EPA
United States
Environmental Protection
Agency

EPA 600/R-16/383 | December 2016 | www.epa.gov/research

Pilot-Scale Demonstration of In Situ Chemical Oxidation Involving Chlorinated Volatile Organic Compounds

Design and Deployment Guidelines

Parris Island, SC - Marine Corps Recruit Depot Site 45 Pilot Study

SITE CHARACTERIZATION

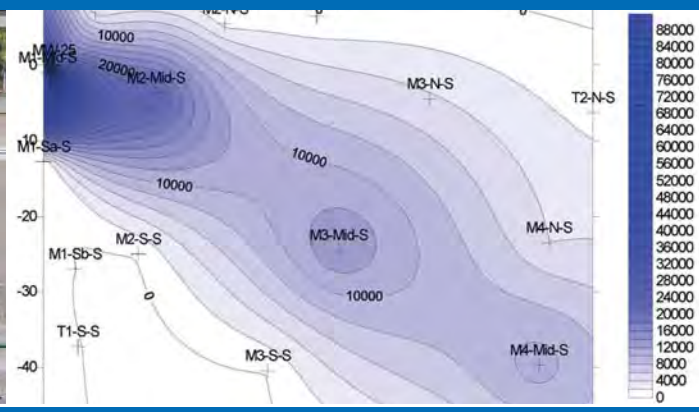

DESIGN

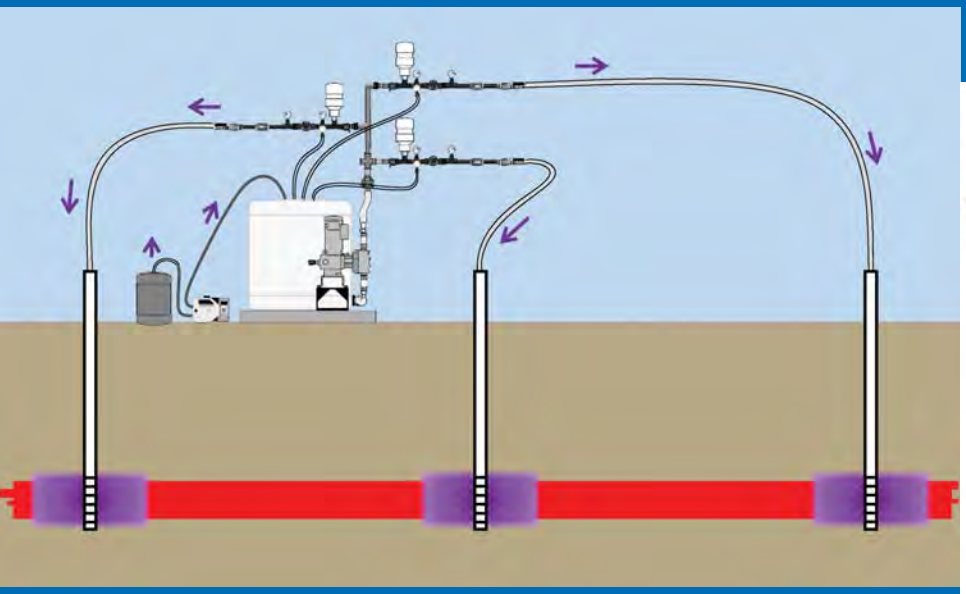

DEPLOYMENT

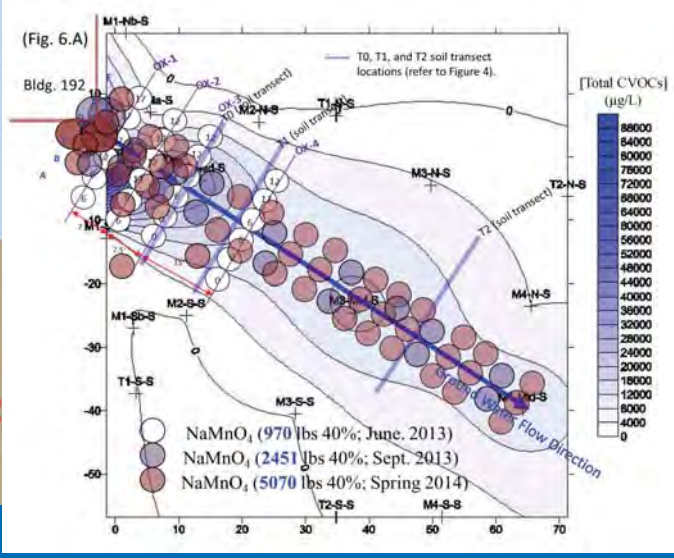

PERFORMANCE EVALUATION

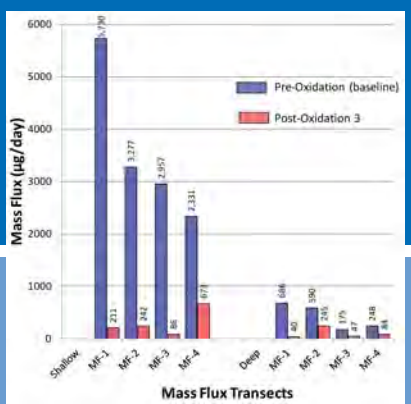

PROJECT REPORT

Office of Research and Development
National Risk Management Research Laboratory

This page intentionally left blank.

EPA 600/R-16/383
December 2016

Pilot-Scale Demonstration of In Situ Chemical Oxidation Involving Chlorinated Volatile Organic Compounds

Design and Deployment Guidelines

Parris Island, SC, Marine Corps Recruit Depot Site 45 Pilot Study

Scott G. Huling
U.S. Environmental Protection Agency
Office of Research and Development
National Risk Management Research Laboratory
Robert S. Kerr Environmental Research Center
P.O. Box 1198, Ada, OK, 74820
huling.scott@epa.gov 580.436.8610

Bruce E. Pivetz
CSS
452 Mountain View Drive
Lewiston, NY 14092

Ken Jewell
U.S. Environmental Protection Agency
Office of Research and Development
National Risk Management Research Laboratory
Robert S. Kerr Environmental Research Center
P.O. Box 1198, Ada, OK, 74820

Saebom Ko
National Research Council
Robert S. Kerr Environmental Research Center
P.O. Box 1198, Ada, OK, 74820

Office of Research and Development
National Risk Management Research Laboratory | Ground Water and Ecosystems Restoration Division

Disclaimer

This document has been reviewed in accordance with U.S. Environmental Protection Agency policy and approved for publication. Any mention of trade names or commercial products does not constitute endorsement or recommendation for use.

Acknowledgements

The Authors wish to acknowledge the collaborative support by the Parris Island Partnering Team (PIPT), including L. Llamas (EPA, Region 4), M. Singletary, D. Owens (US Navy), T. Harrington, L. Donahoe (US Marines), C. Wargo, A. Gerry, M. Amick (SC DHEC).

The EPA field and analytical staff contributing to this project include T. Lankford, L. Callaway, K. Hargrove, R. Neill, K. Jones, and J. Groves (EPA, NRMRL, GWERD, Ada, OK), and P. Clark (EPA, NRMRL, LRPCD, Cincinnati, OH).

Key Words

Site characterization, ground water, CVOCs, permanganate, in situ chemical oxidation, ISCO design, direct-push injection, rebound

Acronyms

ASTM	American Society of Testing Materials
bgs	below ground surface
CMF	contaminant mass flux
CSIA	compound-specific isotopic analysis
CSM	conceptual site model
CVOCs	chlorinated volatile organic compounds
DoD	Department of Defense
c-DCE	cis-1,2-dichloroethylene
t-DCE	trans-1,2-dichloroethylene
1,1-DCE	1,1-dichloroethylene
DNAPL	dense non-aqueous phase liquid
EPA	Environmental Protection Agency
GC/MS	gas chromatography / mass spectroscopy
GWERD	Ground Water and Ecosystems Restoration Division
ICP - OES	inductively coupled plasma – optical emission spectrometry
ID	inside diameter
ISCO	in situ chemical oxidation
MCRD	Marine Corps Recruit Depot
LRPCD	Land Remediation and Pollution Control Division
MSDS	material safety data sheet
NAPL	non-aqueous phase liquid
NOD	natural oxidant demand
NOM	natural organic matter
NRMRL	National Risk Management Research Laboratory
OD	outside diameter
ORD	Office of Research and Development
ORP	oxidation reduction potential
PCE	perchloroethylene
PI, SC	Parris Island, South Carolina
PIPT	Parris Island Partnering Team
PPE	personal protection equipment
PUPS	Palmetto Utility Protection Service, Inc. (Columbia, SC)
PV	pore volume
RAP	research action planning
RCRA	Resource Conservation and Recovery Act
RSKERC	Robert S. Kerr Environmental Research Center
SC DHEC	South Carolina Department of Health and Environmental Control
SHC	Sustainable and Healthy Communities
TCE	trichloroethylene
TEAP	terminal electron accepting process
TOC	total organic carbon
Tt NUS	TetraTech-NUS Corp.
UIC	underground injection control
USGS	United States Geological Survey
UST	Underground Storage Tanks
VC	vinyl chloride

Table of Contents

Abstract

A pilot-scale in situ chemical oxidation (ISCO) demonstration, involving subsurface injections of sodium permanganate ($NaMnO_4$), was performed at the US Marine Corps Recruit Depot (MCRD), site 45 (Parris Island (PI), SC). The ground water was originally contaminated with perchloroethylene (PCE) (also known as tetrachloroethylene), a chlorinated solvent used in dry cleaner operations. High resolution site characterization involved multiple iterations of soil core sampling and analysis. Nested micro-wells and conventional wells were also used to sample and analyze ground water for PCE and decomposition products (*i.e.*, trichloroethyelene (TCE), dichloroethylene (c-DCE, t-DCE), and vinyl chloride (VC)), collectively referred to as chlorinated volatile organic compounds (CVOC). This characterization methodology was used to develop and refine the conceptual site model and the ISCO design, not only by identifying CVOC contamination but also by eliminating uncontaminated portions of the aquifer from further ISCO consideration. Direct-push injection was selected as the main method of $NaMnO_4$ delivery due to its flexibility and low initial capital cost. Site impediments to ISCO activities in the source area involved subsurface utilities, including a high pressure water main, a high voltage power line, a communication line, and sanitary and stormwater sewer lines. Utility markings were used in conjunction with careful planning and judicious selection of injection locations. A portable, low cost injection system was designed, constructed, and deployed at the site. The oxidant delivery design and deployment methods were used to achieve aggressive, effective, and efficient oxidant delivery and oxidation of CVOCs. Specifically, this included numerous injection locations, a narrow radius of influence of the injected oxidant, short vertical screen injection intervals, low injection pressure, outside-in oxidant injection, and a total porosity oxidant volume design.

Three oxidant injection events were carried out, where the oxidant loading was more aggressive and the areal footprints were progressively larger. In this process, the oxidant was delivered into the targeted zones, hydraulic control of the injected oxidant was maintained, the oxidant persisted in zones where heavy oxidant loading was delivered, and significant CVOC destruction was achieved. Ground water and aquifer material sampling and analysis involved an array of parameters, including CVOC, iron, chloride, oxidation reduction potential (ORP), methane, metals, dissolved oxygen, total organic carbon, oxidant demand, molecular biological tools, and compound-specific isotopic analysis. Monitoring these parameters provided insight into the impact of ISCO and ISCO treatment performance, but limited insight was provided by some parameters. Significant reductions in post-oxidation CVOC concentrations in ground water and soil, and a 92% and 76% reduction in total CVOC mass flux in shallow and deep micro-wells, respectively, occurred as a result from the three oxidant injections. CVOC rebound was determined in 3 of the 38 wells. At one depth interval in the source area, elevated post-oxidation CVOC concentrations were measured in the soil, indicating the presence of PCE dense non-aqueous phase liquids. This result suggests that rebound will continue and that subsequent ISCO activities are needed, on a limited scale, in the source area to address CVOC rebound. Specific details and guidelines are provided regarding continued monitoring and recommended ISCO activities. The results of this study are intended to provide details and guidelines that can be used by EPA and Department of Defense remedial project managers regarding ISCO remediation at other sites.

1. Introduction

This research project involved the pilot-scale deployment of in situ chemical oxidation (ISCO) at the United States Marine Corps Recruit Depot (MCRD) (Parris Island, SC), site 45. The purpose of the project was (1) to advance the state of the science of the ISCO technology through improvements in ISCO design, methods, techniques, and tools, and (2) to collaborate with the US Environmental Protection Agency (EPA) Region 4 Comprehensive Environmental Response, Compensation, and Liability Act (CERCLA) program and verify the effectiveness of the ISCO technology at pilot-scale.

In a detailed feasibility analysis (TetraTech, 2012), it was determined that an ISCO remedy, in conjunction with natural attenuation, could be protective of human health and the environment by meeting the cleanup goal of reducing the toxicity, mobility, and volume of groundwater CVOCs, reducing the high-concentration areas, significantly reducing the expansion of the plume, and permanently removing CVOCs in the ground water. Overall, this would accelerate the remediation process. Independently, based on a critical analysis of site-specific conditions and goals, it was determined that the health and safety of project and facility personnel could be assured, that ISCO deployment was appropriate, and stood a moderately good probability to achieve the treatment objectives. The ISCO pilot-scale study was proposed by the U.S. Environmental Protection Agency, Office of Research and Development, National Risk Management Research Laboratory, Ground Water and Ecosystems Restoration Division (EPA, ORD, NRMRL, GWERD) at the Robert S. Kerr Environmental Research Center (RSKERC) (Ada, OK) through an EPA research action plan (RAP). Subsequently, the proposed research was approved by the EPA ORD through the research planning process. The Parris Island Partnering Team (PIPT) oversees the CERCLA program at the Parris Island MCRD, and is comprised of the US EPA Region 4, US Navy, US Marine Corps Recruit Depot, and the South Carolina Department of Health and Environmental Control (SC DHEC). The PIPT determined that ISCO was an appropriate source reduction remedy for site 45 and also

approved the ISCO pilot-scale project. Therefore, fortunate timing between the US EPA CERCLA site remediation process and the EPA ORD RAP project planning allowed collaboration and synergy between these two programs. Overall, the successful implementation and completion of this pilot-scale demonstration was accomplished through the collaboration of EPA, NRMRL, GWERD (Ada, OK); Region 4 (Atlanta, GA); EPA, NRMRL, Land Remediation and Pollution Control Division (LRPCD), (Cincinnati, OH); the Department of Defense including both the US Navy and the US Marine Corps; and the South Carolina Department of Health and Environmental Control (SC DHEC). Through the execution of the pilot-scale ISCO project, valuable data and information was provided that satisfied the remedial steps in the CERCLA feasibility study process, has advanced the state of the science of the ISCO technology, and will be used by the regulatory decision-makers associated with the PIPT to determine whether ISCO should be deployed as the final treatment remedy for site 45.

This project's feasibility analysis included research statistics provided by the Superfund Remedy Report, which includes information and analysis on remedies selected to address contamination at Superfund sites (EPA, 2014).

The US EPA prepared a Superfund Remedy Report that compiled data and information regarding remedies selected that address contamination at Superfund sites (EPA, 2014). In 2009-2011, a critical analysis of the data indicates that decisions regarding the Superfund remedial program selected "treatment" for a large number of source remedies, and in situ treatment continued to make up an increasing portion of the selected treatment technologies. On average, half of recent source treatment decision documents included in situ treatment. The EPA's analysis of remedy selection from FY 2009 to 2011, and a comparison to early data, shows that the Superfund remedial program continues to select treatment at nearly 75 % of Superfund sites over the life of the program.

In situ treatment for ground water continues this overall upward trend, averaging 38 % of decision documents addressing ground water.

Furthermore, in situ chemical oxidation (ISCO) treatment continues to be one of the most frequently selected in situ treatment technologies. Concerning groundwater remedies (EPA, 2014), the selection of pump and treat and monitored natural attenuation (MNA) has decreased slightly, while the selection of in situ treatment has increased. The overall selection of in situ chemical treatment remedies for groundwater remains steady and more than half of the chemical treatment remedies involved ISCO. These trends in technology selection indicate the need for the continued development of ISCO, a technology that has the ability to transform contaminants in the subsurface while minimizing the use of fossil fuel energy, chemicals, and environmental impact (Siegrist *et al.*, 2001; 2011; Huling *et al*., 2006).

Task 4.1 of the sustainable and healthy communities (SHC) research action plan (RAP) involved assessment and management of contaminated ground water to protect human health and ecological services. Section 3.1.5.1 of the SHC research program involved ISCO, a technology that meets the goals and objectives of task 4.1. Contamination of aquifers with organic chemicals remains a significant concern even after decades of research into remedial technologies and field applications. In recent years, various methods of in situ chemical oxidation have emerged involving the injection of different oxidants into the subsurface, including sodium or potassium permanganate ($NaMnO_4$ and $KMnO_4$, respectively), hydrogen peroxide (H_2O_2), and sodium persulfate ($Na_2S_2O_8$). ISCO is a developing technology for hazardous waste treatment in surface and subsurface systems and is used to transform and destroy a wide array of environmental and emerging contaminants of national interest. These contaminants are a national EPA priority and are regulated under numerous environmental programs, including CERCLA, RCRA, and UST; and millions of US dollars are spent annually to treat ground water, soil, and aquifer material. Engineering design criteria and guidelines for ISCO deployment, monitoring, and performance evaluation methods still requires further development. For example, understanding the fate and transport of injected chemical oxidants, in conjunction with the targeted

contaminants in the subsurface, are critical in the successful development and deployment of this treatment technology and is a core competency at the EPA/NRMRL/Ground Water and Ecosystems Restoration Division (Ada, OK). The ISCO project at Parris Island Marine Corps Recruit Depot, (Parris Island, SC) involved multiple EPA priority research areas, including research on the rapid chemical oxidation of chlorinated solvents. The results of this research can be extended to other priority contaminants including biofuels, endocrine disrupting compounds, pharmaceuticals, and other emerging contaminants, so the knowledge gained from the Parris Island ISCO project can be applied to a broader area of contaminant oxidation and subsurface remediation.

Specific technical objectives of this project were to establish an accurate conceptual site model through high resolution aquifer core material and ground water sampling and analysis, to focus oxidant delivery to targeted zones through improved resolution of contaminant distribution data and information, to design and develop a low cost, portable injection system, and to improve the design of oxidant injection dosages (*i.e.*, volume and concentration) and delivery using spatial distribution criteria. Satisfying these objectives would permit an improved critical analysis of ISCO deployment and treatment performance, avoid potential treatment inefficiency and ineffectiveness associated with poorly developed methods, and ultimately advance the state of the science of the ISCO technology.

1.1 In Situ Chemical Oxidation (ISCO)

1.1.1 ISCO Description

ISCO involves the introduction of a chemical oxidant into the subsurface for the purpose of transforming groundwater or soil contaminants into less harmful chemical species (Siegrist *et al*., 2001; Huling and Pivetz, 2006; Siegrist *et al*., 2011). Several forms of oxidants are used for ISCO, including sodium and potassium permanganate ($NaMnO_4$, $KMnO_4$), hydrogen peroxide (H_2O_2), and sodium persulfate ($Na_2S_2O_8$). Sodium permanganate ($NaMnO_4$) was selected as the form of oxidant to use in the pilot-scale deployment of ISCO at site 45. A detailed description of the fundamentals of ISCO using permanganate is described elsewhere (Siegrist *et al*., 2001; Huling and Pivetz, 2006; Petri *et al.*, 2011). Sodium permanganate (40%; 1.36 g/mL) is formulated and produced as a liquid, is a highly soluble form of permanganate, and only requires dilution prior to injection. Potassium permanganate ($KMnO_4$(s)) is a solid, and costs less than $NaMnO_4$, but must be dissolved and rigorously mixed to assure complete dissolution prior to injection. $NaMnO_4$ was selected rather than $KMnO_4$ to minimize the use of mixing tanks and equipment, potential oxidant exposures during mixing, labor associated with oxidant handling and mixing, logistics in staging oxidant mixing and injecting, and the potential for permeability reduction near the injection points and wells. Specifically, this helped to assure the injection of more uniform oxidant concentrations, to limit the on-site footprint of the remedial activity, and to minimize the interruption in through traffic and on-site activities at the dry cleaner.

Successful ISCO is functionally dependent on three basic requirements. First, there must be a strong reaction between the oxidant and target compound, indicating the importance of reaction kinetics. The faster the reaction the better, as this limits the contact time required between the reactants. There must be physical contact between the target chemical and the oxidant, emphasizing the importance of good site characterization and effective oxidant delivery to the specific targeted zone. Finally, a sufficient quantity of oxidant must be delivered to the targeted zone and must persist for a sufficient reaction period to achieve the treatment objectives. These basic tenets must be satisfied for significant contaminant reduction to occur at the site.

1.1.2 ISCO at sites with chlorinated volatile organic compounds (CVOCs)

Reaction 1 (Table 1) is the 3-electron half reaction for permanganate (MnO_4^-) oxidation under most environmental conditions (pH 3.5 to 12). One of the reaction byproducts is MnO_2, and in the pH range of 3.5 to 12 it is a solid precipitate. Under acidic conditions (pH <3.5), Mn in solution or in colloidal form may be present in different redox-dependent oxidative states ($Mn^{+2, +4, +7}$). Additionally, under strongly alkaline conditions, Mn may be present as Mn^{+6}. Under conditions where pH is <3.5 and >12, 5-electron and 1-electron transfer reactions occur, respectively (Table 1, half reactions 2 and 3). Reactions 1 to 3 illustrate the general permanganate reactions in the subsurface. Overall, permanganate oxidation potentially involves various electron transfer reactions (reactions 1 to 3), but is generally considered independent of pH in the range of 4 to 8.

Reactions 4 to 7 (Table 1) illustrate the oxidation of perchloroethylene (PCE), trichloroethylene (TCE), dichloroethylene (DCE), and vinyl chloride (VC), respectively. These are chlorinated volatile organic compounds (CVOCs) commonly found at site 45. Examination of these balanced redox reactions indicates that the oxidant demand is inversely correlated with chlorine substitution. For example, the stoichiometric requirements for PCE, TCE, DCE, and VC are 1.33, 2.0, 2.67, and 3.33 mol $KMnO_4$/mol contaminant, respectively. The reaction rate between MnO_4^- and the CVOCs is fast (Yan and Schwartz, 1999) (Table 2). Assuming conservatively that $[MnO_4^-]$ = 1 mM (120 mg/L), it is projected that the half-lives of target CVOCs found at the ISCO site range from less than an hour for TCE, c-DCE, t-DCE, and 1,1-DCE, to 4.5 hours for PCE. The average ground water temperature is > 20 °C during summer months, and faster reaction rates are expected for these CVOCs.

Table 1. Permanganate oxidation and CVOC mineralization reactions.

pH dependency of MnO_4 reactions

$MnO_4 + 2\,H_2O + 3\,e \longrightarrow MnO_2(s) + 4\,OH$	(pH 3.5-12)	(1)
$MnO_4 + 8\,H^+ + 5e \longrightarrow Mn^{+2} + 4\,H_2O$	(pH <3.5)	(2)
$MnO_4 + e \longrightarrow MnO_4^{-2}$	(pH >12)	(3)

CVOC stoichiometry

$4\,KMnO_4 + 3\,C_2Cl_4 + 4\,H_2O \longrightarrow 6\,CO_2 + 4\,MnO_2 + 4\,K^+ + 8\,H^+ + 12\,Cl$	(4)
$2\,KMnO_4 + C_2HCl_3 \longrightarrow 2\,CO_2 + 2\,MnO_2 + 2\,K^+ + H^+ + 3\,Cl$	(5)
$8\,KMnO_4 + 3\,C_2H_2Cl_2 \longrightarrow 6\,CO_2 + 8\,MnO_2 + 8\,K^+ + 2\,OH + 6\,Cl + 2\,H_2O$	(6)
$10\,KMnO_4 + 3\,C_2H_3Cl \longrightarrow 6\,CO_2 + 10\,MnO_2 + 10\,K^+ + 7\,OH + 3\,Cl + H_2O$	(7)

Table 2. First order transformation of chlorinated volatile organic compounds.

CVOCs	Reaction Rate Constant, k [1] (20 °C) (s^{-1})	Half-Life, $t_{1/2}$ [2] (20 °C) (hours)
PCE	4.5×10^{-5}	4.3
TCE	6.5×10^{-4}	0.3
c-DCE	9.2×10^{-4}	0.2
t-DCE	3.0×10^{-2}	< 0.1
1,1-DCE	2.38×10^{-3}	< 0.1

[1] The estimated pseudo first-order reaction rate constant involving MnO_4 (1 mM, 20 °C) (Yan and Schwartz, 1999).

[2] The half-life is the time required for 50% loss of CVOCs.

1.1.3 Advantages and limitations of the technology

The oxidation of CVOCs in ground water at the Parris Island (PI), MCRD site 45 involved relatively simple and fast reaction kinetics between MnO_4^- and soluble CVOCs. This type of reaction does not require a catalyst. $NaMnO_4$ is highly soluble, and high concentrations of the oxidant can be injected, where appropriate. The long-term persistence of MnO_4^- in the subsurface permits both advective and diffusive transport, which is generally associated with relatively good distribution of the oxidant and good contact between the oxidant and the target contaminants. High concentrations of $NaMnO_4$ can result in a density greater than ground water, causing density-driven vertical transport of the oxidant into the subsurface. This transport mechanism can contribute to improved distribution and contact between the oxidant and CVOCs that may be present in low-permeability materials. Specifically, the oxidant may migrate vertically and accumulate on or near low permeability materials that are contaminated with CVOCs. This condition is desirable, given that CVOC diffusion from low permeability materials, and oxidant diffusion into the low permeability materials can result in a larger and effective reaction zone between the oxidant and the CVOCs.

Permanganate has been successfully delivered into a wide range of hydrogeologic environments: sands, clays, sand-clay mixtures, alluvial materials, fractured shale, and fractured bedrock. A disadvantage of in situ technologies where fluids are injected, including ISCO, is the potential for hydraulic short circuiting of the injected oxidant. Naturally occurring and man-made preferential pathways result in non-uniform delivery of the oxidant, and potentially the transport of the oxidant into non-targeted zones. Consequently, the failure to achieve adequate oxidant coverage and distribution in the target zone results in incomplete contact and limited reaction between the MnO_4^- and CVOCs. Significant efforts to characterize the hydrogeology, CVOC distribution, and CVOC fate and transport at site 45 helped to develop an accurate conceptual site model that was critical in the effective and efficient delivery of the oxidant.

MnO_2(s) is the main reaction byproduct that may accumulate near the injection well or at the dense non-aqueous phase liquid (DNAPL) interface (*i.e.*, encrustment) resulting in mass transport (permeability reductions) and mass transfer limitations, respectively. Permeability reductions may also result from the (1) injection of potassium permanganate solids, such as incompletely dissolved $KMnO_4$(s), and (2) entrapment of CO_2(g) released from CVOC mineralization. Ion exchange of Na^+ in $NaMnO_4$ for divalent cations in the aquifer matrix may disperse soil colloids and also contribute to permeability reductions, however, permeability reductions of this nature are not often reported. These causes of permeability reductions can be largely avoided by adhering to design and operational guidelines. Subsequent increases in the permeability due to dissolution of CO_2(g) and $KMnO_4$(s) suggests that these mechanisms are reversible under ambient conditions. Permeability reduction can also be avoided during oxidant recirculation in ISCO by filtering re-injected fluids, by selection of permanganate with low silicate content, such as $NaMnO_4$, and by assuring adequate mixing of the $KMnO_4$ solution before injection (Luhrs *et al*., 2006). Well-development steps can also be performed to more rapidly restore the permeability of affected injection wells.

Other disadvantages potentially include secondary drinking water standards for manganese and the oxidant impact on microbial activity. The EPA has established a secondary maximum contaminant level (MCL) for drinking water for manganese (0.05 mg/L), based on color, staining, and taste. At site 45, there are no downgradient domestic water wells where the ground water is being used for domestic purposes. A short-term reduction in microbial activity may result from the injection of permanganate; however, this does not appear to be permanent, and post-oxidation increases in microbial numbers, activity, and contaminant attenuation are often reported (Luhrs *et al.*, 2006).

1.2 Site Selection

ISCO has been deployed over a wide range of geologic and hydrogeologic environments. A moderate to high permeability subsurface is preferred, and sandy material is ideal. High permeability allows rapid delivery of the oxidant into the subsurface, and therefore does not require high pressure or extended periods of oxidant injection. A low degree of heterogeneity is preferred since this leads to a more uniform distribution of the oxidant. Low organic content is also preferred since this limits the natural oxidant demand and depletion of the oxidant by non-target reactants. At the PI MCRD ISCO site, the shallow surficial aquifer extends to 18 feet below ground surface (ft bgs) and consists of fine to medium sand. Localized silty, clayey lenses in the surficial aquifer are limited in areal extent and are not expected to be functional confining units, typically associated with extensive low permeability materials. A peat and silty clay layer occurs at 17-27 ft bgs and does effectively function as a local confining unit.

Ideally, the ground water table should be between 10-30 ft bgs, and the contaminated zone should be no deeper than 65 ft bgs. This limits the vertical depth required for site characterization, remedial investigations, and ISCO deployment (*i.e.*, limits the depth of drilling and well construction materials/costs).

At the PI MCRD ISCO site 45, the ground water is 3-4 ft bgs and the water table fluctuates with the tide (0.2-0.6 ft). The contaminated interval is shallow, resulting in a limited overburden pressure to off-set the injection pressure.

Fast and well-established reaction rates between the oxidant and the target contaminant are ideal and emphasizes the importance of oxidation chemistry in ISCO. The reaction between permanganate and the targeted chlorinated ethenes of interest at the PI MCRD ISCO site 45 has previously been established (Yan and Schwartz, 1999). Furthermore, the site should not contain large quantities of dense non-aqueous phase liquids (DNAPL). In general, the presence of excessive DNAPL, especially mobile DNAPL, would make it difficult to accomplish significant contaminant mass reduction. Prior to ISCO deployment, DNAPL removal is an important pretreatment step; however, some DNAPL will likely exist at most sites containing CVOCs. Historical information regarding DNAPL handling and releases, site characterization data, and ongoing remedial efforts is useful to help assess the relative quantity of DNAPL that could be in the subsurface. In preliminary investigations, soil core samples (n= 31) from site 45 were tested for DNAPL using a fluorescent light screening method and no information was found suggesting direct evidence of DNAPL, neither was it found in conjunction with other investigations (Tt NUS, 2012). However, it was projected that small quantities of residual DNAPL were likely at the site, given the PCE handling and release records and the extensive nature of the CVOCs' ground water plume.

Minimal access limitations at ISCO sites are important regarding site characterization, including soil coring, installation and sampling of micro-wells, wells, and remediation, including utilization of injection equipment, chemical storage vessels, etc. Further, the site should not contain significant above- or below-ground utilities that interfere with the deployment of the technology. At site 45, multiple subsurface, surface, and overhead impediments to ISCO required special design and deployment considerations. In the subsurface, these include a sanitary sewer pipe, storm sewer line, an 8-inch high pressure water main, and a high voltage power line. Surface impediments include overhead steam lines, a drive-through at the dry cleaner facility, street and parking traffic, and constant foot traffic. As-built construction maps were obtained and reviewed to help identify the presence of subsurface utilities. Facility dig permits and utility markings were used prior to all subsurface activities, to confirm these locations. The CVOC ground water contamination plume had migrated under the drive-through of the facility, Kyushu Street, an existing parking lot, and all the utilities discussed above (Figure 1). Site activities adhered to appropriate health and safety requirements, and access to the US Marine Corps Recruit Depot was through a security gate, where identification of project personnel and project purpose was required each day.

1.3 Partial plume remediation – source reduction remedy

Source area contaminant mass reduction, or partial plume remediation, was the goal of this pilot-scale deployment of ISCO. The PCE source area located near the corner of Bldg. 192, which housed a new dry cleaner facility, resulted in a CVOC ground water plume that extended to the southeast (Figure 1). As is typically observed, the downgradient ground water plume was much larger than the source area, but lower in concentration. It is well known that significant challenges exist in achieving maximum concentration limits (MCLs) on a site-wide basis for CVOCs at DNAPL sites (McGuire *et al*., 2006; Krembs *et al*., 2010). These challenges are partially attributed to contaminant mass transfer and transport limitations. However, ISCO deployment in the source area, (1) limits the areal extent in which ISCO is deployed, (2) focuses the oxidant delivery in the most contaminated zones, where contact between target and contaminant generally results in fast and efficient reaction rates, (3) and reduces CVOC concentrations and mass flux of contaminants from the source area. A reduction in mass flux leads to a reduction in the transport load of CVOC contaminants in the downgradient direction that must ultimately undergo natural attenuation processes.

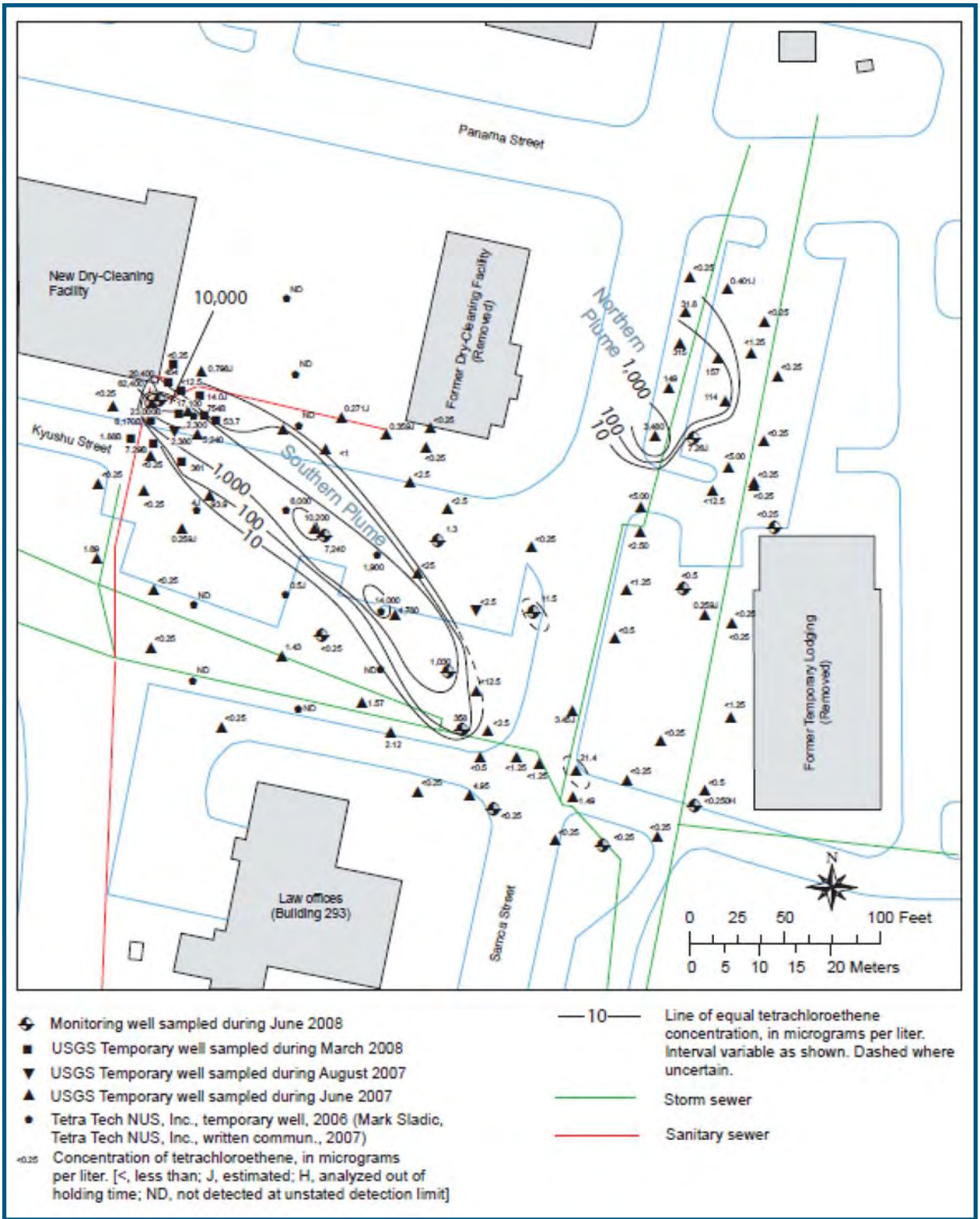

Figure 1. Generalized distribution of tetrachloroethylene in ground water at Site 45, Marine Corps Recruit Depot, South Carolina (2006-2008) (Vroblesky *et al.*, 2009).

In summary, the treatment objective was not to achieve site-wide MCLs for CVOCs, but rather to investigate whether a cost-effective remedy could be achieved through ISCO deployment over a limited area. Ideally, this could lead to a reduction in mass flux, and in conjunction with natural attenuation, achieve acceptable CVOC concentrations at a downgradient compliance plane, eliminate exposure pathways, and reduce risks beyond the compliance plane. Under this scenario, the total mass of contamination would not be completely eliminated, but reduced in a cost-effective manner that limits or minimizes risk. In general, natural attenuation is expected to be an integral component of ISCO remedies at DNAPL sites because of the difficulty and technical challenges to achieve site-wide MCLs. Partial plume remediation does not require 100% removal of contaminant mass, rather this approach recognizes existing technical and economic remediation constraints, and limits exposure pathways and risks at critical site locations.

1.4 Binary mixtures of permanganate and chlorinated volatile organic compounds in ground water samples: sample preservation and analysis

Often, ground water samples collected specifically to be analyzed for organic contaminants at ISCO sites may contain the oxidant and the organic contaminants in a "binary mixture" (Huling *et al.*, 2011; Johnson *et al*., 2012; Ko *et al.*,2012). When organic contaminants and oxidants are commingled in a binary mixture, there is significant potential for oxidative transformation of contaminants to occur after the sample is collected. Consequently, the results of the sample analysis may be non-representative of in situ conditions at the time of sampling, the quality of the ground water sample may be compromised, and false negative results may occur.

An integral component of ISCO is the collection and analysis of representative ground water samples to assess ISCO treatment performance (Ko *et al*., 2012). High quality analytical results are critical to support site assessment and remedial performance monitoring, where ISCO is deployed. Therefore, the guidelines, methods, and procedures presented in Ko *et al*. (2012) were used in this study to preserve binary mixture ground water samples. The visual confirmation of MnO_4^- in ground water samples is possible due to the characteristic pink/purple color of the oxidant. Under this condition, ascorbic acid was amended to the sample to eliminate MnO_4^-. Excess ascorbic acid amended to aqueous samples did not negatively impact the quality of the aqueous samples, nor the analytical instruments used in the analyses (Johnson *et al*., 2012; Ko *et al*., 2012).

1.5 Objectives of the ISCO demonstration at PI MCRD

Bench-, pilot-, and full-scale ISCO applications have been conducted using sodium permanganate and much is already known about process fundamentals and field-scale deployment of this technology (Huling and Pivetz, 2006; Petri *et al.*, 2011). Through the development of new methods, equipment, and techniques, and through utilization and adaptation of existing methods, the overall objectives were to make improvements in both process fundamentals and technology deployment that would lead to improved ISCO effectiveness and efficiency. The specific objectives of the proposed demonstration were (1) to significantly reduce the mass of CVOCs in the source area, (2) to limit the areal extent of the CVOC concentration plume downgradient from the source area and significantly reduce the mass flux of CVOCs from the source area, (3) to quantify pre- and post-oxidation CVOC natural attenuation to assess the short- and long-term impacts of ISCO on the natural attenuation process, and (4) to assess contaminant rebound and focus subsequent oxidant delivery into specific target zones, if needed. The results of this study will provide a conceptual approach and guidelines that can be used by the EPA and DoD remedial project managers when considering ISCO for remediation at other sites.

2. Detailed Site Description

2.1 Site location and history

The MCRD at Parris Island (PI), SC is located along the southern coast of South Carolina, 1 mile south of the city of Port Royal. It covers approximately 8,047 acres of dry land, salt marshes, saltwater creeks, and ponds. The PI MCRD facility is the reception and recruit training facility for the US Marine Corps for enlisted men from states east of the Mississippi River and for enlisted women nationwide. Prior to 2001, the old dry cleaning facility at site 45 was in a building located in the Main Post area of PI MCRD, between Panama Street to the north, Kyushu Street to the south, and Samoa Street to the east (Figure 1). Four above-ground storage tanks, put into place in 1988, were situated along the northern side of the building. Reportedly, one of the tanks was overfilled on March 11, 1994, with PCE and an unknown amount of the PCE solvent flowed into a concrete catch basin (TtNUS, 2004). The PCE overflow was not collected at that time, and heavy rainfall subsequently washed the contaminant onto the surrounding soil and into subsurface storm drains (TtNUS, 2004). Additionally, miscellaneous solvent spills resulted in releases to the sanitary sewer line that were located in and near the old dry cleaner facility. Subsequently, multiple lines of evidence indicate that the PCE leaked from the broken sewer pipe at a location approximately 50-75 yards southwest of the dry cleaner facility (Vroblesky *et al.*, 2009). A new dry cleaner facility was constructed to the southwest of the demolished old dry cleaner building. Prior to construction, a sanitary sewer manhole and a portion of the sanitary sewer line was removed and replaced with a diagonal section to bypass the newly constructed Building 192. The southeast corner of the new dry cleaner facility, Building 192, was constructed over the former manhole and sanitary sewer line. In this report, “the plume” refers to the southern CVOC plume emanating from the southeast corner of Building 192, and the northern CVOC plume emanates from the north side of the former old dry cleaner facility (Figure 1).

Leakage of PCE was from the sanitary sewer and served as the source of contamination for the southern plume, and not from the new dry cleaner facility as was once surmised (Vroblesky *et al.*, 2009). Contaminated soil at the original spill location was excavated, and an interim remedial action was initiated. In early 2001, the main dry cleaning building, solvent tanks, and other related structures were demolished and removed from the site. Currently, the site is mostly a vacant lot covered with mowed grass and isolated shrubs and trees. Physical features remaining at the site consist of three above-ground extraction well housing units and one ground water treatment system shed.

2.2 Site conceptual model, previous investigations

Data and information from previous investigations were available for review, and included contaminant distribution, hydrogeology, and other chemical and physical parameters (TtNUS, 2004; 2012; Vroblesky, 2007; 2008; 2009). This data was important to develop an accurate site conceptual model, to understand site-specific contaminant fate and transport, and to guide additional site characterization activities.

2.2.1 USGS site characterization

The United States Geological Survey (USGS) performed a subsurface investigation of ground water quality and levels which involved the monitoring of existing permanent wells and installation and monitoring of additional permanent and temporary wells (Vroblesky *et al*., 2007; 2008; 2009). Temporary borings were installed using direct-push technology and a membrane interface probe (MIP) was used in temporary borings, which provided information on the depth of the contamination. Collectively, the data and information were used in the development of plan-view isocontour maps illustrating the CVOCs, including PCE, TCE, c-DCE, and VC isopleths (Vroblesky *et al*., 2009). Examination of the CVOC ground water contamination isopleths indicated that the source of the southern plume originated near the corner of the new dry cleaner facility (Bldg. 192) (Figure 1) (TCE, c-DCE, VC isopleth maps not included). However, several lines of evidence indicate that the contaminant source in the southern plume was due to the release of PCE into the sanitary sewer from the old dry cleaner facility, and discharge of the PCE from an incompetent section of the sanitary sewer line, was constructed of vitrified clay, in the vicinity of the new dry cleaning facility (Vroblesky *et al*., 2009). USGS (2009; pg. 28) states "A sewer-inspection camera was used to examine the integrity of the sewer line in 2007. The camera revealed that although the existing pipe between the former and new dry-cleaning facilities contained no collapsed sections, it contained many cracks, and grass roots extended into the pipe. Thus, it is highly probable that the abandoned sanitary sewer is leaky". Several lines of evidence suggest the source of the plume is in the immediate vicinity of the southeast corner of Building 192: the CVOC plume emanates from the southeast corner of Building 192 (Figure 1); the highest CVOC concentrations measured in ground water and soil samples collected during baseline characterization were from the area immediately adjacent to MW-25, approximately 10 ft from the corner of Bldg. 192; and the occurrence of parent and decomposition chlorinated products downgradient from a source at the southeast corner of Bldg. 192, are consistent with the natural attenuation of CVOCs. The USGS investigation also identified ground water table elevations in the lower surficial aquifer, and the presence of subsurface sanitary and storm sewer lines and the roles they play in the fate and transport of CVOCs in the southern plume (Figures 2-3) (Vroblesky *et al*., 2009).

The USGS conducted a detailed assessment of natural attenuation processes in the southern plume and revealed that the surficial aquifer in the southern plume is anaerobic at most locations, with the predominant terminal electron accepting process (TEAP) being iron reduction in the shallowest sediment (Vroblesky *et al.*, 2009). In deeper sediment containing the main body of contamination, the predominant TEAP appears to be sulfate or iron reduction; however, the presence of methane, the high degree of contaminant dechlorination, and a H_2 value (31 nM) in the range of methanogenesis at one well indicates that methanogenic zones probably also are present. In the deepest part of the surficial aquifer, near the peat layer, the predominant TEAP probably is methanogenesis, by virtue of the abundance of available natural organic matter.

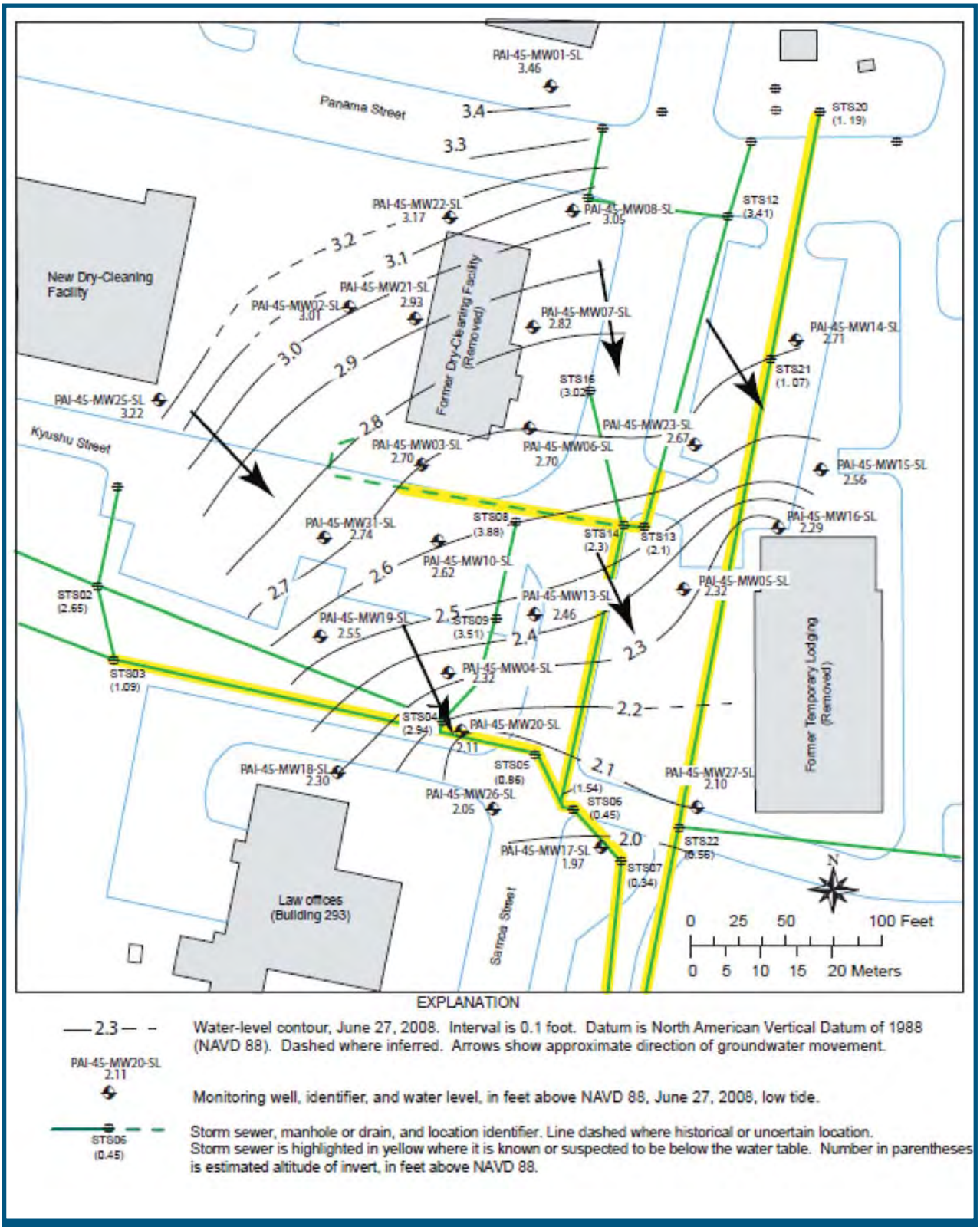

Figure 2. Ground water levels in the lower surficial aquifer at Site 45, Marine Corps Recruit Depot, South Carolina (Vroblesky *et al.*, 2009).

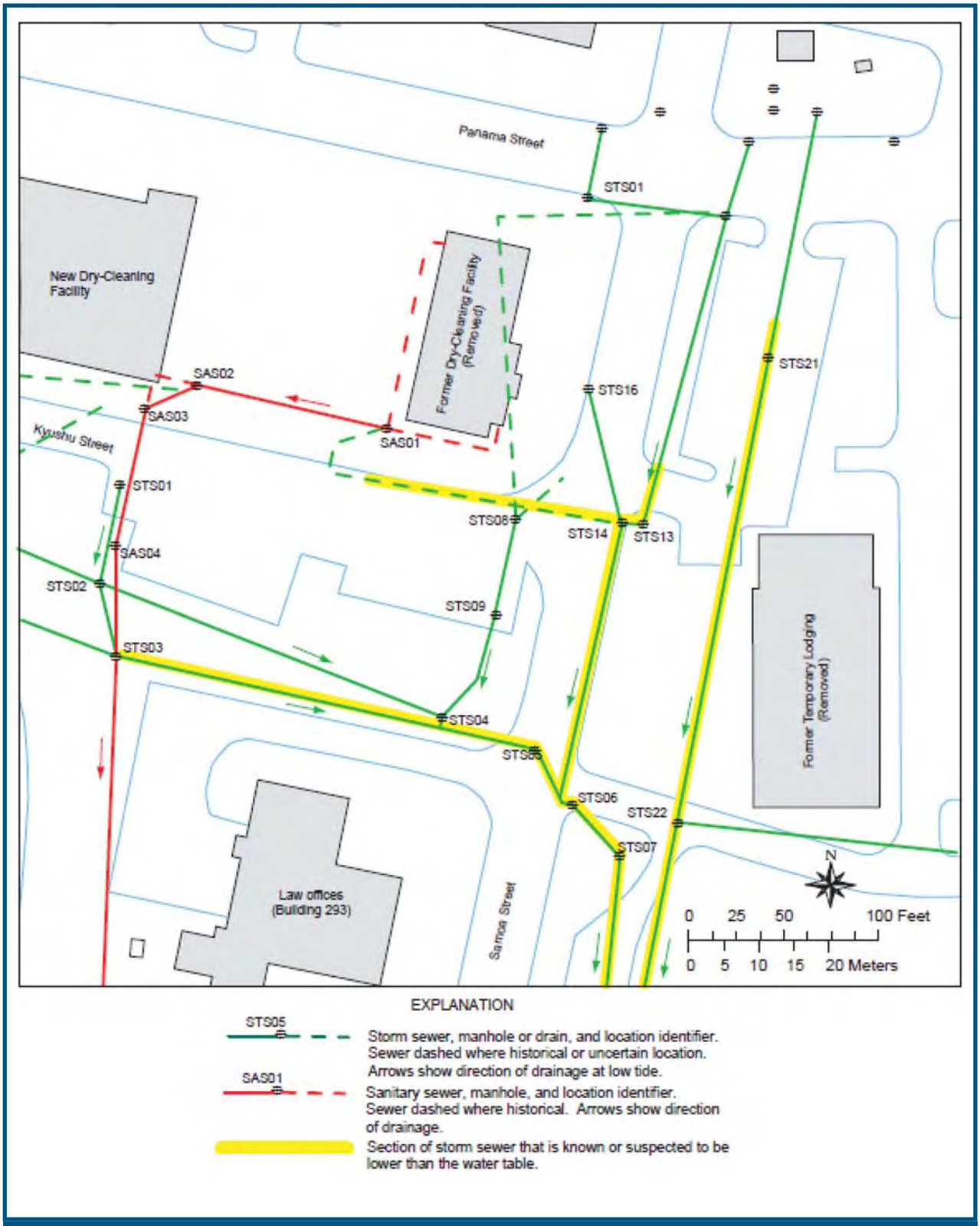

Figure 3. Storm and sanitary sewers at Site 45, Marine Corps Recruit Depot, South Carolina (Vroblesky *et al.*, 2009).

2.2.2 TtNUS (2004; 2012)

The surficial aquifer underlying Site 45 consists of sandy Pliocene to Holocene sediments at an average depth of approximately 18 ft (TtNUS, 2004). In general, the water table encountered within these heterogeneous sediments is shallow and is typically encountered at a depth of 3 to 4 ft bgs, at the site. Ground water is expected to preferentially migrate through the higher-permeability sandy sediments within the surficial aquifer. Because of their limited areal extents, the localized silty/clayey lenses found within the surficial aquifer are not expected to function as significant confining units. However, localized hydraulic effects have been observed because of silt and clay (TtNUS, 2004). Recharge to the surficial aquifer is likely to occur, primarily through infiltration of precipitation.

2.2.3 Aquifer characteristics

Slug tests and aquifer tests were conducted in the area associated with the former dry cleaner building (TtNUS, 2004). Some of these tests were conducted within approximately 120 ft from the proposed ISCO test areas and were useful in conducting a preliminary assessment of the oxidant and reagent fate and transport in the study area. A summary of the slug tests performed in wells in the upper surficial aquifer (3-7' bgs) and lower surficial aquifer (9-14 ft bgs) are summarized (TtNUS, 2004; Table 3-6). The hydraulic conductivity arithmetic and geometric means in the upper surficial aquifer were 12 and 8 ft/day (4.2×10^{-3} cm/s and 2.8×10^{-3} cm/s) (n=8), and in the lower surficial aquifer they were 2.7 and 2.1 ft/day (1.0×10^{-3} cm/s and 7.4×10^{-4} cm/s) (n=6), respectively. Based on these values, this aquifer material would be classified as clean sand or silty sand.

Aquifer test results involving the pumping of well RW-3 were reported; 8 observation wells screened in the upper and lower surficial aquifer were used during the test (TtNUS, 2004; Table 3-7). Although the methods used are generally for confined aquifers, the aquifer core data (*i.e.*, boring log) indicate that the surficial aquifer is unconfined, but the drawdown patterns more closely represent a confined or leaky-confined aquifer. This may be the result of the presence of the relatively finer-grained sediments (silty-sand) within the upper portion of the shallow aquifer, in comparison to the deeper sediments (fine sand). Evidence supporting the occurrence of this clay layer was observed in aquifer cores collected during subsequent site characterization activities, as discussed in section 5.5.1. (*Proposed natural attenuation conceptual model*), below. The average transmissivity was 230 ft^2/day and, assuming an average thickness of 15 ft, the overall hydraulic conductivity of the shallow aquifer sediments is 15.3 ft/day (5×10^{-3} cm/s). The well (RW-3) that was pumped was screened in the upper and lower surficial aquifer (4-16 ft bgs). Given that the water table is approximately 3.5 ft bgs, and the bottom of the surficial aquifer is 16 ft, a more accurate estimate of the aquifer thickness and average hydraulic conductivity is 12.5 ft and 18.4 ft/day (6.6×10^{-3} cm/s), respectively. The results of the slug tests indicate that the majority of water captured by RW-3 was from the upper surficial aquifer.

The surficial aquifer extends to a depth of approximately 17 ft bgs (TtNUS, 2004). The peat and clayey materials found underlying the surficial aquifer sediments throughout the site, at depths ranging from 17 to 27 feet (bgs), are expected

to function locally as a confining unit to ground water flow (Tt NUS, 2004). Based on the results from previous laboratory hydraulic conductivity testing, of six samples from this unit, the geometric mean vertical hydraulic conductivity for this confining unit is 0.00166 ft/day (5.8×10^{-7} cm/sec) (TtNUS, 2004). This, in combination with an average thickness of 5 to 6 ft, indicates that the unit significantly restricts vertical ground water flow.

The low-permeability materials in the 17-27 ft bgs interval are deeper than what was targeted in the ISCO demonstration, and serves as a vertical impediment to downward transport of contaminated water or oxidant solutions. The aquifer cores collected during the site characterization investigation associated with the ISCO study extended to 16 ft bgs, and did not penetrate the confining unit that separates the surficial and deep aquifers. Overall, site characterization efforts and other subsurface investigations associated with the ISCO study at site 45 did not extend beyond 16 ft bgs.

2.2.4 Seepage velocity

Given the following parameter values: porosity 0.32, K = 8 ft/d (geometric mean), dh/dl = 0.005, the seepage velocity in the upper surficial aquifer is 46 ft/yr (clean to silty sand). The lower surficial aquifer is comprised of darker material. Given the following parameter values: porosity 0.32, K = 2 ft/d, dh/dl = 0.006, the seepage velocity is 14 ft/yr (silty sand). Wells in the deep aquifer (17-27 ft bgs) penetrate farther into the dark, silty clay and organic-rich aquifer materials and given the estimated porosity of 0.32, K (1 ft/d), and dh/dl (0.004), the seepage velocity is estimated to be 4.6 ft/yr.

2.2.5 Conceptual site model (CSM)

The data and information provided by the USGS and TtNUS investigations (1) identified the areal and vertical extent of the southern ground water plume, (2) provided important hydrogeologic parameters, and (3) development of probable fate and transport processes. Collectively, this information served as the basis for a CSM upon which to base additional detailed site characterization activities used in the ISCO design.

3. Methods and Materials

3.1 Site characterization of source area targeted for ISCO

Additional site characterization was needed to augment previous work, to improve the resolution of areal and vertical extent of the CVOC contamination. The driver for additional data was (1) to establish a high resolution baseline CVOC concentrations to compare with post-oxidation data, which is required to assess treatment performance, and (2) to identify high priority specific contamination zones (*i.e.*, locations and vertical intervals) for oxidant delivery. It is equally important to identify zones of contamination, where oxidant delivery is critical, as it is to identify non-targeted zones, where oxidant delivery is not needed. Through this approach, the oxidant can be delivered to the high priority, highly contaminated zones of the aquifer.

CVOC analyses of ground water samples represent an integrated measure of contamination mass in the subsurface, including aqueous, sorbed, and NAPL phases. Development of generalized ground water quality isocontour maps is useful in the delineation of source area(s), assessment of CVOC fate and transport, and in evaluating treatment performance. Additionally, analysis of CVOCs in aquifer core samples can be used to identify discrete zones of vertical and areal contamination. Through a critical analysis of ground water and aquifer core CVOC analytical results, an accurate, high resolution CSM can be developed. The CSM can be used to develop an oxidant injection strategy and design for the targeted delivery of the oxidant into high priority contamination intervals.

3.1.1 Aquifer cores

Multiple rounds of aquifer core collection, sampling, and analysis took place over the course of this study. As CVOC concentration data sets were assimilated, data gaps were identified and frozen cores (-15 °C) were sampled (*i.e.*, subcores collected, extracted, and analyzed) at different locations along the core. Also, additional cores were collected at different locations and intervals. Throughout this process, the EPA-RSKERC continued to address data gaps and to refine the CSM.

Initially, aquifer cores were collected along six transects (T1-T6), spaced approximately 33 ft apart along the longitudinal axis of the projected ground water plume (Figure 4). Cores were collected at three locations (A, B, and C) along each transect. Core location "B" was collected along the longitudinal axis of the ground water plume. Core locations "A" and "C" were located 20 ft laterally from core location "B". Two cores were collected, 4 ft in length, at each location which extended from approximately 8-16 ft below ground surface (bgs), (*i.e.*, 8-12 ft bgs, 12-16 ft bgs). Aquifer cores were collected in transparent acetate sleeves, allowing a visual inspection of the core. The cores were frozen on-site, by placing the cores on dry ice, and transported to the EPA-RSKERC where they were stored (-15 °C) until analyzed. A cement/bentonite mixture (4% bentonite, by weight) was pressure injected, bottom-up, into each abandoned core location to seal the exploratory boring preventing it from becoming a potential preferential pathway.

The frozen aquifer cores were partially thawed and subsamples were collected and analyzed for CVOCs, metals, and total organic carbon (TOC). Sub-cores analyzed for CVOCs were collected at specific intervals, extracted with methanol (MeOH), and the MeOH extracts were analyzed via gas chromatography/mass spectroscopy (GC/MS). The soil cores were visually examined for general lithology (sand, silt, clay), stratigraphy (layering, lenses, geochemistry), and permeability. The hydraulic conductivity of subsamples collected from the cores was measured in a lab permeameter (ASTM method D2434).

An additional transect (T0) (Figure 4) of aquifer cores, and several additional source area core locations were collected near the southeast corner of Bldg. 192, sampled, and analyzed. Through this effort, numerous sub-core samples provided valuable CVOC concentration data and information, leading to the development of an accurate CSM regarding the CVOC distribution in the source area. This information was used to design oxidant injection locations and intervals.

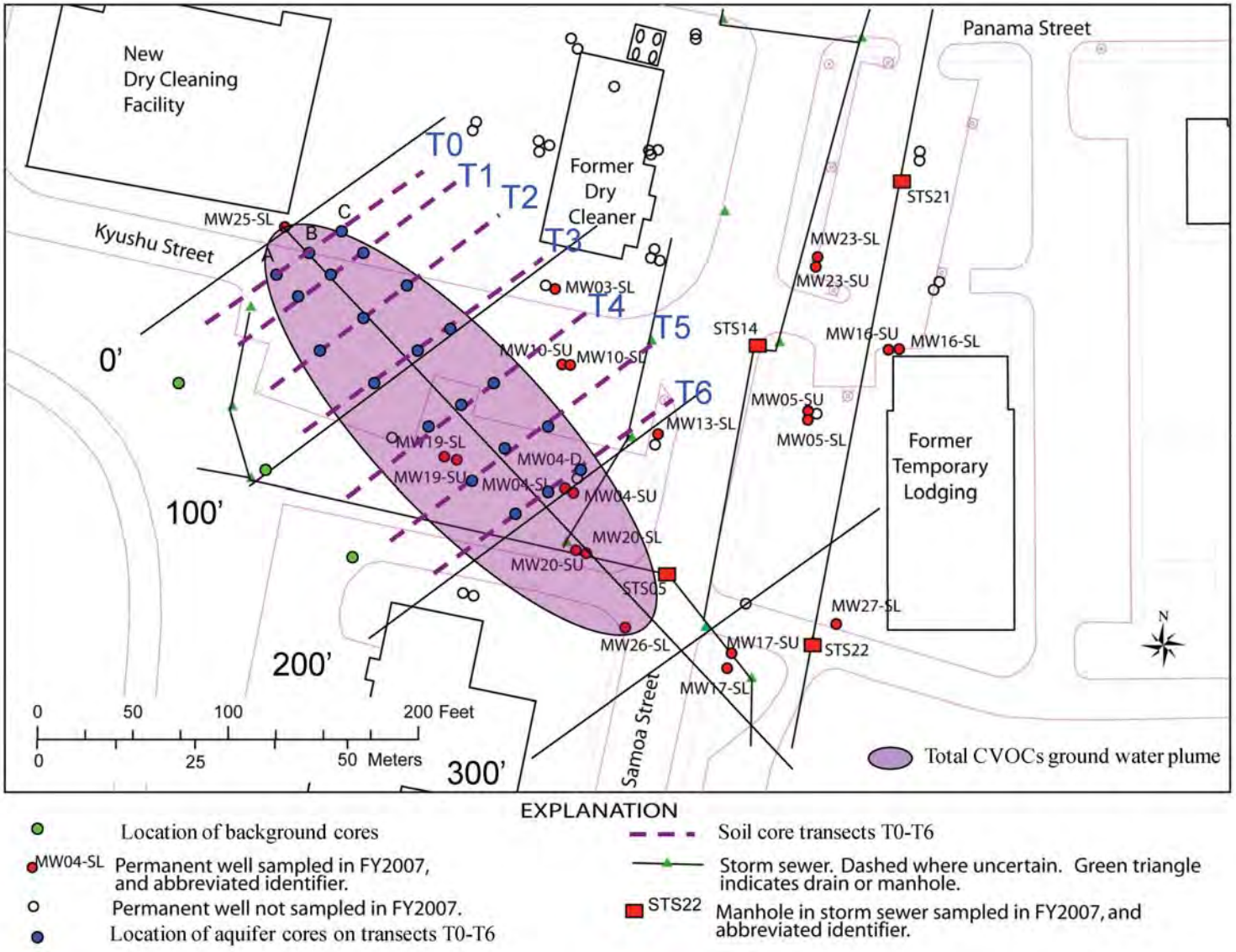

Figure 4. Conceptual model of the CVOCs ground water plume and aquifer core transect locations. Transects T0 – T6, centered on the approximate longitudinal axis of the CVOCs ground water plume, involve 3 aquifer locations (A, B, C) extending from left to right (see transect T0). The ordinate of the longitudinal transect is MW 25-SL located at the southeast corner of the new dry cleaning facility. Transects are located approximately 16.5 ft (T0), 33 ft (T1), 66 ft (T2), 99 ft (T3), 132 ft (T4), 165 ft (T5), and 198 ft (T6) downgradient from MW 25-SL.

3.1.2 Ground water monitoring micro-wells

Four transects of ground water monitoring micro-well clusters were installed to assess fate and transport of the contaminants and injected oxidant (Figure 5). The micro-wells were installed at two depths, shallow and deep. Transect M1 includes 5 monitoring clusters, and transects M2-M4 includes 3 monitoring clusters. This results in 14 monitoring locations along four transects, and 28 monitoring points total. Four sets of sentry micro-wells were also installed to assess the fate and transport of MnO_4^- and CVOCs on the periphery of the study area. Micro-wells were constructed with PTFE tubing, and 21 inch stainless steel GeoProbe screens; they were clustered at depths approximately 7-10 ft and 10.25-12.25 ft bgs. A 1¼ inch GeoProbe rod was driven to depth, and an assembly consisting of ¼ inch stainless steel screen, 21 inch in length, was attached to 5/16 inch (I.D.) PTFE tubing and inserted into the rod to the bottom. The rod was then removed and the surficial aquifer material collapsed around the screen and PTFE tubing. The upper 3-4 ft of the hole was sealed with a cement/bentonite mixture to the ground surface. The micro-wells were covered by a traffic-rated vault box set in concrete, and set for 4 months before they were sampled. Well development procedures involved the removal of 10-20 pore volumes of the micro-well tubing and screen using a peristaltic pump. The turbid purge water produced during development, and the purge water produced during each ground water sampling event, was collected and stored in the investigation derived waste (IDW) storage drum at the site 45, and transferred to the Horse Island Hazardous Waste Processing facility.

3.1.3 Direct-push Injection well

A temporary direct-push injection well (Inj.-1, Deep) was installed in the source area, approximately 7 ft to the northwest of MW-25. The objective of the well was to more aggressively deliver oxidant into the source area underlying the suspected leaking sanitary sewer line, now decommissioned. The hole was pre-punched (≈ 3 in) over the length of the solid pipe and the well was installed using direct-push. Inj.-1, Deep was constructed vertically with a screened interval over 11.5-15 ft bgs (2.5 inch outside diameter (OD), 1.99 inch ID, stainless steel, 0.010 inch slot size, wire wrapped). Natural collapse of the aquifer material above the screen (≈ 1 ft) was followed by a cement-bentonite grout to within 2 ft from the surface. A traffic-rated, flush-mounted vault cover was installed. Prior to pre-punching, aquifer cores were collected from 5-15 ft bgs. These cores were frozen on-site, transported back to the GWERD facility, and stored at -15 ^{o}C. Partially frozen sub-cores were collected, extracted with MeOH, and analyzed for CVOCs, as described in section 3.1.1. Upon completion of the well, and prior to oxidant injection, ground water samples were collected and analyzed for CVOCs.

Originally, it was proposed to construct the injection well at an angle to direct the oxidant under the corner of the building. However, it was discovered that a thick concrete layer extended 5 ft from the building in the general vicinity of the SE corner of Bldg. 192. The exact thickness could not be determined but “mat-slab” foundations are common at the MCRD and involve a wide-based footing-foundation. Specifically, the foundation extended approximately 5 ft from the exterior wall of Bldg. 192. Consequently, the injection well could not be constructed at an angle and was constructed vertically.

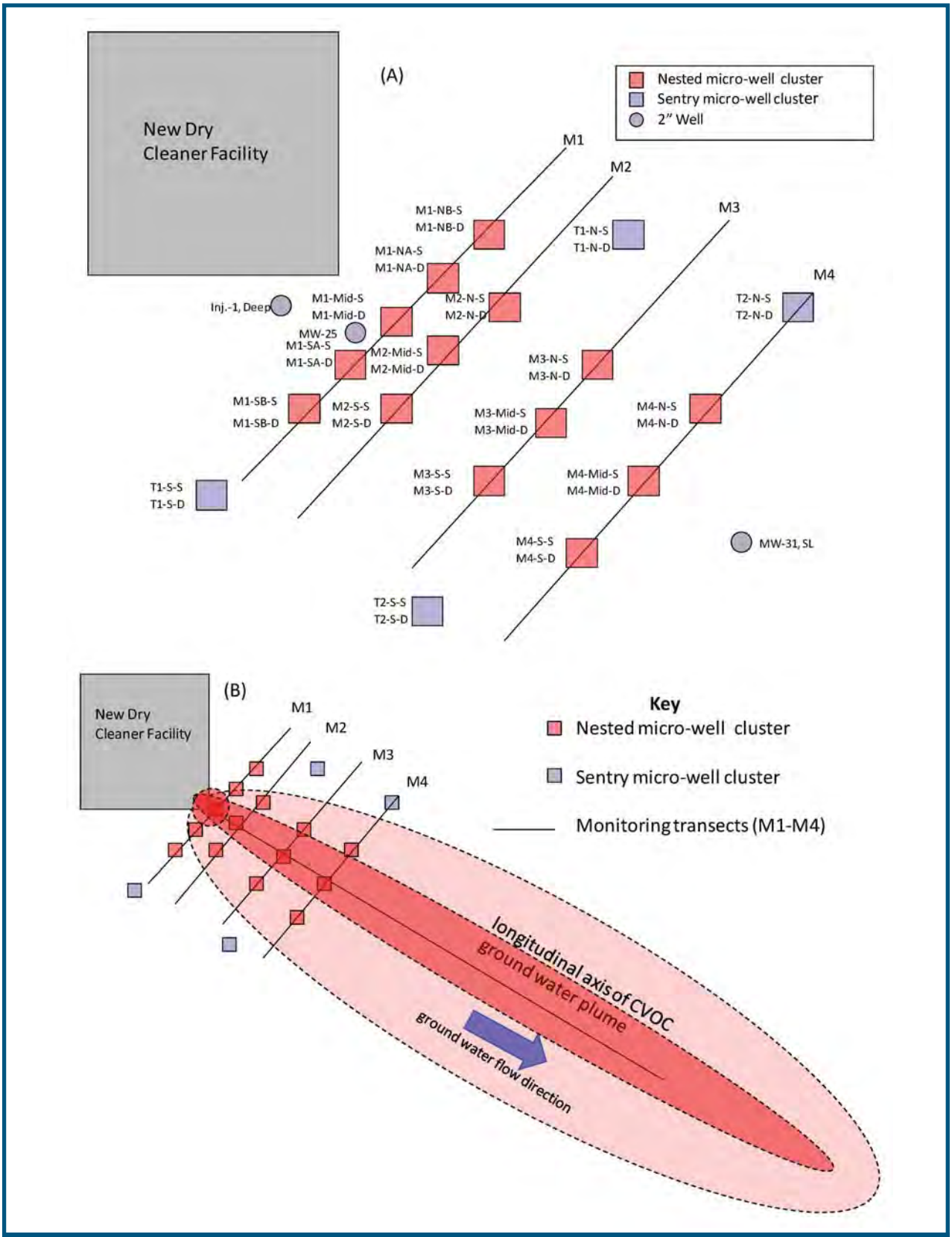

Figure 5. U.S. MCRD (Parris Island, South Carolina) Site 45 (A) well and micro-well numbers and locations; (B) plan-view schematic.

3.1.4 Natural oxidant demand (NOD)

The permanganate injected into the subsurface will react with a range of species in the aquifer material, including natural organic matter (NOM), reduced inorganic species, and the organic chemicals that are the intended target of the oxidant (Mumford *et al.*, 2005; Huling and Pivetz, 2006; Urynowicz, 2008; Urynowicz *et al.*, 2008). In some cases, excessive NOD may preclude the feasibility of ISCO due to cost and to projections involving limited reaction with the target compounds. Therefore, the NOD is often measured as a preliminary screening tool to assess the general feasibility of ISCO. A standardized 48-hour test method was used (ASTM, 2007) to measure the NOD. In general, the ASTM test method involves the use of a complete-mix test reactor allowing full contact between oxidant and reactants. Due to these physical differences between lab and field conditions, NOD results generally represent higher NOD values than might be encountered in the field.

The NOD was measured using aquifer core material in the central portion of the plume, at location T2-B. Approximately 35 g of wet soil was collected at depths of 5, 7, 9, 11, and 13 ft bgs and was amended with a $NaMnO_4$ solution (5 g/L $NaMnO_4$). The test reactors were shaken periodically throughout the day and the $NaMnO_4$ was replenished in the test reactors when the solution was pink or clear over a 48 hour period. The $NaMnO_4$ was replenished one time in test reactors containing soil from 5, 7, 9, and 11 ft bgs, and four times in the reactor containing soil from 13 ft bgs. At the end of the testing period, the NOD was estimated to be < 2.7 g/kg in the 5-11 ft bgs interval, and approximately 5.0 g/kg in the 13 ft bgs interval. Given that TOC concentrations are generally proportional to NOD, these results are consistent with the TOC data which exhibited increasing TOC concentrations with depth (refer to Section 4.1.2 *Total Organic Carbon*).

3.2 ISCO approach, design, and critical analysis

3.2.1 Oxidant selection

Sodium permanganate was selected as the oxidant to use in this ISCO project for several important reasons. As described in section 1.1.2 above, fast reaction rates occur between the permanganate anion (MnO_4^-) and the chlorinated ethenes found at site 45. Half-lives have been estimated to be less than an hour for TCE, c-DCE, t-DCE, 1,1-DCE, and 4.5 hours for PCE (20 °C). Since the average ground water temperature is > 20 °C at site 45 during the summer months, faster reaction rates and shorter half-lives are expected for these CVOCs. Furthermore, no catalyst is required, $NaMnO_4$ is highly soluble, long-term persistence of $NaMnO_4$ will result in good contact with the target contaminants near NAPL interfaces and in low permeability conditions, preliminary results indicated that the natural oxidant demand was low, and oxidant delivery was not projected to be limited due to reported values of hydraulic conductivity.

3.2.2 ISCO Approach

There were three objectives of the first injection event: (1) assure that the newly designed injection equipment could be operated in a manner that protected the health and safety of the field crew and the general public, (2) assess the fate and transport of the oxidant, and (3) assess the impact of ISCO activities on the CVOC concentrations and mass flux.

Previously, an unknown number of subsurface exploratory borings had been performed at site 45 by several organizations and it was unclear to what extent the abandoned borehole locations had been properly grouted and sealed. Potentially, old unsealed exploratory borings could significantly contribute to "daylighting", where the oxidant migrates upward along the former borehole location and seeps out at the ground surface. Numerous subsurface utilities are known to occur in the source area, including an 8-inch high pressure water main, high voltage power line, communication lines, sanitary sewer, and a stormwater sewer. Although the proposed oxidant injection intervals were below these buried utilities, it was unclear whether the injected oxidant could migrate though preferential pathways, enter into utility line trenches, and short-circuit the intended targeted zones. The overhead high pressure steam lines also represented a hazard when raising and lowering the mast height of the direct-push rig (GeoProbe 6610DT). Subsurface structures from former buildings were probable, as per discussion with long-term MCRD employees, and as observed via GeoProbe rejection in areas known to be utility-free. Given these details and complexities in site conditions, the primary objective was to ensure the health and safety of the field crew and the general public. Regarding oxidant fate and transport, the objective was to confirm that the oxidant could be successfully delivered to the targeted zone as designed, to assess oxidant persistence, and determine whether hydraulic control could be achieved. Essentially, it was critical to ensure that the oxidant did not seep into the sanitary or storm sewers, or seep into non-targeted areas. Consequently, the first oxidant injection event involved a small-scale, low volume oxidant loading approach designed to limit potential risk, to gather oxidant fate and transport information, and to assess the impact on the CVOCs. Assuming it could be confirmed as a result of the first oxidation event that the oxidant was injected safely, and was successfully delivered to the targeted zone(s), subsequent aggressive remediation involving greater oxidant loading was planned.

This approach integrated well with the overall treatment approach involving multiple oxidant injections. Consequently, in order to assess the impact of ISCO activities on the CVOC concentrations and mass flux, multiple monitoring events were used to quantify treatment performance, to understand the fate and transport of CVOCs, and to guide subsequent injections. Therefore, ground water sampling of all monitoring wells was performed prior to and following each oxidant injection event.

3.2.3 Injection strategy

The soil core analytical results, presented in section 4.1 below, indicated that the main source of CVOC contamination was near the sanitary sewer line southeast of Building 192, at a depth of 8-14 ft bgs, and 8-12 ft bgs for the downgradient portion of the plume. Therefore, the targeted oxidant injection intervals occurred over these zones. The CVOC data from the discrete, non-composited soil cores was used to identify specific CVOC contamination intervals. This soil core data and information was critical to the continued development of a conceptual site model, documenting and refining the CVOC source areas, and to guide the design of the first oxidant injection event. Post-oxidation ground water monitoring of CVOC concentrations was also used to assess treatment performance and to guide subsequent injections. Persistent CVOC concentrations, measured as a result of post-oxidation ground water sampling, are indicative of high contaminant mass, insufficient delivery and persistence of oxidant, and/or slow oxidant or CVOC mass transfer and mass transport. Three sequential oxidant injection events targeting these zones was needed to address CVOC persistence. Additionally, pre- and post-oxidation ground water monitoring was performed to help assess and improve treatment performance.

3.2.4 Oxidant delivery methods – direct-push and injection wells

The most commonly used methods for oxidant delivery are through direct-push injection probes and conventional ground water injection wells (Krembs, 2008). Direct-push injection provides wide flexibility, both in terms of injection location and vertical interval (Huling and Pivetz, 2006). During field deployment, significant flexibility is needed in oxidant delivery to avoid the site utilities, to evaluate the ability of the subsurface system in accepting the oxidant solution, and to acquire new site characterization data and information generated during ongoing field activities. In shallow, unconsolidated porous media, direct-push injection can be fast and cheap, and multiple injection locations are possible. However, there is direct-push depth limitation of approximately 100 ft bgs, which may prevent the use of this technology in deeper contamination zones. Also, it may not be possible in some geologic environments where rocks, cobbles, or boulders prevent the injection probe from advancing into the subsurface (Huling and Pivetz, 2006). But these limitations do not apply at site 45. Due to the limited contact area between the injection tip and aquifer material, and the shallow injection depths, low injection rates were projected.

Injection wells are designed and constructed for the effective delivery of oxidant into the subsurface. The continuous slotted well screen and coarse sand pack associated with the conventional injection well facilitate the flow of liquid from the screen, providing excellent contact between the well and aquifer material, and a high area of contact between the injected fluids and the aquifer (Payne *et al*., 2008). Specifically, the large contact area between the sand pack and the native materials allows the oxidant to more easily penetrate into the adjacent aquifer materials at appreciable oxidant injection rates. Often, these injection wells are constructed with long-screened intervals of 10-15 ft (Simpkin *et al.*, 2012) relative to direct-push intervals of 2-5 ft. Longer screened intervals (>15 ft) are not uncommon, however, long well screens are generally discouraged for conventional injection wells due to the risk of preferential flow of the oxidant into zones exhibiting greater permeability. The use of packers may help isolate sections of a long screen and therefore deliver oxidant over partial sections of the screened interval. Oxidant transport along the sand pack, and around the packer, may limit the ability to deliver oxidant to specific zones, however (Payne, 2008). A bentonite seal constructed above the sand pack is designed to prevent vertical transport of the injectate along the disturbed aquifer materials adjacent to the well. The final design for the injection well screen length must be appropriate for site-specific conditions.

Overall, greater rates of oxidant injection and oxidant injection volumes can be delivered into injection wells than into direct-push injection tips. This is mainly attributed to the high level of contact area between the screen interval and the aquifer materials. Disadvantages of conventional injection wells include (1) higher capital costs for the construction of the injection wells, (2) oxidant injection being restricted to the same injection location, (3) oxidant injection is restricted to the same injection interval, unless packers can be successfully deployed, (4) long-screened intervals in heterogeneous aquifer materials being vulnerable to disproportionate oxidant delivery into high-permeability zones, (5) large radii of influences often leading to heterogeneous spatial oxidant delivery and distribution, as a result of heterogeneity and anisotropy.

For this ISCO demonstration, direct-push was selected as the main method of oxidant delivery at site 45 due to spatial flexibility, lower initial capital cost, and the disadvantages of injection wells, presented above. Utilizing the existing site infrastructure, an existing

monitoring well was used to augment oxidant injection, discussed in section 3.2.5 below. Additionally, a newly constructed, temporary direct-push injection well was used to assist in the delivery of a heavy oxidant dosage into the source area. This well was a conventional well but was advanced into the subsurface using direct-push, and is therefore a hybrid of each. Overlapping, narrow ROIs (2-5 ft) and short injection intervals (2 ft) were used to assure oxidant delivery to the targeted zones. The equipment used for oxidant injection using the direct-push, the conventional injection well, and the temporary, direct-push injection well was mobilized for each injection event.

3.2.5 Monitoring well as an oxidant injection well

Utilizing existing infrastructure at hazardous waste sites is an important component of remedial design and can lead to minimizing remedial cost and improving remedial efficiency and effectiveness. Construction details of ground water monitoring wells are different than the construction details of injection wells (Driscoll, 1986; Payne, 2008). However, monitoring wells are often constructed in ideal source area locations, indicating their unique potential to deliver oxidants into the heart of the source area. Despite differences in construction details between monitoring and injection wells, monitoring wells are capable of delivering large quantities of oxidant into the subsurface. Assuming monitoring wells are constructed in appropriate locations and screened over appropriate intervals, they may successfully serve this application. The dual purpose role of a monitoring well serving as an injection well is becoming more common and accepted given the scientific rationale for their use, the compressed remediation schedules, and the potential for time and cost savings.

At the PI MCRD ISCO site, monitoring well MW-25 was located in the source area near the southwest corner of Building 192 and was screened over the targeted contaminated interval of 10-15 ft bgs. MW-25, the most contaminated well at the site, represented a convenient opportunity to inject oxidant into a highly contaminated, utility-congested source area. Given the numerous potential impediments causing direct-push refusal, and the associated hazards of direct-push in this zone, the use of MW-25 as an injection well (1) reduced the need and risk of additional oxidant delivery subsurface borings in an already congested utility zone, and (2) permitted convenient delivery of a high oxidant loading into the heart of the source area. MW-25 was incorporated into the injection plan and was successfully used in all three oxidant injection events, and in post-oxidation monitoring events.

3.2.6 Top-down versus bottom-up injection methods

Two oxidant injection approaches used with direct-push oxidant injection technology include, (1) the top-down and (2) the bottom-up. The top-down approach involves advancing the injection tip to the first depth interval, delivering the oxidant, driving to the next depth, and delivering the oxidant, etc. This sequence of events continues until the final targeted depth is reached. Subsequently, the direct-push rod and injection tip string is removed and the hole is sealed with an appropriate mixture of bentonite and cement. The bottom-up approach starts at the lowest injection depth where oxidant injection is initiated. The drill string is moved upward to a shallower injection interval, and oxidant injection continues. This sequence of events continues until the shallowest targeted depth is achieved. A potential disadvantage of the bottom-up oxidant injection approach is that there is hydraulic short circuiting of the oxidant around the injection tip into the underlying collapsed, or open hole. The underlying collapsed, or open borehole serves as

a proximal preferential pathway. Short circuiting in this manner would occur in a downward direction since there is only a short (2-4 inch) segment of the injection tip separating the open hole below from the injection interval at the injection tip. Pressurized oxidant injection may potentially erode and collapse the porous media near the injection tip. Consequently, erosion of the porous media adjacent to the injection tip would allow short circuiting of oxidant between the injection interval and the open/collapsed hole below. Anecdotal evidence of this condition has been observed, where the rate and volume of oxidant delivered during the bottom-up method is greater than when using the top-down injection method. During the top-down injection method, soil erosion due to injected fluids does not occur at the top end of the injection string, or in the upward direction since the direct-push hole is tightly sealed by the direct-push assembly. Therefore, the top-down injection configuration results in less risk of oxidant short circuiting and greater certainty that the oxidant is delivered at the targeted interval. The top-down injection method was used at the PI MCRD ISCO site.

3.2.7 Outside-in oxidant injection

ISCO application over the entire plume footprint, including the source area and downgradient plume, is generally infeasible given the scope of such activities and the associated cost. Rather, ISCO is most commonly used as a partial plume remediation technology, where injection locations are designed to target the source area in an effort to achieve maximum contaminant oxidation and mass reduction, and to reduce contaminant concentrations at a downgradient compliance plane. A critical analysis of partial plume remediation indicated that partial DNAPL removal from the source zone is likely to lead to large reductions in plume concentrations and mass, and a reduction in the longevity of the plume. Furthermore, when the mass discharge from the source zone is linearly related to the DNAPL mass, it is shown that partial DNAPL depletion leads to linearly proportional reductions in the plume mass and concentrations (Falta *et al.*, 2005a; 2005b). Therefore, a common strategy is partial source treatment to a level allowing subsequent passive management or natural attenuation (Stroo *et al*., 2014).

The outside-in oxidant injection strategy is used in source area applications to minimize the lateral displacement of contaminated ground water. When more than two adjacent injection locations are designed, the outside-in approach targets injection locations on the periphery of the targeted zone, then moves inward. Through this process, oxidant injection in the central portion of the plume would still displace ground water, but would likely contain the oxidant solution and lower concentrations of contaminants, thus minimizing contaminant dispersal. This strategy also helps to limit the development of stagnation zones and hydraulic interference between injection locations.

3.2.8 Injection pressure and overlying hydrostatic pressure

In saturated porous media, the overlying hydrostatic and overburden pressure plays an important role in counterbalancing the oxidant injection pressure at the injection tip and screened interval of the injection well. During oxidant injection into shallow aquifers, this is especially important due to the lack of hydrostatic and overburden pressure. In a simple homogeneous aqueous system, approximately 2.3 ft of water is required to counterbalance 1 lb/in^2 of injection pressure. In porous media, the weight of porous media plays a role as overburden pressure. The density and weight of dry and wet aquifer material above the injection point, relative to the weight of water, can be used to estimate the maximum injection pressure prior to failure or breakout of the injected

liquid (Appendix A. *Oxidant Injection Pressure Calculations – Role of Hydrostatic and Overburden Pressure*). These calculations represent ideal conditions, and do not take into consideration existing discontinuities in porous media, either naturally occurring or man-made. Discontinuities represent weaknesses in the fabric of the lithology and may cause breakout at low injection pressures.

3.2.9 Direct-push disruption of aquifer lithology

The horizontal hydraulic conductivity (K_X) is typically greater than the vertical hydraulic conductivity (K_Z); this is attributed to the orientation of clay minerals in unconsolidated aquifer materials (Freeze and Cherry, 1979). The vertical hydraulic conductivity of many aquifers is approximately 10 % of the horizontal hydraulic conductivity (Payne *et al.*, 2008). GeoProbe pneumatic hammering of the direct-push rod assembly used at the PI MCRD site 45 resulted in the disturbance of the unconsolidated, saturated porous media adjacent to the injection string (*i.e.*, GeoProbe rod and injection tip). Under this condition, it was projected that the lithologic integrity of the porous media, and the associated hydraulic properties, were altered in a way that permitted preferential pathways along the direct-push string assembly. Consequently, during injection activities at the PI MCRD ISCO site, a settling period of 15-30 minutes was permitted after the drill string was advanced to the targeted injection interval. It was projected that the settling period would allow the porous media to re-settle, to partially re-establish the lithologic properties, and to limit the preferential pathway along the direct-push assembly. Although re-settling and repositioning of the aquifer particles in this manner unlikely achieved pre-disturbed aquifer material density values, empirical observations indicated that oxidant daylighting was limited when the settling period preceded injection, relative to immediate pressurization and injection.

3.2.10 Field-scale ISCO deployment

The oxidant injection strategy included (1) the injection of progressively greater quantities of the oxidant into the source areas with each successive oxidant injection event, and (2) the complete oxidant coverage of the source area. The source area was defined as zones within the aquifer that contained the greatest CVOC mass. The two main source areas included the PCE release area from the sanitary sewer near the southeast corner of Building 192, and along the longitudinal axis of the plume. Three oxidant injection events took place, where 970 lbs, 2450 lbs, and 5070 lbs of 40% $NaMnO_4$ were injected during the 1st, 2nd, and 3rd oxidant injection events, respectively.

The first round of $NaMnO_4$ oxidant injection in the ISCO pilot study was carried out in June, 2013. Seventeen (17) 5-gallon pails of 40% remediation grade (Rem-Ox) $NaMnO_4$ (57 lbs 40% $NaMnO_4$/pail; 970 lbs 40% $NaMnO_4$) (Carus Chemical, Peru, IL) was injected into the subsurface using direct-push injection and using the existing monitoring well MW-25 as an injection well (Figure 6). The second oxidant injection event (September, 2013) was more aggressive than the first as greater quantities of oxidant were injected over a larger area (Figure 6). During the second injection event, 43, 5-gallon pails of 40% $NaMnO_4$ (57 lbs 40% $NaMnO_4$/pail; 2451 lbs 40% $NaMnO_4$) were delivered using direct-push injection, the existing monitoring well, MW-25, and a newly constructed direct-push injection well, Inj.-1, Deep. The third injection event (March, 2014) involved the injection of 89, 5-gallon pails of 40% $NaMnO_4$ (57 lbs 40% $NaMnO_4$/pail; 5073 lbs 40% $NaMnO_4$) using direct-push, MW-25, and Inj.-1, Deep.

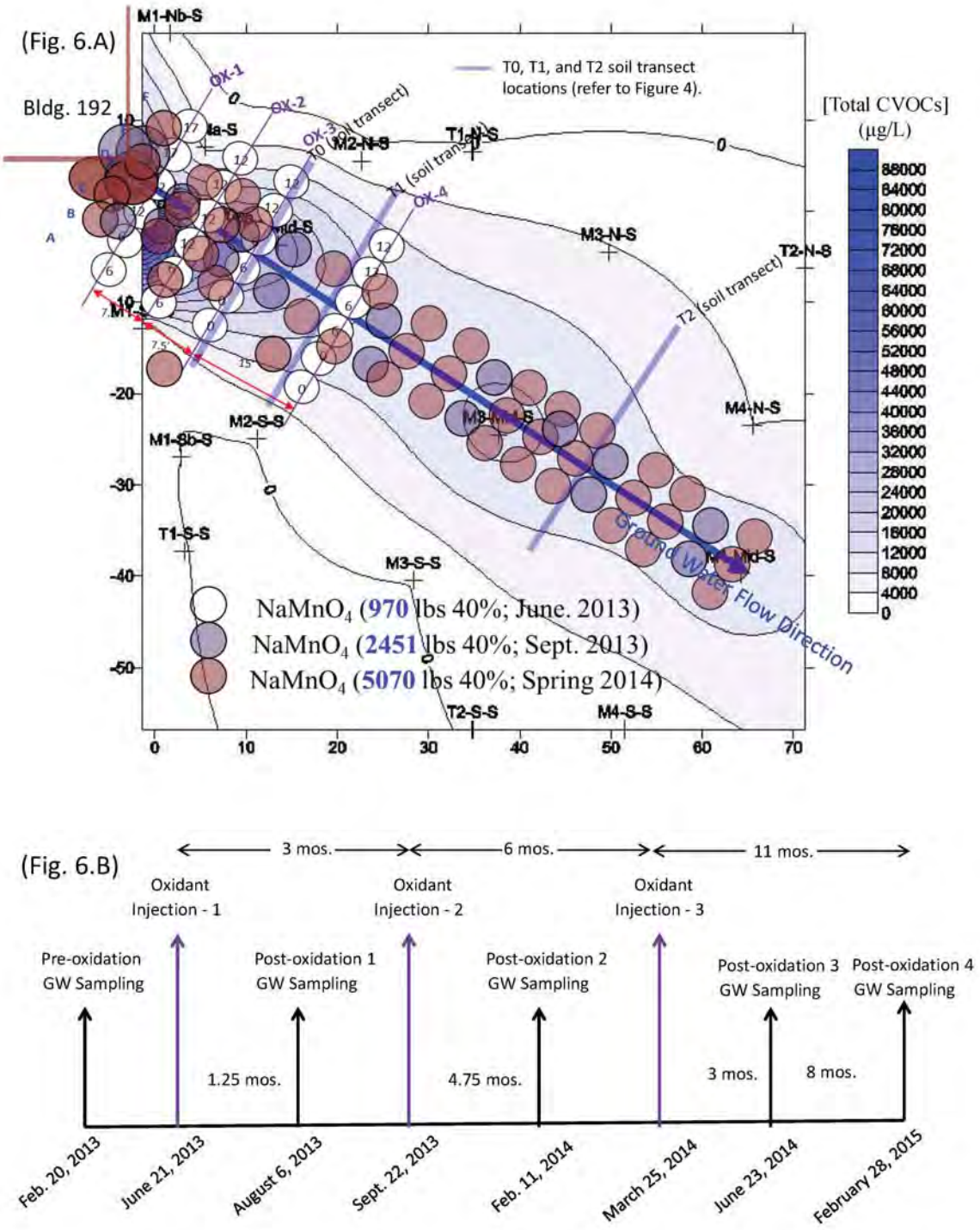

Figure 6. (A) Oxidant injection locations for injection 1 (June, 2013), injection 2 (September, 2013), and injection 3 (March, 2014). Oxidant injection transects (OX-1 through OX-4) were used in the first injection, radial distribution of MnO_4 represented by small white circles, ground water flow direction, and nomenclature for injection locations (A-F). The ordinate of the axis system (*i.e.*, (0, 0) is well MW-25 which is used as an injection well. The large circles near Bldg. 192 represent oxidant injected into wells in the source area (MW-25; Inj.-1, Deep), and the small purple circles represent oxidant from direct push injection. T1, T2, and T3 represent soil core sampling transects depicted in Figure 4. (B) Pre- and post-oxidation ground water sampling and oxidant injection timeline.

The oxidant was injected using an outside-in approach, where the oxidant was injected on the perimeter and progressively moved towards the center of the plume. In the case where two adjacent injection points were used, as in injection event 2, the outside-in approach was not used. The oxidant was injected starting at the lower concentration end of the plume and moved towards the higher concentration source area. The area surrounding these wells and the first two transects was considered the high-strength source area, likely containing PCE-DNAPL; the mass of oxidant used here accounted for approximately 30% of the total oxidant mass injected. During each injection event, several injection locations were not amenable to injection due to proximity to utilities, rejection of the direct-push string, or daylighting. Minor adjustments to the injection locations, depths, and volumes were made in the field to account for these contingencies. The subsurface utilities were marked prior to each injection and a 2 ft buffer distance on either side of the utility was maintained. The accurate marking of utilities by Palmetto Utility Protection Service, Inc. (PUPS) (Columbia, SC) and by the MCRD was critical to ensure that utilities were avoided during oxidant injection and soil coring activities.

3.2.11 Natural oxidant demand (NOD) and oxidant loading

NOD tests are performed to satisfy different objectives, including (1) as a screening tool to assess the general feasibility of ISCO, and (2) as a design parameter in the oxidant loading design. Oxidant loading, or dosage, involves the oxidant mass delivered (*i.e.*, oxidant volume × concentration) per mass of aquifer material in the targeted zone, or the mass of oxidant per mass of aquifer material (g $NaMnO_4$/kg aquifer material). One approach used in the design of oxidant loading involves measuring the NOD of the aquifer material in laboratory tests, applying different adjustment factors to the laboratory-determined NOD value, and estimating the oxidant dosage for field delivery. These adjustment factors are applied by ISCO practitioners and are generally based on previous experience, site-specific contaminant and hydrogeologic parameters, and possibly other factors. The final oxidant loading involves the delivery of a "proportional" quantity of the NOD into the subsurface.

In this study, the NOD tests were conducted and the results were used as a preliminary screening tool to determine whether the NOD was within a reasonable range of oxidant demand values and to assess the general feasibility of the technology. The NOD results were also used as a general check in the oxidant loading. The average oxidant demand was approximately 2.7 g/kg (n=4) and 5.0 g/kg (n=2) in the shallower aquifer material (5-11 ft bgs) and deeper aquifer material (13 ft bgs), respectively. Rough correlations between soil TOC and NOD have previously been established with some success (Honning *et al.*, 2007; Xu and Thompson, 2009). Given the increase in TOC with depth at site 45 (Section 4.1.2 below), the increase in NOD is consistent with previous correlations reported in the literature. In one study, where the 48 hour NOD test was performed using 274 samples from 46 sites, a histogram indicated that a NOD of ≤ 5 g/kg was measured in approximately 70% of the samples measured, and ≥ 5 g/kg at the remaining sites (Petri *et al.*, 2011, and references therein). These results suggested that the average value of the NOD in the shallow aquifer was lower than the range of values measured at 70% of the 46 sites tested.

The oxidant loading was based on delivering $NaMnO_4$ into the two source areas defined from the pre-oxidation soil and ground water monitoring data and information. Specifically, this included the area adjacent to the southeast corner of Bldg. 192, where PCE was reported to have leaked from the broken sewer pipe and where the source of the

CVOC ground water plume originates, and along the longitudinal axis of the CVOC plume. The incremental volume of oxidant solution to be injected at each location was based on a radial flow, cylindrical, total porosity porous media conceptual model (Eqn. 1).

$$V_{OXIDANT} = \Pi\ ROI^2\ \eta\ h \qquad \text{(Eqn. 1)}$$

Where,

$V_{OXIDANT}$ = volume of oxidant (gal)

ROI = radius of influence (ft)

η = total porosity

h = vertical injection interval (ft)

The first oxidant injection event involved a small-scale, low volume oxidant loading approach designed (1) to limit potential risk, (2) to gather oxidant fate and transport information, and (3) to assess the impact on the CVOC concentration in the ground water. A small range in $NaMnO_4$ concentration (18.9-19.6 g/L) was delivered using direct-push injection during all three oxidation events. Assuming a range in soil bulk density (100-120 lbs/ft^3) in the targeted zone, the radial-flow, total porosity, and a cylindrical, porous media conceptual model) the oxidant loading (*i.e.*, oxidant volume × concentration) delivered to the idealized pore volume, was projected to be
3-4 g $NaMnO_4$/kg aquifer solids.

Based on the average NOD values measured in the 5-11 ft bgs interval (*i.e.*, 2.7 g $NaMnO_4$/kg aquifer material), the oxidant loading was projected to exceed the laboratory-measured NOD. The persistence of unreacted oxidant residual in ground water would be vulnerable to transport through advection and diffusion beyond the immediate targeted zone. Thus, it was projected that the injected oxidant would cover a larger aquifer volume than the radial flow, cylindrical, total porosity porous media conceptual model. Given the projected moderate costs in oxidant and labor required to deliver 3-4 g $NaMnO_4$/kg aquifer solids, a decision was made by the Parris Island Partnering Team to move forward with pilot-scale deployment of ISCO and to further evaluate the feasibility of ISCO as a final remedy.

3.3 Ground water sampling and analysis

Additional site characterization data and information was initiated to augment the previous work by the USGS and to refine the conceptual site model. Specifically, the CVOC distribution in the source area and along the longitudinal axis of the plume, where the majority of CVOCs were surmised to occur was quantified.

3.3.1 Ground water

A comprehensive pre-oxidation baseline ground water sampling event was performed prior to injection of the oxidant. Ground water samples were collected from 39 micro-wells, MW-25, Inj.-1, Deep, and MW-31SL (Figure 5). Post-oxidation ground water sampling was performed, involving the same set of micro-wells and other wells, to assess oxidant fate and transport, treatment performance, and to guide subsequent injections. The samples were analyzed for an array of parameters using either standard EPA methods, or procedures developed and approved for use at the R.S. Kerr Environmental Research Center and referred to as R.S. Kerr standard operating procedures (RSKSOP) (Table 3) (please refer to section 3.7 for information on the analytical methods). Laboratory-based analyses were performed at RSKERC as well as contract laboratories. Field analysis was performed by the EPA field crew.

Molecular biological tools (MBT) and compound-specific isotope analyses (CSIA) were performed by the contractors at Microbial Insights and Microseeps, Inc., respectively. Prior to ground water sample collection, a YSI multi-parameter probe with a flow through cell was used to collect field parameters, including pH, dissolved oxygen (DO), oxidation reduction potential (ORP), temperature, specific conductivity, and turbidity. Ground water samples were collected when field parameters stabilized (<10% variability).

During ground water sampling, some ground water samples contained visible concentrations of permanganate, in binary mixture samples, as per the pink-purple color. Previous studies indicate that without appropriate preservation, the quality of the ground water sample may be compromised, and false negative results may occur. Therefore, the guidelines, methods, and procedures presented in Ko *et al*. (2012) were used in this study to preserve binary mixture ground water samples.

Table 3. Ground water parameters and methods used in analysis of samples.

Parameters	Method
pH, turbidity, temperature, ORP, DO	YSI Multi-parameter system with flow-through cell
CVOCs (PCE, TCE, cis-1,2-DCE, trans-1,2-DCE, 1,1-DCE, VC)	EPA Method 8260B/C GC/MS
Metals	EPA Method 6010C (ICP-AES); EPA Method 200.7
Dissolved methane gas	[1]RSKSOP-194/175,Rev. 5
Ferrous and total iron	EPA Method 3500-Fe D
Chloride and sulfate	EPA Method 6500 (refer to RSKSOP-276, Rev. 4 below)
Compound specific isotope analysis (CSIA)	[2] analyses performed by Microseeps, Inc. 220 William Pitt Way, Pittsburgh, PA 15238
Molecular biology tools (MBT)	[2] analyses performed by Microbial Insights, 2340 Stock Creek Blvd., Rockford TN 37853

[1] There is no existing EPA method for dissolved methane gas. Please refer to Kampbell and Vandegrift, 1998 in the reference section.

[2] CSIA and MBT were measured in six wells in the source area (M1-mid-shallow and -deep, M1-NA-shallow and -deep, and M1-SA-shallow and -deep).

EPA Method 8260B - Volatile organic compounds by purge and trap GC/MS.

EPA Method 6010C (EPA SW-846) and EPA Method 200.7 - Inductively coupled argon plasma with atomic emission spectrometry.

RSKSOP-194, Rev. 4 - Gas Analysis by Micro Gas Chromatograph.

RSKSOP-175, Rev. 5 - Sample Preparation and Calculations for Dissolved Gas Analysis in Water Samples Using a GC Headspace Equilibration Technique.

EPA Method 3500-Fe D - Phenanthroline method.

RSKSOP-276, Rev. 4 - Determination of Major Anions in Aqueous Samples Using Capillary Ion Electrophoresis with Indirect UV Detection and Empower 2 Software.

3.3.2 Contaminant mass flux

Contaminant mass flux is a quantitative parameter describing the contaminant mass transported through a prescribed plane over time (Eqn. 2). Contrasting mass flux estimates before and after ISCO deployment is a useful metric to critically assess changes in contaminant mass transport across the site, and ISCO performance. The calculation is based on Darcy's Law, where the ground water velocity, total CVOCs concentration, and aquifer cross-sectional area are used to estimate mass flux. Site-specific parameters used in these calculations are provided in Table 4. Given the clusters of micro-wells in the shallow and deep zones (Figure 5), four mass flux transects across the CVOC plume were established as zones MF-1 through MF-4 (Figure 7). The ground water velocity associated with transect MF-1 was corrected to include directional differences between the ground water flow direction and the coordinate system at the MF-1 transect (*i.e.*, the y-direction ground water flow component does not go through MF-1; the x-direction is perpendicular, $V_x = V_D \cos 33.6^o$, $V_x = 0.833\ V_D$). The distances between monitoring locations in transects MF-2 through MF-4 were calculated based on the relative differences between the ground water flow direction and the coordinate system (*i.e.*, $\cos 33.6^o = V_D/V_Y$, $V_Y = 1.2\ V_D$). Micro-well location M3-N-S did not function correctly during ground water sampling and a reliable ground water sample was unobtainable. The concentration of CVOCs from T1-N-S was used as a substitute for M3-N-S in mass flux calculations for MF-3.

$$\text{Contaminant Mass Flux (CMF)} = V_S \times [\text{CVOC}] \times \text{Area} \qquad \text{(Eqn. 2)}$$

Where,

$V_S = V_D/\eta = K \times (dH/dL)/\eta$

V_S = Seepage velocity (ft/day)

[CVOC] = Total CVOC concentration (µg/L)

A = cross sectional area (depth × width)

V_D = Darcy velocity (ft/d)

η = porosity

K = hydraulic conductivity (ft/d)

dH/dL = hydraulic gradient (ft/ft)

3.3.3 Impact on natural attenuation

As reported above in section 2.2.1 (USGS Site Characterization), an abundance of site specific indicator parameters strongly suggest that natural attenuation processes are playing a significant role in the attenuation of CVOCs at the site. The surficial aquifer is anaerobic at most locations with the predominant terminal electron accepting process being iron reduction in the shallowest sediments, and sulfate or iron reduction in the deeper sediment, including methanogenesis (Vroblesky *et al.*, 2009). Molecular biology tools and contaminant specific isotope analysis were utilized to assess the impact of ISCO on microbial populations and natural attenuation processes.

Table 4. Parameters used in the contaminant mass flux calculations.

Aquifer Zone	Hyd. Conc. (K)[1]	Hyd. Grad. (dH/dL) (ft/ft)[1]	Cross sectional area (A) (ft^2)[2]	Porosity η[1]
Shallow (7-10)	4.30E-03	0.006	171 (MF-1)	0.3
			153 (MF-2)	0.3
			168 (MF-3)	0.3
			183 (MF-4)	0.3
Deep (10-12.25)	1.00E-03	0.004	114 (MF-1)	0.3
			102 (MF-2)	0.3
			112 (MF-3)	0.3
			122 (MF-4)	0.3

[1] Hydraulic properties used in these calculations were based on previous investigations (Vroblesky *et al.*, 2009).

[2] Width of mass flux transect: MF-1 (57'); MF-2 (51'); MF-3 (56'); MF-4 (61') (Figure 7).

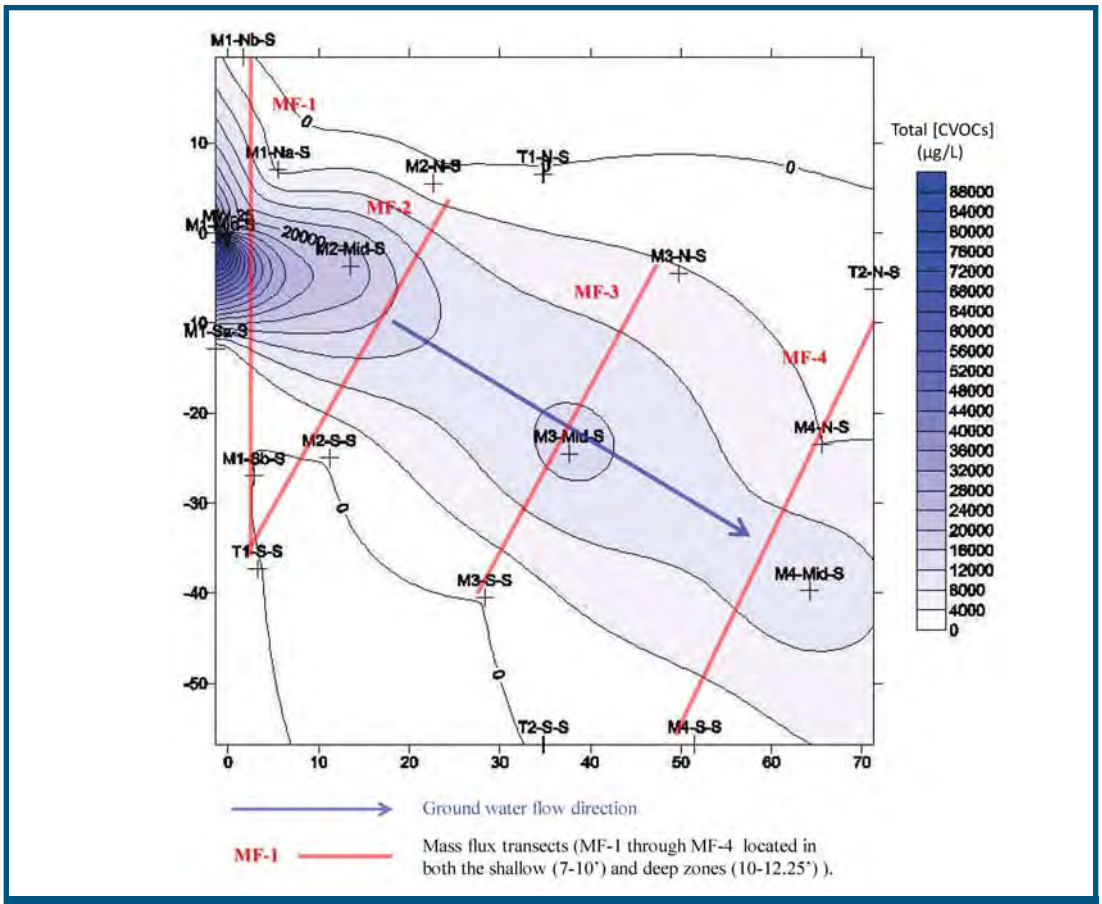

Figure 7. Pre-oxidation baseline contaminant mass flux transects (MF-1 through MF-4) used in the shallow and deep zones of the aquifer in the ISCO study area. Due to clustering of shallow and deep micro-wells at the field site, a similar set of transects was used for both the shallow and deep zones of the aquifer.

3.4 Health and safety plan and permits

3.4.1 Health and safety plan

A project-specific and site-specific health and safety plan (HASP) was prepared in 2008, prior to field activities carried out at Site 45. The HASP was prepared in accordance with the requirements of the EPA - Robert S. Kerr Environmental Research Center (EPA-RSKERC). It was reviewed and approved by the RSKERC Safety, Health and Environmental Management Program Manager and was provided to the Parris Island Partnering Team (PIPT) as part of the in-situ chemical oxidation pilot study work plan. The PIPT provided comments to the draft HASP based on their individual site-specific knowledge. A Material Safety Data Sheet (MSDS) was provided by the manufacturer (Carus Corp., Peru, IL) of the sodium permanganate and included as an attachment to the HASP. A presentation "*The Safe Use and Handling of Permanganate Products*", prepared by Carus Corp. was included as an attachment to the HASP. The HASP was updated as needed prior to each new stage of the study. In 2013, the HASP was revised, updated, and re-formatted to meet new HASP guidelines adopted by the US EPA National Risk Management and Research Laboratory (NRMRL). Each member of the field crew reviewed the HASP prior to beginning field work, and daily safety meetings were held to discuss current site conditions.

The HASP included detailed information on a range of important topics: project description, field activities, laboratory activities, physical hazards summary, personal protective equipment (PPE) summary, equipment requirements, chemicals to be used, waste management, sample management, spill response, authorized personnel, staff concurrence, job hazard analysis, controls, and PPE, emergency telephone numbers and hospital information, a generic emergency response plan, emergency recognition and prevention, electrical safety, physical hazards, personnel roles, lines of authority, and communication procedures during an emergency, procedures for emergency medical treatment and first aid, and emergency contacts. The job hazard analysis covered all the tasks for each stage of the field and laboratory work.

3.4.2 Injection permit

The injection of permanganate during the field study required the issuance of an underground injection control (UIC) permit by the South Carolina Department of Health and Environmental Control (SC DHEC), Ground-Water Protection Division. The application was submitted by MCRD environmental staff to SC DHEC on behalf of the RSKERC ISCO team. Once the UIC permit application was approved by SC DHEC, a construction permit to install the direct-push rods was issued by SC DHEC and the permanganate injections were subsequently fully permitted to commence.

3.4.3 Well permit

The installation of monitoring wells, including micro-wells and direct-push temporary well, at Site 45 required the approval of SC DHEC, Bureau of Water. Information on the location, type, and construction details of the wells to be installed was provided to the SC DHEC for technical review and approval. Once SC DHEC staff members were satisfied with the proposed well installation, approval for construction was given by the SC DHEC. Following the monitoring well installation, SC DHEC required the submission of SC DHEC Form 1903, Water Well Record.

3.4.4 Dig permit

Submission and approval of a Ground Penetrating Activity Permit Request, or the "dig permit", was required by MCRD for all activities that disturbed the subsurface. A dig permit form was prepared and distributed to all relevant MCRD departments (*i.e.*, those with a stake in subsurface activities). Each stage of investigation involving soil coring, well installation, and oxidant injection activities required that a dig permit be prepared and approved prior to commencement of field activities.

3.5 Oxidant handling

The 40% sodium permanganate oxidant (permanganate) delivered to the site was a hazardous chemical; it is a strong oxidizing agent and can react violently with oxidizable materials and was handled in accordance with the proper safety requirements. Before permanganate oxidant injections began, MCRD placed a metal hazardous materials storage unit at the site for secure storage of the 40% liquid sodium permanganate. Upon delivery of the 40% sodium permanganate, by Carus Corp., the 5-gallon buckets of 40% sodium permanganate were placed in the storage unit. The storage unit was placarded with "oxidizing material" signs and was locked. Individual 40% sodium permanganate 5-gallon pails were removed one at a time from the storage unit, as they were needed, and moved a short distance to the 350-gallon injection tank. The appropriate personal protective equipment (PPE), including a face shield, plastic gloves, and a rubber apron over a Tyvek suit, was used during the transport and transfer of the 40% sodium permanganate. The oxidant was transferred from the 5-gallon pail to the mixing tank, where it was mixed with water to create the dilute (~1%) injection solution. The 40% sodium permanganate solution was metered into the mixing tank via a peristaltic pump to avoid potential contact and exposure. The much lower oxidant solution concentration (~1%) was less hazardous and appropriate PPE consisted of Tyvek suits, vinyl gloves, and eye protection.

Potential release and exposure to the 1% solution was mitigated through the presence of shut-off valves, pressure relief valves with return lines to the mixing tank, pressure gauges, secondary containment, and high pressure-rated and corrosion-resistant hoses in the injection manifold and distribution lines. A dilute ascorbic acid solution was kept in pressurized spray bottles near each of the permanganate handling locations for neutralization of minor spills and leaks of the diluted oxidant solution.

3.6 Design and operation of injection system/equipment

The selection of direct-push as the main method of oxidant delivery in the pilot study (see section 3.2.4 above, *Oxidant delivery methods – direct-push and injection wells*) required that an oxidant injection system be designed, constructed, and operated as a part of the pilot-scale study project. Preliminary calculations indicated that the three proposed oxidant injection events, if contracted with an ISCO vendor, would significantly exceed the research budget. Therefore, the design criteria for the injection system included low cost, and ease of mobility, so that it could be transported back and forth between the EPA, GWERD facility (Ada, OK) and the MCRD site 45 (Parris Island, SC). The injection system was designed and constructed by the GWERD staff at the GWERD facility and the details of the injection system, including a schematic and description of injection pallet components, component manufacturers, part numbers, cost, and relevant description details are included in Appendix B.

The cost of the injection system for injection arm (*i.e.*, header) was $16,000. Three arms were designed and constructed in the system, allowing the oxidant to be injected at three locations simultaneously. All parts were constructed with corrosion-resistant components allowing the system to be used with strong oxidants, or other corrosives. These include reductants, acids, solvents, or surfactants, if needed. Each injection arm, or header, was equipped with a flow dampener, pressure release valve and return line, pressure control valve, pressure gauge, flowmeter/totalizer, emergency cutoff ball valve, and a 45-60 ft long, high pressure injection hose. The injection hose was designed to fit inside the GeoProbe rod as a separate unit and attached directly to the injection tip. The rationale of this design was to maintain hydraulic control of the oxidant. Alternatively, oxidant can be injected down through the GeoProbe rod but there is a greater potential for leaks to develop, risk personnel exposure.

The oxidant injection occurred at low pressures, resulting in low to average injection rates (0.5-1.5 gpm) per location. However, at three injection locations, the overall injection rate was tripled (1.5-4.5 gpm). This was due to (1) the shallow injection intervals and limited overburden pressure, and (2) to the subsurface utilities and the potential for other preferential pathways, such as improperly sealed exploratory borings. Only low injection pressures (<10-15 psi) were used throughout the demonstration. The use of high oxidant injection pressure can lead to hydraulic short circuiting and breakout of the injected oxidant into preferential pathways. Consequently, an unintentional and disproportionately high volume of oxidant may be transported into non-targeted zones.

The on-site monitoring well, MW-25, and the direct-push injection well (Inj.-1, Deep) are 2-inch wells constructed with screened intervals approximately 10-15 feet bgs. Oxidant injection into these wells was accomplished with above-ground, 55-gallon HDPE drums, using a peristaltic pump with Phar-Med tubing (¾ inch) and PTFE pipe (Figure 8). All components in contact with the oxidant were corrosion resistant. The fittings between the injection hose and the 2-inch wells involved PTFE couples, ¾ inch nipples, and hose clamps. Slow oxidant injection rates (0.5-1.0 gpm) were used to limit mounding of oxidant and ground water and to reduce the potential for discharge into nearby storm and sanitary sewers.

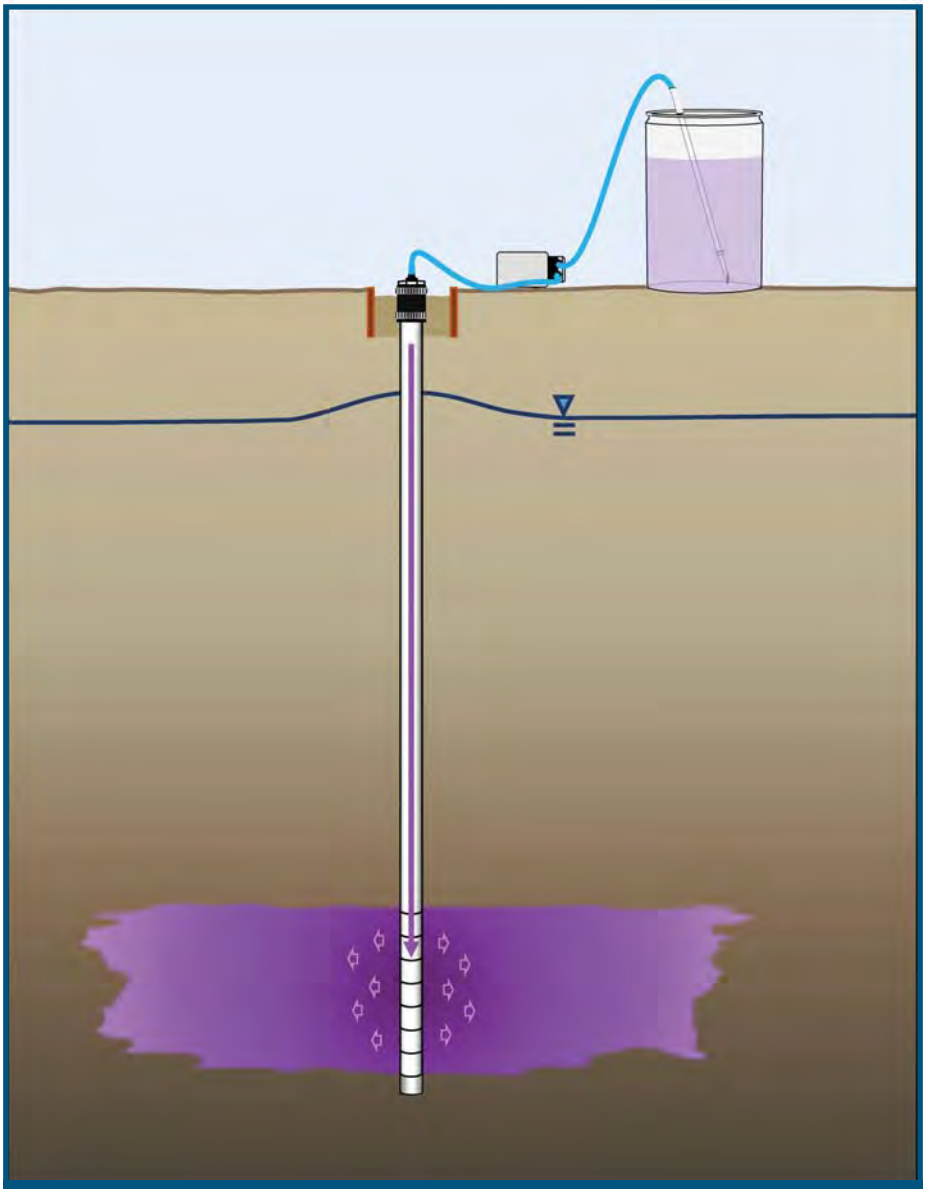

Figure 8. Schematic of injection apparatus used in the delivery of oxidant into injection wells MW-25 and Inj.-1, Deep.

3.7 Analytical and Quality Assurance/Quality Control

Upon collection, ground water samples collected for CVOC analysis were preserved with HCl. Aquifer subcores were collected from aquifer cores, placed in 40 mL vials, and amended with Methanol (MeOH) (15 mL). The MeOH-soil slurry was shaken intermittently and allowed sufficient contact time for CVOC extraction (>48 hr). The MeOH extracts of the soil cores were analyzed for CVOCs at the EPA GWERD, using EPA Method 8260C with headspace sample introduction using EPA Method 5021A as implemented in GWERD analytical method RSKSOP-299/2 "Determination of Volatile Organic Compounds (Fuel Oxygenates, Aromatic and Chlorinated Hydrocarbons) In Water Using Automated Headspace GC/MS." All quality control (QC) results met criteria established in RSKSOP-299/2. MeOH extracts were further prepared by adding 250 µL of the methanol/water mix to a vial containing 10 mL of boiled milli-Q water and two grams of sodium chloride. CVOC analytical results were reported per dry weight of soil extracted.

Metals analysis of ground water samples was performed via inductively coupled plasma, optical emission spectrometry (ICP OES) (Perkin Elmer, Model Optima 3300 DV, Norwalk, CT), using EPA Method 200.7 as implemented in RSKSOP-213, Rev. 5 "Standard Operating Procedure for Operation of Perkin Elmer Optima 3300DV ICP". All QC results met criteria established in RSKSOP-213/5. Metals analysis of soil core samples collected at site 45 were also analyzed by RSKSOP-213/5 after the soil samples were extracted using EPA Method 3051A as implemented in GWERD method RSKSOP-180/3 "Standard Operating Procedure for Total Nitric Acid Extractable Metals from Solids and Sludges by Microwave Digestion". Here, representative soil samples were digested, using nitric acid (40 mL, 10%) in a microwave oven (40 min; 150 °C; 1000 kPa).

Loss of the on-site analytical contract at the EPA GWERD during the course of this demonstration required that analytical support be provided by an off-site laboratory. Shealy Environmental Services (Columbia, SC), accredited by the National Environmental Laboratory Accreditation Program, was contracted and carried out similar GC/MS and ICP OES analytical methods. They analyzed ground water and MeOH extracts using equivalent methods of analysis (EPA method 8260B; EPA Method 6010C, (water only)) and QA/QC requirements.

Chloride (Cl^-) and sulfate (SO_4^{2-}) in ground water samples were analyzed using EPA Method 6500 as implemented in GWERD method RSKSOP-276/4, "Determination of Major Anions in Aqueous Samples Using Capillary Ion Electrophoresis with Indirect UV Detection and Empower 2 Software". All quality control results met the criteria established in RSKSOP-276, Rev. 4. Ferrous iron (Fe^{+2}) and total Fe in ground water was measured using the EPA Phenathroline method (EPA Method 3500-Fe D). Prior to ground water sample collection, a YSI multi-parameter probe with a flow through cell was used to collect field parameters, including pH, dissolved oxygen, oxidation reduction potential, temperature, specific conductivity, and turbidity. Ground water samples were collected when field parameters stabilized.

Aquifer sub-cores collected from aquifer cores for TOC analysis were treated with hydrochloric acid to remove inorganic carbon and then analyzed by RSKSOP-120, Rev. 3 for organic carbon by combustion and subsequent detection and quantitation of carbon dioxide using a LECO CR-412 carbon analyzer with an infrared detector.

Ground water samples collected for dissolved methane analysis by RSKSOP-194/175, Rev. 5 were placed in 60 mL serum bottles, without headspace and preserved with HCl. A headspace of helium was created in the sample bottle and shaken to allow the gases to equilibrate between the aqueous and gas phases. A gas-tight syringe was used to withdraw a portion of the headspace and injected into a micro-gas chromatograph for separation of the gases and detection and quantitation by a thermal conductivity detector.

Molecular biology tools (Microbial Insights, 2017) and compound-specific isotope analysis (CSIA) (Pace Analytical, 2017) were analyzed in ground water samples collected from six micro-wells. Analyses included total eubacteria (qEBAC), Dehalococcides (qDHC), and DHC functional genes (TCEa reductase, BAV1 vinyl chloride reductase (BVC), and vinyl chloride reductase (VCR). The CSIA for carbon on PCE, TCE, c-DCE, and vinyl chloride were analyzed. These micro-wells included both the shallow and deep micro-wells at locations M1-S-A, M1-Mid, and M1-N-A. Samples for analysis by molecular biology tools (MBT) and compound-specific isotope analyses (CSIA)

were collected by the Navy and submitted to contract laboratories for analysis. Sample preservation and handling of samples analyzed using MBT (qPCR or quantitative polymerase chain reaction) and CSIA were performed by the contractors at Microbial Insights and Microseeps, Inc., respectively. The data was made available to the EPA. The quality assurance and quality control procedures established by these laboratories for these analyses were followed.

As required by US EPA QA policy, a Quality Assurance Project Plan (QAPP) was prepared and approved for this project prior to collection of data and implemented without significant deviations. A QAPP describes the technical and QA/QC activities of an environmental research project that is implemented to ensure that the results will satisfy the intended used of the data.

Field sampling quality control included the collection of duplicates (both ground water and aquifer subcores) and blanks for ground water including field, equipment, and trip blanks. Analytical quality control included positive controls (calibration checks, matrix spikes, and second source checks), negative controls (blanks), and duplicates. Data quality acceptance was initially determined by the analyst using the procedure's acceptance criteria. The Principal Investigator ultimately determined whether or not data was usable for the project. All data used in this report satisfied QA/QC requirements.

CVOCs in both the ground water and aquifer cores were considered a critical parameter needed to meet the project objectives. As mentioned earlier in this section, all QC criteria performed at the EPA GWERD were met for RSKSOP-299/2 (EPA Method 8260C). These included method blanks which should not have analyte concentrations above the Method Detection Limit (MDL), calibration checks and second source standards should be within +/-20% of their known value, matrix spikes and laboratory control spikes should have 70-130% recovery, and laboratory duplicates should have a Relative Percent Difference of ≤20%. Surrogates were also added to all samples and QC samples with a required recovery of 80-120%. The MDL and QL (Quantitation Limit) were 0.5 and 0.09 – 0.22 µg/L in the water samples, and 0.004 and 0.02 mg/kg in the aquifer core samples (assumes 25 ml total MeOH extract (MeOH + soil water) and 25 g dry soil). Note, the range in QL for water samples reflects the 6 CVOCs detected (*i.e.*, VC, 1,1-DCE, trans-1,2-DCE, cis-1,2-DCE, TCE, PCE). Sample results below the QL were considered to be estimated.

Samples analyzed for CVOCs by Shealy Environmental Services also met the QC criteria for EPA Method 8260B based on the criteria in the DOD Quality Systems Manual for Environmental Laboratories, Version 4.2. These included method blanks which should not have analytes detected above ½ the RL (Reporting Limit) and > 1/10 the amount in any sample, for calibration checks the average Response Factor for VOC SPCCs (System performance check compounds) should be ≥0.30 for chlorobenzene and ≥0.1 the remainder, second source standards should be within +/-20% of true value, matrix spike and laboratory control spikes should be trans-1,2-Dichloroethene 60-140%, cis-1,2-Dichloroethene 70-125%, 1,1-Dichloroethene 70-130%, Tetrachloroethene 45-150%, Trichloroethene 70-125%, Vinyl chloride 50-145%. Surrogates were also added to all samples and QC samples with a required recovery of 1,2-Dichloroethane-d4 70-120%, Toluene-d8 85-120%, Bromofluorobenzene 75-120%, and Dibromofluoromethane 85-115%. The MDL and QL (Quantitation Limit) for undiluted samples were 0.25 and 0.5 µg/L in the water samples, respectively. The MDL and QL in soil were 0.002-0.02 mg/kg and 0.025 mg/kg, respectively (assumes 25 ml total MeOH extract (MeOH + soil water) and 25 g dry soil). Sample results below the QL were considered to be estimated.

3.8 Data analysis

Statistical analysis involving the 95% confidence interval (*i.e.,* 95% CI = Avg. ± standard error (S.E.), where S.E. = $(t_{0.05} \times \text{std. dev.}) / (n)^{0.5}$; std. dev. = standard deviation; $t_{0.05}$ = two tail t-values at the 0.05 level of significance and n-1 degrees of freedom) in post-oxidation $[CVOCs]_{SOIL}$ involved the two-tailed , standard t-tables 0.05 level of significance.

Isocontour plots of chemical parameters were prepared for the study area using Surfer® 7.0 (Golden Software). Linear kriging was used for the gridding method, and filled contours over similar concentration ranges for specific parameter data sets were used. Post maps showing well locations were used based on an (X, Y) coordinate system where the ordinate (*i.e.*, 0, 0) was selected as well MW 25-SL.

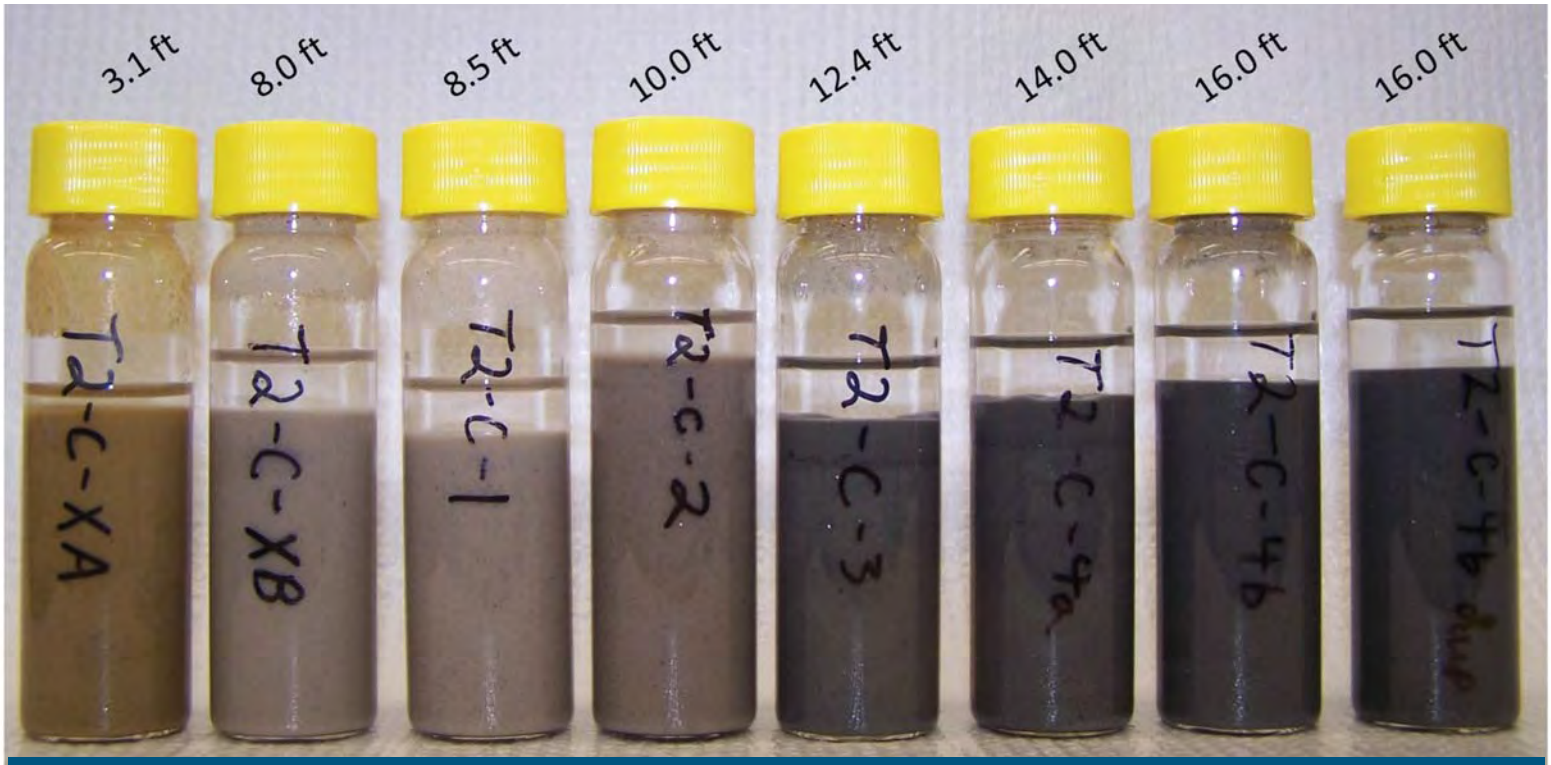

4. Results

A visual perspective of site activities is provided through numerous site photographs in Appendix C (*Photographic compendium of ISCO activities at the site 45 ISCO demonstration project (Parris Island, MCRD, SC)*). A short narrative is provided for each photo to give background information of the ISCO and ISCO-related site activities.

4.1 Soil/aquifer cores

4.1.1 Visual inspection of core material

Visual inspection of the subsamples collected from the soil and aquifer cores revealed distinct geochemical conditions and layering. The shallow, 3-10 ft bgs, aquifer material was comprised of light-colored sandy material. This depth interval was sometimes overlain by a distinct orange-colored sandy layer, indicating the presence of iron oxides resulting from exposure to air during low water table events (Figure 9). The light-colored sandy material graded into a darker sandy material with depth containing greater levels of silt, clay, and organic matter. Aquifer cores collected from 16 ft and lower were very dark and consistently exhibited pieces of decaying wood of natural origin (*i.e.*, not building or commercial debris).

Figure 9. (See above.) Photo of soil cores and depth below ground surface.

4.1.2 Total organic carbon

Total organic carbon (TOC) was analyzed in aquifer cores collected at transects T1-B, T3-B, and T5-B (8-16 ft bgs) (Figure 4) over 0.5-1.0 ft intervals. The average TOC values were lower in the 8-12 ft bgs interval than in the 12-16 ft bgs interval (see summary below). A distinct correlation between TOC and depth was not established though (Figure 10), suggesting that there is not a distinct, high organic, lithologic layer in the subsurface over this interval. Rather, a general increasing trend in TOC concentration with depth is observed. Examination of aquifer cores at 16 ft bgs indicated an abundance of organic materials, such as wood or peat, underlying the contamination zone. The darker color of aquifer material in the deeper cores was partially attributed to the organic matter, which is characteristically dark.

Transect-Location	Interval	TOC (%)	Number of samples analyzed
T1-B	8-12 ft	0.120	9
	12-16 ft	0.227	8
T3-B	8-12 ft	0.112	7
	12-16 ft	0.259	6
T5-B	8-12 ft	0.107	10
	12-16 ft	0.281	6

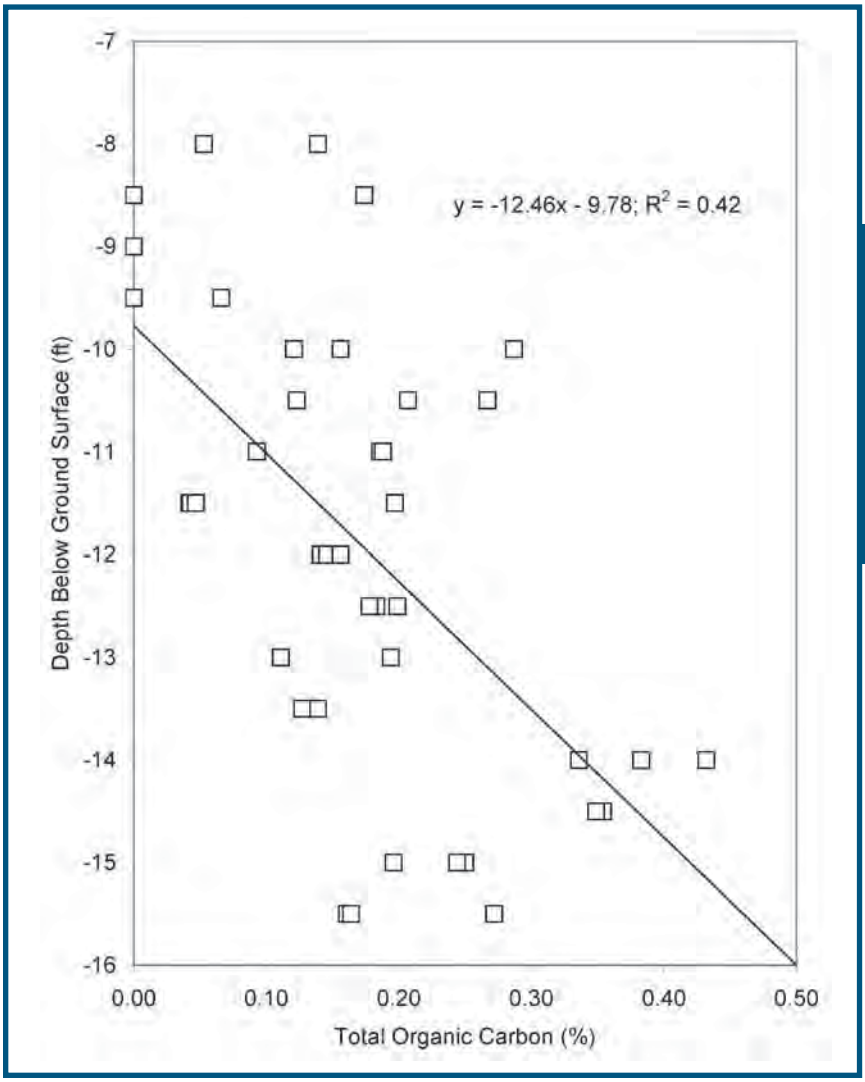

Figure 10.
TOC concentration with depth from aquifer samples collected at transect locations T1-B, T3-B, and T5-B (refer to Figure 4 for transect locations).

4.1.3 Metals and Sulfur

Sub-cores were collected from the 8-12 ft and 12-16 ft bgs cores in replicate, extracted, and analyzed for metals via ICP OES. Results of these analyses indicate that iron, manganese, and sulfur increase with depth (Figure 11). An abundance of iron and sulfur at the site suggests that naturally occurring minerals containing these elements likely serve as a source of terminal electron acceptor in reductive dehalogenation natural attenuation mechanisms. Under reduced conditions, these geochemical minerals would provide an abundance of dissolved species in the ground water. Upon oxidant injection however, it is projected that a significant increase in the oxidation potential would alter the geochemistry resulting in a decline in the solubility of these species.

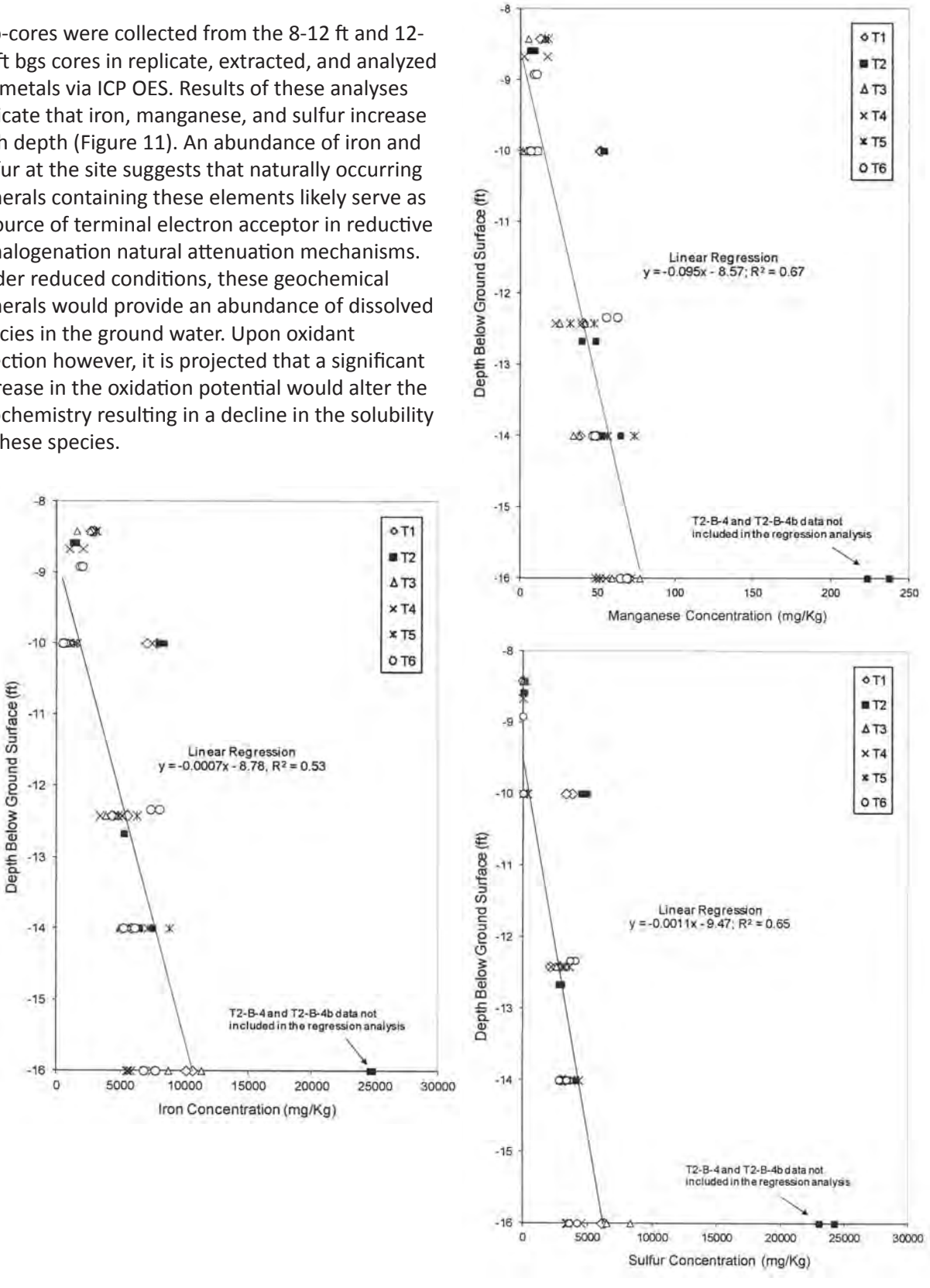

Figure 11. Concentration of iron, manganese, and sulfur in soil with depth.

4.1.4 CVOCs

Aquifer cores were collected at the locations illustrated in transects T-1 through T-6 (Figure 4; Appendix D, Figure D.1). Sub-cores were collected at a minimum of five locations for each core at the following depths: 8 ft, 10 ft, 12 ft, 14 ft, and 16 ft bgs. Sub-core aquifer samples (~25-40 g dry weight) were extracted with methanol and analyzed for CVOCs via GC/MS. These total-extract samples represent CVOCs found in both the aqueous and solid (adsorbed) phases. Based on a contaminant mass distribution analysis, it was determined that NAPLs were not present in these subsamples. Total CVOCs were mostly limited to the 8-12 ft bgs interval (Appendix D, Figures D.2-D.3).

Additional site characterization in the source area was performed approximately 20-22 ft upgradient of transect T-1, closer to the decommissioned sanitary sewer line near the south-southeast corner of Building 192 (Figure 4; Appendix D, Figure D.1). Aquifer cores were collected along a transect (T-0) located very near the corner of the dry cleaner building, and adjacent to well MW-25 (Figure 4). Cores were also collected (1) at the same location where injection well Inj.-1, Deep was installed, and (2) at other locations near the decommissioned sanitary sewer line. The total CVOCs analytical results of cores collected along transect T-0 and in the source area clearly indicated that the total CVOCs concentrations in these areas were the highest at the site, the contamination extended over a broader vertical interval extending from ≈7.5-15 ft bgs, that the contamination was predominantly distributed along the longitudinal axis, and that lateral distribution was limited (Appendix D, Figures D4-D5). Furthermore, based on a contaminant mass distribution analysis of the total CVOCs concentration data, it was concluded that PCE DNAPL was present in the aquifer core collected at the Inj.-1, Deep location (*i.e.*, PCE DNAPL was likely when PCE concentrations were greater than 225 mg/kg).

The aquifer core collection and analysis provided data and information used to refine the conceptual site model. Specifically, that contamination was predominantly constrained between 8-12 ft bgs, except in the source area where it extended over a broader interval (≈7.5-15 ft bgs). Consequently, the oxidant injection strategy was designed to focus oxidant injections into the 8-12 ft bgs contaminated interval, and that more aggressive oxidant loading was needed in the source area at the southeast corner of Bldg. 192.

Based on the general lithology performed for well PAI-45-MW-28D, loose sand existed at approximately 6-11 ft bgs (Vroblesky *et al*., 2009; Figure 17). The loose sand was underlain by silty sand that extended down to 16 ft bgs. The loose sand and silty sand were expected to have high and low hydraulic conductivity, respectively. Conceptually, the general interface area between these two zones would represent a lower boundary that limited downward contaminant migration and distribution. Given that the source of contamination was introduced above this elevation, the vertical migration would have been impeded by the silty sand layer. This conceptual model was consistent with ground water samples collected and analyzed in temporary wells collected above and below this zone (Vroblesky *et al*., 2009). Further, as discussed below, aggressive natural attenuation conditions in the lower surficial aquifer were also projected to limit the transport of CVOCs into the lower surficial aquifer. Overall, given the elevation of the TCE release from the vitrified clay pipe, the high hydraulic conductivity of aquifer material ≤ 12 ft bgs, and the aggressive natural attenuation fate mechanisms and lower hydraulic conductivity occurring ≥ 12 ft bgs, aquifer core CVOC concentrations were consistent with TCE presence, persistence, and rapid transport in the 8-12 ft bgs interval.

4.2 Oxidant delivery and impact on total CVOCs in ground water

The oxidant loading design predominantly included direct-push delivery of MnO_4^- at 15 g/L (17.9 g/L $NaMnO_4$), in 2-ft increments into the 8-10 ft bgs and 10-12 ft bgs intervals. Assuming a range in bulk density (1.61-1.93 kg/L, 100-120 lbs/ft^3), the oxidant loading calculated within the design radius of influence was 3-3.6 g $NaMnO_4$/kg, but the actual oxidant loading delivered into the subsurface ranged slightly higher (3.0-3.9 g/kg). The oxidant loading was greater than the measured oxidant demand of <2.7 g/kg (see Section 3.1.4 *Natural Oxidant Demand*), suggesting some oxidant residual persisted and was transported in the ground water over a limited time frame. During the third and final injection event, a higher oxidant concentration (30 g/L MnO_4^-) was delivered to the centerline of the CVOC contaminant plume, where high concentrations of CVOC were known to occur. Given the repeated delivery of oxidant in the high concentration CVOC source areas of the site during oxidant injection events 1-3, it is likely that the oxidant demand was satisfied and that downgradient oxidant drift occurred in some areas. In the source area located at the southeast corner of Building 192, the highest concentrations of CVOCs were measured during baseline ground water and soil monitoring events. Consequently, greater oxidant loading in the source area was achieved by injecting higher concentrations (36.5 g/L) and volume of MnO_4^- into the wells (MW-25; Inj.-1, Deep) present in the source area.

The density of the $NaMnO_4$ oxidant solution at 2% (*i.e.*, 20 g/L) is slightly greater than water and would have a mild downward transport component. It is reasonable to assume that the oxidant injected in the source zone at a higher average concentration (*i.e.*, 3.65%) also underwent vertical transport and eventually rested on or near the lower permeable materials at 15 – 16 ft bgs. Conceptually, this is ideal since it is a known hot spot area, the oxidant will naturally migrate into the low permeable media with time, and oxidant transport will be limited due to low permeability. Overall, this helps to assure oxidant delivery into the source zone, long term persistence of the oxidant, and good contact between the oxidant and contaminated media, an important requirement for successful chemical oxidation.

4.2.1 First oxidant injection event (June 23-29, 2013)

Sodium permanganate was injected at multiple direct-push locations and depths near the corner of Building 192, and into MW-25 (Figures 6, 8, 12). The injection interval was 2 ft and the injection depths reported below represent the top of the interval. Specifically, there were six injection locations along the first oxidation transect, OX-1, at four depths (6 ft, 8.5 ft, 11 ft, 13.5 ft bgs) per location. On the other three transects (OX-2, OX-3, OX-4) there were two depths (8 ft, 10 ft bgs) (Figure 12). Not all of the projected injection locations were successful or precisely located due to proximity of subsurface utilities, daylighting, and refusal of the injection tip. Refusal was attributed to competent, but unknown subsurface material possibly including a former building pier, construction debris, etc. An oxidant solution was injected (0.5 gpm) into MW-25 using a 55-gallon drum, a peristaltic pump, and a 2 in × 2 in flexible coupling pumping system (Figure 8). A total of 17, 5-gallon pails of $NaMnO_4$ (57 lbs, 40% $NaMnO_4$/pail) were injected. During the first oxidant injection event, approximately 2205 gallons ($[NaMnO_4]_{AVG}$ = 18.1 g/L) and 480 gallons ($[NaMnO_4]_{AVG}$ = 13.6 g/L) were injected using direct-push technology and the existing monitoring well MW-25, respectively. The sanitary and storm sewers in the vicinity of the injection zone were routinely inspected over the course of the oxidant injection activities. The absence of visual observation of MnO_4^- in these sanitary and storm sewers indicates that there were no releases into these conduits.

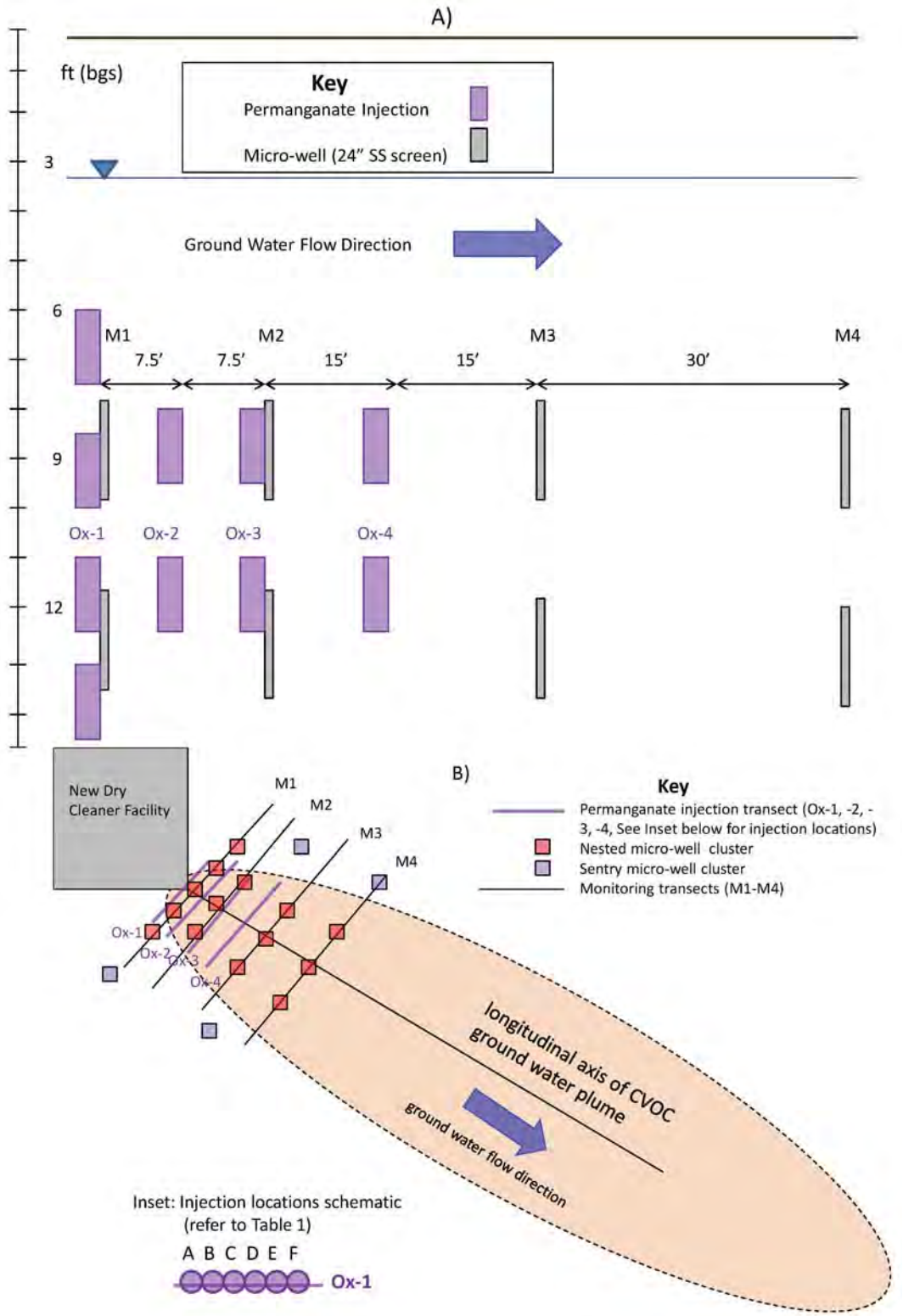

Figure 12. Conceptual model of permanganate injection in the south CVOC plume at Parris Island MCRD site 45. A) Cross section schematic of permanganate injection and micro-well screened intervals; B) Plan view schematic of ground water plume, oxidant injection, and ground water monitoring micro-well transects.

As a result of the first oxidant injection event, it was apparent that (1) a significant volume and quantity of oxidant could be injected into the contaminated interval(s), (2) the oxidant was delivered and was contained within the specific targeted zone, and (3) there was no oxidant solution leakage into the nearby sanitary or storm sewers. Wells in the southern plume were sampled on August 5-9, 2013, and indicated that $NaMnO_4$ persisted (0.05 to < 1 g/L) in several wells in the source area (MW-25, M1-mid-shallow, M2-mid-deep), indicating that the $NaMnO_4$ had not completely reacted. $NaMnO_4$ was not detected in the downgradient sets of micro-wells along the longitudinal axis of the plume (M3-mid-shallow/deep; M4-mid-shallow/deep) (Figure 5) where oxidant loading had not occurred. This result suggested that rapid transport of oxidant down the longitudinal axis of the plume did not occur.

4.2.2 Post-oxidation 1 CVOC concentrations

A schematic illustrates the base map locations of the micro-well clusters, shallow and deep, and MW-25 (Figure 13). This is the base map used in Figures 6-7, illustrating oxidant injection locations and mass flux transects, respectively. The pre-oxidation concentrations of CVOC in ground water in the shallow (7-10 ft) and deep (10-12.25 ft) zones are represented by isocontours and provide useful information regarding CVOC fate and transport trends in the ISCO study area (Figure 14a). These results confirmed the conceptual model: that the source of the CVOCs is located near the corner of the new dry cleaner building, ground water flow is from the northwest to the southeast, and that total CVOC plume is limited laterally. These results were consistent with previous investigations indicating that the source of PCE was from the old dry cleaner facility; the PCE entered the sanitary sewer system and then leaked from the sanitary sewer located at the corner of the new dry cleaner facility (Vroblesky *et al*., 2009). Faster transport, greater plume length, and more widespread distribution of the CVOCs in the shallow zone relative to the deeper zone is partially attributed to higher hydraulic conductivity and hydraulic gradient in the shallow zone, and aggressive natural attenuation processes in the deeper zones.

The areal extent of oxidant distribution during the first oxidant injection event was limited relative to the plume footprint. Because the oxidant was injected in the source area, significant CVOC destruction was achieved as observed by contrasting the pre- and post-oxidation CVOC isocontours (Figures 14a and 14b). Results of the first oxidant injection indicated that the oxidant was successfully delivered to the targeted zones, hydraulic control of the injected oxidant was achieved, and the oxidant persisted in the source zone. Furthermore, based on a comprehensive ground water monitoring program, significant CVOC destruction was evident through lower CVOC concentrations.

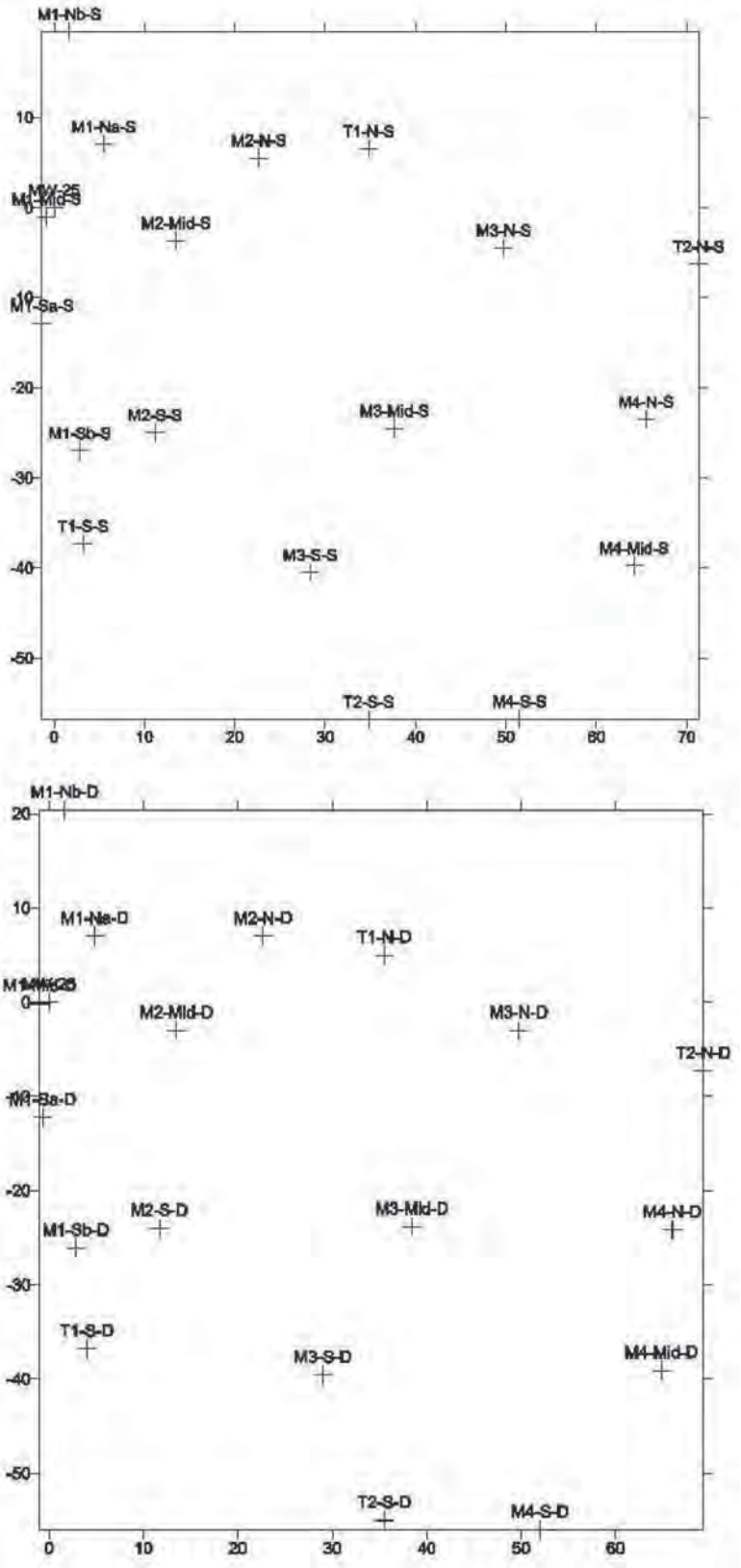

Figure 13. Shallow (7-10') (top figure) and deep (10.25-12.25') (bottom figure) well locations and names at Parris Island, SC Marine Corps Recruit Depot (MCRD) Site 45.

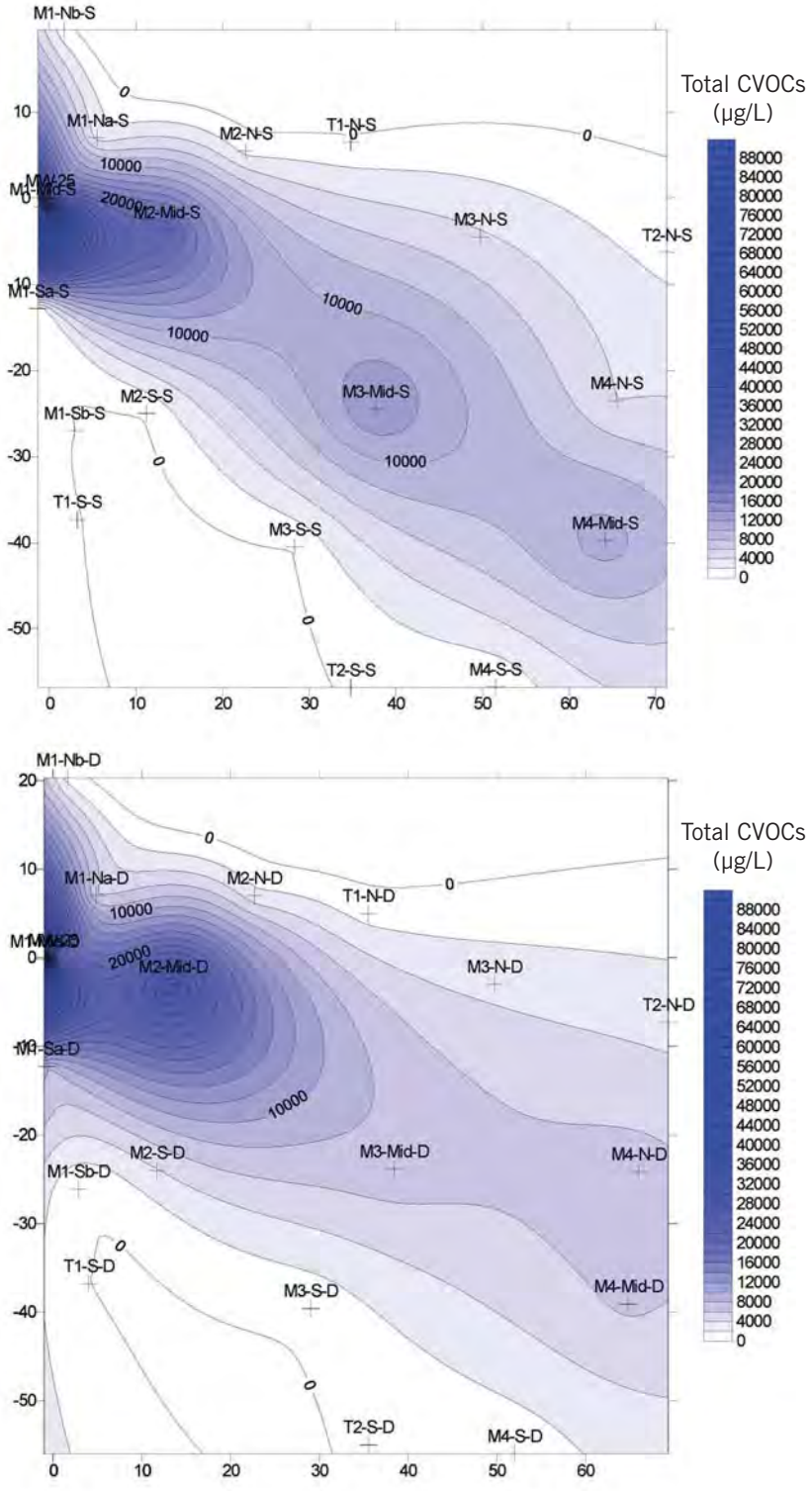

Figure 14.A. Pre-oxidation shallow (February, 2013) (7-10 ft bgs) (top figure) and deep (10-12.25 ft bgs) (bottom figure) total chlorinated volatile organic compounds (µg/L) (replicates) at Parris Island, SC MCRD Site 45.

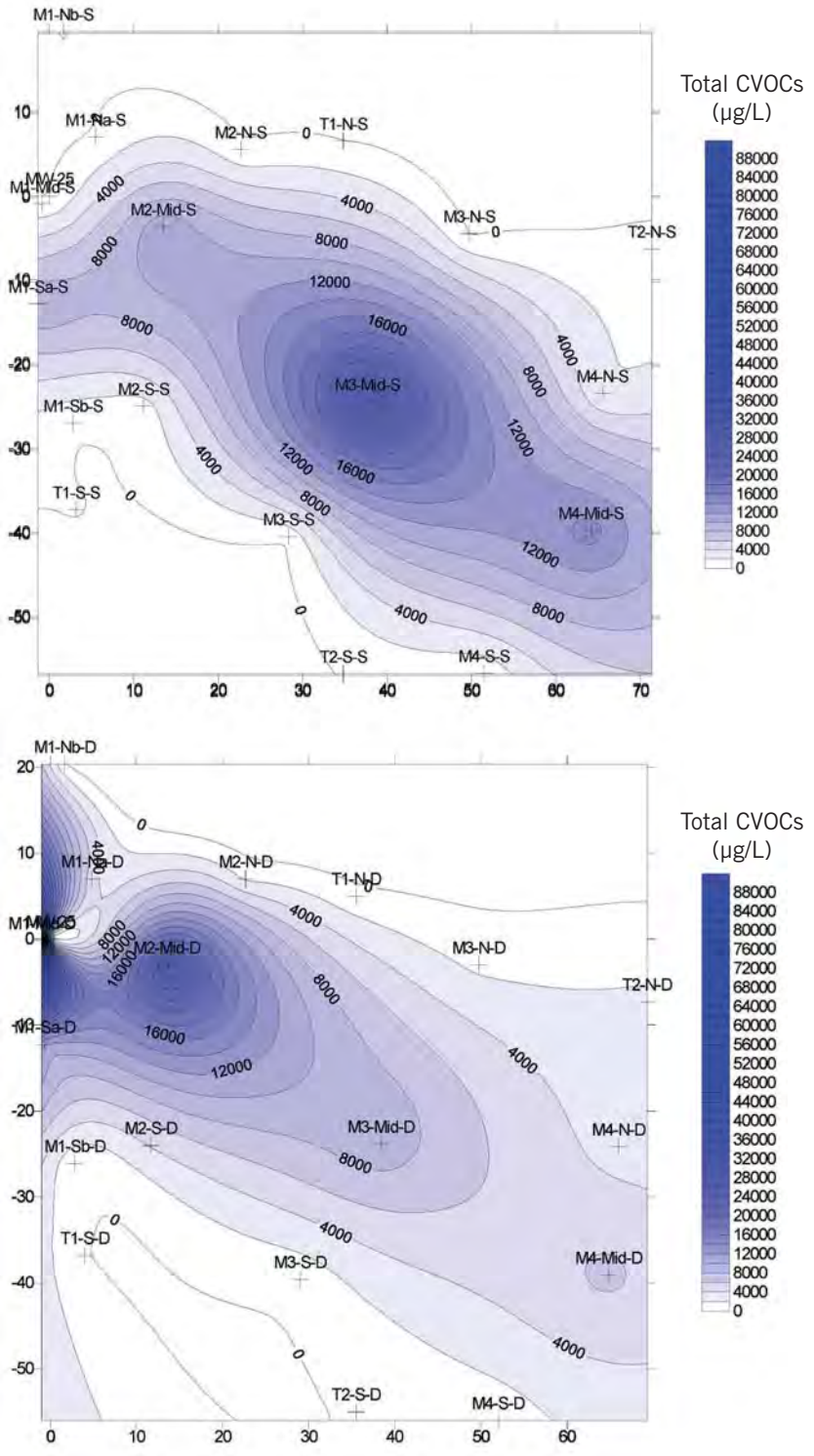

Figure 14.B. Post-oxidation 1 (August, 2013) shallow (7-10 ft bgs) (top figure) and deep (10-12.25 ft bgs) (bottom figure) total chlorinated volatile organic compounds (µg/L) at Parris Island, SC MCRD Site 45.

4.2.3 Second oxidant injection event (September 22-27, 2013)

Based on the results and conclusions from the first injection event, the strategy developed for the second oxidant injection was to more aggressively target the source area near the corner of Building 192 and along the longitudinal axis of the downgradient plume, where the majority of the CVOCs mass resided. Sodium permanganate was injected at multiple direct-push locations and depths in the source area and along the longitudinal axis of the plume (Figure 6). Additionally, a greater oxidant dosage was injected into MW-25 and into the newly constructed injection well (Inj.-1, Deep) (Figure 8). Overall, 43, 5-gallon pails of $NaMnO_4$ (57 lbs, 40% $NaMnO_4$/ pail) were injected.

Direct-push injection. Oxidant was injected along eight transects on the longitudinal axis of the plume, consisting of two injection locations per transect (14 locations), and at two additional single locations in the source area and downgradient from M3-mid (Figure 6). At each transect, the oxidant was injected approximately 7 ft apart and at two depth intervals (8-10, 10.5-12.5 ft bgs). Approximately 135 gallons of $NaMnO_4$ oxidant solution was injected, resulting in a theoretical 3 ft radius of influence (ROI). This ROI ideally assumes a cylindrical shape, a 2 ft vertical interval, and a porosity = 0.3. The locations of these transects were selected to lie between previous oxidant injection locations and to extend further down the plume. Relocation of some of the pre-determined oxidant injection locations was required due to the proximity of subsurface utilities.

Injection wells. MW-25, an existing monitoring well used as an injection well, is screened 10-15 ft bgs in both the loose sand (6.5-11.5 ft bgs) and in the underlying silty sand (11.5-17.5 ft bgs) (USGS, 2009). It was estimated that the permeability in the loose sand is approximately four times greater than in the underlying silty sand (TetraTech, 2004). It was projected that the oxidant volume injected into MW-25 during the first injection (480 gallons; $[NaMnO_4]_{AVG}$ =13.6 g/L) was predominantly delivered into the overlying loose sand, but was also introduced into the silty sand. During the second oxidant injection event, an increase in the oxidant dosage was delivered into MW-25 (640 gallons; $[NaMnO_4]_{AVG}$ = 37 g/L) to achieve an approximate 4-5 ft radius of influence (*i.e.*, assuming a 5 ft screened interval, porosity = 0.3).

The direct-push injection well (Inj.-1, Deep) was installed in the source area, approximately 7 ft to the northwest of MW-25. The objective was to deliver more oxidant into the source area adjacent to and underlying the suspected leaking sanitary sewer line. The construction of this well, is described above in section 3.1.3. A heavy oxidant loading (125 gallons; $[NaMnO_4]_{AVG}$ = 111 g/L) was successfully injected into this well to achieve approximately a 2-3 ft radius of influence.

4.2.4 Post-oxidation 2 CVOC concentrations

Contrasting Figures 14a and 14c, it is evident that significant and more widespread CVOC destruction was achieved through the second oxidant injection. Results of the second oxidant injection confirmed the findings from the first oxidant injection event: (1) the oxidant was successfully delivered to the targeted zones, (2) hydraulic control of the injected oxidant was achieved, (3) the oxidant persisted in zones where a heavy oxidant loading was delivered, and (4) that significant CVOC destruction was achieved.

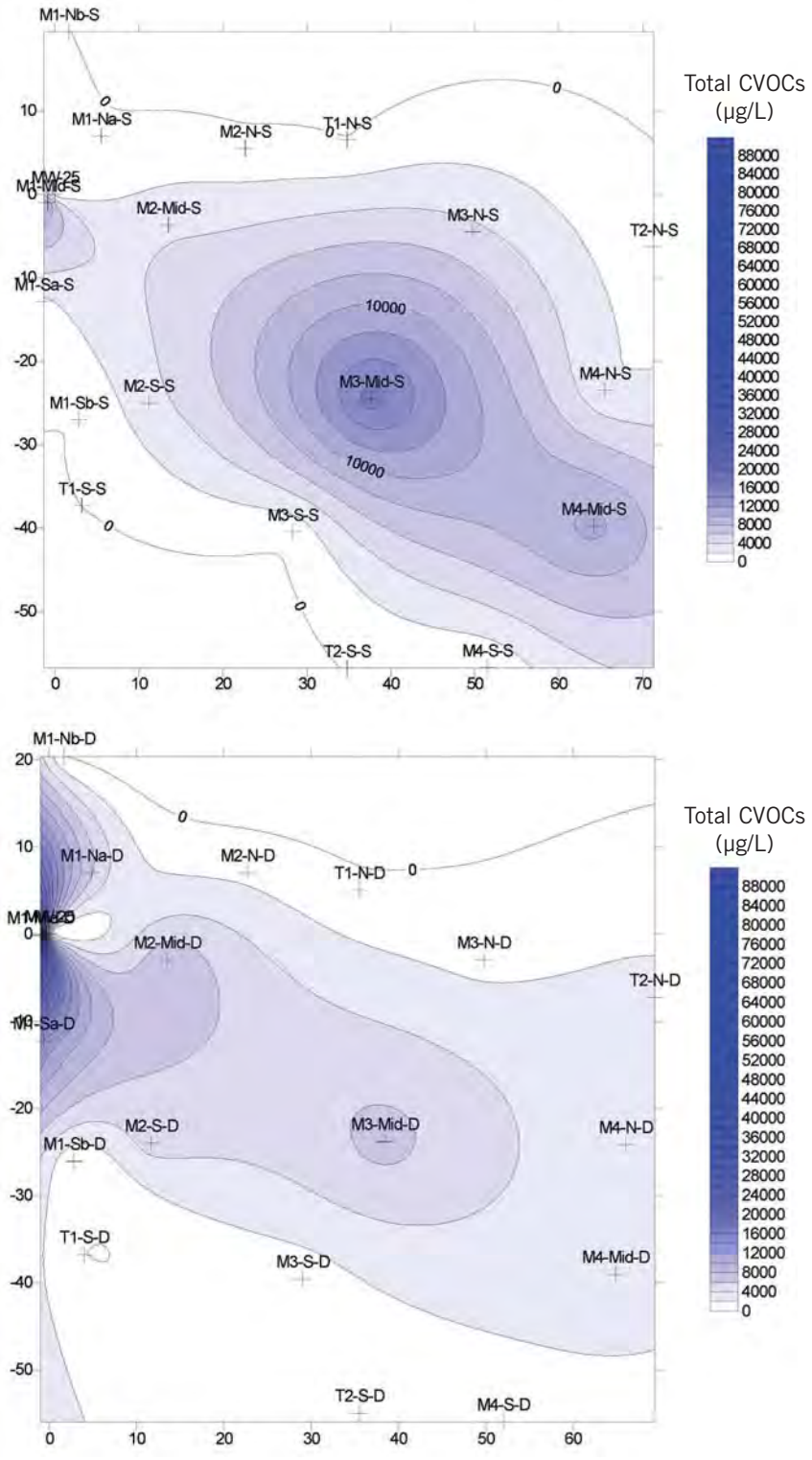

Figure 14.C. Post-oxidation 2 (February, 2014) shallow (7-10 ft bgs) (top figure) and deep (10-12.25 ft bgs) (bottom figure) total chlorinated volatile organic compounds (µg/L) at Parris Island, SC MCRD Site 45.

4.2.5 Third oxidant injection event (March 24-29, 2014)

Based on the results from the first two oxidant injection events, the ISCO strategy during the third oxidant injection was to aggressively target the source area(s) and to deliver the oxidant into zones where CVOCs had persisted. Again, this included the southeast corner of Building 192 and along the longitudinal axis of the CVOC plume. Greater oxidant dosages of sodium permanganate were delivered at multiple direct-push locations and depths in the source area and along the longitudinal axis of the plume (Figure 6). Greater oxidant dosage was also injected into MW-25 and Inj.-1, Deep (Figure 8). Overall, there were 87, 5-gallon pails of $NaMnO_4$ (57 lbs, 40% $NaMnO_4$/pail) injected, which was greater than the mass of oxidant injected during the first two events combined. Given the repeated delivery of oxidant in the high concentration CVOC source areas during oxidant injection events 1-3, it is likely that the oxidant demand was satisfied and that oxidant residuals in some areas would drift downgradient.

Direct-push injection. Oxidant was injected at 14 transects along the longitudinal axis of the plume, consisting of 3-5 injection locations per transect and at two additional locations in the source area and downgradient from M3-mid (Figure 6). Approximately 7900 gallons ($[NaMnO_4]_{AVG}$ = 26 g/L) was injected using direct-push technology. At each transect, the oxidant was injected approximately 7 ft apart and at two depth intervals (8-10, 10.5-12.5 ft bgs). Approximately 135 gallons of $NaMnO_4$ oxidant solution was injected per interval, resulting in a theoretical 3 ft ROI. This ROI ideally assumes a cylindrical shape, a 2 ft vertical interval, and porosity = 0.3. The locations of transects were selected to lie between previous oxidant injection locations and to extend further down the plume. The oxidant was injected using an outside-in approach, where the middle injection was last. Specific transect locations targeted high CVOC concentration zones in the subsurface, and the oxidant was injected starting at the lower concentration end of the plume and moved towards the higher concentration source area.

Injection wells. An aggressive oxidant dosage was delivered into MW-25 (640 gallons, $[NaMnO_4]_{AVG}$ = 41 g/L) to achieve an approximate 4-5 ft ROI, and into Inj.-1, Deep (218 gallons, $[NaMnO_4]_{AVG}$ = 41 g/L) to achieve an approximate 3-4 ft ROI.

4.2.6 Post-oxidation 3 CVOC concentrations

By contrasting Figures 14.A and 14.D, it is evident that significant and widespread CVOC destruction was achieved by the third oxidant injection event. Noticeably absent are the high concentration isocontours near the source area and at the M3-Mid-shallow micro-well monitoring location, where CVOC concentrations were historically high and persistent. Results of the 3rd oxidant injection confirmed the findings from the first two injection events: (1) the oxidant was successfully delivered to the targeted zones, (2) hydraulic control of the injected oxidant was achieved, (3) the oxidant persisted in zones where the heavy oxidant loading was delivered, and (4) that significant CVOC destruction was achieved.

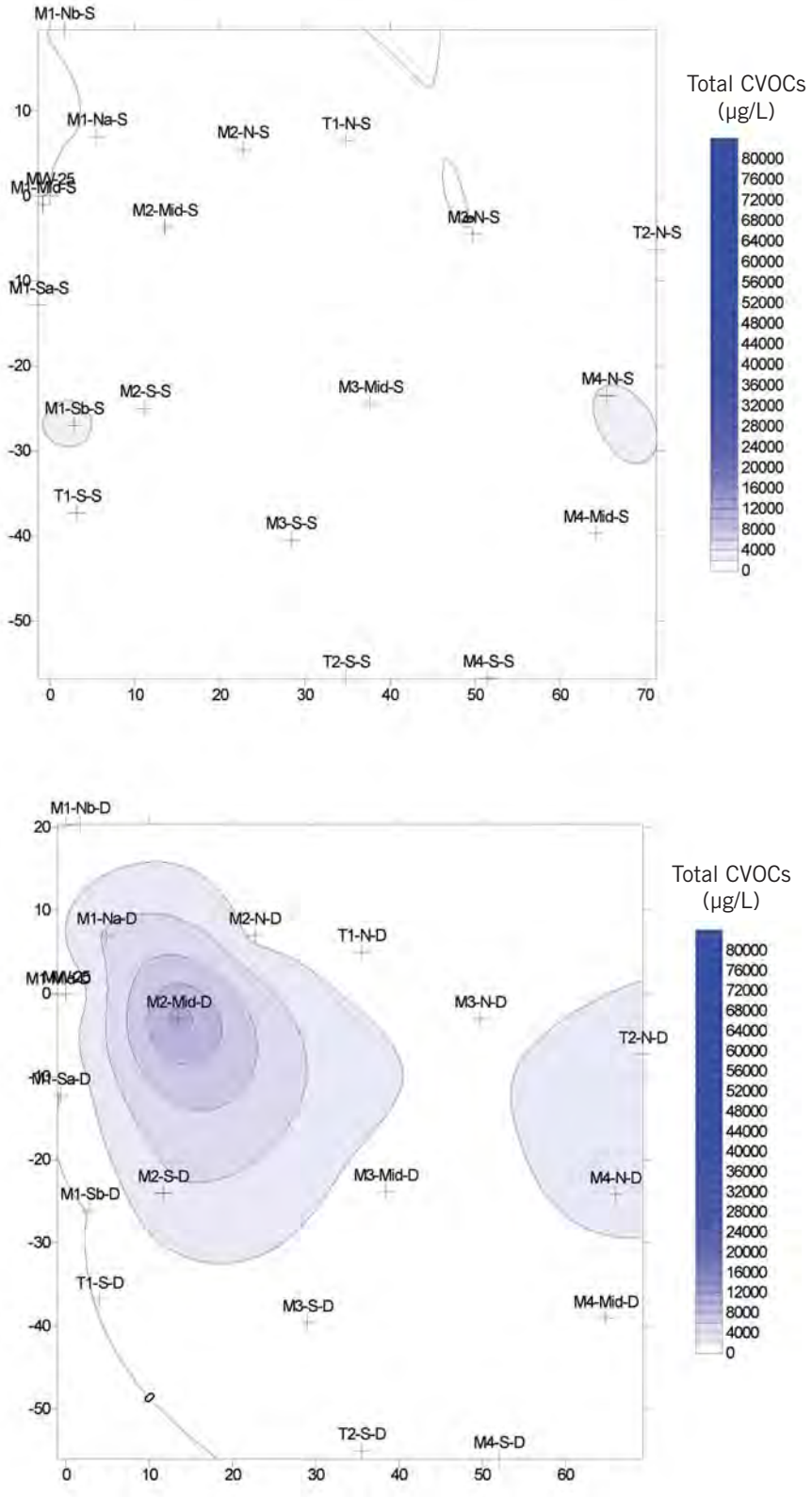

Figure 14.D. Post-oxidation 3 (June, 2014) shallow (7-10 ft bgs) (top figure) and deep (10-12.25 ft bgs) (bottom figure) total chlorinated volatile organic compounds (µg/L) at Parris Island, SC MCRD Site 45.

4.3 Mass flux

The CVOC mass flux (refer to Eqn 2 in Section 3.3.2 *Contaminant mass flux*) is an estimate of the VOC mass in ground water, passing through a plane. The mass flux is defined, or quantified, by the micro-wells used in each of the four monitoring transects (Figure 7). It was evident that the majority of the CVOC mass flux was attributed to the shallow interval (7-10 ft bgs) rather than the deeper interval (10-12.25 ft bgs) (Figure 15.A). This was attributed to lower CVOCs concentration, slower transport, and smaller cross sectional area associated with the deeper interval. Below the 12.25 ft bgs elevation, the CVOC concentrations in the aquifer material were significantly limited (refer to section 4.1.4, above), and the hydraulic conductivity was lower due to the increase in clay content. The baseline mass flux results indicated that focusing the oxidant in the 7-12 ft bgs interval should efficiently destroy the most mobile and greatest mass of CVOCs at the site. Ideally, this approach was projected to significantly reduce the CVOC concentrations and have the greatest impact on limiting CVOC transport from the site.

The oxidant injected during the first oxidant injection event was focused only in the areas represented by mass flux transects 1 and 2. The oxidant was not injected near mass flux transects 3 and 4 and therefore, the greatest reduction in CVOCs occurred in the areas of mass flux transects 1 and 2 (Figure 15.A). A significant reduction in mass flux was not observed in the deeper interval, suggesting that greater oxidant delivery was needed in that interval during subsequent injection events. An unexpected increase in mass flux was estimated at MF-3. During oxidant injection, the displacement of ground water by the injected oxidant can temporarily change ground water flow lines and directions. This can potentially result in changes in ground water CVOC concentrations in side and downgradient directions. The spike in CVOC mass flux in transect MF-3 was attributed to an increase in [CVOCs] in downgradient micro-well M3-Mid-S. Overall, a 22.6% and 2.5% reduction in mass flux was measured in the shallow and deep intervals respectively (Table 5).

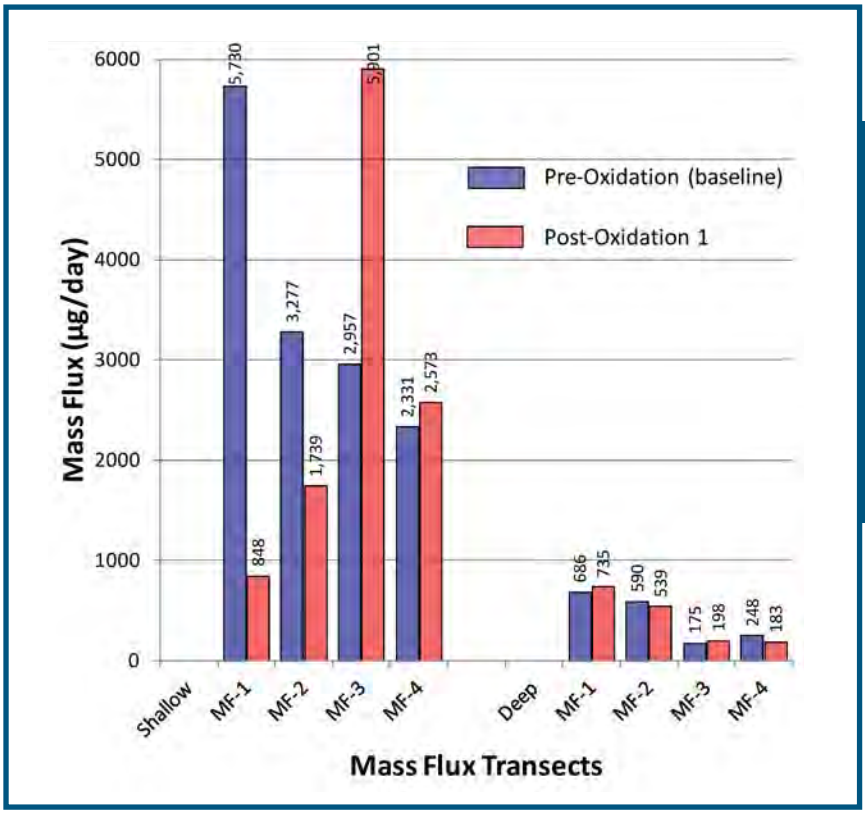

Figure 15. A. Pre-oxidation (baseline) and post-oxidation 1 CVOC mass flux across transects MF-1 through MF-4 in shallow and deep zones in the study area (refer to Figure 7 for locations of mass flux transects).

Table 5. Summary of mass flux results for baseline and post-oxidation events 1-3.					
Mass Flux Transect	Total CVOCs Mass Flux (µg/day)				Total mass flux decline (%)[1]
	MF-1	MF-2	MF-3	MF-4	
Shallow					
Baseline	5730	3280	2960	2330	
Post-Oxid. 1	850	1740	5900	2570	22.6
Post-Oxid. 2	770	1000	3550	1940	49.3
Post-Oxid. 3	210	240	90	670	91.5
Deep					
Baseline	690	590	170	250	
Post-Oxid. 1	740	540	200	180	2.5
Post-Oxid. 2	560	220	150	120	50.4
Post-Oxid. 3	40	245	50	80	75.5

[1] The total mass flux decline is relative to baseline (pre-oxidation conditions).

The second oxidant injection event caused the continued decline in total CVOC mass flux in the shallow mass flux transects MF-1 and MF-2, and significant declines at MF-3 and MF-4 (Figure 15.B). This was attributed to the more aggressive and widespread oxidant injection associated with the second oxidation event. A greater impact was also observed at the deep interval mass flux transects relative to the first injection, but the magnitude was small compared to the shallow interval. Approximately a 50% decline in mass flux was achieved in both the shallow and deep intervals after the second oxidation event (Table 5).

More oxidant was delivered in the targeted source zones in the third injection event than in both the first and second injections combined (Figure 6; section 4.1.3). Correspondingly, a significant and widespread decline in CVOC mass flux was observed in both the shallow and deep intervals (Figure 15.C). Overall, a 91.5% and 75.5% reduction in total CVOC mass flux occurred as a result from oxidant injections 1-3 (Table 5).

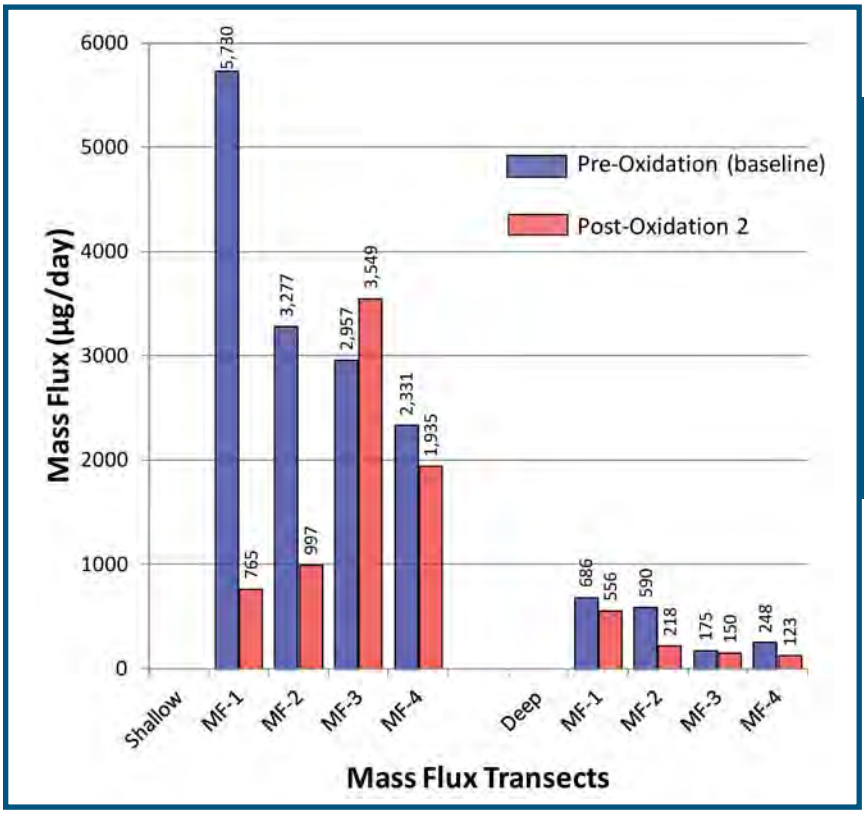

Figure 15. B. Pre-oxidation (baseline) and post-oxidation 2 CVOC mass flux across transects MF-1 through MF-4 in shallow and deep zones in the study area (refer to Figure 7 for locations of mass flux transects).

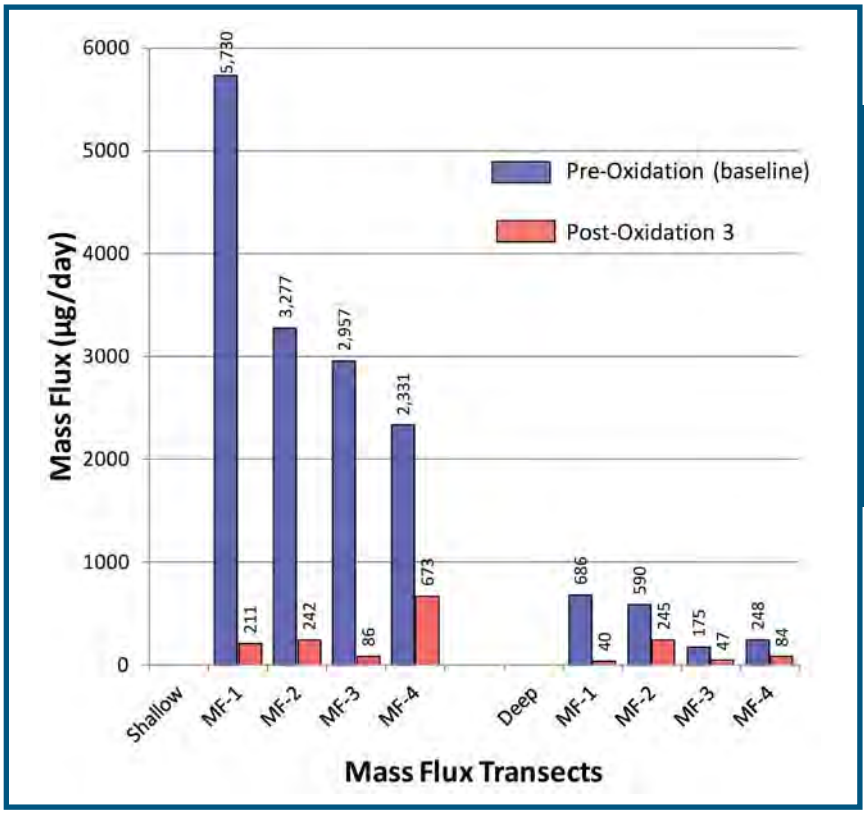

Figure 15. C. Pre-oxidation (baseline) and post-oxidation 3 CVOC mass flux across transects MF-1 through MF-4 in shallow and deep zones in the study area (refer to Figure 7 for locations of mass flux transects).

4.4 Oxidant distribution and persistence

The design ROI was approximately 3 ft for direct-push oxidant injection. The post-injection distribution of oxidant was evaluated by sampling micro-wells in all locations within 2-3 days of oxidant injection. Elevated concentrations of $NaMnO_4$ were measured in micro-wells located within 3-4 ft from the direct-push injection locations. Further, non-detect concentrations of oxidant were measured in all micro-wells located greater than 3-4 ft away from the injection locations. Therefore, the schematic depicting oxidant distribution (Figure 6) was generally an accurate estimate of oxidant distribution. However, as a result of aquifer heterogeneities and preferential pathways, it is projected that the transport of $NaMnO_4$ beyond the design ROI may have occurred to some extent but could not be quantified given the spatial distribution of micro-well locations. In all direct-push and injection well oxidant delivery locations, the ground water and aquifer material just beyond the design ROI was contaminated with CVOCs. Therefore, any unintentional delivery of oxidant beyond the design ROI and transport into non-targeted zones most likely resulted in the oxidation of CVOCs.

The post-oxidation 1 ground water sampling event occurred 1.25 months after the first injection. During this sampling event, permanganate was measured in three wells (MW-25, M1-Mid-shallow, M2-Mid-deep) that were located in an area where the greatest oxidant dosages were delivered. The persistence of MnO_4^- in these wells was an indication of the slow reaction of the oxidant and that the oxidant demand in the nearby aquifer materials was being depleted over time. The post-oxidation 2 ground water sampling event occurred 4.75 months after oxidant injection 2 and revealed a wider range of oxidant persistence in the ground water. Permanganate was measured in 6 wells (MW-25; Inj.-1, Deep; M1-Mid-shallow; M1-Mid-deep; M2-Mid-shallow; M4-Mid-deep)

over the length of the injection zone. The post-oxidation 3 ground water sampling event occurred three months after the third oxidant injection and revealed oxidant persistence over the length of the injection zone. Permanganate was measured in 6 wells (MW-25; Inj.-1, Deep; M1-Mid-shallow, M1-Mid-deep, M1-S-A-shallow; M4-Mid-deep). Finally, the post-oxidation 4 ground water sampling event (Feb. 27-28, 2015) occurred > 11 months after the third permanganate injection and permanganate was found in six wells (MW-25; M1-SA-shallow; M1-Mid-shallow; M1-Mid-deep; M2-S-deep; M4-Mid-deep).

It is evident from these results that permanganate persisted mainly in the source area near the southeast corner of Building 192, where heavy oxidant dosages were delivered near the suspected PCE release point(s) along the sanitary sewer line. Ideally, oxidant persistence in this area results in long-term contact between the oxidant and the contaminated media. Oxidant persistence along the longitudinal axis, over the length of the injections, was also evident from ground water monitoring results. Long term persistence of the oxidant resulted in improved contact between the oxidant and contaminated media, as a result of enhanced CVOC mass transfer and transport processes: (1) CVOCs slowly dissolving from DNAPL, (2) CVOCs desorbing from aquifer solids, and (3) CVOCs diffusing from low permeability silty media. Further, oxidant diffusion into low permeability media can be improved through long term oxidant persistence.

Given the repeated delivery of oxidant and the potential for overlapping ROIs during oxidant injection events 1-3, it is probable that the oxidant demand was satisfied, that downgradient drift of oxidant residual occurred, and that oxidant distribution occurred over a greater area than depicted by the ROIs. Excessive oxidant persistence may allow oxidant transport into non-targeted areas. At the time of the last ground water sampling event (Feb. 27-28, 2015), permanganate had not been detected in downgradient well MW-31 SL, which is 75 ft downgradient of monitoring transect M4 (*i.e.*, the furthest downgradient location where oxidant was injected).

4.5 General indicators of oxidation

The indicator parameters including chloride (Cl^-), ferrous iron (Fe^{+2}), and oxidation reduction potential (ORP) were measured prior to and after the oxidant injections. These parameters potentially provide insight regarding the impact of oxidant injection on total CVOC oxidation and dechlorination, or Cl^- release, and change in the redox potential in the subsurface.

4.5.1 Chloride (Cl^-)

Dechlorination of the CVOCs results in the release of Cl^- ions in solution. Background Cl^- levels in surficial aquifers near marine environments typically exhibit elevated concentrations of Cl^-. Further, elevated Cl^- levels in the study area can also be attributed to the long term dechlorination of CVOCs through natural attenuation reductive dechlorination mechanisms known to occur at this site as described by Vroblesky *et al.* (2009). Contrasting pre-oxidation Cl^- isocontours in the study area with post-oxidation isocontours revealed marginal evidence of the formation of Cl^- ions released as a result of total CVOC oxidation. It is evident that the pre-oxidation baseline concentration of Cl^- in the shallow aquifer interval is lower than in the deeper interval. However, despite significant reductions in total CVOCs (Figures 14.A-D), a stark contrast was not observed between pre-oxidation and post-oxidation Cl^- isocontours (Figures 16.A-D). Consequently, Cl^- data resulting from post-oxidation ground water sampling provided limited insight into ISCO treatment performance due to elevated background levels of Cl^-.

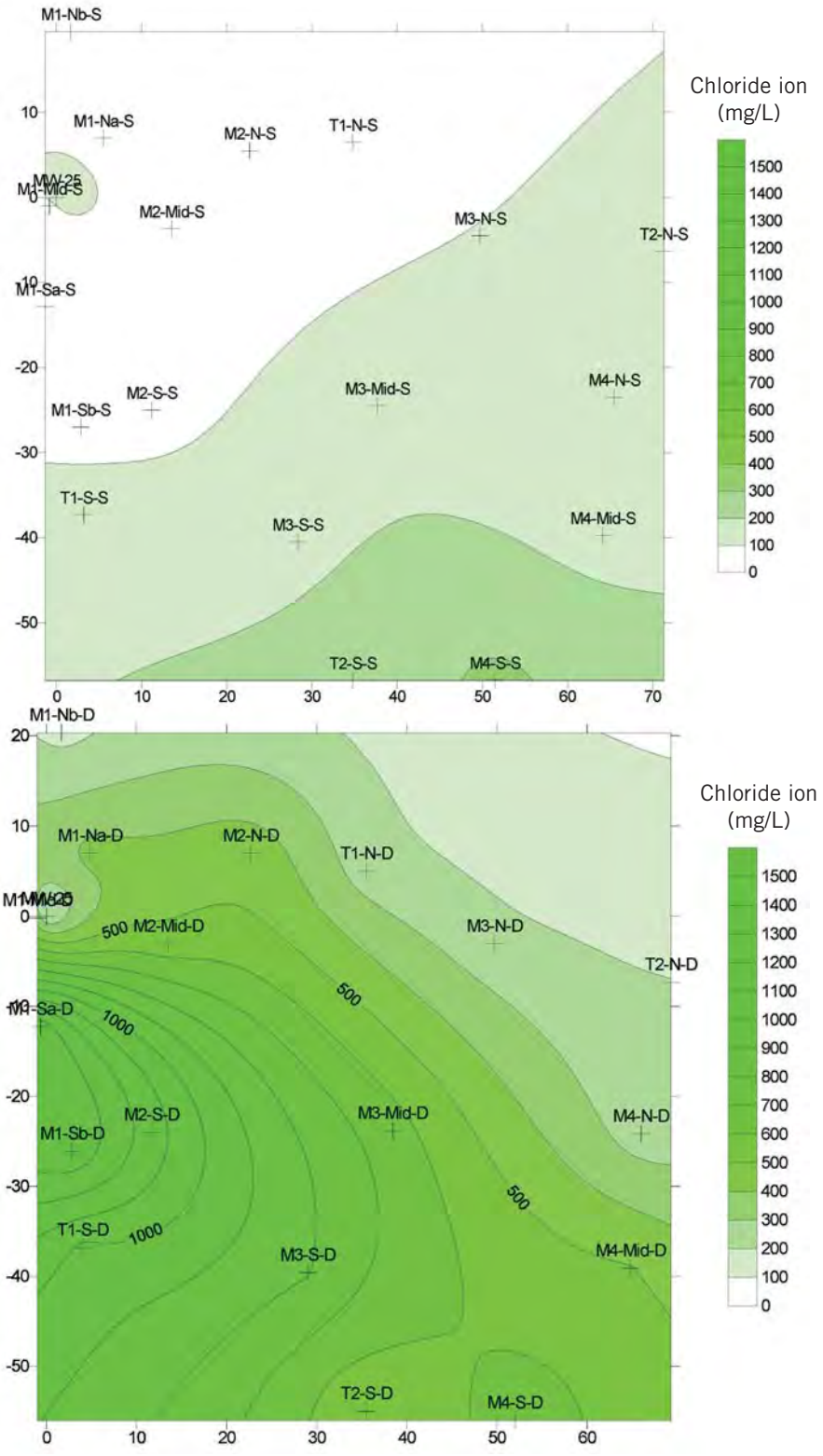

Figure 16.A. Pre-oxidation shallow (7-10') (top figure) and deep (10.25-12.25') (bottom figure) chloride ion (Cl) concentrations (mg/L) at Parris Island, SC MCRD Site 45 (2/19/13 - 2/21/13). Note: there was an outlier data point in T1-N-S (763 mg/L) that was deleted from the data set. All 3 samples that followed were < 100 mg/L.

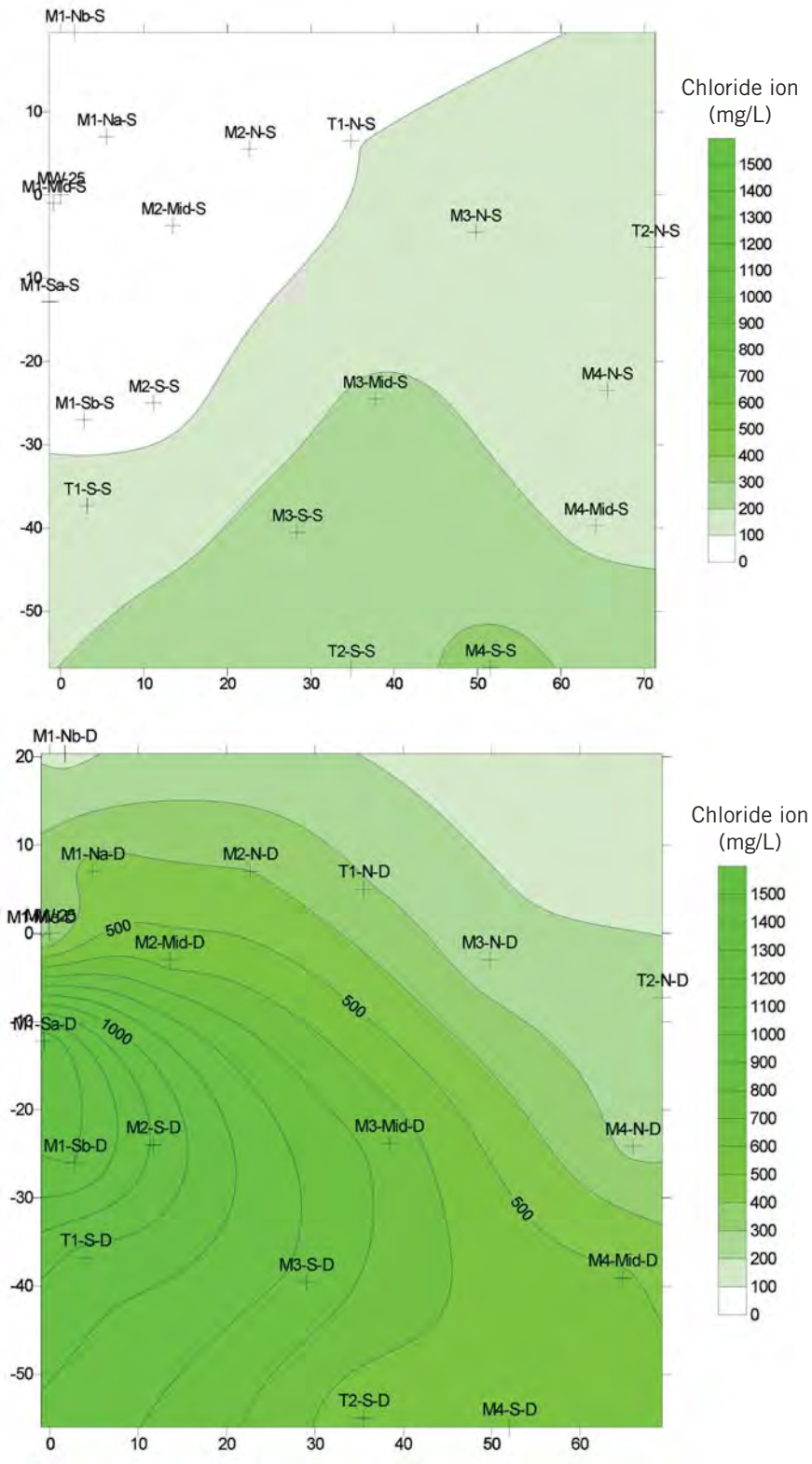

Figure 16.B. Post-oxidation 1 shallow (7-10') (top figure) and deep (10.25-12.25') (bottom figure) chloride ion (Cl) concentrations (mg/L) at Parris Island, SC MCRD Site 45.

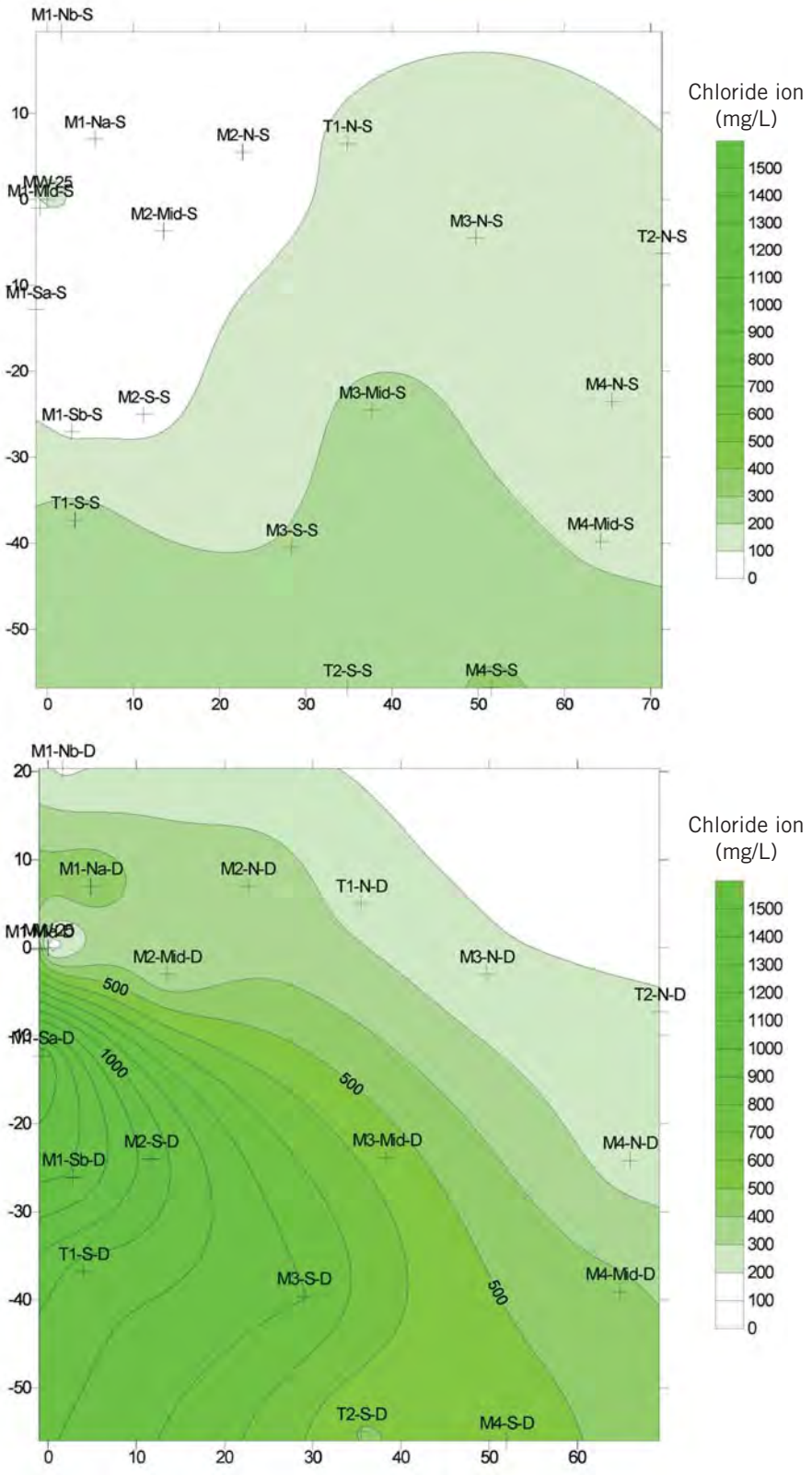

Figure 16.C. Post-oxidation 2 shallow (7-10') (top figure) and deep (10.25-12.25') (bottom figure) chloride ion (Cl) concentrations (mg/L) at Parris Island, SC MCRD Site 45.

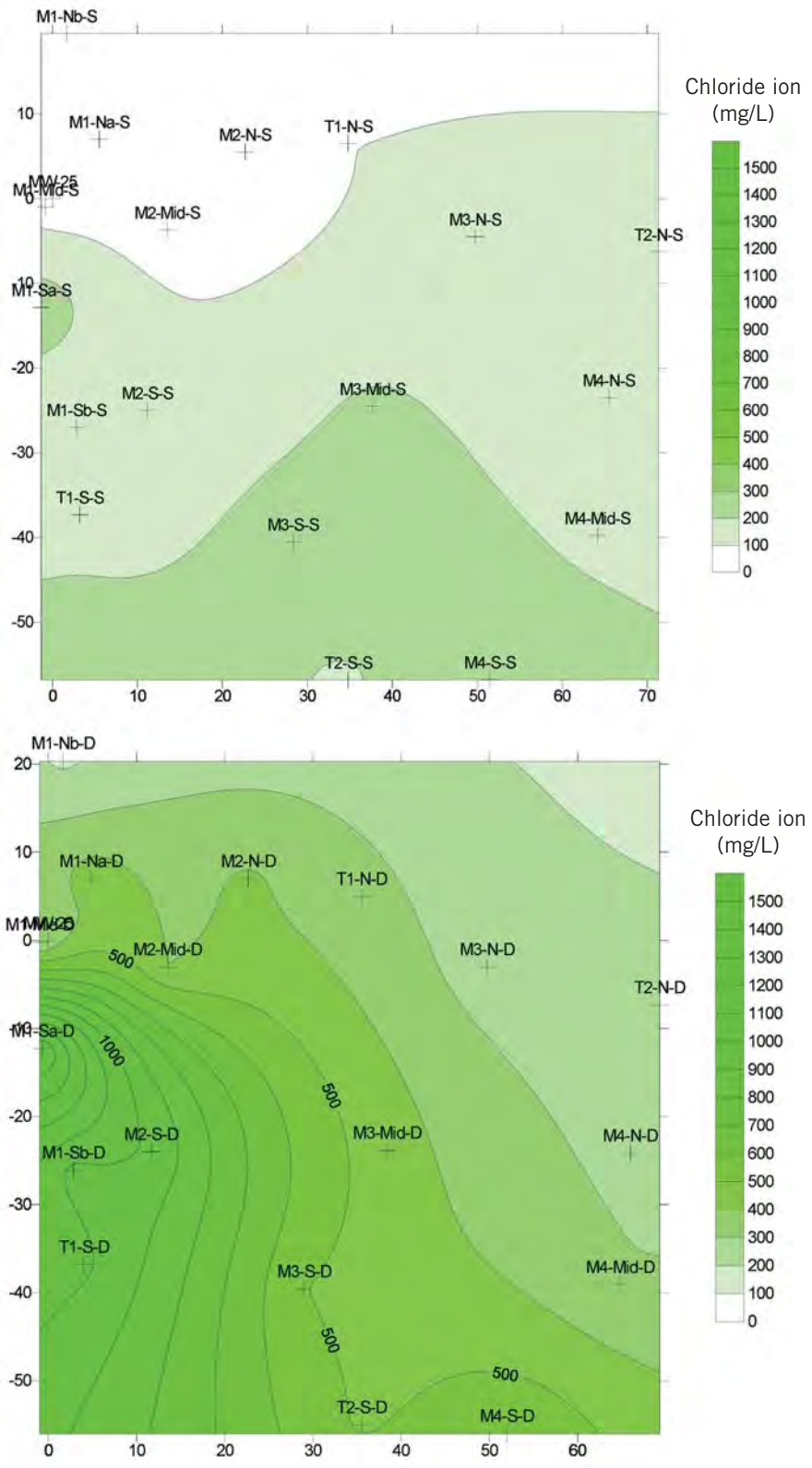

Figure 16.D. Post-oxidation 3 shallow (7-10') (top figure) and deep (10.25-12.25') (bottom figure) chloride ion (Cl) concentrations (mg/L) at Parris Island, SC MCRD Site 45.

4.5.2 Ferrous iron (Fe^{+2})

The presence of naturally occurring organic matter in the aquifer material was a general indicator that reducing conditions existed at the site. This was especially the case at depth, where an abundance of organic material, such as decaying wood material and wood chips, was visibly present in the aquifer cores. Further, sewage inputs into the subsurface were known to occur as a result of leaking sanitary sewer line(s). Sewage odors emanating from the work area during the collection of aquifer cores provided anecdotal evidence supporting the presence of sewage residuals in the subsurface. Ferrous iron, a byproduct of ferric iron (Fe^{+3}) reduction, is a general indicator of reducing conditions and was projected to be present in the ground water, especially since the aquifer material sampled and analyzed contained up to 10 g/kg (Figure 11). Under increasingly reduced conditions, iron solubility increases and soluble ferrous iron was measured in abundance under pre-oxidation, or baseline, conditions in the ground water (Figure 17.A). Ferrous iron concentrations progressively declined with increasing applications of oxidant (Figures 17.B-D). The redox shift towards oxidized conditions was expected to be temporary, however, given the significant quantity of organic materials and the abundance of iron in the subsurface. Nevertheless, the absence of ferrous iron in ground water along the longitudinal axis of the plume and in the source area indicated the significant impact of the oxidant injected in these areas.

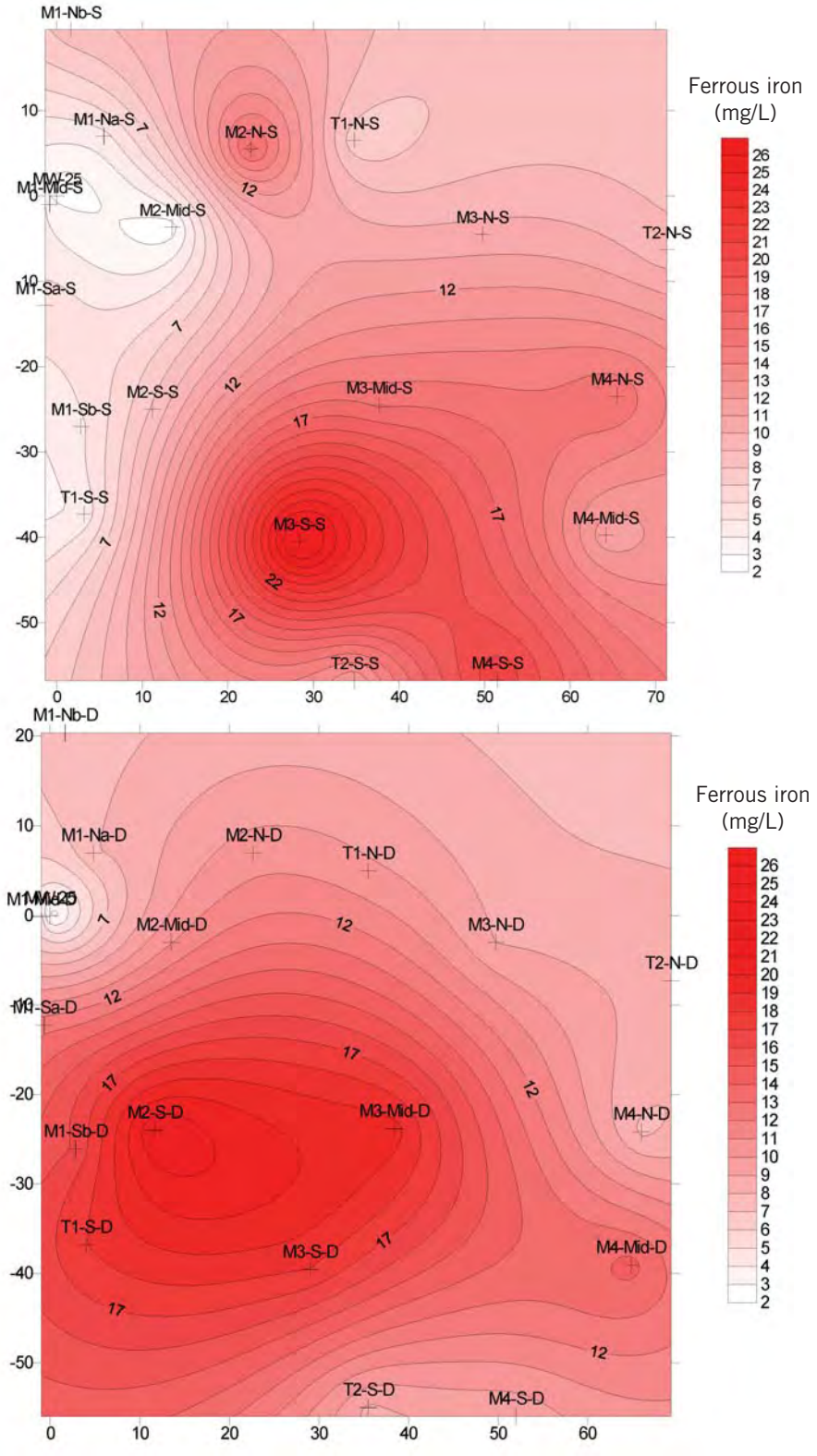

Figure 17.A. Pre-oxidation shallow (7-10') (top figure) and deep (10.25-12.25') (bottom figure) ferrous iron (Fe^{+2}) concentrations (mg/L) at Parris Island, SC MCRD Site 45 (2/19/13 - 2/21/13).

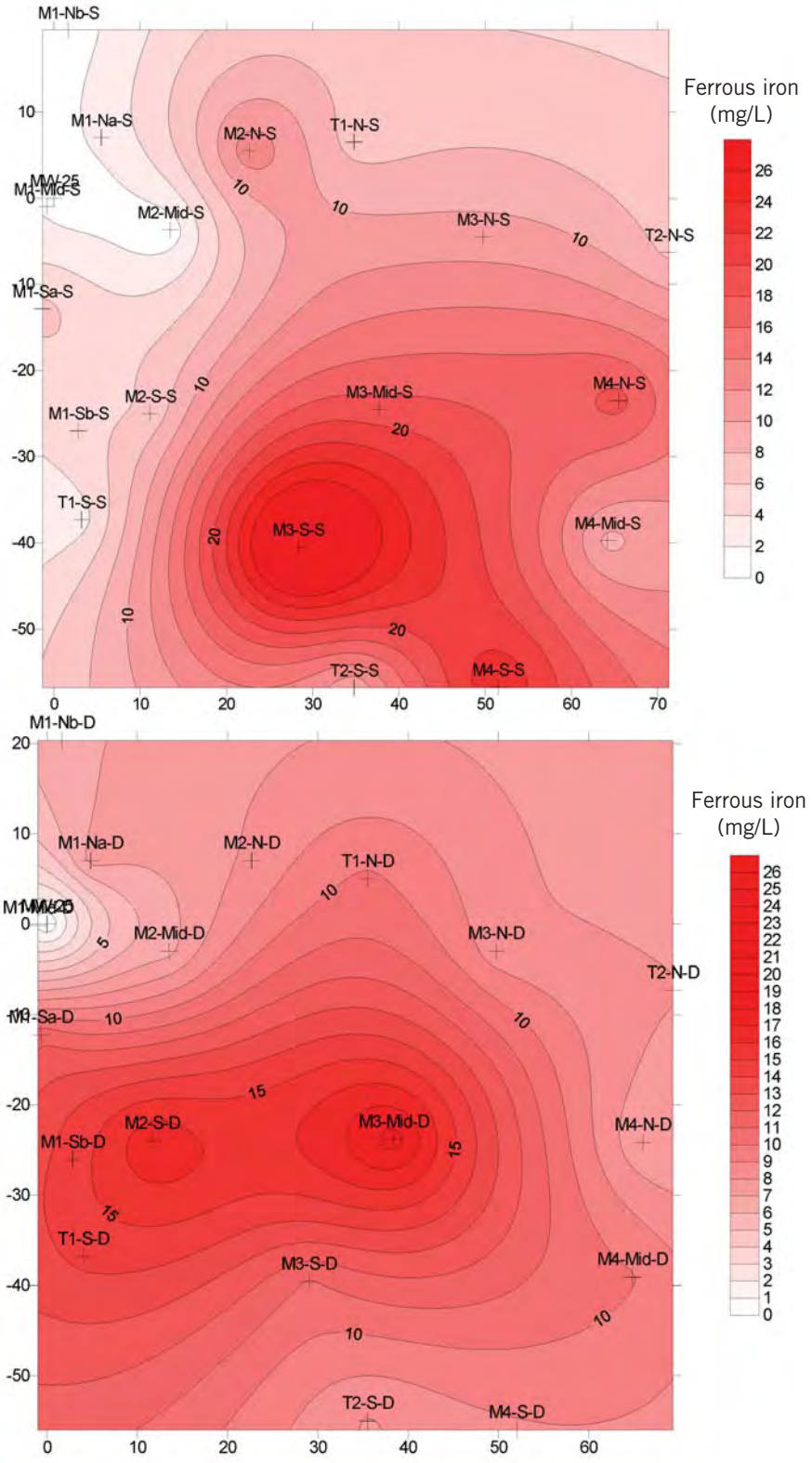

Figure 17.B. Post-oxidation 1 shallow (7-10') (top figure) and deep (10.25-12.25') (bottom figure) ferrous iron (Fe^{+2}) concentrations (mg/L) at Parris Island, SC MCRD Site 45.

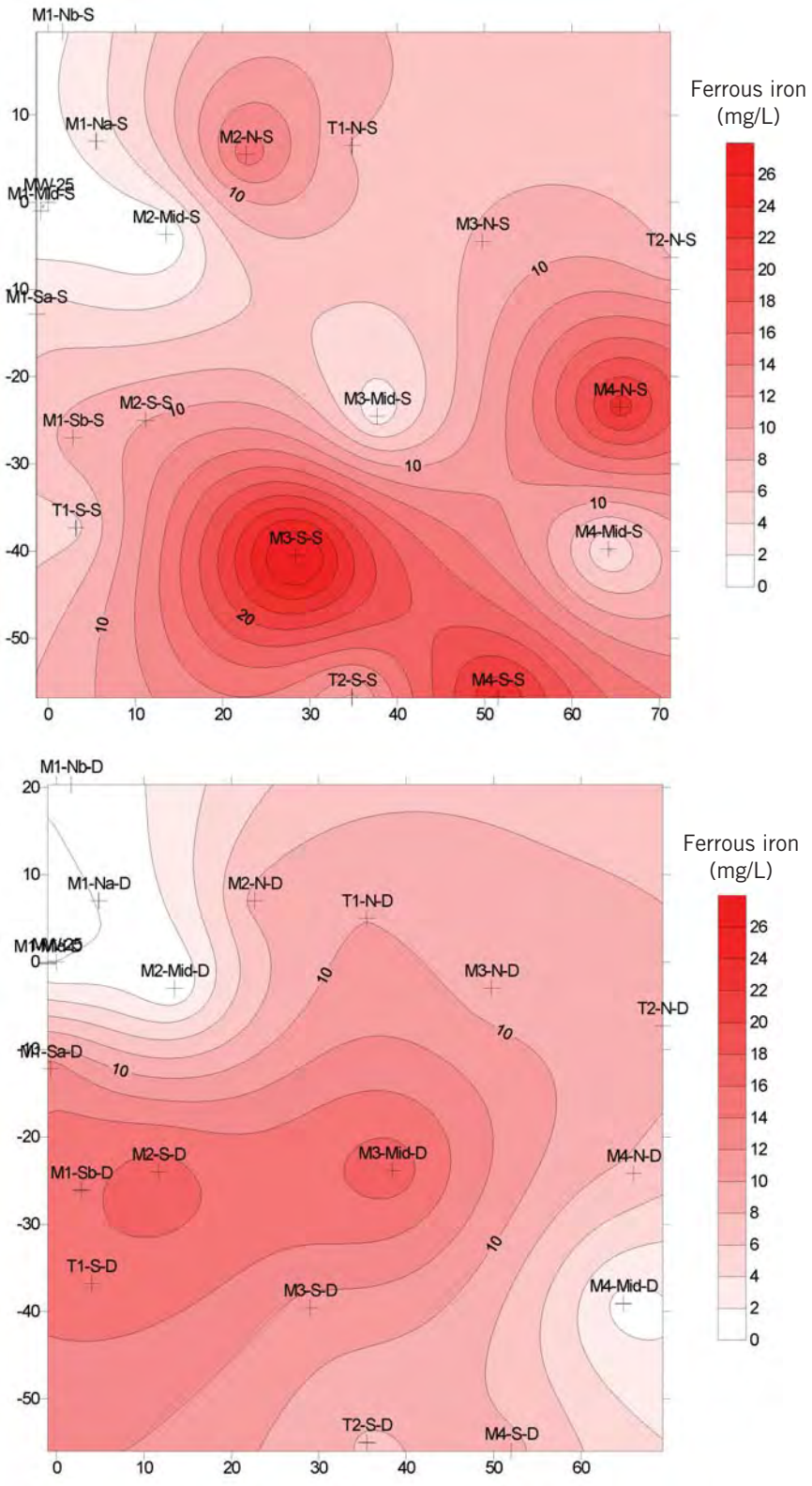

Figure 17.C. Post-oxidation 2 shallow (7-10') (top figure) and deep (10.25-12.25') (bottom figure) ferrous iron (Fe^{+2}) concentrations (mg/L) at Parris Island, SC MCRD Site 45.

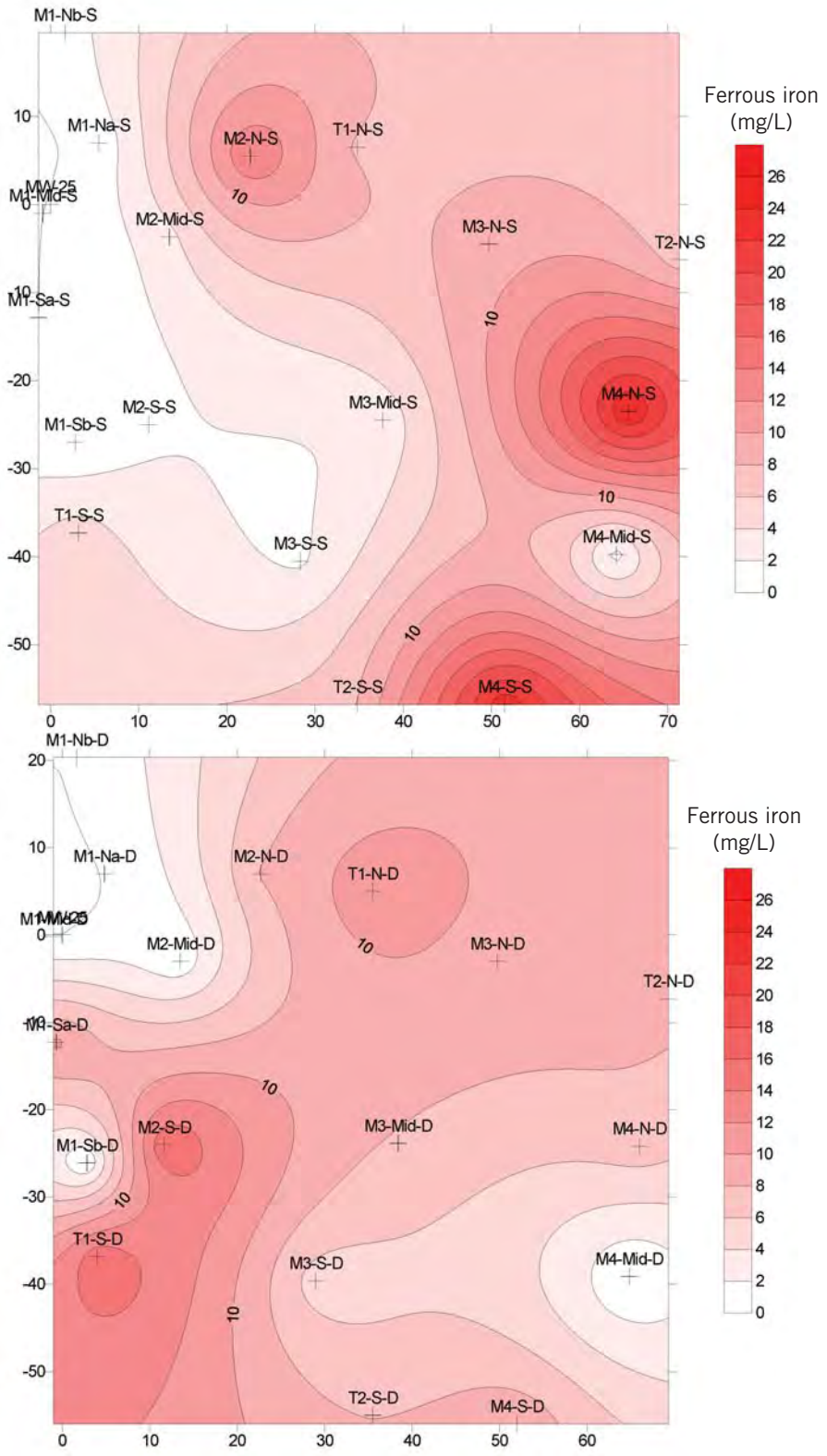

Figure 17.D. Post-oxidation 3 shallow (7-10') (top figure) and deep (10.25-12.25') (bottom figure) ferrous iron (Fe^{+2}) concentrations (mg/L) at Parris Island, SC MCRD Site 45.

4.5.3 Oxidation reduction potential (ORP)

Pre-oxidation measurements of ORP were only measured in three shallow and deep micro-well clusters along monitoring transect M1, including M1-S, M1-Mid, and M1-N. The pre-oxidation ORP values indicated that the ground water was under reducing conditions (6.6-66.6 mV) for the three nested well pairs (Table 6). A significant post-oxidation increase in ORP was measured in all wells along monitoring transect M1, indicating the impact of nearby oxidant injection.

Table 6. Summary of ORP measurements in micro-wells near the source area.

Sampling event [1]	ORP (mV)					
	M1-S-A-D	M1-S-A-S	M1-Mid-D	M1-Mid-S	M1-N-A-S	M1-N-A-D
Baseline	22	44	29	67	45	7
Post-Oxid. 1	31	113	392	629	65	14
Post-Oxid. 2	415	484	591	617	263	121
Post-Oxid. 3	478	658	523	651	30	56

[1] Baseline pre-oxidation (6/21/13), Post-Ox 1 (8/6/13), Post-Ox 2 (2/13/14), Post-Ox 3 (6/24/14)

4.5.4 Dissolved methane

Pre-oxidation elevated concentrations of dissolved methane were measured in the ground water, indicating methanogenic conditions along the longitudinal axis of the plume in the shallow (7-10 ft bgs) aquifer (Figure 18.A). Despite this distinct zone of elevated dissolved methane, concentrations were lower and dispersed in the deeper (10.25-12.25 ft bgs) interval.

Multiple lines of evidence have been presented indicating that the PCE release in the southern CVOCs plume at site 45 originated from a leak in the sanitary sewer line at the southeast corner of Building 192. Given this observation, it is reasonable to assume that raw sewage would also have been released at the same location(s) of the broken sewer line. The continuous discharge of sewage into the subsurface at an elevation of 5-6 ft bgs would have introduced large quantities of biodegradable organic matter. The organic matter associated with raw sewage is readily degradable and would have resulted in the depletion of dissolved oxygen and rapid onset of anaerobic and methanogenic conditions. Introduction of the dissolved organic matter in the highly permeable aquifer material would follow the southeastern ground water flow direction previously described. Therefore, the high levels of methane measured in the shallow interval are generally consistent with this conceptual model. The aquifer material directly above the 8-12 ft bgs interval exhibited a lower permeability and may potentially limit vertical dispersal of the methane. Conceptually, it is surmised that the lower permeability materials may serve to form a “methane trap” where gas-phase methane may accumulate.

Lower post-oxidation 3 concentrations of methane were measured in the shallow interval (Figure 18.B). This trend in dissolved methane may be an indication that (1) the heavy and repeated oxidant dosages applied in the subsurface may have impacted methanogenic microbial activity, (2) chemical oxidation of easily biodegradable organic matter lowered the availability of organic substrate and thus the formation of the methane byproduct, and/or (3) the methane may itself have been oxidized as a result of chemical oxidative treatment.

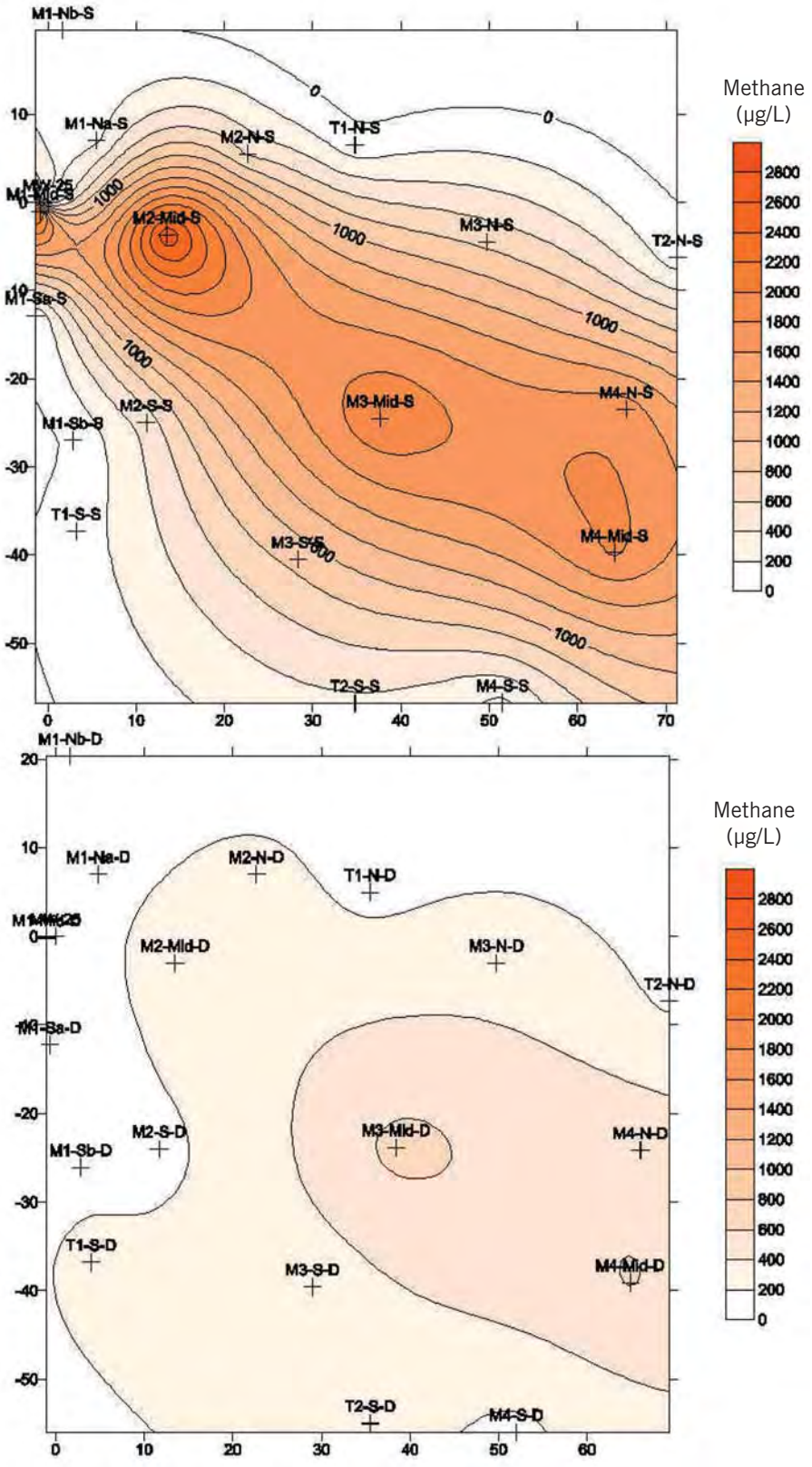

Figure 18.A. Pre-oxidation shallow (7-10') (top figure) and deep (10.25-12.25') (bottom figure) methane (µg/L) at Parris Island, SC MCRD Site 45 (February, 2013).

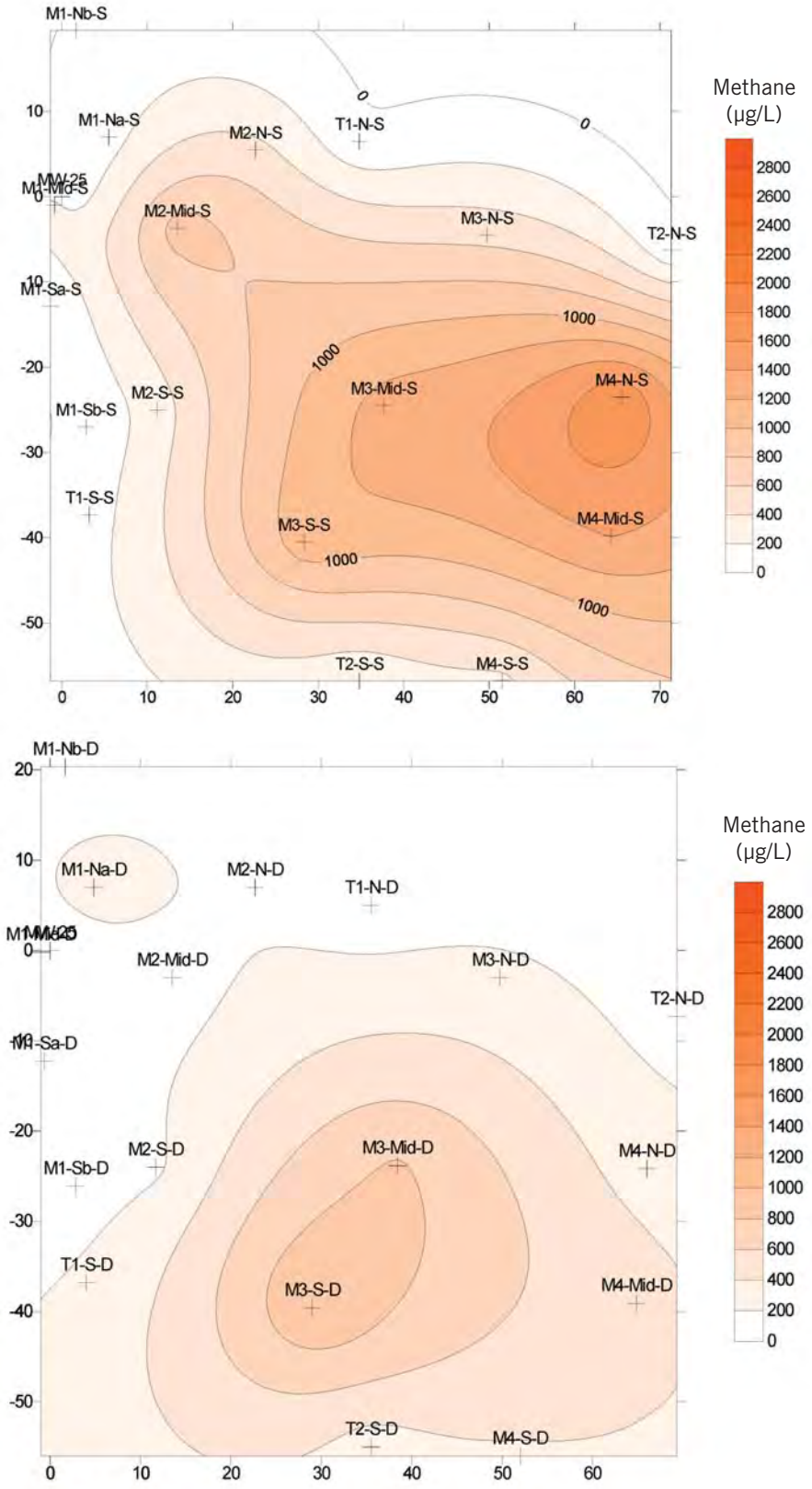

Figure 18.B. Post-oxidation 3 shallow (7-10') (top figure) and deep (10.25-12.25') (bottom figure) methane (µg/L) at Parris Island, SC MCRD Site 45 (June, 2014).

4.5.5 pH

The pre-oxidation pH was measured in micro-well clusters M1-S-A, M1-mid, and M1-N-A and the pH ranged from 5.5 to 5.8. Post-oxidation pH was measured in micro-wells and wells where there was no residual permanganate, the pH ranged from 4.4-6.5 (post-oxidation 1), 5.4-7.4 (post-oxidation 2), and 5.3-7.3 (post-oxidation 3). An elevated pH (pH 9) was measured in a limited number of wells where permanganate persisted during the post-oxidation ground water sampling event.

4.5.6 Metals

An increase in heavy metals concentration in ground water may result from heavy metals impurities contained in the permanganate, as well as in situ mobilization of pre-existing redox- or pH-sensitive heavy metals by the oxidant. Chromium (Cr) and arsenic (As) have historically been the impurities of concern. Field investigations generally reveal that these metals attenuate through various mechanisms and within acceptable transport distances, but monitoring and assessment is needed for confirmation. Ground water samples were collected in all nested micro-wells and analyzed for metals via ICP OES.

Chromium. The concentration of total chromium increased in the ground water, from background concentrations in all wells that were below the quantitation limit (10 µg/L), to elevated concentrations in a few wells (Figure 19). The elevated chromium concentrations were measured in wells where residual MnO_4^- had persisted and spatial correlation between elevated chromium and elevated ORP was also evident (Figure 20). Approximately 11 months after the third oxidant injection, the post-oxidation 4 ground water sampling event (Feb. 27-28, 2015) occurred and the concentration of chromium had declined in M3-mid-shallow from 1500 µg/L to 95 µg/L, and had declined in M4-mid-shallow from 950 µg/L to 17 µg/L. MW-31 SL is located approximately 75 ft downgradient of the M4 monitoring transect and the concentration of chromium there was < 10 µg/L. Empirical evidence provided by the ORP ground water data indicates that MW-31 SL was representative of a downgradient well in the ISCO area. Prior to oxidant injection (June 19, 2013), the ORP was 63 mV in MW-31 SL. After the oxidant injections, the ORP in MW-31 SL was 236 mV and 152 mV during the post-oxidation 3 (June 23, 2014) and 4 (Feb. 27-28, 2015) monitoring events, respectively. The increase in the ORP between pre- and post-oxidation indicated that MW-31 SL was downgradient and hydraulically connected with ground water in the ISCO area.

Arsenic. The background pre-oxidation concentration of arsenic in the ground water was measured in the monitoring network at the site (Figure 21). Given the lack of waste management activities involving heavy metals in this area, it is assumed that this is naturally-occurring arsenic. The impact of ISCO on lowering the arsenic concentrations in the ground water is evident by examining the post-oxidation 3 and 4 ground water arsenic isocontours (Figure 21). Arsenic species in ground water are functionally dependent on the pH and the redox state of the aquifer and thus significant changes were the result of the elevated ORP (Figure 20) measured in the ground water between the pre-oxidation and post-oxidation conditions. Consequently, the attenuation of the arsenic in the ground water occurred as a result of ISCO activities. The geochemistry associated with arsenic attenuation is discussed below (Section 5.4, *Metals Mobilization*).

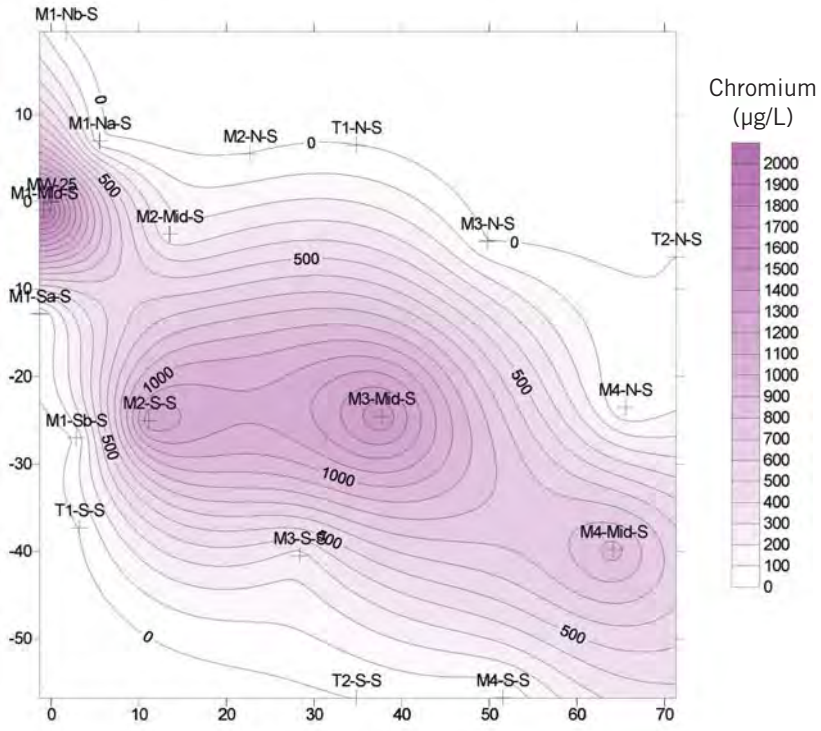

Figure 19. Post-oxidation 3 concentration of chromium (µg/L) (pink isocontours).

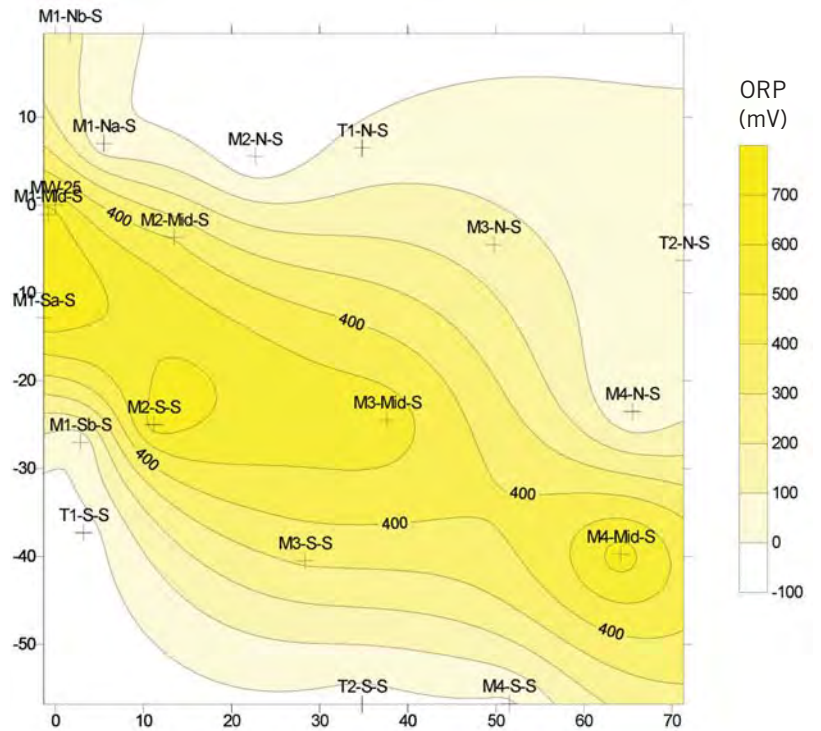

Figure 20. Post-oxidation 3 oxidation reduction potential (ORP) (mV) (yellow isocontours).

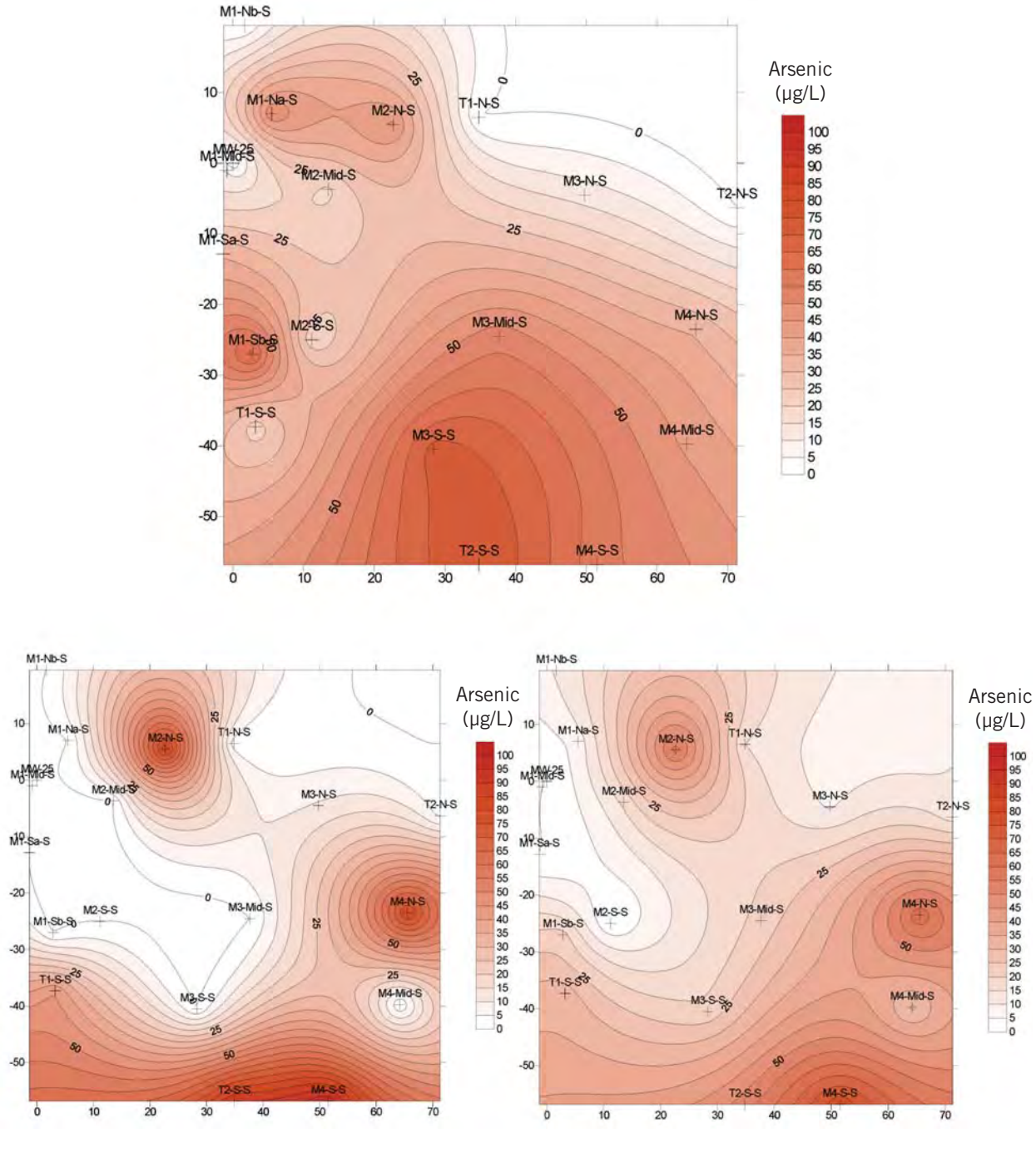

Figure 21. (Top Figure) Pre-oxidation (February, 2013) shallow (7-10') arsenic concentration (µg/L) at Parris Island, SC MCRD Site 45. Similar sample locations were also collected in the deep aquifer as in the shallow aquifer. All ground water samples collected in the deep (10.25-12.25') zone of the aquifer were reported as non-detect for arsenic. (Bottom Left Figure) Post-oxidation 3 (June, 2014) shallow (7-10') arsenic concentration (µg/L) at Parris Island, SC MCRD Site 45. (Bottom Right Figure) Post-oxidation 4 (February/March, 2015) shallow (7-10') arsenic concentration (µg/L) at Parris Island, SC MCRD Site 45.

4.6 Oxidant delivery and impact on total CVOCs in aquifer solids

Oxidant residuals from ISCO were visually observed in most of the post-oxidation soil cores collected at site 45. Manganese dioxide ($MnO_2(s)$) is characteristically dark in color, and permanganate is characteristically purple in color. Due to the clear acetate sleeves used to collect soil cores, the purple oxidant and the dark staining of the $MnO_2(s)$ in the aquifer material could be observed, indicating the presence of the oxidant and oxidant residuals. Although these visual indicators were often observed in soil cores removed from the subsurface, comprehensive mapping of the oxidant and/or oxidant residuals in the soil cores was not conducted.

The macro-, meso-, and micro-scale heterogeneities in lithology and depositional mixtures of sand, silt, clay, and total organic carbon impact the hydraulic conductivity, the transport of ground water, the predominant advective transport pathways involving aqueous phase CVOCs, and the transport and distribution of DNAPL in the subsurface. Similarly, variability in the TOC concentration in aquifer material will significantly alter the extent of CVOCs sorbed to the aquifer solids. These heterogeneities in aquifer composition and hydraulic properties ultimately impact the distribution of the CVOCs. Contrasting pre- and post-oxidation soil CVOC concentrations for the purpose of performance evaluation must recognize the inherent variability in subsurface systems and in the distribution of the CVOCs. Consequently, simple empirical differences between pre- and post-oxidation CVOC concentrations are used here as one line of evidence to assess treatment performance.

Post-oxidation soil cores were collected in high CVOC concentration areas and were consistent with locations where the permanganate oxidant was injected. Soil cores were not collected in downgradient areas of the plume, where CVOC concentrations were limited and where oxidant injection did not occur. Sub-cores were collected from the 17 core locations and analyzed using similar procedures as used during the pre-oxidation soil sampling program. Based on the (X, Y) coordinate system used in the study, distance calculations were performed to quantify the distance between the pre- and post-oxidation points using the distance formula (Eqn. 3).

$$\text{Distance (d)} = [(X_2-X_1)^2 + (Y_2-Y_1)^2)]^{1/2} \qquad \text{Eqn. 3}$$

Where,

X_1 and Y_1 = the X, Y coordinates for the first point

X_2, Y_2 = the X, Y coordinates for the second point

d = distance between the two points

The distance calculations were made to contrast the vertical distribution of the concentration of CVOC in soil ($[CVOC]_{SOIL}$) in post-oxidation sampling locations with 2-5 nearby pre-oxidation sampling points (Appendix D, Figures D.6-D.22). These sampling points ranged from 2.2 to 25.6 ft away from the post-oxidation sampling location. As per Eqn. 3, the average distance between pre- and post-oxidation soil core locations was 11 ft (n=47). The figures represent contrasting $[CVOC]_{SOIL}$ profiles with increasing distance from the source zone. Visual examination of Figures D.6-D.22 indicate that the post-oxidation $[CVOC]_{SOIL}$ are consistently lower than the pre-oxidation $[CVOCs]_{SOIL}$ profiles. There is one isolated depth interval where elevated post-oxidation $[CVOC]_{SOIL}$ were measured. Specifically, at the (-5, -4) sampling location (-14 ft bgs interval), the highest CVOC concentration was measured (576 mg/kg) (Appendix D, Figure D.6) indicating the presence of DNAPL. This result is consistent with a complex DNAPL distribution conceptual model, often observed at DNAPL sites, where nearby soil samples are contaminated with CVOC, but do not contain DNAPL (Appendix D, Figures D.6-D.23). The CVOC concentrations (0.3-10.4 mg/kg), measured in the same core at higher intervals (6.5-12 ft bgs), contained much lower CVOC concentrations. The (-5, -4) soil sample location was from the most contaminated portion of the source zone. Two other nearby sampling locations, (0, -5) (35.3-50.1 mg/kg) and (11, -3) (10.6-18.9 mg/kg), also exhibited persistent CVOCs concentrations at the 12-14 ft bgs interval indicating CVOC persistence at this location. Correspondingly, additional oxidant injection and long-term persistence of permanganate in this

general vicinity will be required for the continued oxidation and depletion of CVOCs in the source area.

The bar chart inset in Figures D.6-D.22 illustrates the average pre- and post-oxidation $[CVOCs]_{SOIL}$ for each core location, where the average value was based on the post-oxidation soil sample depth interval (*i.e.*, ≈ 8 – 14 ft bgs). The post-oxidation concentrations of total CVOCs are generally lower than the pre-oxidation concentrations. However, sampling locations close to and upgradient of the ordinate (0, 0), at MW 25-SL, indicated sporadic $[CVOC]_{SOIL}$ ranging from very low (1.1 mg/kg total CVOCs) to elevated (101.3 mg/kg total CVOCs), suggesting a CVOC source area. Specifically, in the X-distance range of -5 to 11 ft from MW 25-SL (*i.e.*, 5 ft upgradient to 11 ft downgradient), the average $[CVOC]_{SOIL}$ was 20.6 mg/kg and the 95% confidence interval was high (95% CI = 0 – 60.2 mg/kg), indicating significant variability. High variability in total CVOC concentrations is consistent with DNAPL source areas and is in agreement with the conceptual site model for site 45. Much lower $[CVOC]_{SOIL}$ variability was measured in the downgradient direction (*i.e.*, X-distance > 11 feet) from this zone, where the average $[CVOC]_{SOIL}$ is 1.29 mg/kg and the 95% CI indicated much lower variability in total CVOC concentration (95% CI = 0.90 – 1.60 mg/kg).

Overall, contrasting post-oxidation and pre-oxidation CVOC concentrations (Figures D.6-D.22) indicated a declining trend in post-oxidation CVOC concentrations. The declining trend is attributed to the successful delivery of permanganate oxidant into these areas and the subsequent oxidation of the CVOCs. The $[CVOC]_{SOIL}$ data provide additional evidence of the destruction of CVOCs in the soil media associated with the source area and the longitudinal axis of the plume. Although it is probable that chemical oxidation of CVOCs occurred in the aqueous, sorbed, and DNAPL phases of contaminated media, differentiation between the CVOC mass oxidized between these phases was not possible.

4.7 Molecular biology tools

Under aerobic conditions, oxygen is the most energetically favorable terminal electron acceptor (TEA) in the biodegradation of organic compounds. Given the limited solubility of oxygen in water, dissolved oxygen is rapidly depleted, resulting in anaerobic conditions (Huling *et al*., 2002). Under anaerobic conditions, however, the biochemical oxidation of organic compounds also occurs (Lovley and Phillips, 1986; Hutchins *et al*., 1998). The sequential order of TEA utilization under anaerobic conditions is nitrate (NO_3^-), manganese (Mn(IV)), ferric iron (Fe(III)), sulfate (SO_4^{2-}), and carbon dioxide (CO_2). Although biodegradation of BTEX has been correlated with this sequential utilization of TEA under field conditions (Borden *et al*., 1995), the distribution of the terminal electron accepting processes is highly dynamic in both time and space (Vroblesky and Chapelle, 1994). In anaerobic conditions, certain bacteria utilize the chlorinated ethenes: PCE, TCE, DCE, and VC, as electron acceptors in biotic reductive dechlorination processes. The net result is the sequential dechlorination of PCE and TCE, through daughter products DCE and VC, to non-toxic ethene, which volatilizes or can be further metabolized biochemically.

The microbial species *Dehalococcoides* (sp.) is capable of complete sequential dechlorination of PCE to ethylene, and *Dehalobacter* (sp.) can also dechlorinate chloroethenes. Dechlorination of CVOCs can be carried out by mixed cultures of dechlorinators under anaerobic conditions (Bradley, 2003); however, *Dehalococcoides* (Dhc) (spp.) is the only known bacteria that completely dechlorinates PCE and TCE to non-toxic ethene. Site-specific analysis of Dhc in ground water provides information regarding whether sufficient Dhc are present on site and potentially capable of carrying out this desirable biodegradation pathway. Further analysis of the functional Dhc genes responsible for encoding enzymes that transform the CVOCs also provides information regarding the microbial characteristics of the subsurface microbial

system. Microbial Insights Inc., a commercial laboratory, was contracted to analyze ground water sample filters for Dhc, and the enzymes responsible for the CVOC biotransformation pathway. Specifically, qTCE and qVC are the functional genes in Dhc that encode reductive dehalogenases for TCE and VC. The presence of TCE reductase indicates the ability to reduce TCE to DCE and VC. The presence of VC reductase indicates the potential for reductive dechlorination of VC to ethene, and the absence of VC reductase suggests that VC may accumulate (Microbial Insights Inc., 2014). *Dehalococcoides* sp. strain BAV1 couples growth with the reductive dechlorination of VC to ethene (Krajmalnik-Brown *et al*., 2004). Identification of these genes, qTCE and qVC, provides information on potential sustainability of the reductive dechlorination mechanism at the site. The comprehensive analysis of these microbial characteristics (Microbial Insights, CENSUS®), involving the enumeration of specific organisms or genes encoding specific biological functions, provides a direct avenue to investigate the potentials and limitations to implementing corrective action plan decisions and to target a variety of organisms involved in the reductive dechlorination pathway. Further, total Eubacteria is a measurement that targets universal regions of bacterial 16S rRNA genes to provide a broad index of total bacterial biomass.

Pre-oxidation (*i.e*., baseline) and post-oxidation ground water samples were collected from six micro-wells in the source area and analyzed for *Dehalococcoides*, the enzymes TCE-A reductase, BAV1 VC reductase, VC reductase, and total Eubacteria (cells/mL) (Table 7). The pre-oxidation microbial enzyme markers *Dehalococcoides* TCE-A reductase, BAV1 VC reductase, and VC reductase were notably absent as they were mostly reported as U (not detected). The same condition existed in the post-oxidation samples from five of the wells. The pre- and post-oxidation populations of total Eubacteria were measurable but a definitive trend between pre- and post-oxidation conditions was not established. For example, in four wells the total Eubacteria populations increased but in two wells it decreased. Lu *et al*. (2006) suggested that a density of 10^7 Dhc cells/L is necessary for reductive dehalogenation natural attenuation rate that provides significant degradation in a reasonable time frame. The ground water samples collected from the micro-wells located in the source zone do not meet this general requirement and therefore no firm conclusions are possible regarding the impact of ISCO on biotic natural attenuation processes in the source zone.

Table 7. Pre- and post-oxidation molecular biology tool analysis (Microbial Insights) [(1)] for micro-wells M1-Mid-shallow and deep, M1-NA-shallow and deep, and M1-SA-shallow and deep. The baseline (pre-oxidation) sampling event occurred on 6/21/2013; oxidant injections 1 and 2 occurred on 6/23-29/2013 and 9/22-27/2013, and post-oxidation 2 (post-ox 2) ground water sampling occurred 2/13/2014.

Micro-well ID	Sample Date	Sampling Event	*Dehalococcoides* (cells/mL)	tceA Reductase (cells/mL)	BAV1 VC Reductase (cells/mL)	VC Reductase (cells/mL)	Total Eubacteria (cells/mL)
M1-Mid-S	6/21/13	Baseline	0.5 U	0.5 U	0.5 U	0.5 U	3,330
	2/13/14	Post-ox 2	0.5 U	0.5 U	0.5 U	0.5 U	1,930
M1-Mid-D	6/21/13	Baseline	0.3 U	0.3 U	0.3 U	0.3 U	479
	2/13/14	Post-ox 2	1.7	1.7	1.7	1.7	3,390
M1-NA-S	6/21/13	Baseline	0.5 U	0.5 U	0.5 U	0.5 U	5,770
	2/13/14	Post-ox 2	0.7 U	0.7 U	0.7 U	0.7 U	9,290
M1-NA-D	6/21/13	Baseline	0.5 U	0.5 U	0.5 U	0.5 U	437
	2/13/14	Post-ox 2	0.5 U	0.5 U	0.5 U	0.5 U	1,200
M1-SA S	6/21/13	Baseline	0.5 U	0.5 U	0.5 U	0.5 U	693
	2/13/14	Post-ox 2	0.8 U	0.8 U	0.8 U	0.8 U	21,200
M1-SA D	6/21/13	Baseline	0.3 U	0.3 U	0.3 U	0.3 U	3,390
	2/13/14	Post-ox 2	0.6 J	0.7 U	0.7 U	0.7 U	2,590

[1]U - analyte not detected above reporting limit; J - concentration estimated.

The MBT results were derived from samples collected in micro-wells in the heart of the source area. This suggests that limited quantities of the microbial indicators may have been measured as a result of inhibitory levels of CVOCs known to occur in these micro-wells. Specifically, the pre-oxidation average CVOC was 31.4 and 32.2 mg/L in the three shallow and deep wells, respectively. Subsequently, three aggressive injections of $NaMnO_4$ in the source area near these wells caused additional microbial toxicity. Therefore, it is proposed that the low concentrations of pre- and post-oxidation microbial indicators: *Dehalococcoides*, TCE-A reductase, BAV1 VC reductase, VC reductase, and total Eubacteria are consistent with highly toxic conditions for microbial populations both from elevated concentrations of CVOCs, or $NaMnO_4$, or both. Future efforts to assess the impact of ISCO on biotic natural attenuation should include the collection of ground water samples in a downgradient direction from the source area. In a previous study at Site 45, several groundwater samples collected near, within 50-200 ft, the source area contained *Dehalococcoides* sp. at $>10^7$ cells/L. This suggests that sufficient quantities of *Dehalococcoides* sp. were present and robust biodegradation of the CVOCs to ethylene is possible in downgradient portions of the plume (Vroblesky *et al*., 2009).

4.8 Compound-specific isotope analysis (CSIA)

CSIA can potentially distinguish destructive chemical oxidation transformation reactions from non-destructive mechanisms (*e.g.*, dilution, displacement, dispersion, desorption, advection, etc.). Stable isotope analysis of carbon involves measurement, quantifying, and contrasting of the relative abundance of the naturally occurring stable isotopes of carbon, ^{13}C and ^{12}C, in organic chemicals (US EPA, 2008). Since the chemical bonds associated with ^{13}C are stronger than ^{12}C, ^{13}C destructive reactions are slower and permit the abundance of ^{13}C to increase over time in the parent compound, relative to ^{12}C. In contrast, dilution, displacement, and desorption mechanisms that are non-destructive have little impact on the distribution of ^{13}C and ^{12}C in an aqueous solution containing the organic compounds. Consequently, destructive reactions such as chemical oxidation and biodegradation will preferentially destroy ^{12}C, resulting in a higher quantity of ^{13}C, relative to ^{12}C. Typically, the abundance of ^{12}C is much greater than ^{13}C, which represents approximately 1% of the total naturally occurring organic carbon.

In order to ensure inter-laboratory comparability and accuracy, the ratios of ^{13}C and ^{12}C are expressed relative to an international standard. Therefore, for a "sample" compound, the data are reported as $R_{sample} = (^{13}C_{sample}/^{12}C_{sample})$ relative to the ratio of the international standard (R_{std}) where $R_{std} = ^{13}C_{std}/^{12}C_{std}$. Measured values are reported as $\delta^{13}C$ (Eqn. 4) (US EPA, 2008).

$$\delta^{13}C\ (‰) = \frac{[^{13}C_{sample}/^{12}C_{sample}] - [^{13}C_{std}/^{12}C_{std}]}{[^{13}C_{std}/^{12}C_{std}]} \times 1000 \quad \text{(Eqn. 4)}$$

Since the resulting δ values are very small (*e.g.*, for $\delta^{13}C$, typically < 0.05), they are generally multiplied by 1000 for convenience and reported as parts per thousand or "per mill", indicated by the symbol ‰ (US EPA, 2008). In the common delta (δ) notation, the deviation of the stable isotope value of the sample from the standard will be either negative or positive. A negative value means that the sample is depleted in its ^{13}C-content, relative to the $^{13}C/^{12}C$ content of the standard whereas a positive sign implies an enriched ^{13}C-content (US EPA, 2008).

To be significant, the extent of fractionation must be greater than the total analytical uncertainty. In addition, the observed difference in the values of $\delta^{13}C$ must exceed the spatial and temporal variability introduced by different sources of contamination at the site, by the mixing of ground water flow lines, and by what are typically the minor effects of processes such as sorption or volatilization. The total analytical uncertainty for $\delta^{13}C$ analyses was estimated to be approximately ± 0.5‰ (US EPA, 2008). As a result, the observed fractionation must be at a minimum > 1‰. To ensure reliable interpretation, it was recommended that fractionation on the order of 2‰ be used as a criterion for positive identification of degradation in order to minimize the possibility of an erroneous interpretation (US EPA, 2008).

Pre-oxidation (*i.e.,* baseline) and post-oxidation ground water samples were collected from six micro-wells in the source area and analyzed for CVOCs; and CSIA was performed for the corresponding CVOCs from the same micro-wells (Table 8). CSIA values were not reported by the contract laboratory for some ground water samples and therefore comparisons between pre- and post-oxidation conditions were not possible in these cases (these cells are shaded in gray in Table 8). As indicated by others (US EPA, 2008), spatial and temporal variability in CVOCs and CSIA can result from analytical variability, the heterogeneous distribution of CVOCs at the site, the mixing of ground water flow lines, and by the variability in transport and fate processes such as sorption or volatilization. Further, non-equilibrium conditions resulting from oxidant injection and incomplete oxidant reaction can also introduce variability in CVOCs and CSIA results. Consequently, as recommended by US EPA (2008), fractionation values of < 2 ‰ between pre- and post-oxidation were omitted from the pool of results (these cells are shaded in blue in Table 8). An increase in the abundance of ^{13}C, relative to ^{12}C, is an indication of the chemical oxidation of CVOCs. This condition occurred in six of the samples analyzed, indicating evidence of CVOC destruction in the source area (Table 8, shaded in yellow). Conversely, there were four ground water samples where both the CVOC concentration and the $^{13}C/^{12}C$ increased (Table 8, shaded in red). One possible explanation for this occurrence could be that pre-oxidation conditions involved aggressive biodegradation that was responsible for lower CVOCs and CSIA. After ISCO activities, a temporary decline in biodegradation due to ISCO, in conjunction with CVOCs influx due to rebound and upgradient CVOC-contaminated ground water, could have raised both the CVOC concentration and the CSIA values. The post-oxidation CVOC and CSIA data represent a highly transient non-equilibrium ground water chemistry condition resulting from disturbances in ground water flow paths from fluids injection, chemical oxidation destruction of CVOCs, inhibitory response of biotic processes to the highly oxidative conditions, spatial variability in CVOC distribution, major changes in redox and concentration gradients, etc. Overall, the CSIA results are variable and represent ground water in a highly mixed and disturbed condition. Consequently, due to these complexities, it was difficult to establish firm and definitive trends in the analytical results. Nevertheless, it can be concluded that in several wells located close to the oxidant injections (*i.e.*, M1-Mid-S and D, M1-NA-S), where significant reductions in CVOCs were measured, the CSIA data provides proof of concept that PCE, TCE, DCE, and VC were destroyed.

Table 8. Pre- and post-oxidation CSIA (Microseeps, Inc.) and CVOCs summary table for micro-wells M1-Mid-shallow and deep, M1-NA-shallow and deep, and M1-SA-shallow and deep. The baseline (pre-oxidation) sampling event occurred on 6/21/13; oxidant injections 1 and 2 occurred on 6/23-29/2013 and 9/22-27/2013, and post-oxidation 2 (post-ox 2) ground water sampling occurred 2/13/2014[1, 2].

Micro-well ID	Sample Date	Sampling Event	PCE $\delta^{13}C/^{12}C$ (‰)	TCE $\delta^{13}C/^{12}C$ (‰)	Cis 1,2-DCE $\delta^{13}C/^{12}C$ (‰)	VC $\delta^{13}C/^{12}C$ (‰)
M1-Mid-S	6/21/13	Baseline	-28.52	-29.81	-29.41	-23.26
	2/13/14	Post-ox 2	-24.03	-22.39	-18.68	-
CVOCs (µg/L)	6/21/13	Baseline	67100	10800	7310	1180
	2/13/14	Post-ox 2	6400	1400	2300	61
M1-Mid-D	6/21/13	Baseline	-27.66	-29.9	-29.97	-
	2/13/14	Post-ox 2	-24.87	-15.1	-14.09	-
CVOCs (µg/L)	6/21/13	Baseline	76300	3990	536	1.7
	2/13/14	Post-ox 2	13000	3900	39000 Q	40 U
M1-NA-S	6/21/13	Baseline	-	-	-25.53	-25.85
	2/13/14	Post-ox 2	-24.23	-24.54	-23.86	-16.80
CVOCs (µg/L)	6/21/13	Baseline	1670	1110	154	22.3
	2/13/14	Post-ox 2	80	44	58	9.4
M1-NA-D	6/21/13	Baseline	-14.81	-14.75	-25.28	-
	2/13/14	Post-ox 2	-23.68	-23.62	-25.08	-17
CVOCs (µg/L)	6/21/13	Baseline	2050	627	3630	5
	2/13/14	Post-ox 2	92	48	6100	U
M1-SA-S	6/21/13	Baseline	-18.91	-29.55	-43.87	-
	2/13/14	Post-ox 2	-24.64	-25.04	-28.39	-
CVOCs (µg/L)	6/21/13	Baseline	60	47	34	0
	2/13/14	Post-ox 2	99	58	1500	U
M1-SA-D	6/21/13	Baseline	-23.58	-24.87	-32.27	-
	2/13/14	Post-ox 2	-24.85	-26.42	-31.15	-
CVOCs (µg/L)	6/21/13	Baseline	2640	2780	2160	2
	2/13/14	Post-ox 2	6000	4200	3600	U

[1] Shading description for cells:
light gray - CSIA data not reported for either baseline or post-oxidation sampling event 2, or both, preventing a comparison of data;
light blue - data eliminated due to low fractionation criteria (< 2‰);
yellow - aggressive oxidation, indicated by CSIA where ^{13}C becomes more abundant relative to ^{12}C (*i.e.*, $^{13}C/^{12}C$ is less negative as per Eqn 4 in section 4.8);
red - increase in both CVOC and CSIA, suggesting possible influx of CVOCs.

[2] U - contaminant not detected above reporting limit; J - concentration estimated; Q - surrogate recovery failure.

4.9 Preliminary Cost Analysis

The cost of remediation is of great interest to the site stakeholders (*e.g.*, federal, state, and potentially responsible party (PRP) project managers). Lowering the cost of remediation is an important consideration in the overall remedial goal; however, the successful outcome is also contingent upon achieving the remedial goals. For example, greater costs are justified when a more expensive remedial option is effective and achieves the remedial goal, relative to a less-costly remedial alternative that falls short of achieving the remedial goal. Further, greater remedial costs may also be considered relative to a desired time frame for remediation.

The two sections below present a preliminary cost analysis involving actual costs of the pilot-scale ISCO demonstration. The pilot-scale demonstration of ISCO is expected to be the first stage of a final remedy at site 45. Therefore, the costs presented are intended to be used to project additional costs associated with a final ISCO remedy. As will be discussed below in section *5.8 Recommendations*, assuming the recommended limited-scale ISCO and monitoring activities are adopted, projected costs for ISCO deployment as a final remedy will be limited. The costs presented below do not include travel costs. The site 45 pilot-scale ISCO demonstration originated as a research study and travel costs for EPA research staff traveling from Oklahoma to South Carolina would be unlikely to be incurred assuming remediation deployment involved local or regional expertise. Labor and analytical costs represented the primary costs for the site characterization. The primary remediation costs were divided among injection system capital costs, oxidant, labor, and analytical costs.

4.9.1 Site characterization

The collection and analysis of aquifer cores and ground water samples were carried out to develop and refine the site conceptualization model.

Cores. The initial site characterization for the pilot study consisted of the collection of soil cores along six transects of the ground water plume, involving three locations at each transect (Figure 4). Pre-oxidation soil cores were collected to better understand contaminant distribution in aquifer materials at the site, and post-oxidation soil cores were collected and analyzed to assess treatment performance, and to quantify the remaining contaminant residuals. The soil cores were collected using Geoprobe equipment, owned by RSKERC, so no capital costs were incurred. Each soil core characterization event incurred costs for items such as core sleeves and caps, dry ice to preserve the cores for shipping, and other miscellaneous supplies. The bulk of the cost incurred for the site soil characterization involved labor of the personnel during the field work, and in analytical costs for analyzing the cores.

Micro-wells. Micro-wells were installed to use as sentry wells, to better understand contaminant distribution in ground water, and to help assess the ISCO process and treatment performance. The costs incurred for these wells included micro-well screens, tubing, traffic-rated vault boxes, and miscellaneous supplies, such as grout. The bulk of the cost involved labor by the RSKERC field team and research staff.

Analytical. Analytical costs for the site characterization activities at site 45 were incurred for analysis of chlorinated compounds, metals, and field parameters in ground water samples, and for chlorinated compounds in soil samples. The laboratory ground water and soil analyses for the site characterization were predominantly conducted using contract staff at RSKERC. These costs depended on the level of analyst and the time spent for the analyses, and cannot be easily quantified. A number of field parameters for ground water were measured in the field, incurring costs for sample containers, reagents, disposable PPE, and the labor required for sample collection and field analyses. During the course of this project, the RSKERC was unable to retain the on-site analytical contract. Consequently, off-site analyses of ground water and soil samples at Shealy Environmental Inc. (Columbia, SC) were conducted.

Personnel. Labor costs were the second of the two major categories of expenses for the site characterization activities at site 45. The duration (in days) of the work conducted for site characterization and the level of personnel involved have been estimated (Table 9). The monetary cost for the labor performed for the site characterization activities is difficult to calculate, due to different rates for different personnel.

Table 9. The duration of work days, the number of personnel utilized, and the personnel work days associated with the site characterization and remediation activities for the pilot-scale ISCO demonstration at Site 45

Activity	Duration of work (days)	Number of Personnel utilized	Personnel days (days)
Site Characterization			
Initial site reconnaissance	1	Research staff 1	Research staff 1
Soil core collection	4	Research staff 2 Field crew 4	Research staff 8 Field crew 16
Micro-well installation	5	Research staff 2 Field crew 2	Research staff 10 Field crew 10
Total days for site characterization	10		Research staff 19 Field crew 26
Remediation			
Baseline sampling	1.5	Research staff 2	Research staff 3
First injection	9	Research staff 2 Field crew 3	Research staff 18 Field crew 27
First post oxidation sampling	1.5	Research staff 1 Field crew 1	Research staff 1.5 Field crew 1.5
Second injection	5	Research staff 1 Field crew 2.5	Research staff 5 Field crew 12.5
Second post oxidation sampling	1.5	Research staff 1 Field crew 1	Research staff 1.5 Field crew 1.5
Third injection	7	Research staff 1 Field crew 2	Research staff 7 Field crew 14
Third post oxidation sampling	1.5	Research staff 1 Field Crew 1	Research staff 1.5 Field Crew 1.5
Post-oxidation soil core sampling	2	Research staff 1 Field crew 2	Research staff 2 Field crew 4
Total for remediation	29		Research staff 39.5 Field crew 62

4.9.2 Remediation

The costs for the remediation portion of the pilot-scale ISCO deployment at site 45 included the capital costs of the injection equipment, injection process equipment (peristaltic pumps), oxidant, analytical, and personnel costs. The cost of the injection unit was $15,400, the supporting injection process equipment was approximately $4,500, and the total capital cost was about $19,900. The total cost of the oxidant injected was approximately $26,000.

Injection system. An injection system was constructed specifically to be used for the pilot-scale ISCO demonstration at Site 45 (Appendix B – Oxidant Injection System). The ISCO approach was to carry out three oxidant injection events involving increasing oxidant loading for each successive event, and rigorous monitoring between oxidant injections. Consequently, a portable injection system was required that could be mobilized, set up on-site, safely and effectively deployed, and demobilized. The design included sizing the injection system (*e.g.*, dimensions, injection solution volume, weight loaded/empty), three-manifold injection arms, safety considerations, portability, corrosion resistant components from inlet to outlet, etc. The injection system was designed to allow additional injection lines to be added. For example, two injection lines were used during the first oxidant injection, and three injection lines during the third injection. The cost of the components for the injection system, including one injection arm, was $15,400. Additional injection lines could be added (*i.e.*, > 3 arms), with the cost being approximately $2,860 per injection arm. The field injection process utilized additional equipment such as a peristaltic pump and tubing to transfer the 40% oxidant into the mixing tank ($2,946), Geoprobe drive caps (custom-made in-house), top-down injection tools and drive rod ($1,211), and oxidant neutralizer and absorbent socks ($351), for a total cost of $4,508.

Oxidant. The oxidant was purchased from Carus Corp. (Peru, IL), and included 5-gallon pails of 40% liquid sodium permanganate (*i.e.*, Carus Corp., Remox-L, 57 lb Jerrican). The oxidant cost approximately $2.50-$2.70/lb of 40% $NaMnO_4$ (*i.e.*, $143-$154/5-gallon Jerrican). The cost of the oxidant plus shipping charges resulted in an approximate actual cost of $175 per five-gallon pail. The number of 40% $NaMnO_4$ pails and cost for the 1st, 2nd, and 3rd oxidant injections was 17 pails ($2,975), 43 pails ($7,525), and 89 pails ($15,575), respectively. The total cost of oxidant, including freight, was $26,075.

Analytical. Analytical costs for the remediation activities of the pilot-scale study at site 45 were incurred primarily for analyses of chlorinated compounds and field parameters in ground water. Additional analytical costs occurred throughout the study, involving the analyses of soil cores used to further delineate CVOC concentrations in the source area. The additional site characterization was needed to help focus oxidant injections in the source area. The laboratory ground water analyses for the ISCO baseline sampling were conducted using contract staff at RSKERC. The laboratory ground water analyses for the subsequent ISCO performance monitoring were conducted using Shealy Environmental (Columbia, SC). The basic cost for CVOC analysis of ground water samples and methanol extracts of soil was $50/sample. A number of field parameters for ground water were measured in the field, incurring additional costs for sample containers, reagents, disposable PPE, and the labor required for sample collection and field analyses.

Personnel. Labor costs contributed significantly to the total cost of the remediation activities at site 45. The duration of the work and the level of personnel involved in remediation and monitoring the remediation (*i.e.*, additional site characterization) are approximated and summarized (Table 9). The cost for the labor performed for these activities will vary based on the hourly rate of personnel, therefore, “personnel-days” equivalence is reported and can be used to estimate cost based on local and/or regional hourly rates.

The duration of the first injection trip was lengthy since the research and field crew were conducting the initial set-up, operation, and monitoring procedures for the injection equipment for the first time. This was required for the safe and effective deployment of the oxidant injection process. The total volume of oxidant solution injected during the first, second, and third injections was 2688, 4450, and 8814 gallons, respectively. One method of analyzing manpower efficiency is to examine the ratio of the volume of oxidant injected and the combined (*i.e.*, research and field crew) personnel-days. Given the personnel-days (Table 9), the combined oxidant injection efficiency was 60, 254, and 419 gallons oxidant/personnel-day for the 1st, 2nd, and 3rd injections, respectively.

5. Discussion

5.1 Injection equipment, design, and impact

5.1.1 Injection equipment

The cost of the oxidant injection system was approximately $15,400, which included one injection arm. Each injection arm, including the 45 ft injection hose and the injection tip, cost $2,860 each, excluding the GeoProbe rod (Appendix B. *Detailed description of injection equipment (schematics, manufacturers, part numbers, cost)*). The injection pallet proved to be compact and portable, making it easy to accommodate transport of the system between the RSKERC facility and the ISCO site. The pallet has a 4 ft × 4 ft footprint and was easily transported on a flatbed trailer or on the bed of a 1-ton truck. The injection arms are easily removed from the injection pallet, allowing for easy storage and transport when not in use. A temporary catchment system was constructed for the injection pallet, serving as secondary containment. This was performed for added safety, to contain the oxidant, if there were an unexpected catastrophic spill. The injection pallet was moved to different locations during injection events to accommodate large distances between the source area injection locations and other injection locations further downgradient. At little additional cost, a longer injection hose (60 ft vs 45 ft) was purchased, allowing greater reach between the injection pallet and the injection location. Even longer hoses could have been ordered that would have been able to access all the injection locations without moving the injection pallet. Once mobilized and set up, the injection pallet was moved between injection locations using multiple methods, including a fork lift, a Tommy-lift on the 1-ton truck, and the GeoProbe sonic rig that the field crew mobilized for a subsequent project on the second leg of the field trip.

The addition of the 2nd and 3rd arms on the injection pallet allowed injection to occur at three locations simultaneously. This contributed significantly to the overall efficiency in delivering the oxidant into the subsurface. Each arm was individually equipped with a flow dampener, pressure relief valve, pressure control valve and return line, injection pressure valve, flow meter, and emergency shut-off valve. This design allowed each of the injection arms and tips to be operated individually in the delivery of the specific oxidant dosage for each injection location. An injection tip could be advanced to another injection interval or moved from one location to another while simultaneously injecting into the other two injection tips, thus being efficient, effective, and flexible.

5.1.2 Incremental benefits of soil core sampling and analysis

Ground water samples represent an integrated measure of CVOCs in the subsurface. For example, CVOC concentrations in ground water spatially represent the sorbed and DNAPL mass distributed nearby in the subsurface. Specifically, CVOCs partition into the ground water from the aquifer solids and DNAPL. However, it is difficult to refine in detail the distribution of CVOCs in the subsurface using ground water samples alone. This is especially true in the vertical scale, given the screen lengths of monitoring wells that tend to represent the average CVOC concentration. Short screened intervals, such as the 2 ft stainless screened micro-wells used in the study area at this site, help to limit the vertical averaging of long screened intervals.

Collection and analysis of soil cores for CVOC can help to refine the CVOC conceptual model, especially in the vertical scale. Examination of historical ground water concentration data from monitoring wells at the site suggested that CVOC contamination extended from 3-18 ft bgs. This observation is due to the wells' screen lengths, which occur over this vertical interval. Constructing ground water monitoring wells with screen lengths of 5-10 ft, or greater, is common. Consequently, the length of the well screen can preclude an accurate vertical discretization of CVOCs present in the aquifer solids or as DNAPL. At this site, the majority of the CVOC contamination was found within a loose sand layer. Consequently, wells partially screened over the loose sand layer, containing CVOC contamination, would suggest that contamination occurred over the entire length. A 5 ft well screen is considered to be relatively short, but these wells partially screened across a highly contaminated interval may give a false impression that contamination extends over a greater vertical interval than it actually does. The benefit of the soil core data was that it allowed greater differentiation between contaminated and uncontaminated intervals and therefore established a relatively narrow contaminated interval. This information allowed the development of an oxidant delivery strategy that predominantly targeted the 8-12 ft bgs contaminated interval rather than the 3-18 ft bgs interval. Thus, the soil core data provided the scientific basis to reduce the vertical interval over which ISCO should be deployed from 15 ft (*i.e.*, 3-18 ft bgs) to 4 ft (*i.e.*, 8-12 ft bgs). This is nearly a 75% reduction in the vertical interval requiring treatment. If oxidant were injected outside the targeted interval of 8-12 ft bgs, the oxidant would have served a limited purpose. This is especially the case at lower depths where the NOD was high due to the elevated organic material, the CVOC concentrations were low or non-detect, and the oxidant transport and persistence would have been limited. It is evident that this modification in the ISCO design resulted in an overall cost savings to the pilot-scale ISCO demonstration project. In addition to the cost savings attributed to purchasing a smaller quantity of oxidant, significant cost savings resulted in a reduction in the labor costs associated with injecting a much lower volume of oxidant. The investment in additional site characterization involving soil core sampling and analysis provided a high value dividend, a refined conceptual site model. This allowed ISCO activities to be focused over a specific targeted interval which limited remedial costs.

5.1.3 Oxidant delivery design and methods

The oxidant delivery design and methods used in the pilot-scale ISCO demonstration at site 45 resulted in more effective and efficient oxidation of CVOCs. Specifically, narrow ROIs, short vertical screened injection intervals, low injection pressure, outside-in oxidant injection, and total porosity oxidant volume design were used to help assure oxidant delivery to the targeted zones. The narrow ROIs required additional labor due to the greater number of injection locations required to cover the source areas, but did not add significantly to the overall injection time. The short 2-ft vertical screened injection intervals required the injection tip to be advanced in 2 ft increments at the same injection location. Relative to longer injection tips, this additional injection time at each injection location was marginal. However, the short (2-ft) injection increments limited the potential of injecting oxidant across vertical intervals with contrasting hydraulic conductivity. Collectively, these oxidant delivery methods and design were beneficial as they helped to limit the role of preferential pathways and the unintentional delivery of oxidant into non-target areas, and to increase the probability and confidence that the oxidant was delivered to the targeted zones.

The role of preferential pathways during oxidant injection and remedy failure can be correlated with high injection pressure (Suthersan *et al.*, 2011). High injection pressures can also promote fracturing, fluid movement along the fractures, and compromise the ability to uniformly distribute the oxidant. In these cases, delivery of oxidant into the subsurface does not equate to appropriate distribution. Parameter values for density of dry soil and saturated soil, the thickness of the vadose zone, and the height of the saturated zone above the injection point, were used to calculate the maximum injection pressure (Appendix A). Given the shallow injection depths, and hydrostatic and overburden pressure to counter-pressure the oxidant injection pressure, low injection pressures were calculated. For the injection intervals of 8-10, 10-12, and 12-14 ft bgs, maximum injection pressures were 4.8, 5.6, and 6.4 lb/in^2 (psi) respectively. Therefore, it was evident that low injection pressures were critical for effective oxidant delivery at site 45 to limit the potential for breakout and daylighting of the oxidant. Because of the low flow rate under this low oxidant injection pressure, an informal trial and error method was used to test higher injection pressures. As a result, an operational injection pressure of ≤ 10 lb/in^2 was developed as a guideline. Due to the frictional head loss of the injected fluids in the injection hose, connectors, and injection tip, the downhole pressure was less than the gauge pressure on the injection arm. The ≤ 10 lb/in^2 injection pressure permitted a higher flow rate of oxidant, while preventing breakout and daylighting of the oxidant. Higher injection pressures *(i.e.*, > 10 lb/in^2) were avoided as this could have resulted in daylighting of the injected solution.

5.2 Critical analysis of oxidant loading

Concepts and fundamentals used to design the volume of oxidant injected into a targeted treatment zone often involves porosity. A detailed critical analysis of oxidant loading has been presented in a manuscript entitled, "In Situ Chemical Oxidation: Oxidant Volume Design Considerations", and is included as Appendix E (Huling *et al.*, 2016a). A summary of the salient technical issues from the manuscript, involving oxidant loading design, will be presented here. Also, ISCO design parameters used at site 45 will be contrasted with conventional ISCO design parameters to clarify the unique and aggressive oxidant loading design approach used.

5.2.1. Estimating oxidant volume for injection

The targeted treatment zone (TTZ) defined here refers to the contaminated volume of porous media in a source area requiring oxidative treatment. Adequate coverage of the oxidant in the TTZ requires the delivery of a sufficient volume of oxidant, containing a sufficient mass of oxidant, to achieve the treatment objectives. An estimate of the volume of oxidant to inject to fill the pore volume in the TTZ can vary depending on the assumptions used in the calculation. Assuming the simplified radial-flow, cylindrical, porous media conceptual model (Eqn. 1) (refer to section *3.2.11 Natural oxidant demand and oxidant loading*), two methods used to estimate the volume of oxidant are contrasted, involving the mobile porosity and the total porosity. The oxidant injected into the subsurface will fill the pore spaces in the unconsolidated porous media. The total porosity (η) of unconsolidated porous media is defined as the volume of voids (V_V) relative to the total volume (V_T) of aquifer material ($\eta=V_V/V_T$). However, unconnected, poorly connected, and dead-end pores are responsible for a fraction of water in the porous media but minimally contribute to fluid displacement.

Therefore, the concept of total porosity was broadened to include effective porosity, and refers to that fraction of the total volume of pore space where pore fluid can be readily displaced; *i.e.*, the interconnected pore volume or void space in an aquifer that contributes to fluid flow or permeability. Specifically, the fraction of the total porosity that contributes to advective flow and transport of ground water in aquifers is the mobile porosity (θ_M), and the portion of the void space that does not contribute to the advective flow of ground water, and behaves as immobile or slowly moving ground water, is the immobile porosity (θ_I) (Payne *et al.*, 2008). The total porosity is the sum of mobile and immobile porosity ($\eta = \theta_M + \theta_I$). The selection of mobile porosity or total porosity in designing the volume of oxidant to be injected into the TTZ can have major implications to ISCO.

5.2.2 Contrasting ISCO design at site 45 with other treatment systems

Krembs *et al*. (2010; 2011) compiled methods and results of field applications of ISCO case studies, specifically involving permanganate ISCO sites. Several oxidant injection design parameters were compiled including the design and observed ROI (ft), oxidant dosage (g/kg), number of pore volumes delivered, number of delivery events, and duration of delivery events (days) (Table 10). The ISCO design parameters from the MCRD site 45 ISCO project were also compiled to contrast with the ISCO database used by Krembs *et al.* (2010; 2011) (Table 10). A critical analysis of the median design parameters reported by Krembs *et al.* (2010; 2011) is preceded by the caveat that the number of case studies for the median value of each design parameter varied, and therefore only general observations are possible.

Table 10. A compilation of the median value for ISCO design parameters from field application case studies (Krembs *et al.*, 2011) contrasted with design details used in the pilot-scale ISCO demonstration at Site 45.

Design Parameter	Median Value Reported Krembs *et al.* (2011)[1]	Site 45 ISCO project Parris Island, SC
Design ROI (ft)	14 (n=29)	2-4
Observed ROI (ft)	25 (n=11)	≈ 2-4
Oxidant dose (g/kg)	0.4 (n=24)	3.8-5.2[2]
Number of pore volumes delivered	0.16 (n=32)	1
Number of delivery events	2 (n=65)	3
Duration of delivery events (days)	4 (n=45)	5.5 (n=3)[3]
Vertical injection interval (ft)	NA[4]	2

[1] The median design value and number of case study sites is reported.
[2] The range in oxidant dose was estimated, assuming a bulk density of 1.2-1.6 g/cm^3.
[3] Average duration of delivery events = site mobilization, de-mobilization, and oxidant delivery.
[4] The vertical injection interval was not reported in Krembs *et al.* (2011).

Radius of Influence (ROI), Oxidant Dosage, and Pore Volume. The observed ROI (25 ft) is considerably greater than the design ROI (14 ft) (Table 10) suggesting that oxidant distribution was more extensive than designed. A firm explanation cannot be provided regarding this anomalous difference, but some speculation is warranted. The difference could be attributed to a number of factors, including an increase in the median ROI value simply based on the weighted values of the reduced number of case studies reported. Assuming preferential pathways, a disproportionate volume of oxidant could have been delivered into high permeability layers present within the screened interval. Non-uniform oxidant transport, perhaps unidirectional, and breakthrough in monitoring wells under these conditions may account for the misinterpretation and the large ROI discrepancy. Regardless of the design method or value of porosity used, the volume of oxidant required to achieve a 25 ft ROI, relative to a 14 ft ROI, would involve greater than 3× more oxidant volume. Heterogeneities in aquifer hydraulic properties invite vulnerability to disproportionate transport of the oxidant in preferential pathways. Smaller ROIs have several advantages including lower probability that preferential pathways will play a role in oxidant transport, greater potential for hydraulic control, greater accuracy in the spatial emplacement of the oxidant, and greater confidence that the oxidant can be delivered to the ROI. However, a reduction in the ROI translates into smaller injection well spacing, leading to the installation of additional injection wells or more direct-push injection locations.

Natural oxidant demand impact on oxidant volume design. The design of ISCO oxidant loading, defined here as mass of oxidant per mass of soil (*i.e*., units of g oxidant/kg aquifer material), is sometimes based on natural oxidant demand (NOD) values measured in bench-scale studies. The NOD by soil and aquifer material for permanganate often involves a 48-hour test procedure (ASTM D 7262-07, 2007). However, the results from these tests must be qualified, given that the reaction between MnO_4^- and the reactants responsible for the NOD varies with time, the reactants are often comprised of multiple reactive components that exhibit varying reactivity (*i.e*., fast and slow reaction), the measured values of NOD may increase substantially with longer testing periods, and the reaction of MnO_4^- is concentration dependent (Mumford *et al*., 2005; Hønning *et al*., 2007; Urynowicz, 2008 Urynowicz *et al*., 2008; Xu and Thomson, 2009; Cha *et al*., 2012). More quantitative methods have been developed that utilize NOD results and can be used to project oxidant distribution and/or dosages (Heiderscheidt *et al.*, 2008; Borden *et al.*, 2010; Cha and Borden, 2012). Cha *et al.* (2012) reported that most of the NOD in soil and aquifer samples was slow reacting, and that results from the 48-hr NOD measurements are poor predictors of total NOD and cannot be used accurately to estimate long-term MnO_4^- consumption. Once the fast NOD fraction is rapidly consumed, the remaining MnO_4^- may persist for weeks to months, diffusing into low permeability zones where contaminants may reside. Use of these NOD results in field-scale applications must recognize that these laboratory measured oxidant demand values, whether based on short-term or long-term testing procedures, are derived from the total aquifer solids, including both the mobile and immobile porosity fractions of the media.

In one study, 50 samples of aquifer solids were analyzed from 12 different facilities in the US, where ISCO with MnO_4^- was being considered as a possible remedial alternative (Cha *et al.*, 2012). The total oxidant demand, measured over a long period (up to 41 days) in 80% of the samples exhibited a broad range in total NOD, between 0.24 and 18.8 g MnO_4^-/kg soil; and the median value was 3.33 g/kg, and the overall range in values was 0.2 to 150 g/kg. This range of values was similar to previously reported ranges (Mumford *et al.*, 2005; Huling and Pivetz, 2006; Hønning *et al*., 2007; Urynowicz, 2008; Xu and Thomson, 2009). The MnO_4^- dosage generally applies to the mass of MnO_4^- delivered per mass of aquifer material within the ROI, in the TTZ. The median value of MnO_4^- dosage reported by Krembs *et al*. (2010; 2011) is low (0.4 g/kg) (n = 24) (Table 10), relative to these values. Assuming that long-term persistence of MnO_4^- was needed to address contaminant mass transport and mass transfer limiting processes, contrasting the MnO_4^- dosage with total NOD values reported in the literature suggests that median range values used at many ISCO sites have been under-designed, either in terms of oxidant volume or concentration.

The pore volume (PV) represents the volume of voids within the TTZ, spatially defined by the ROI and vertical interval. The median number of permanganate pore volumes delivered (PV = 0.16; n=32 sites) (Table 10), as reported by Krembs *et al*., (2010; 2012), was less than the pore volume delivered (PV = 1.0) at site 45 (Table 10). The low pore volume of oxidant delivered appears inconsistent with both the ROI and the oxidant loading (Table 10). The volume of oxidant required to achieve a 25 ft ROI, relative to a 14 ft ROI, would involve greater than 3× more oxidant volume. Further, the post-injection oxidant dispersal would require significant persistence and transport to achieve coverage in the remaining 0.84 pore volume in a TTZ where oxidant was not initially delivered. Finally, the median oxidant dosage was low (0.4 g/kg) and it would be unlikely to persist long enough to broadly disperse within the TTZ while satisfying both the fast and slow acting NOD.

Overall, contrasting the ISCO design parameters reported by Krembs *et al.* (2010; 2011) and the pilot-scale ISCO demonstration at site 45 reveals significant differences. The median values for oxidant dosage (0.4 g/kg) and pore volume delivery (PV = 0.16) associated with the ISCO field site data base (Krembs *et al.* 2010; 2011) suggest a less aggressive, low oxidant volume ISCO design that appears to be consistent with a mobile porosity ISCO design. Such designs could result in incomplete oxidant distribution within the TTZ, insufficient oxidant dosage within the TTZ, and short duration oxidant persistence. Conversely, the more aggressive ISCO design at site 45 (Table 10), based on the total porosity oxidant volume design, involved a greater oxidant dosage (3.8-5.2 g/kg) and pore volume delivery (PV = 1), permitting long duration oxidant persistence (> 1 year) in some areas.

5.3 Assessment of achieving objectives

An accurate conceptual site model (CSM) was established by first examining existing data and information. This was followed by an aggressive pre-oxidation aquifer core and ground water sampling and analysis effort, designed to augment existing information and to fill data gaps. Multiple iterations in gathering additional site characterization data and information continued throughout the ISCO deployment, in an effort to develop and refine the CSM. This information was used to identify the source areas, which were subsequently targeted through the focused delivery of oxidant. A low cost, portable injection system was designed, constructed, and successfully deployed in the delivery of oxidant during three injection events. Post-oxidation ground water samples were collected from the nested, on-site micro-wells and used to assess the fate and transport of the permanganate and CVOCs. This information was used to guide subsequent oxidant dosages and injections into the source zones. Post-oxidation soil sampling and analysis was executed after the third and final ISCO deployment. Contrasting the pre- and post-oxidation CVOC soil data served as a metric by which to critically assess ISCO treatment performance. Overall, significant reduction in the mass of CVOCs in the ISCO targeted areas was achieved through the three oxidant injection events. This was apparent through the significant reductions in the CVOC concentration evident by contrasting CVOCs isocontours (Figures 14a and 14d) and the overall 91.5% and 75.5% reduction in total CVOC mass flux in the shallow and deep surficial aquifer (Figure 15.c).

5.4 Metals mobilization

There are two main mechanisms for increasing concentrations of metals in the ground water during ISCO: (1) the $KMnO_4$ or $NaMnO_4$ provided by the manufacturer may contain elevated levels of the heavy metals, and (2) mobilization of pre-existing redox- or pH-sensitive heavy metals (in situ) by the oxidant (Huling and Pivetz, 2006). The content of heavy metals in permanganate is dependent on the type and source of the oxidant. Because of the manufacturing process, $NaMnO_4$ has lower concentrations of heavy metals than $KMnO_4$. Both forms of the oxidant are manufactured in the US, Germany, and China. In 2006, Carus Chemical, a manufacturer of permanganate in the US provided analytical data for heavy metal impurities in their products. The remediation-grade $KMnO_4$ was developed by Carus Chemical to contain minimal quantities of metal impurities.

Chromium (Cr) and arsenic (As) have historically been the impurities of concern. Due to the low maximum contaminant level (MCL) in drinking water, established by EPA for these metals (0.1 mg/L total Cr MCL, 0.01 mg/L As MCL) (U.S. EPA, 2002), injection of technical-grade $KMnO_4$ may exceed the MCL for these elements. Generally, natural attenuation of these metals has been achieved within acceptable transport distances and time frames. Due to the possibility of exposure pathways and potential receptors, monitoring of these parameters may be needed under some conditions. A site-specific evaluation of the potential impact of heavy metals should be conducted to assess whether ground water monitoring for these metals is needed (Huling and Pivetz, 2006).

5.4.1 Chromium (Cr)

Enhanced transport of pre-existing, or naturally occurring, redox- or pH-sensitive metals may occur when deploying ISCO using permanganate. Changes in ORP and pH may change the fate and transport of chromium. Depending on pre-ISCO site conditions, permanganate ISCO can drop the pH of a system to below 3, or raise it to above 10 (Petri *et al*., 2012, and references therein). Further, highly oxidizing conditions involving permanganate ISCO can raise the system ORP to as high as +800 mV (Siegrist *et al.*, 2001). Oxidation of Cr(III) to Cr(VI) by MnO_4^-, and the subsequent mobilization, have been demonstrated in the laboratory (Li and Schwartz, 2000; Chambers *et al*., 2000b). Additionally, Cr(VI) and Ni mobilization has been observed under field conditions, where MnO_4^- has been injected (Crimi and Siegrist, 2003). Several field studies have reported anomalously high post-oxidation concentrations of Cr(VI), but natural attenuation of Cr(VI) was observed (Crimi and Siegrist, 2003), and cleanup concentrations have been achieved within acceptable transport distances and time frames (Chambers *et al.*, 2000a).

The ground water monitoring data for chromium (section *4.5.6 Metals*) indicated that chromium mobilization occurred as a result of injecting permanganate at site 45, but that attenuation mechanisms were efficient and effective, and that chromium persistence and transport was limited. Cr^{+6} undergoes natural attenuation through several mechanisms (McLean and Bledsoe, 1992; Palmer and Puls, 1994), including adsorption to MnO_2(s) and various other mineral species containing iron. Given the abundance of manganese and iron mineral species at the site (Figure 11), and the abundance of MnO_2(s) resulting from permanganate ISCO, elevated concentrations of chromium were not projected. Further, Cr^{+6} attenuation mechanisms were expected to play a major role, where chromium transport would be temporary, attenuation rapid, and transport distance limited. This pilot-scale study provided an excellent opportunity to assess whether metals mobilization was an issue, and whether attenuation occurred at a rate that was acceptable prior to implementing a final ISCO remedy.

5.4.2 Arsenic (As)

Table 11. Stability of arsenic species (Vu *et al.*, 2003).

Reducing Conditions		Oxidizing Conditions	
pH	As(III)	pH	As(V)
0-9	H_3AsO_3	0-2	H_3AsO_4
10-12	H_2AsO_3	3-6	H_2AsO_4
13	$HAsO_3^{2}$	7-11	$HAsO_4^{2}$

The two main forms of arsenic are arsenite (As(III)) and arsenate (As(V)), and specific arsenic species are dependent on redox conditions and pH (Table 11). It is apparent that numerous arsenic species may occur in ground water under varying pH and redox conditions. The reduced form, arsenite, is more toxic, soluble, and mobile than the oxidized form, arsenate. There are several mechanisms in which arsenic removal from the ground water may occur as a result of the oxidation of aquifer materials. Complex arsenic chemistry and variability in subsurface geochemical conditions contribute to the varying roles of removal mechanisms, and consequently the relative role of each mechanism may be difficult to quantify (Huling *et al*., 2016b).

As(III) and As(V) adsorb to iron (Fe) minerals found in aquifer material through complexation reactions, which form various As-Fe species (Sun *et al.*, 1999; Vu *et al*., 2003; Akai *et al.*, 2004). Under most environmental systems (*i.e*., pH 6-9), As(V) adsorbs more strongly than As(III), and Fe(III) complexes more arsenic than Fe(II). Complexation and adsorption of arsenic species involve electrostatic attraction between the anionic form of arsenic species (Table 11) and the cationic forms of iron and other positively charged sorption sites and surfaces. Through this mechanism, oxidized aquifer materials, containing greater quantities of ferric iron, have greater potential for the arsenic adsorptive removal mechanism than reduced aquifer materials.

Arsenic removal may occur by co-precipitation with iron and other metals. Specifically, in ground water containing Fe(II) and As(III), a shift towards oxidative conditions would result in the oxidation of As(III) to As(V), Fe(II) to Fe(III), the precipitation of ferric iron (Fe(III)) and co-precipitation, or coagulation, of As(V) (Johnston and Heijnen, 2001). Once MnO_4^- is applied to aquifer materials, the predominant manganese reaction byproduct is MnO_2(s), which is a stable form of manganese. Further, MnO_2(s) readily oxidizes As(III) to As(V), which becomes adsorbed to the hydroxyl group on the MnO_2(s) surface (Oscarson *et al.*, 1981; Sun *et al.*, 1999), forming birnessite ($(MnO)_2AsOOH$) (Manning *et al*., 2002).

Microbial mechanisms responsible for the reduction of arsenate to arsenite can result in the enrichment of arsenic in ground water (Akai *et al*., 2004). However, oxidative conditions resulting from the application of permanganate, persulfate, or H_2O_2, yield antiseptic conditions that are detrimental to microbial species and activity. Consequently, inhibition of microbial activity that carries out reductive processes, limits the arsenic dissolution process. The aquifer materials at site 45 exhibit high concentrations of naturally occurring iron (Fe 2-10 g/kg) and manganese (Mn 20-70 mg/kg) (Figure 11), and were supplemented with MnO_2(s) through the $NaMnO_4$ ISCO processes, suggesting that these arsenic attenuation mechanisms could play a significant role.

5.5 Natural attenuation

5.5.1 Proposed natural attenuation conceptual model

Based on the available data and information, several lines of evidence indicate that natural attenuation of the CVOCs was occurring in both the source area and downgradient zones of the aquifer. Attenuation of CVOCs occurs via biotic and abiotic reductive dehalogenation, and through other fate mechanisms (US EPA, 1998). The naturally occurring total organic carbon (TOC) (Figure 10) in the aquifer material is an available source of substrate material supporting biotic activity and serves as an important parameter, impacting CVOC fate and transport, potential electron donor materials, and the natural attenuation processes in the subsurface. A general increasing trend in TOC concentration with depth was observed, but a correlation between TOC and depth was not established (Figure 10), suggesting that there is not a distinct, high organic, lithologic layer in the subsurface over this interval. Nevertheless, the presence, abundance, and availability of TOC over the profile supports biotic activity and reducing conditions. The presence of terminal electron acceptors in the deeper zone including solid phase iron, manganese, and sulfate, is projected to support reductive transformation processes (Huling *et al.*, 2002); these appear to be more abundant in the deeper zone (Figure 11). The occurrence of reduced conditions is evident by the presence of ferrous Fe (Figure 17.A) and the presence of sulfides, hydrogen, and methane, measured in the ground water at depth (Vroblesky *et al.*, 2009). High sulfate concentration (112-130 mg/L) in downgradient wells indicates that the sulfate reducing condition is outcompeting methanogenesis. Hydrogen measurements (1.1-3.4 nM/L) in six of the seven wells are indicative of sulfate reducing conditions (Vroblesky *et al.*, 2009). The increase in acid-extractable Fe with depth suggests that Fe reduction could be a predominant terminal electron acceptor process to a depth of 16 ft bgs. However, acid extractable Fe is not necessarily a measure of bioavailable ferric iron, so the actual availability of microbially-reducible ferric iron is not known. The co-existence of ferrous iron, sulfide, and methane at the site is an indication that multiple terminal electron accepting processes are occurring simultaneously, either at different locations of the site, or at different micro-sites in the same subsurface location. Lower redox in the deeper zone (Vroblesky *et al.*, 2009) could result in faster rates of reductive dechlorination (*i.e.*, natural attenuation) of the CVOCs.

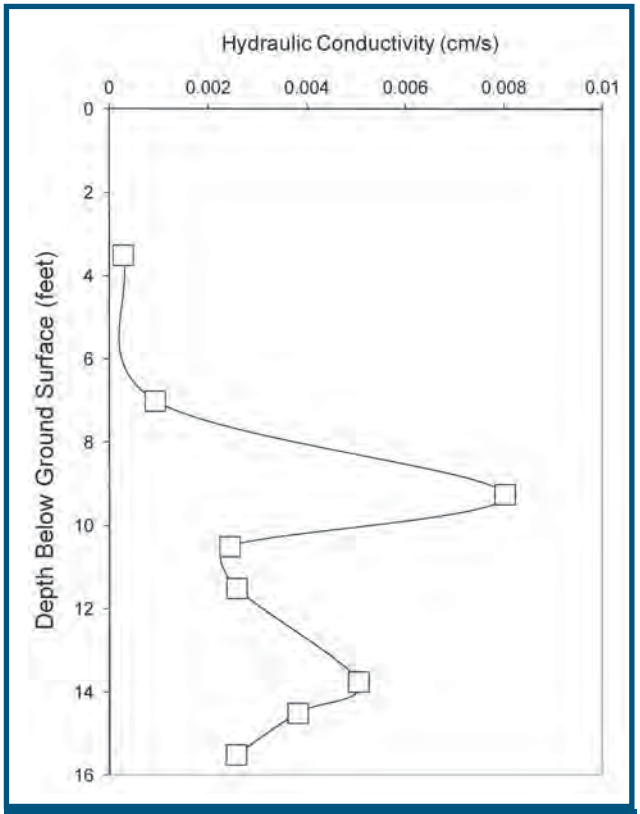

Figure 22. Hydraulic conductivity values in aquifer material collected from Parris Island, SC, MCRD, site 45 using a laboratory permeameter (ASTM Method D2434).

Although the surficial aquifer is considered unconfined, drawdown patterns more closely represent a confined or leaky-confined aquifer (TtNUS RI report, 2004). This may be the result of the presence of the relatively finer-grained, silty-sand sediments within the upper portion of the shallow aquifer, in comparison to the deeper sediments of fine sand (Figure 22). This observation is consistent with aquifer cores collected and visually examined by EPA-RSKERC staff, which indicated that a thin clay layer exists in the 3-6 ft bgs interval. Specifically, hydraulic conductivity measurements using ASTM method

D2434 were performed at EPA-RSKERC, using aquifer cores collected at site 45 (Figure 22). It is evident that there is a thin, low permeability clay layer at approximately 3-6 ft bgs, and that a highly conductive zone co-exists at and just below that depth, contributing to CVOC persistence and transport. Further, the permeability decreases with depth, in conjunction with the increased clay content of the aquifer solids. The low permeability of aquifer media with depth would result in slow ground water transport conditions and would contribute to restricted transport and dispersal of CVOCs at this depth.

Despite the significant source strength of CVOCs at the corner of the dry cleaner building (Figure D.2-D.3 in Appendix D), low concentrations or the absence of CVOCs in deeper aquifer intervals at downgradient transect locations (T1-T6) (Figure D.4-D.5 in Appendix D) are an indicator that natural attenuation mechanisms play a significant role in the fate of CVOCs with depth. Overall, multiple lines of evidence suggest that permeability, ground water velocity, and CVOC transport decreases with depth and that biotic and abiotic natural attenuation of CVOCs is greater in the deeper zone than the shallow zone.

5.5.2 ISCO impact on natural attenuation

ISCO can potentially change or affect several parameters and mechanisms associated with natural attenuation. These impacts may enhance or inhibit, be significant or negligible, or be short-term or long-lasting. $NaMnO_4$ is an antiseptic (*i.e.*, biocide) and will kill and inhibit microbial activity at much lower concentrations than what was injected into the subsurface at site 45. Typically, microbial toxicity is evaluated in simple laboratory systems that generally permits excellent contact between oxidant and microbes, therefore, results project a high impact of the oxidant on microbial activity at low oxidant concentrations. In subsurface systems, there are heterogeneities in aquifer material that cause short circuiting, dead zones, low-flow areas, and micro-niches that result in incomplete contact between the injected oxidant and microbial populations in aquifer material. This allows microbial populations to survive rigorous applications of oxidants during ISCO. The same heterogeneous, anisotropic condition that limits the ability to uniformly deliver oxidant into the subsurface, is probably also the same condition that prevents the injected oxidant from impacting microbial activity in subsurface systems. Therefore, laboratory studies conducted in ideal, complete-mix systems provide insight into the microbial toxicity but do not represent actual non-ideal systems, which permit microbial survival and activity under harsh oxidative field conditions. These basic differences between laboratory and field conditions help explain discrepancies between microbial toxicity and inhibition results reported from laboratory studies and the seemingly low impact of ISCO on microbial activity at field-scale (Luhrs *et al.*, 2006).

The oxidation reduction potential (ORP) is a general indicator of oxidation conditions in the subsurface. The generally accepted sequential order of TEA utilization, under aerobic and anaerobic conditions is:

O_2 Aerobic → NO_3 nitrate reducing → Fe^{+3}, Mn^{+4} iron, manganese reducing → SO_4^{2} sulfate reducing → CO_2 methanogenesis

It is generally accepted that methanogenesis is the least efficient TEAP. Iron and sulfate reducing conditions are the most favorable for reductive dehalogenation processes for the CVOCs at site 45. These transformations are more energetic and efficient, relative to methanogenesis. The injection of $NaMnO_4$ oxidant into the subsurface will result in a strong increase in ORP and shift the TEAP to the left, killing or inhibiting some microbial species. Examination of the process residuals suggests that ISCO would shift the predominant terminal electron accepting process from an inefficient one (methanogenesis) to more efficient processes, such as Fe^{+3} and SO_4^{2-} reduction, and provide a sustained long-term source of TEA. The injection of oxidants into the subsurface will result in the rapid oxidation of aquifer sediments and increase the relative bioavailability and abundance of TEA. For example, ferrous iron is oxidized to ferric iron, sulfides to sulfate, and so on. In general, the short-term impact of ISCO was projected to negatively impact natural attenuation, but the long-term impact is projected to enhance and help sustain natural attenuation, given the shift in electron accepting conditions, and the long-term bioavailability and abundance of TEAs.

Some oxidation reactions are acid producing, so pH changes can occur under some conditions. Since pH is widely known as the master variable in water chemistry, this parameter has direct and indirect effects on biotic and abiotic attenuation processes. However, the ground water is well-buffered at site 45 and pH changes in the post-oxidation ground water were not significant. Oxidation of organic contaminants by different oxidants, and formation of simpler organic molecules, results in an increase in the solubility, bioavailability, and biodegradability of the reaction byproducts (Allen and Reardon, 2000; Klens *et al*., 2001; Droste *et al.*, 2002; Chapelle *et al*., 2005; Luhrs *et al.*, 2006; Rivas, 2006). For example, many post-oxidation reaction byproducts are identified as carboxylic acids, chloroacetic acids, and other unregulated compounds. Finally, ISCO was deployed in the source area and along the longitudinal axis of the plume at site 45; this resulted in a physical separation between the ISCO area and other downgradient and side-gradient areas where ISCO had minimal impact on natural attenuation processes.

In summary, the large volume of the $NaMnO_4$ solution injected into the subsurface was broadly dispersed. As a result, it is projected that (1) there will be a localized decline in microbial activity near the injection points and farther away from the injection points, where there was direct contact between the $NaMnO_4$ and microbial populations, (2) the inhibitory effects on microbial activity will diminish with time, leading to microbial rebound after the oxidant is reacted, and (3) increased bioactivity will result from improved bioavailability of trace constituents, greater abundance of easily oxidized substrates, lower concentrations of challenging chemicals, increased levels of TEAs, and more efficient TEAPs.

5.6 Contamination rebound

Rebound is a site condition where contaminant concentrations in ground water decrease as a result of remediation, but then increase over time. In general, this term should be applied to parent compounds only (*i.e.*, PCE at site 45); this is due to the potential for other mechanisms to alter the concentration of decomposition products.

In ISCO, rebound has been attributed to several mechanisms and conditions, including the slow post-oxidation equilibrium of contaminant mass transfer (*i.e*., the dissolution of NAPL residuals and desorption of residual contaminants in solid-phase media), and the back diffusion of contaminants from low permeability media, etc. Other complexities in contaminant rebound include long-term persistence of oxidants, or impact on hydraulic conductivity by entrapment of O_2(g), especially with H_2O_2-based ISCO. Various methods have been used to quantify rebound. For example, in one case it was considered to have occurred with concentrations increased greater than or equal to 25% over the post-treatment monitoring period (McGuire *et al.*, 2006). Assuming one year of post-treatment data, the geometric mean of the first half of the year would be compared to the second half of the year; for two years of post-treatment data, the geometric mean of the first year would be compared to the second year. In Krembs *et al.* (2010), rebound was determined when the increase in the concentration of total contaminants of concern (COCs) in groundwater during the post-ISCO monitoring period was greater than 0.25 of the pre-ISCO baseline value (Eqn. 5).

$$\frac{[\text{COCs}]_{\text{1 Year post-ISCO}} - [\text{COCs}]_{\text{lowest post-ISCO}}}{[\text{COCs}]_{\text{pre-ISCO baseline}}} \geq 0.25 \qquad \text{(Eqn.5)}$$

Rebound at site 45 may be attributed to several potential mechanisms associated with the incomplete oxidation of CVOCs. These mechanisms have a cumulative overall effect on CVOC concentrations and include, but are not limited to: (1) the non-uniform distribution of injected oxidant, and the heterogeneous distribution of CVOCs (*i.e*., simply not delivering a sufficient volume of oxidant for adequate contact with the TTZ), (2) the back diffusion of CVOCs from low permeability materials, (3) the accumulation of MnO_2(s) at DNAPL interfaces, which impede CVOC mass transfer and CVOC and MnO_4^- mass transport, (4) insufficient delivery of oxidant to the contaminated media (*i.e*., the mass of oxidant delivered was inadequate to satisfy the natural oxidant demand and to oxidize the CVOCs), and (5) slow mass transfer associated with the dissolution of DNAPL residuals and desorption of residuals on solid-phase media.

Overlapping oxidant ROIs, total porosity oxidant volume design, heavy oxidant loading, and multiple oxidant injections into the source zone were components of the ISCO design at site 45, to ensure aggressive oxidant delivery to the CVOC targeted zones. Other oxidant injection strategies were used to limit the role of heterogeneous porous media and to improve oxidant coverage in the TTZ, including low injection pressure, short injection intervals, and small ROIs at numerous injection points. However, the impact of heterogeneities on oxidant transport cannot be completely avoided and non-uniform distribution of oxidant occurred at site 45. The inability to achieve ideal contact between oxidant and the TTZ can be amplified due to the heterogeneous distribution of CVOCs. Consequently, the oxidation of CVOCs may range from being highly effective in areas where good contact was achieved, to less effective in other areas where good contact was not achieved. Persistent CVOC ground water concentrations can be used as an empirical measure of incomplete contact between the oxidant and the TTZ, and the identification of hot spots of CVOCs, DNAPL, and NOD.

The lithology of the aquifer material at site 45 ranges from highly permeable sand to sandy clay, and the study area is underlain by a peat-clay material. This lithology suggests that the downward transport of PCE DNAPL would be limited, and that diffusion transport of the CVOCs would dominate in the lower permeability material, relative to advective transport. Oxidant delivery into higher permeability material would sweep through relatively quickly via advection. However, diffusion, a much slower transport process would dominate CVOC and oxidant transport in the lower permeability material. Specifically, both the transport of permanganate into the low permeability material and transport of CVOCs from the low permeability materials would be limited. Overall, CVOC oxidation may also be limited in these zones, allowing CVOCs to slowly diffuse and rebound in the ground water.

The accumulation of MnO_2(s) at NAPL interfaces in the source area at site 45, may have occurred and is projected to slow mass transfer (*i.e.*, dissolution of the DNAPL components in the ground water). In some respects, this result may be desirable in that the CVOC transport distance may be significantly reduced under this condition, when considering the role of natural attenuation (*i.e.*, the CVOC plume length and dimensions are limited, static, and/or declining).

The PCE concentrations measured in the pre-oxidation, post-oxidation 3, and post-oxidation 4 ground water monitoring events were used to assess rebound of PCE at site 45, using Eqn. 5. The following data sets were used for the parameters in Eqn. 5 for all ground water micro-wells, MW-25, and MW-31 SL.

Eqn. 5 parameters	Ground water monitoring data sets
[COCs] pre-ISCO baseline	Pre-oxidation baseline [PCE] (Feb. 20, 2013)
[COCs] lowest post-ISCO	Post-oxidation 3 [PCE] (June 23, 2014)
[COCs] 1 Year post-ISCO	Post-oxidation 4 [PCE] (Feb. 27, 2015) (11 mos. post ox)

The results of this analysis indicated that 3 of the 37 wells evaluated showed rebound. These wells were either in the source area (M1-S-A-shallow, M1-S-A-deep) or were along the centerline of the plume (M2-S-shallow). The post-oxidation performance evaluation metrics used in this study indicated that reductions in soil and aqueous CVOC concentrations and in mass flux have been achieved.

However, based on the elevated concentrations of CVOCs measured in the source area soil samples, further CVOC rebound is probable. One depth interval where elevated post-oxidation $[CVOC]_{SOIL}$ were measured (*i.e.*, (-5, -4) sampling location, -14 ft bgs interval) exhibited the highest CVOC concentration (576 mg/kg) (Appendix D, Figure D.6), indicating the presence of DNAPL. The oxidant loading into the source area was insufficient to fully oxidize this material. Consequently, it is projected that rebound would occur in the source area and subsequent ISCO activities are recommended to target the source area and to address CVOC rebound.

5.7 Sustainability

The ISCO design and deployment associated with this study was aimed at achieving a sustainable solution through various design steps and approaches. First, the remedy is expected to be fully integrated with a final natural attenuation remedy since it is projected that ISCO will not achieve the MCLs for CVOCs. Due to the high resolution site characterization method and the development of an accurate site conceptual model, clean portions of the aquifer were eliminated from further consideration for oxidant delivery. The most contaminated portions of the aquifer were then targeted to receive appropriate oxidant dosages, thus achieving good oxidation reaction and oxidant efficiency. These aspects of the ISCO design and deployment helped to limit the overall amount of oxidant used, and indirectly the amount of fossil fuels consumed and the project's carbon footprint.

5.8 Recommendations

It is recommended to continue ground water monitoring and to carry out additional, but limited, ISCO activities.

5.8.1 Proposed monitoring activities

It is recommended to perform semi-annual ground water monitoring for CVOCs, metals, MnO_4^-, and indicator parameters (*i.e.*, pH, oxidation-reduction potential (ORP), specific conductance (SC), dissolved oxygen (DO), and temperature) to assess MnO_4^- persistence, metals mobilization and attenuation, and CVOC destruction and rebound. A proposed ground water monitoring plan has been included as Appendix F. Dissolved methane gas, ferrous and total iron, chloride, and sulfate are optional parameters that could be measured and may provide useful background data and information to assess natural attenuation.

5.8.2 Proposed ISCO activities

It is recommended that continued, but limited, ISCO activities be deployed to address the CVOC residuals at the site. The basis for recommended ISCO activities includes the following:

(1) It is assumed that there are CVOC residuals in the source area located near the suspected point of origin. The point of origin is in the area of the former sanitary sewer that existed adjacent to the southeast corner of Bldg. 192.

(2) It is assumed that CVOC rebound will continue to occur, mainly in the source area, and that the CVOC concentration could eventually exceed acceptable levels. It is also assumed that CVOC concentrations may generally rebound downgradient from the source area. Additional ground water monitoring is needed to assess this potential occurrence and determine whether additional ISCO activities are needed.

(3) It is assumed that periodic injection of the permanganate oxidant in the source area will prevent the re-development of the CVOC plume and will limit and/or prevent the capture of CVOCs in the downgradient storm sewer.

Regarding source area ISCO, it is recommended to periodically inject oxidant into 3-5 injection wells located in the source area. Two of these wells are existing and were used as injection wells during the ISCO pilot study (*i.e.*, MW-25 and Inj.1-deep). The other 1-3 proposed wells are located close to the existing wells but serve to inject the oxidant across a broader footprint in the source area. Collectively, these wells would deliver oxidant into the source area across a broader lateral direction, transverse to the ground water and CVOC plume transport direction (Figure 23). Given these stationary injection wells, oxidant injection would involve more simplified mobilization and oxidant delivery than the direct-push injection method. The specific details of the recommended design include 4 ft ROIs, used to cover a broader oxidant footprint in the source area; screened intervals of 4-5 ft are needed to address the suspected CVOC residuals that occur in the deeper source area (Table 12). Inj.-1, Deep is located upgradient from MW-25, and therefore, post-injection oxidant transport will occur along the longitudinal axis of the PCE source zone. This aggressive oxidant loading delivery is designed to continue targeting the precise locations where the highest $[CVOCs]_{SOIL}$ were measured. Inj.-2 and -3 are located transversely to the longitudinal axis of the PCE source zone to address PCE that may have migrated laterally from the source zone. However, these wells are not located very far from the suspected release point, given the limited lateral distribution of CVOC in the soil and ground water near this location.

Previous oxidant loadings to the source area, during injection events 1-3, were aggressive and are expected to have met the oxidant demand of the aquifer material. Therefore, the proposed oxidant concentration (20 g/L) in this design is expected to achieve long-term oxidant residuals needed to address the long-term source of CVOCs that exists in this area. The overall cost of oxidant using this oxidant injection strategy is estimated to be approximately $3,000. It is projected that 2-3 additional oxidant injections may be needed but should be based on continued ground water monitoring results.

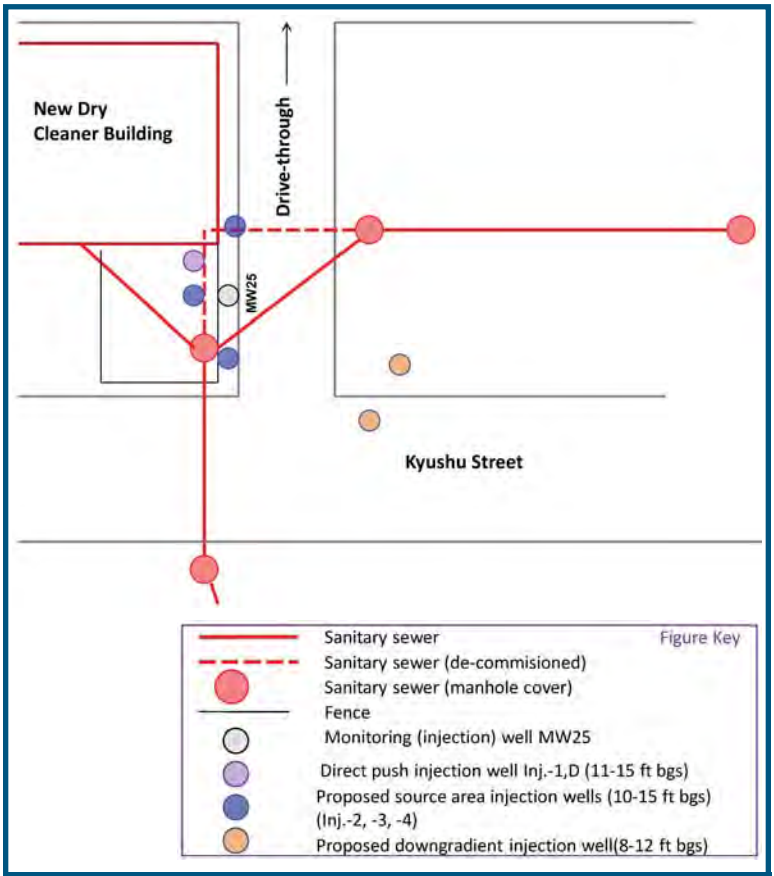

Figure 23. Existing and proposed oxidant injection well locations for recommended continued oxidant injection activities at site 45.

Table 12. Summary of oxidant ($NaMnO_4$) volume and loading for the long-term ISCO activities. Injection wells Inj.-2, Inj.-3, and Inj.-4 are proposed and depicted in Figure 23.

Injection Wells	$NaMnO_4$ Volume (gal)	$NaMnO_4$ Mass (lbs)	Projected total cost of oxidant [1] ($)
MW-25, Inj.-2, Inj.-3 [2]	600 (1800)	360	
Inj.-1, deep	480 (480)	96	$3080

[1] Carus Chemical method of estimating involves the following steps: divide lbs of $NaMnO_4$ by 0.4 since it is 40% $NaMnO_4$; since each pail of 40% contains 57 lbs, divide the weight in step 1 by 57 then round up to the next number, multiply the round number of pails by 57 lbs/pail, then $2.70 / lb.

[2] Assumes (1) a 4 ft ROI, (2) 5 ft screened interval for MW-25, Inj.-2, -3, and -4, a 4 ft screened interval for Inj.-1, deep, (3) 20 g/L $NaMnO_4$, and (4) $2.70/lb $NaMnO_4$.

6. Conclusions

A pilot-scale ISCO demonstration involving subsurface injections of sodium permanganate was performed at the Marine Corps Recruit Depot, site 45 (Parris Island, SC). The ground water at the site is contaminated as the result of the release of tetrachloroethylene (PCE), a chlorinated solvent used in dry cleaner operations. The treatment objective was to evaluate the feasibility of ISCO as an effective remedy, over a limited area, to reduce CVOC concentrations and mass flux in conjunction with natural attenuation. The results of this study are intended to provide details and guidelines that can be used by EPA and DoD remedial project managers regarding ISCO for remediation at other sites.

A preliminary site conceptual model was based on ground water samples collected from temporary and permanent ground water wells and was effective in delineating the plan view distribution of CVOCs. The well screen lengths and placement of these wells tended to average the vertical distribution of CVOCs. Therefore, the vertical extent of CVOC contamination was subsequently quantified and the conceptual site model was refined through the analysis of soil cores collected at locations transverse to the ground water flow and along the longitudinal axis of the CVOC plume transport direction. These data were augmented to fill in data and information gaps by sampling and analyzing archived cores that were frozen and stored at EPA RSKERC. Additional soil cores were collected and analyzed to further refine the CSM, as further data gaps were identified. High resolution site characterization also involved the installation of nested micro-wells used to sample and analyze ground water. This overall site characterization methodology was critical in the continued refining of the CSM and the ISCO design, not only by identifying CVOC contamination, but also by identifying and eliminating uncontaminated portions of the aquifer from further ISCO consideration. Throughout this process, ISCO activities were focused on the most contaminated portions of the aquifer, resulting in efficient and effective ISCO deployment. Overall, both the soil and ground water data were critical in further developing and refining the conceptual site model, the ISCO design, and in assessing the ISCO treatment performance.

Sodium permanganate was selected as the oxidant, and direct-push was selected as the main method of oxidant delivery, due to its flexibility and low initial capital cost. Numerous impediments and subsurface utilities existed in the source area where the oxidant was to be injected, including an 8-inch high pressure water main, a high voltage power line (230 V), a communication line, a sanitary sewer, a stormwater sewer, and the drive-through to the dry cleaner. An existing monitoring well and a newly constructed, temporary direct-push injection well were used in the oxidant injection. Utilizing these wells augmented the delivery of a heavy oxidant load into the source area.

A portable, low cost injection system was designed, constructed, and deployed at the site. All parts of the system, from inlet to outlet, were constructed with corrosion-resistant components, and included a 150-gallon tank, a teflon diaphragm pump, three oxidant injection arms, and an injection hose designed to fit inside the GeoProbe rod as a separate unit and attach directly to the injection tip. This design was used to help maintain hydraulic control of the oxidant and to limit the potential for leaks and the risk of exposure. Several oxidant delivery designs and methods used in the ISCO deployment resulted in an aggressive, effective, and efficient oxidation of CVOCs. Specifically, this includes narrow ROIs (3-5 ft), short vertical screen injection intervals, low injection pressure, outside-in oxidant injection, and a total porosity oxidant volume design. The injection tip was designed with a 2 ft screened interval. The top-down approach involved advancing the injection tip to the first depth interval, delivering the oxidant, driving to the next depth, and delivering the oxidant, etc. This configuration resulted in less risk of oxidant short-circuiting and greater certainty that the oxidant was delivered to the targeted interval. The outside-in oxidant injection strategy was used to minimize the lateral displacement of contaminated ground water. Due to the shallow water table and injection depths, low injection pressures and flow rates were required to minimize the potential for daylighting of the oxidant and to limit the role of preferential pathways.

The volume of oxidant solution to be injected at each location was based on a radial-flow, cylindrical, total porosity porous media conceptual model. This design method was expected to result

in the delivery of a large volume of oxidant over a large volume of contaminated aquifer media. Based on the average NOD values measured in the 5-11 ft bgs interval (*i.e.*, <2.7 g $NaMnO_4$/kg aquifer material), and accounting for natural variability, the actual oxidant loading (3.8-5.2 g/kg) was expected to exceed the majority of the NOD measured in the subsurface. Due to heterogeneities in aquifer characteristics, heavy oxidant loading, overlapping ROIs, and multiple oxidant injections, it was projected that the oxidant would be transported beyond the projected ROIs in the targeted treatment zones. In contrast, the mobile porosity design method sometimes used at ISCO sites was not used at site 45; it is based on the delivery of oxidant to the most conductive portions of the aquifer, where ground water transport is fastest. It was projected that using the mobile porosity design method would be less aggressive, involve a smaller injection volume and oxidant footprint, and leave some zones oxidant-free within the targeted treatment zone.

Administrative requirements associated with ISCO activities at site 45 included the preparation of health and safety plans, dig permits, injection and monitoring well construction permits, and oxidant injection permits. Coordination of these plans and permits with the responsible parties, EPA, and state regulatory agencies was an important component in the remediation approval and deployment process.

Three oxidant injection events were carried out where the oxidant loading and areal footprint were progressively larger. Given the proximity of the targeted treatment zones with surface and subsurface utilities, it was necessary to first establish the oxidant could be delivered safely, and without migration into non-targeted zones. The measurement of $NaMnO_4$ in nearby wells and micro-wells indicated that oxidant injection was successful: the oxidant was delivered into the targeted zones, hydraulic control of the injected oxidant was achieved, the oxidant persisted in zones where a heavy oxidant loading was delivered, and that significant CVOC destruction was achieved. Overall, a 91.5% and 75.5% reduction in total CVOC mass flux occurred in the shallow and deep zones, respectively, as a result from oxidant injections 1-3. Contrasting numerous post-oxidation and pre-oxidation CVOC concentrations in soil samples indicated a declining trend in post-oxidation $[CVOCs]_{SOIL}$, relative to pre-oxidation $[CVOCs]_{SOIL}$. A CVOC rebound analysis indicated that rebound has occurred in 3 of 37 wells and micro-wells at the site. At one depth interval in the source area, elevated post-oxidation $[CVOCs]_{SOIL}$ was measured and indicated the presence of DNAPL. For this reason, it is probable that CVOC rebound will continue to occur in the source area, but would likely play a lesser role in the downgradient portions of the plume, where lower CVOC mass and mass flux were measured. Subsequent ISCO activities are recommended to target the source area and to address CVOC rebound.

The permanganate persisted mainly in the source area near the southeast corner of Building 192, where heavy oxidant dosages were delivered to the suspected PCE release zone. Long-term oxidant persistence in this area is desirable as it permits the long-term contact between the oxidant and (1) CVOCs slowly dissolving from DNAPL, (2) CVOCs desorbing from aquifer solids, and (3) CVOCs diffusing from low permeability, silty media.

A significant post-oxidation increase in ORP was measured in the source area and along the longitudinal axis of the plume, where the oxidant was injected. The redox shift towards oxidized conditions is projected to be temporary, given the significant quantity of organic materials in the subsurface that favor reduced conditions. The reduction in ferrous iron concentrations in ground water along the longitudinal axis of the plume and in the source area indicates the significant

impact of the oxidant injected in these areas. Despite significant reductions in total CVOCs, a stark contrast between pre- and post-oxidation chloride isocontours was not observed. This was attributed to the high background chloride levels in the ground water, typical of surficial aquifers near marine environments, and a source of Cl^- attributed to long term reductive dechlorination at the site. The concentration of total chromium increased in the ground water from background concentrations in a few wells. A significant decline in the post-oxidation concentration of chromium was measured. Given the abundance of manganese and iron mineral species at the site, the continued attenuation of chromium is projected to be rapid and elevated concentrations to be temporary. The attenuation of background, naturally occurring arsenic occurred as a result of ISCO activities. Multiple attenuation mechanisms associated with ISCO geochemistry indicated that the arsenic species in the ground water were immobilized, or adsorbed onto the aquifer solids as a result of oxidation.

Firm conclusions were not possible from the MBT results regarding the impact of ISCO on biotic processes in the subsurface. Further, it was difficult to establish firm and definitive trends in the CSIA analytical results. Nevertheless, it can be concluded that in several wells located close to the oxidant injections, where significant reductions in CVOCs were measured, the CSIA data provides proof of concept that PCE, TCE, c-DCE, and VC were destroyed.

Recommendations are provided to perform semi-annual ground water monitoring for CVOCs, metals, MnO_4^-, and indicator parameters to assess MnO_4^- persistence, CVOC destruction and rebound, and metals attenuation. It is recommended to periodically inject oxidant into 3-5 injection wells located in the source area; two of these wells are existing and used during the ISCO pilot study. The other three proposed wells are located close to the existing wells and serve to inject the oxidant across a broader footprint in the source area. Specific details and guidelines are provided regarding these recommendations.

7. References

Akai, J., Izumi, K., Fukuhara, H., *et al*., 2004. Mineralogic and geomicrobiological investigations on groundwater arsenic enrichment in Bangladesh. *Applied Geochemistry* 19, 215-230.

ASTM (American Society of Testing Materials). 2007. ASTM D7262-07 Standard test method for estimating the permanganate natural oxidant demand of soil and aquifer solids. ASTM International, West Conshohocken, PA, USA. 5p.

Borden, R.C., C.A. Gomez, and M.T. Becker. 1995. Geochemical indicators of intrinsic remediation, *Ground Water*, (33)2, 180-189.

Bradley, P.M., 2003, History and ecology of chloroethene biodegradation—A review: *Bioremediation Journal*, (7)2, 81–109.

Chambers, J., A. Leavitt, C. Walti, C.G. Schreier, J. Melby, and L. Goldstein. 2000a. *In situ destruction of chlorinated solvents with $KMnO_4$ oxidizes chromium*. In: Chemical Oxidation and Reactive Barriers, The Second International Conference on Remediation of Chlorinated and Recalcitrant Compounds. Wickramanayake, G.B., A.R. Gavaskar, and A.S.C. Chen (Eds.), Battelle Press, Columbus, OH. pp. 49-55.

Chambers, J., A. Leavitt, C. Walti, C.G. Schreier, and J. Melby. 2000b. *Treatability study: Fate of chromium during oxidation of chlorinated solvents*. In: Chemical Oxidation and Reactive Barriers, The Second International Conference on Remediation of Chlorinated and Recalcitrant Compounds. Wickramanayake, G.B., A.R. Gavaskar, and A.S.C. Chen (Eds.), Battelle Press, Columbus, OH. pp. 57-65.

Crimi, M.L. and R.L. Siegrist. 2003. Geochemical effects on metals following permanganate oxidation of DNAPLs. *Ground Water*. 41(4):458-469.

Driscoll, F.G., 1986, Groundwater and Wells, 2nd ed.: Minnesota, Johnson Division, 1089 p.

Falta, R.W., Basu, N., Rao, S.P. 2005a. Assessing the impacts of partial mass depletion in DNAPL source zones : I. Analytical modeling of source strength functions and plume response, *J. Contam. Hydrol*. 78 (2005) 259–280.

Falta, R.W., Rao, S.P., Basu, N. 2005b. Assessing impacts of partial mass depletion in DNAPL source zones: II. Coupling source strength functions to plume evolution, *J. Contam. Hydrol.* 79 (2005) 45– 66.

Honning, J., Broholm, M.M., and Bjerg, J.L. 2007. Quantification of potassium permanganate consumption and PCE oxidation in subsurface materials, *J. Contam. Hydrol*. 90:221-239.

Huling, S.G., B. Pivetz, and R. Stransky. 2002. "Terminal Electron Acceptor Mass Balance: NAPLs and Natural Attenuation". *J. Environ. Engin*., 128(3), 246-252.

Huling, S.G. and B. Pivetz. 2006. "In Situ Chemical Oxidation – Engineering Issue". US Environmental Protection Agency, National Risk Management Research Laboratory, R.S. Kerr Environmental Research Center, Ada, OK. EPA/600/R-06/072.

Huling, S.G., Ko, S., and Pivetz, B. 2011. Ground water sampling at ISCO sites – binary mixtures of volatile organic compounds and persulfate. *Ground Water Monit. Remed.* (31)2, Spring 72-79.

Huling, S.G., Ross, R.R. and Meeker Prestbo, K. 2017. In situ chemical oxidation: permanganate oxidant volume design considerations. *Ground Water Monit. Remed.* (37)1, Spring.

Huling, J.R., Huling, S.G., and Ludwig, R. 2016b. (*In Preparation*) Enhanced Adsorption of Arsenic on Aquifer Solids and Soil: Oxidative Treatment and Feasibility Assessment. *Wat. Res.*

Hutchins, S.R., D.E. Miller, and A. Thomas. 1998. Combined laboratory/field study on the use of nitrate for in situ bioremediation of a fuel-contaminated aquifer. *Environ. Sci. Technol*., (32)12, 1832-1840.

Johnston, R. and Heijnen, H. 2001. "Safe Water Technology for Arsenic Removal." In: Ahmed, M.F. *et. al.* [Eds]. *Technologies for Arsenic Removal from Drinking Water*. Bangladesh University of Engineering /Technology, Dhaka, Bangladesh.

Johnson, K.T., Wickham-St. Germain, M., Ko, S. and Huling, S.G. 2012. "Binary Mixtures of Permanganate and Chlorinated Volatile Organic Compounds in Groundwater Samples: Sample Preservation and Analysis." *Ground Water Monit. Remed.* 32(3), Summer 84–92.

Kampbell, D.H. and S.A Vandegrift. 1998. Analysis of Dissolved Methane, Ethane, and Ethylene in Ground Water by a Standard Gas Chromatographic Technique. J. of Chromatographic Science. 36: 253-256.

Ko, S., Huling, S.G., and Pivetz, B. 2012. Ground Water Sample Preservation at In Situ Chemical Oxidation Sites – Recommended Guidelines, EPA Ground Water Issue Paper. US Environmental Protection Agency, National Risk Management Research Laboratory, R.S. Kerr Environmental Research Center, Ada, OK. EPA/600/R-12/049.

Krajmalnik-Brown, Hölscher, T., Thomson, I.N., Saunders, F.M., Ritalahti, K.M., Löffler, F.M. 2004. Genetic Identification of a Putative Vinyl Chloride Reductase in *Dehalococcoides* sp. Strain BAV1, *Appl. Environ.Microbiol.* 70(10): 6347–6351.

Krembs, F.J., Siegrist, R.L., Crimi, M.L., Furrer, R.F., and Petri, B.G. 2010. ISCO for ground water remediation: Analysis of field applications and performance. *Ground Water Monit. Remed.*, 30(4) 42-53.

Krembs, F.J., Clayton, W.S., Marley, M.C. 2012. Chapter 8 Evaluation of ISCO field applications and performance. In: In Situ Chemical Oxidation for Remediation of Contaminated Groundwater; Siegrist, R.L.; Crimi M. L.; Simpkin T.J. (Eds). Springer Science and Business Media, LLC, New York, New York. A volume in SERDP/ESTCP Remediation Technology Monograph Series, C.H. Ward (Series Ed). Pgs. 319-354.

Li, X.D. and F.W. Schwartz. 2000. Efficiency problems related to permanganate oxidation schemes. In: Chemical Oxidation and Reactive Barriers, The Second International Conference on Remediation of Chlorinated and Recalcitrant Compounds. Wickramanayake, G.B., A.R. Gavaskar, and A.S.C. Chen (Eds.), Battelle Press, Columbus, OH. pp. 41-48.

Los Angeles Regional Water Quality Control Board - In Situ Remediation Reagents Injection Working Group. 2009. Technical Report: Subsurface Injection of In Situ Remedial Reagents Within the Los Angeles Regional Water Quality Control Board Jurisdiction. http://www.swrcb.ca.gov/rwqcb4/water_issues/programs/ust/guidelines/.

Lovley, D.R. and E.J.P. Phillips. 1986. Availability of ferric iron for microbial reduction in bottom sediments of the freshwater tidal Potomac River. *Appl. Environ. Microbiol*., (52)4, 751-757.

Lu, X., D.H. Kampbell, and J.T. Wilson. 2006. Evaluation of the role of *Dehalococcoides* organisms in the natural attenuation of chlorinated ethylenes in groundwater: U.S. Environmental Protection Agency EPA/600/R-06/029, 101 p.

Luhrs, R.C., R.W. Lewis, and S.G. Huling. 2006. "ISCO's Long-Term Impact on Aquifer Conditions and Microbial Activity." In, Proceedings of the 5th International Conference on Remediation of Chlorinated and Recalcitrant Compounds, Monterey, CA, USA, May 22-25, Paper D-48.

Manning A.B., Fendorf E.S., Bostick B. and Suarez L.D. (2002) "Arsenic (III) Oxidation and Arsenic (V) Adsorption Reactions on Synthetic Birnessite." *Environ. Sci. Technol.* 36(5), 976-981.

McLean, J.E. and B.E. Bledsoe. 1992. "Behavior of Metals in Soils." US EPA Ground Water Issue Paper EPA/540/S-92/018, Pp. 25.

Microbial Insights, 2017. http://www.microbe.com/how-it-works-census/

Mumford, K.G., Thomson, N.R., Allen-King, R.M., 2005. Bench-scale investigation of permanganate natural oxidant demand kinetics. *Environ. Sci. Technol.* 39 (8), 2835–2849.

Oscarson, D.W., Huang, P.M., Liaw, W.K. 1981. Role of manganese in the oxidation of arsenite by freshwater lake sediments. *Clay and Clay Minerals* 29(3) 219-225.

Pace Analytical, 2017. https://www.pacelabs.com/environmental-services/energy-services-forensics/csia/fundamentals-of-csia.pdf

Palmer, C.D., Puls, R. 1994. Natural Attenuation of Hexavalent Chromium in Ground Water and Soils. US EPA, Office of Research and Development, USEPA/540/5-94/505.

Payne, F.C., Quinnan, J.A., and Potter, S.T., 2008, Remediation Hydraulics, Florida, CRC Press; Taylor & Francis Group LLC, 408 p.

Petri, B., Thomson, N.R., Urynowisz, M.A. 2011. Chapter 3 – Fundamentals of ISCO using permanganate, In: In Situ Chemical Oxidation for Remediation of Contaminated Groundwater; Siegrist, R.L., Crimi, M.L., Simpkin T.J. (eds). Springer Science and Business Media, LLC, New York, New York. A volume in SERDP/ESTCP Remediation Technology Monograph Series, C.H. Ward (Series ed). Pgs. 89-146.

Ptak, T. Piepenbrink, M., Martac, E. 2004. Tracer tests for the investigation of heterogeneous porous media and stochastic modelling of flow and transport—a review of some recent developments, *J. Hydrol.* 294, 122–163.

Russo, D. 2012. Numerical analysis of solute transport in variably saturated bimodal heterogeneous formations with mobile–immobile-porosity, *Advances in Water Resources* (47) 31–42.

Siegrist, R.L., Urynowicz, M.A., West, O.R., Crimi, M.L., Lowe, S.L. 2001. Principles and Practices of In Situ Chemical Oxidation Using Permanganate. Battelle Press, Columbus, OH, USA, 336 p.

Simpkin, T.J., Palaia, T., Petri, B.J., and Smith, B. 2012. Chapter 11 Oxidant delivery approaches and contingency planning, In: In Situ Chemical Oxidation for Remediation of Contaminated Groundwater; Siegrist, R.L., Crimi, M.L., Simpkin, T.J. (eds). Springer Science and Business Media, LLC, New York, New York. A volume in SERDP/ESTCP Remediation Technology Monograph Series, C.H. Ward (Series ed). Pgs. 449-480.

Simunek, J., Jarvis, N.J, van Genuchten, M., Gardenas, A. 2003. Review and comparison of models for describing non-equilibrium and preferential flow and transport in the vadose zone, *J. Hydrol.* 272, 14–35.

Sun, X., Doner, H.E., and Zavarin, M. 1999. Spectroscopy study of Arsenite [As(III)] oxidation on Mn-substituted goethite. *Clay and Clay Minerals* 47(4), 474-480.

Suthersan, S., J. Horst, D. Nelson, M. Schnobrich. 2011. Insights from years of performance that are shaping injection-based remediation systems, *J. of Remediation*, Spring, 9-25.

TetraTech NUS, 2004. Remedial Investigation RCRA Facilities Investigation for Site /WMU 45 Former MWR Dry Cleaning Facility (Contract No. N62467-94-D-0888).

TetraTech NUS, 2012. Remedial Investigation Addendum for Site/SWMU 45 - Former MWR Dry Cleaning Facility Marine Corps Recruit Depot Parris Island, South Carolina Contract Task Order 0335 April 2012.

TetraTech, 2012. Feasibility Study for Site 45 – Former Morale, Welfare and Recreation Dry Cleaning Facility, Marine Corps Recruit Depot Parris Island, South Carolina Contract Task Order 0335, April 2012.

Urynowicz, M.A. 2008. In-situ chemical oxidation with permanganate: Assessing the competitive interactions between target and non-target compounds. *Soil Sediment Contam*. 17:53-62.

Urynowicz, M.A., Balu, B., Udayasankar, U. 2008. Kinetics of natural oxidant demand by permanganate in aquifer solids. *J. Contam. Hydrol*. 96:187-194.

US EPA, 1998. Technical Protocol for Evaluating Natural Attenuation of Chlorinated Solvents in Ground Water, US EPA Office of Research and Development, 600-R-98-128, 1998.

US EPA, 2008. A Guide for Assessing Biodegradation and Source Identification of Organic Ground Water Contaminants using Compound Specific Isotope Analysis (CSIA), EPA 600/R-08/148, December 2008.

US EPA, 2012. GWERD Quality Assurance Project Plan for the In Situ Chemical Oxidation Using Permanganate in the Remediation of Contaminated Groundwater at Solid Waste Management Unit 45, Marine Corps Recruit Depot, Parris Island, South Carolina.

US EPA, 2013. Health and Safety Plan for the In Situ Chemical Oxidation Using Permanganate in the Remediation of Contaminated Groundwater at Solid Waste Management Unit 45, Marine Corps Recruit Depot, Parris Island, South Carolina.

US EPA, 2014. Superfund Remedy Report, 14th Ed. EPA 542-R-13-016, November 2013, Solid Waste and Emergency Response.

US EPA GWERD RSKSOP 299.2. Determination of Volatile Organic Compounds (Fuel Oxygenates, Aromatic and Chlorinated Hydrocarbons) in Water Using Automated Headspace Gas Chromatography/Mass Spectrometry (Agilent 6890/597 Quadrupole GS/MS System).

US EPA GWERD RSKSOP 259.1. Determination of Volatile Organic Compounds (Fuel Oxygenates, Aromatic and Chlorinated Hydrocarbons) in Water Using Automated Headspace Gas Chromatography/ Mass Spectrometry (TEKMAR 7000 HS-Varian 2100T GC/MS System-ION Trap Detector).

US EPA GWERD RSKSOP 215.3. Quality Control Procedures for General Parameters Analysis Using Manual Methods for pH, Conductivity, Salinity, Total Dissolved Solids, and Total Suspended Solids.

US EPA GWERD RSKSOP 180.5. Total Nitric Acid Extractable Metals from Solids and Sludges by Microwave Digestion.

US EPA GWERD RSKSOP 120.3 Determination of Total Carbon and Total Organic Carbon in Solids using the LECO CR-412 Carbon Analyzer.

Vroblesky, D.A. and F.H. Chapelle. 1994. Temporal and spatial changes of terminal-electron accepting processes in a petroleum hydrocarbon contaminated aquifer and the significance of biodegradation. *Wat. Resour. Res*., (30)5, 1561-1570.

Vroblesky, D. 2007. "Preliminary Results: USGS Investigation of Site 45 MCRD, Parris Island, April-July, 2007. PowerPoint presentation given to the Parris Island Environmental Team on July 30, 2007.

Vroblesky, D. 2008. Progress Report for US Geological Survey FY 2007 Activities and Work plan for FY 2008 Field Activities at Site 45, Marine Corps Recruit Depot, Parris Island, South Carolina. U.S. Geological Survey, 720 Gracern Road, Suite 29, Columbia, SC, 29210-7651.

Vroblesky, D.A., Petkewich, M.D., Landmeyer, J.E., and Lowery, M.A., 2009, Source, transport, and fate of groundwater contamination at Site 45, Marine Corps Recruit Depot, Parris Island, South Carolina: U.S. Geological Survey Scientific Investigations Report 2009–5161, 80 p.

Vu, K.B., M.D. Kaminski, and L. Nunez. *Review of Technologies for Contaminated Groundwater.* ANL-CMT-03/2Argonne Natl. Laboratories, Argonne, IL 60439.

Xu, X., and Thompson, N.R. 2009. A long-term bench-scale investigation of permanganate consumption by aquifer materials. *J. Contam. Hydrol.* 110:73-86.

Yan, X., and G.E. Schwartz. 1999. Oxidative degradation and kinetics of chlorinated ethylenes by potassium permanganate. *J. Contam. Hydrol*. 37, 343–365.

Appendices

Appendix A

Oxidant Injection Pressure Calculations – Role of Hydrostatic and Overburden Pressure

(Los Angeles Regional Water Quality Control Board - In Situ Remediation Reagents Injection Working Group, 2009)

The rate that an aquifer can accept fluids and the lateral migration of these fluids before reaching structural failure is significantly influenced by the vertical acceptance rate. Maximum injection pressure can be estimated by the density of the dry soil and saturated soil, the thickness of the vadose zone, and the height of the saturated zone above the injection point using the following equation (Eqn. A.1):

$$P_{max} = [(\rho_{dry}\, g\, h_{dry} + \rho_{sat}\, g\, h_{sat}) - \rho_{water}\, g\, h_{sat}]\ psi\ (or\ dynes/cm^2) \qquad (Eqn.\ A.1)$$

Where:

P_{max}	Pressure maximum
ρ_{dry}	Density dry soil – vadose zone
ρ_{sat}	Density saturated soil
g	Gravitational acceleration
h_{dry}	Height dry or thickness of vadose zone above the injection point
h_{sat}	Height saturated of saturated zone above the injection point
ρ_{water}	Density water
psi	Pounds per square inch (lbs/in^2)
cm^2	Centimeters squared

It is important to note, there are several units conversions that make these calculations clearer:

dyne = $g\text{-}cm/s^2$ so the units of $g\text{-}cm/cm^2\text{-}s^2 = dyne/cm^2$;

1 cm $H_2O \times 980 = dyne/cm^2$;

$dynes/cm^2 \times 0.1 = pascals$,

and $psi \times 6.89 = kPa$ (or $psi = kPa / 6.89$).

It is recommended that for injection applications a 60 percent safety factor be applied to the maximum calculated pressure as part of the derivation of $P_{injection}$ (Payne, 2008). As fluids are injected into an aquifer the pressure applied to deliver these fluids is expressed upward against the effective hydraulic conductivity and the downward gravitational force of the water mound. Commonly the vertical hydraulic conductivity of many aquifers is approximately 10 percent of horizontal hydraulic conductivity and can be used as the effective hydraulic conductivity. The vertical acceptance is then determined by the relationship between pressure and the effective hydraulic conductivity as the vertical mounding expands. The following equation can be used to express this relationship between effective hydraulic conductivity and vertical mounding:

$$Q/A = K_{effective} (P_{injection} - \rho_{water} g h)/h \qquad \text{(Eqn. A.2)}$$

Where:

Q/A	the flow rate applied over the area of the expanding mound. Vertical flow ceases as the mound height (h) reaches the pressure limit or the selected "not to exceed" injection pressure (Payne, 2008).
$K_{effective}$	vertical hydraulic conductivity
$P_{injection}$	injection pressure (60% of the allowable injection pressure)
ρ_{water}	Density of water
g	Gravitational acceleration
h	mound height above water table

Example Calculations for site 45 at the MCRD (Parris Island, SC)

A spreadsheet was used to calculate the injection pressures that the aquifer could accept fluids before reaching structural failure. The following parameter values were used in these calculations:

ρ_{dry}	1.5 g/cm^3 (usually 1.1 – 1.6 g/cm^3, higher values for sandy material)
ρsat	1.9 g/cm^3 (using a ρ_{dry} = 1.5 g/cm^3; a particle density = 2.65 g/cm^3; total porosity (η) was estimated ($\eta = 1-(\rho_{BULK}/\rho_{PD})$ and assumed to be saturated with water
g	981 cm/s^2
h_{dry}	91.4 cm
h_{sat}	214-336 cm (8-10, 10-12, 12-14 ft bgs injection intervals)
ρ_{water}	1 g/cm^3

The maximum injection pressures were 4.8, 5.6, and 6.4 lbs/in^2 for the 8-10, 10-12, and 12-14 ft bgs intervals, respectively.

Appendix B

Oxidant Injection System

This section provides the details of the oxidant injection system used in the ISCO demonstration at site 45, Parris Island, MCRD, SC. It consists of a detailed schematic of the oxidant injection pallet (Figure B-1) and a detailed description of injection pallet components, component manufacturers, part numbers, cost, and relevant description details (Table B-1). Other miscellaneous and/or optional equipment and supplies are also provided that were used for backup contingencies or health and safety matters. The estimated cost to construct the injection pallet involving one injection arm was approximately $15,400, and the cost per injection arm (i.e., components 15-27 in Figure B-1) was $2860.

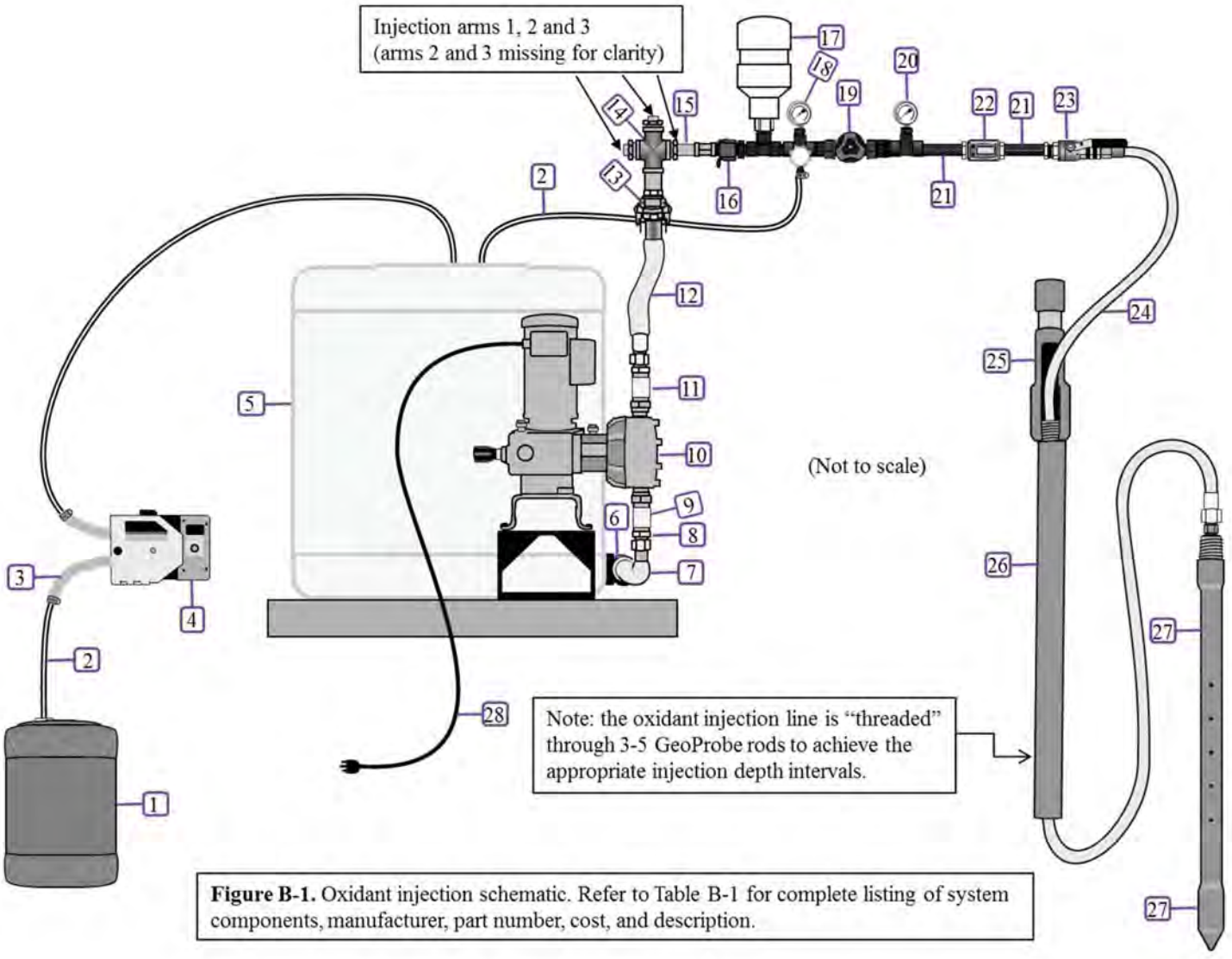

Figure B-1. Oxidant injection schematic. Refer to Table B-1 for complete listing of system components, manufacturer, part number, cost, and description.

Table B-1. Injection system details (components, manufacturer, part numbers, cost, and description). Miscellaneous and optional supplies and equipment associated with oxidant injection system and activities are included. Oxidant injection system components follow the component number identified in the *Oxidant Injection System Schematic* (Figure B-1, above). "poly" and "SS" refer to polypropylene and 316 stainless steel, respectively. Blue Monster pipe compound was used to join and seal threaded parts. Screw clamps were used to join tubing.

Component	Manufacturer	Part number	Cost	Description
1. RemOx-L 57 lb Jerrican (pail)	Carus Chemical	2195-110-500	$143/pail ($2.50/lb $NaMnO_4$)	40% sodium permanganate.
2. PTFE tubing (50 ft)	Chemfluor, or Cole Parmer	T-96000-28 T-06605-46	$399/50 ft $162/25 ft	5/8" O.D. Tubing either fits inside of Phar-Med tubing and serves as the oxidant transfer line, or serves as a pressure relief return line to oxidant tank.
3. Phar-Med pump tubing (25 ft)	Cole Parmer	T-06508-82	$226	Phar-Med pump tubing for peristaltic pump w/ 0.5" I.D.
4. Peristaltic pump I/P variable speed, brushless process drive I/P high performance pump head	Cole Parmer	S-77410-10 S-77600-82	$1886 $824	Oxidant transfer peristaltic pump w/ Phar-Med corrosion resistant tubing.
5. PTFE tank (150gal) and rod rack pallet	GeoProbe	207104	$2979	150 gal corrosion resistant tank on skid mounted metal pallet. Outlet 2" F-NPT polypropylene.
6. Between tank and hose 2"-1.5" poly reducer M-NPT 1.5" poly ball valve F-NPT 1.5" poly male adapter M-NPT 1.5" poly nipple M-NPT 1.5" poly Tee F-NPT *Right side* 1.5"-1" poly bushing 1"- ¾" poly bushing ¾" poly in-line ball valve ¾" poly nipple NPT ¾" hose to pipe adapter *Left side* 1.5" poly male adapter M-NPT	Grainger, Banjo	 1MKF1 1MKK7 1DPN1 1MJZ8 1MKH3 1MKC3 1MKB8 3ELV6 1MJZ5 4KG88 1DPN1	 $3.70 $75 $3.70 $4.40 $12.60 $3.90 $3.20 $18.60 $1.70 $5.00 $3.70	The 1.5" poly ball valve opens the tank allowing oxidant flow to the arms. The right side of Tee involves a check valve leading to a water hose adapter for cleaning the lines and arms. The left side leads to the pump inlet.

Table B-1 (continued). Injection system details (components, manufacturer, part numbers, cost, and description).

Component	Manufacturer	Part number	Cost	Description
7. Pureflex Ultraflex PTFE [1] convoluted hose with polypro braid (1.5"×2') and quick connect: one end SS JIC w/ SS 1.5" F-NPT; other end SS JIC w/ SS 1.5" F-NPT	Corrosion Fluid Products Corp. (hose)	Custom	$563	Corrosion resistant hose from tank to pump.
8. 1.5"×1.5" SS nipple M-NPT on both ends of 1.5"×1.5" SS coupling	Grainger	1XBC2	$14.60	
9. 1.5" SS coupling F-NPT	Grainger	6JK17	$27.30	
10. Neptune 7000 series metering pump; SS dosing head, check valves, and teflon diaphragm, 300-gph @ 30-psi performance w/ 1% $NaMnO_4$ solution; 1-HP, 115/230-volt, 1-phase motor.	Phoenix Pumps	7250-N3-100753	$4768	Corrosion (oxidant) resistant pump. Inlet is 1/5" SS M-NPT/check valve; outlet is 1.5" SS M-NPT/check valve.
11. 1.5"×1.5" SS nipple M-NPT on both ends of 1.5"×1.5" SS coupling	Grainger	6JK17 1XBC2	$27.80 $14.60	
12. Pureflex Ultraflex PTFE [1] convoluted hose (1.5"×4') w/ poly braid: one end SS JIC w/ SS 1.5" Female-NPT; other end SS JIC with SS 1.5" Female NPT	Corrosion Fluid Products Corp. (hose) Grainger	Custom	$683	Corrosion resistant hose from pump to header.
13. 1.5" SS male adapter (quick coupler) SS F-NPT (cam/groove) 1.5"×4" SS nipple M-NPT	Festenal Zoro	0400659 G2961147	$36.80 $26.40	Quick connect between hose and 3-way cross.
14. SS 1.5" F-NPT threaded cross 1.5"×1" SS bushing M-NPT	Grainger	1LVF2 1LUR7	$82.30 $20.80	45° or 90° depending on the angle for arm 1, 2, or 3.
15. 1"×4" SS nipple M-NPT SS elbow (45° or 90°) F-NPT	Zoro Grainger	G2812022 6JK43	$20.20 $15.30	
16. 1" poly F-coupler × M-NPT 1" poly M-adapter quick couple 1" Tee FPT poly F-NPT	Banjo Banjo Grainger	1DPJ9 1DPK4 1MKH1	$7.60 $3.60 $7.50	

Table B-1 (continued). Injection system details (components, manufacturer, part numbers, cost, and description).

Component	Manufacturer	Part number	Cost	Description
17. *Flow dampener* 4" PVC end cap 4"×6" long PVC schedule 40 4" to 2" PVC reducer 2" to 1" PVC bushing 1" PVC male adapter	Grainger	 5WPW6 WKJ4 5WPN9 22FJ17	 $5.30 $10.90 $1.90 $0.60	Provides flow dampening due to pump surge action.
18. *Pressure relief valve system* 1"-3/4" poly reducing bushing M-NPT×F-NPT ¾" 150 psia poly relief valve w SS pressure gauge 1" poly Tee F-NPT to 3/8" barb fitting for return line ¾" poly Tee F-NPT	 Grainger Valworx Sprayer Depot Sprayer Depot Grainger	 1MKB7 36472 2312034PP 36472 3XVP2	 $3.20 $45 $26.40 $45 $6.70	Measures delivery pressure and pressure relief valve that directs oxidant back to oxidant tank as a safety feature.
19. ¾" *Pressure control valve* 1" poly nipple M-NPT 1" poly diaphragm valve, 2-way 1"- ¾" poly reducing bushing	Grainger	 1MJZ6 33Z902 1MKB8	 $2.30 $143.40 $3.20	Controls pressure from pump to downhole pressure.
20. *Injection pressure system* ¾"-1" poly reducer M-NPT ¾" poly Tee F-NPT ¾"-1/4" poly reducing bushing SS pressure gauge	 Grainger Grainger Grainger Valworx	 1MJZ5 1MKG9 1MKB3 36472	 $1.70 $5.60 $3.10 $45	Measures the downhole injection pressure.
21. ¾"×6" poly pipe nipple	Grainger	3DTJ7	$ 2.80	A 10" nipple at this location would be better for flow meter operation.
22. ¾" flowmeter/totalizer	Grainger	1XPR8	$708	Measure flow and volume (totalizer) in each arm of the injection system.
23. 1"-¾" SS hex bushing F-NPT/ M-NPT 1" SS ball valve w/ handle option 1"- ¾" SS coupling to ¾" bevel hose fitting M-NPT	Grainger Zoro Tools Inc. Grainger	1LTF1 WMY4	$7.30 $44	Flow control valve for quick shut-off.
24. Pureflex Ultraflex PTFE [1] convoluted hose with polypro braid (¾"× 45') SS JIC ends w/ ¾" SS male NPT adapters	Corrosion Fluid Products Corp. (hose)	Custom	$1308	Corrosion resistant hose from injection header to oxidant injection tip.

Table B-1 (continued). Injection system details (components, manufacturer, part numbers, cost, and description).				
Component	**Manufacturer**	**Part number**	**Cost**	**Description**
25. Drive cap		Custom made		Drive cap allows the GeoProbe to drive the injection string (rods + injection tip, *i.e.*, oxidant hose is threaded through rods.)
26. 2.25" × 4' GeoProbe drive rod (GeoProbe, Salina, KS)	GeoProbe	204766	$139	GeoProbe rod is used to drive the injection tip; Oxidant delivery hose is threaded inside the rod.
27. 2.25"×2' top-down injection tool. Removable injection tip head (GeoProbe threads) allows to clean out injection tip	Environmental Services Products	INJP225-2	$405	Oxidant injection tip and drive head.
28. Electric cord for 115V	Hardware store		$10	Electric cord did not come with the pump.
Other Miscellaneous and/or Optional Equipment and Supplies				
Component	**Manufacturer**	**Part number**	**Cost**	**Description**
Alternative oxidant injection tip 2.25"×2' retractable injection tool	Environmental Services Products	INJP7K-2	$602	Retractable oxidant injection tip.
Spill contingency Pig hazard. materials adsorb sock	New Pig (Tipton, PA)	124CR (3"×46")	$139	Absorptive socks.
Oxidant neutralizer Ascorbic acid (bulk, 55 lbs)	Nextag Inc. / My Spice Sage		$212	Food-grade oxidant neutralizer.
Micro-well screen 21" SS screen; 3/16' hose bar	GeoProbe	AT-8717S	$65	Stainless steel micro-well screen.
Spare parts kit Includes spare parts for Phoenix 7000 series pump	Pump Locker	004334 1	$1028	Field contingencies Pump.
Extra oxidant injection hose Pureflex Multiflex PTFE convoluted hose with polypro braid (¾"× 60') SS JIC ends w/ SS ¾" male NPT adapters	Corrosion Fluid Products	Custom	$1889	A 60' length allows greater flexibility in depth and location w/o moving the injection pallet.

[1] Hose is full vacuum rated; operating pressures 1.5" 250 psi; ¾" 400 psi.

Appendix C

Photographic compendium of ISCO activities at the site 45 ISCO demonstration project (Parris Island, MCRD, SC).

Photo 1. Front gate of the Parris Island Marine Corps Recruit Depot at Parris Island, SC.

Photo 2. Site 45 looking west from the middle of Kyushu Street, and the new Dry Cleaner building (Bldg 192) is on the right.

Photo 3. Site 45 looking upgradient from the middle of Kyushu Street towards the new Dry Cleaner building. The approximate centerline of the plume is from the near corner of the dry cleaner building and extends in the southeastern direction.

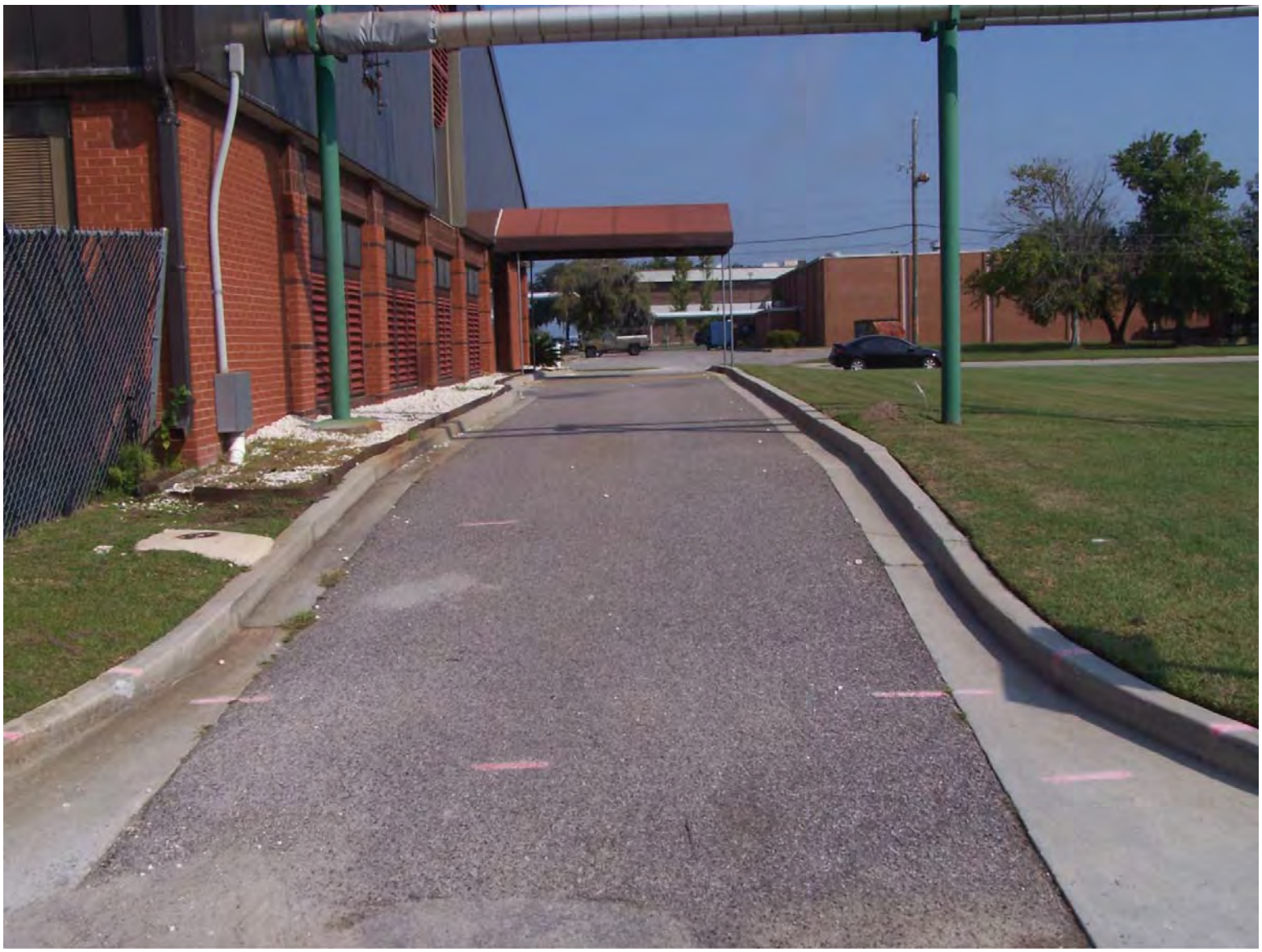

Photo 4. Looking north from the southeast corner of the new Dry Cleaner building and laundry pick-up drive-through. The source area of the plume is the general area in the southeast corner of the building (left side of drive-through).

Photo 5. Utility notification prior to subsurface activity at Site 45 involved detection of utilities and marking. Marked utilities included a high pressure 8 inch water main (blue), communication line (orange), high voltage (230V) power line (red), storm and sanitary sewers (green). The approximate mid-line of the CVOCs plume was marked by the research staff (yellow).

Photo 6. Retrieving soil cores using the GeoProbe equipment along transects extending across (perpendicular) the ground water plume.

Photo 7. Soil core collection using a GeoProbe (background), and soil core processing (capping, cutting, sealing, and freezing) for shipment to RSKERC facility for analysis.

Photo 8. Preparation of cement-bentonite grout using GeoProbe grout pump. The grout was pumped into the bottom of boreholes where soil cores were collected. A tremie tube and a "bottom-up" method was used to properly seal abandoned soil coring locations.

Photo 9. Preparation and staging of materials used in the installation of the micro-wells.

Photo 10. Close-up of the micro-well screen and tubing.

Photo 11. Installing the micro-well well screen and tubing by threading it through the Geoprobe rod to the target depth.

Photos 12-13. Closeup of the installation of the micro-well well screen and tubing through the Geoprobe rod. The GeoProbe rod and tubing is filled with water to prevent heaving and sand-binding of the tubing inside the rod. The tubing and screen are held in place as the GeoProbe rod is retrieved.

Photo 14. Construction of flush-mounted paired micro-wells (*i.e.*, shallow and deep). Paired micro-wells with identification markings M4-N-S and M4-N-D indicate monitoring transect 4, north side of the plume, shallow and deep intervals.

Photo 15. Looking upgradient from the middle of Kyushu Street towards the new Dry Cleaner building. The approximate centerline of the plume (yellow) is from the corner of the dry cleaner building and extends in the southeastern direction. The open, flush-mounted micro-wells (M3-mid-shallow and M3-mid–deep) are shown in the immediate foreground.

Photos 16-17. Post-installation development of micro-wells was carried out by pumping ground water at a slow rate. A few liters of ground water was generally required to "develop" the micro-wells until stabilized general parameters and clear ground water could be achieved.

Photo 18. Storage of 5 gal pails (jerricans) of 40% liquid sodium permanganate in the hazardous waste storage and containment unit.

Photo 19. The injection tool with holes (left) for oxidant delivery into the subsurface is connected with corrosion-resistant stainless steel fittings. The corrosion-resistant, oxidant delivery line (blue) is Pureflex Ultraflex PTFE (45-60 ft in length) and is a convoluted hose with polypro braid.

Photo 20. The oxidant injection line is strung through each of the GeoProbe rods needed to achieve the target depth at each location. The direct push injection tip, GeoProbe rod, and injection hose connected prior to injection.

Photo 21. The oxidant injection system under a rain/shade canopy with 2 injection arms and secondary containment.

Photo 22. Three (3) oxidant injection arms in use at site 45. Each is equipped with flow dampener, pressure gauge, pressure relief valve and return line, flow control valve, pressure gauge, in-line flow totalizer, and on the end is the (not shown) emergency shut-off valve.

Photo 23. The oxidant injection system delivering oxidant to 3 injection locations.

Photo 24. Using a peristaltic pump to transfer a specific volume of 40% liquid sodium permanganate into the mixing tank. Water was introduced into the mixing tank at high flow rates to assure mixing of the sodium permanganate and to achieve the targeted oxidant solution concentration needed for injection. A secondary containment system was constructed under the oxidant injection system.

Photo 25. Access restrictions along Kyushu Street while oxidant handling and injection activities were ongoing.

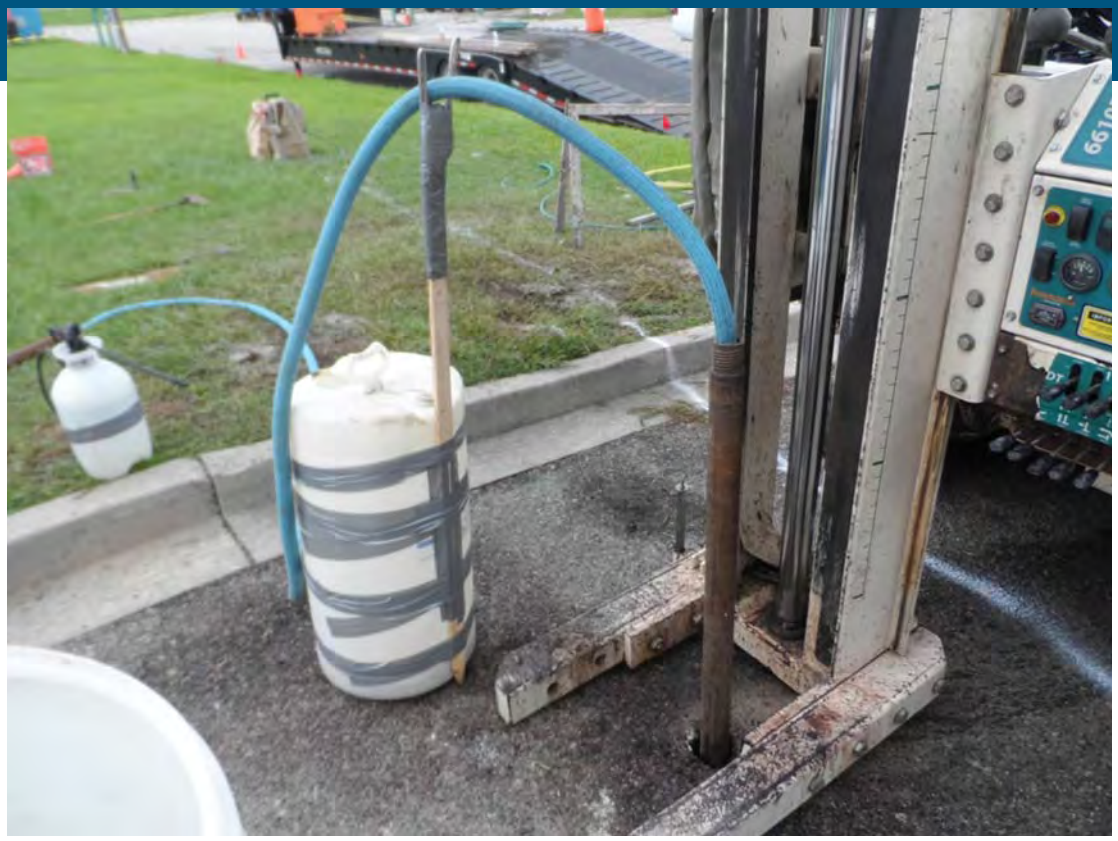

Photo 26. Oxidant injection at one location in the drive-through to the dry cleaner.

Photo 27. Simultaneous injection of oxidant into three locations on Kyushu Street while avoiding subsurface utilities. Facing the west, these injection locations straddle the communication line and flank the south side of the 8" high pressure water main and 230V high voltage line.

Photo 28. Rain/shade canopy used for injection pallet while oxidant is delivered to three locations.

Photo 29. Direct-push at an angle of the injection tip to access the subsurface corner of building 192 in the drive-through of the dry cleaner. This technique was used to avoid the "mat apron" concrete foundation extending 5 ft from the building.

Photo 30. Direct-push of oxidant under corner of the Bldg. 192 into the source area associated with the former leaking sanitary sewer line in this area. This was performed while avoiding the communication lines (orange-marked utility box is the communication line), and the overhead steam line supported by the green post in the background of the photo.

Photos 31-32. Pumping oxidant into well MW-25 and Inj. 1-Deep at approximately 2-4% $NaMnO_4$.

Photo 33-34. Decontamination of GeoProbe rig prior to departure; capture of investigation derived wastewater for subsequent testing and disposal.

Photo 35. Ground water sampling at micro-wells involved "binary mixtures" of ground water and the oxidant solution that was injected as seen by the pink-purple color in the tubing. Ground water samples exhibiting presence of $NaMnO_4$ were neutralized using ascorbic acid.

Photo 36. The color of the sodium permanganate solutions at different concentrations were prepared to provide a field "quick test" to approximate permanganate concentrations.

Appendix D

Pre- and post-oxidation soil CVOCs concentrations

Pre-oxidation (baseline) and post-oxidation soil core analytical results for total CVOCs. Pre-oxidation soil core transects are located approximately 16.5 ft (T0), 32 ft (T1), 65 ft (T2), 98 ft (T3), 131 ft (T4), 164 ft (T5), and 197 ft (T6) downgradient from the X,Y ordinate at MW 25-SL. The X-Y coordinate system used in the pre- and post-oxidation soil core locations is depicted in Figure D.1 below. There were three core locations (A, B, C) on each pre-oxidation soil core transect T0-T6. Core B was on the longitudinal axis of the plume, and cores A and C were located approximately 20 ft on the south and north sides, respectively. The vertical distribution of pre-oxidation total CVOCs at Transects T0-T6 are presented (Figures D2-D5).

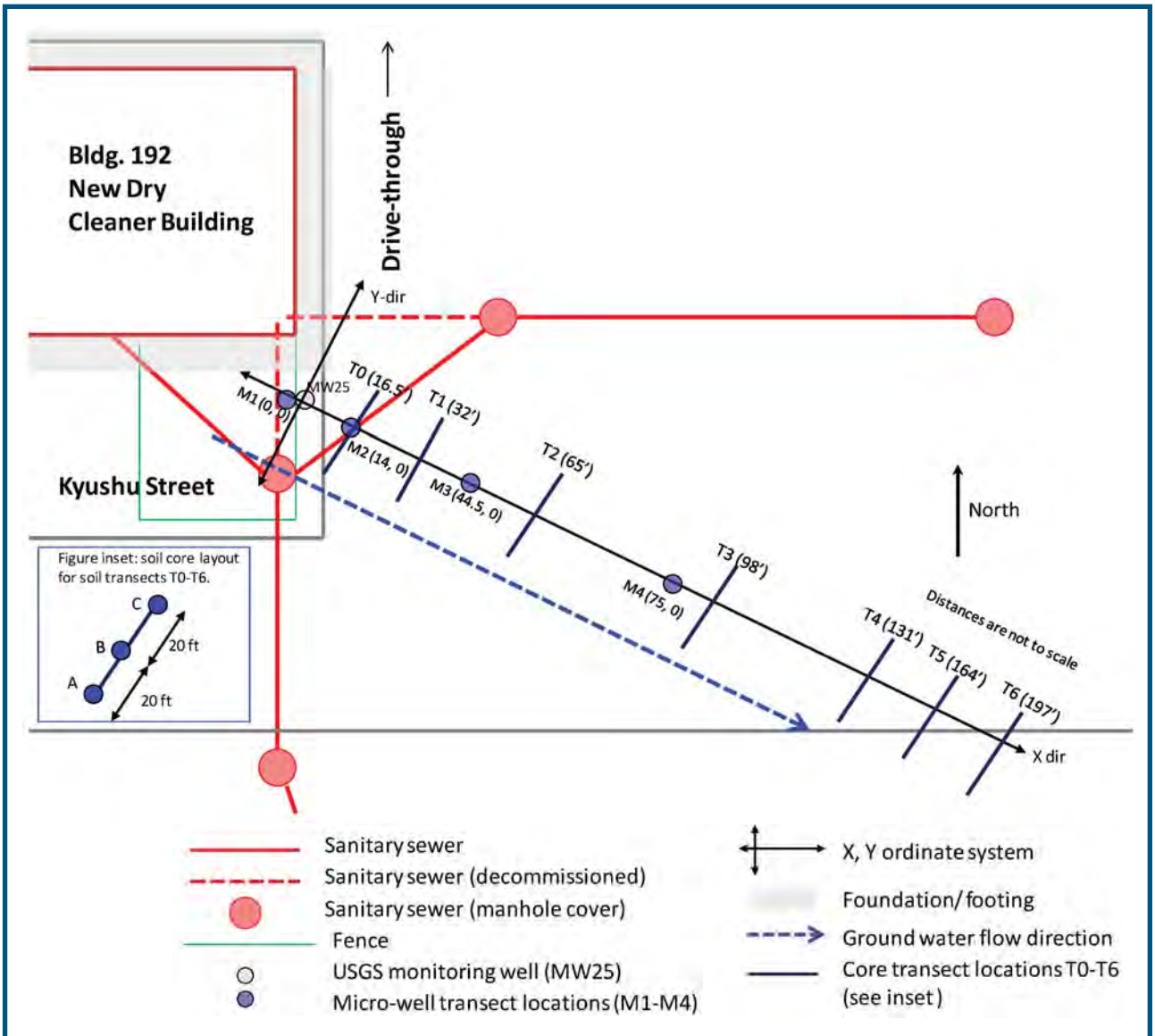

Figure D1. The X, Y-coordinate system used to illustrate the relative locations and distances between monitoring well MW 25-SL, micro-well transects M1-M4, and soil core location transects T0-T6 specified in the following figures.

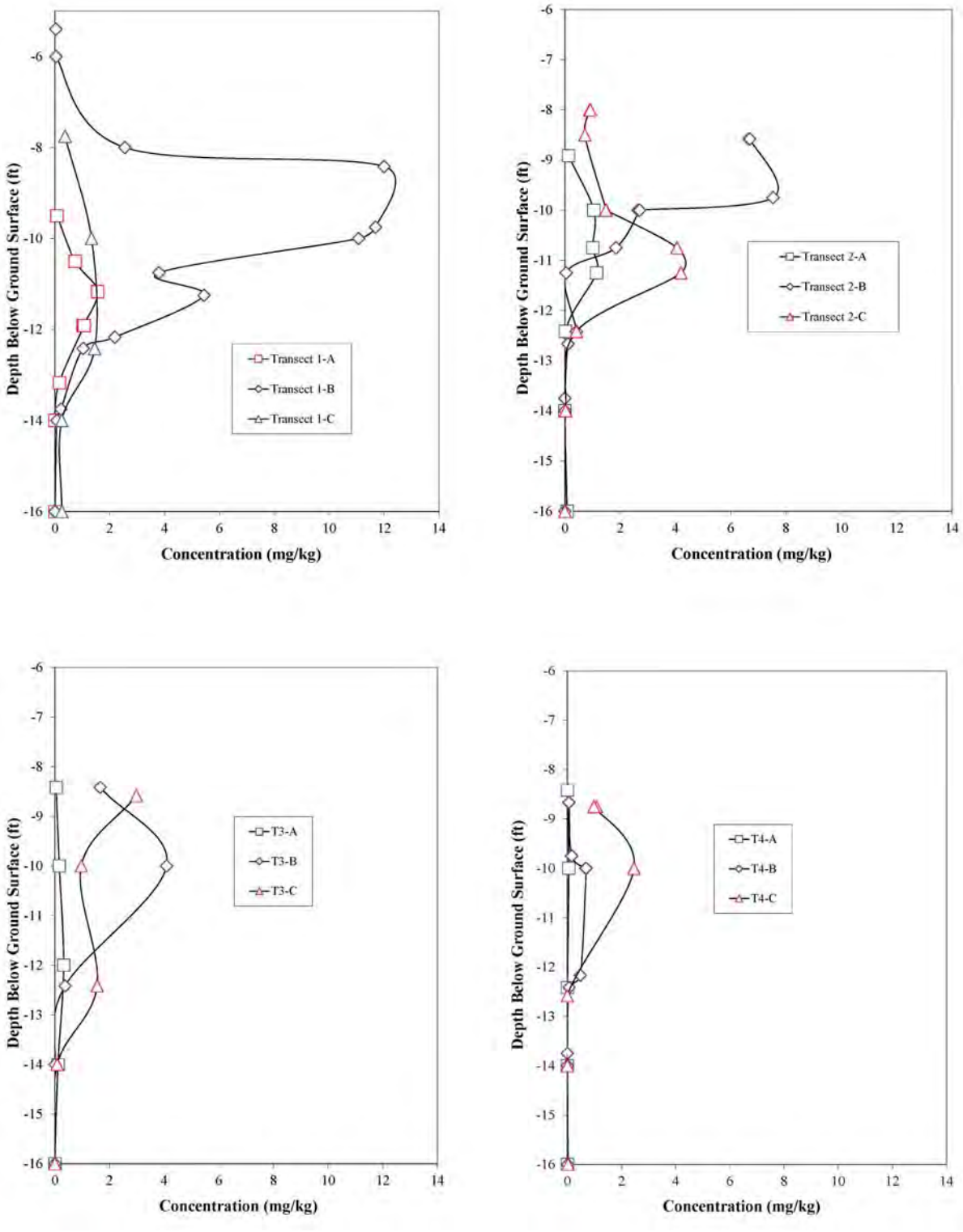

Figure D2. Vertical distribution of pre-oxidation total VOCs at Transects T1-T4 (refer to Figure D1). Transects are located approximately 33 ft (T1), 66 ft (T2), 99 ft (T3), 132 ft (T4) downgradient from MW 25-SL.

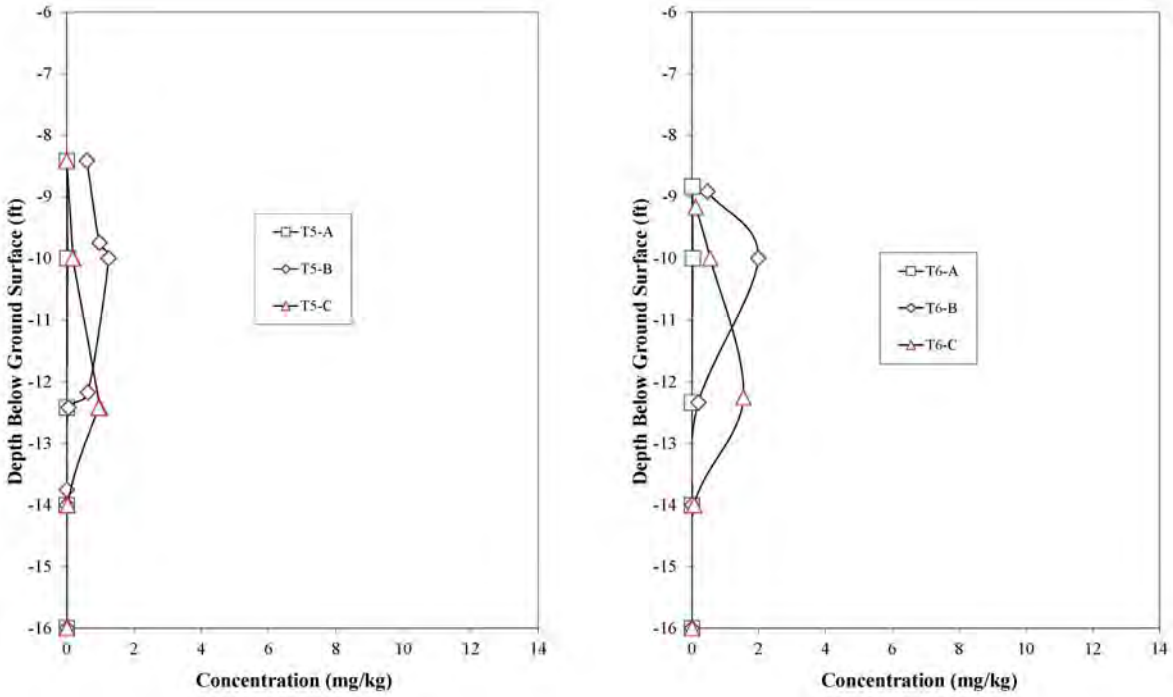

Figure D3. Vertical distribution of pre-oxidation total VOCs at Transects T5-T6 (refer to Figure D1). Transects are located approximately 165 ft (T5) and 198 ft (T6) downgradient from MW 25-SL.

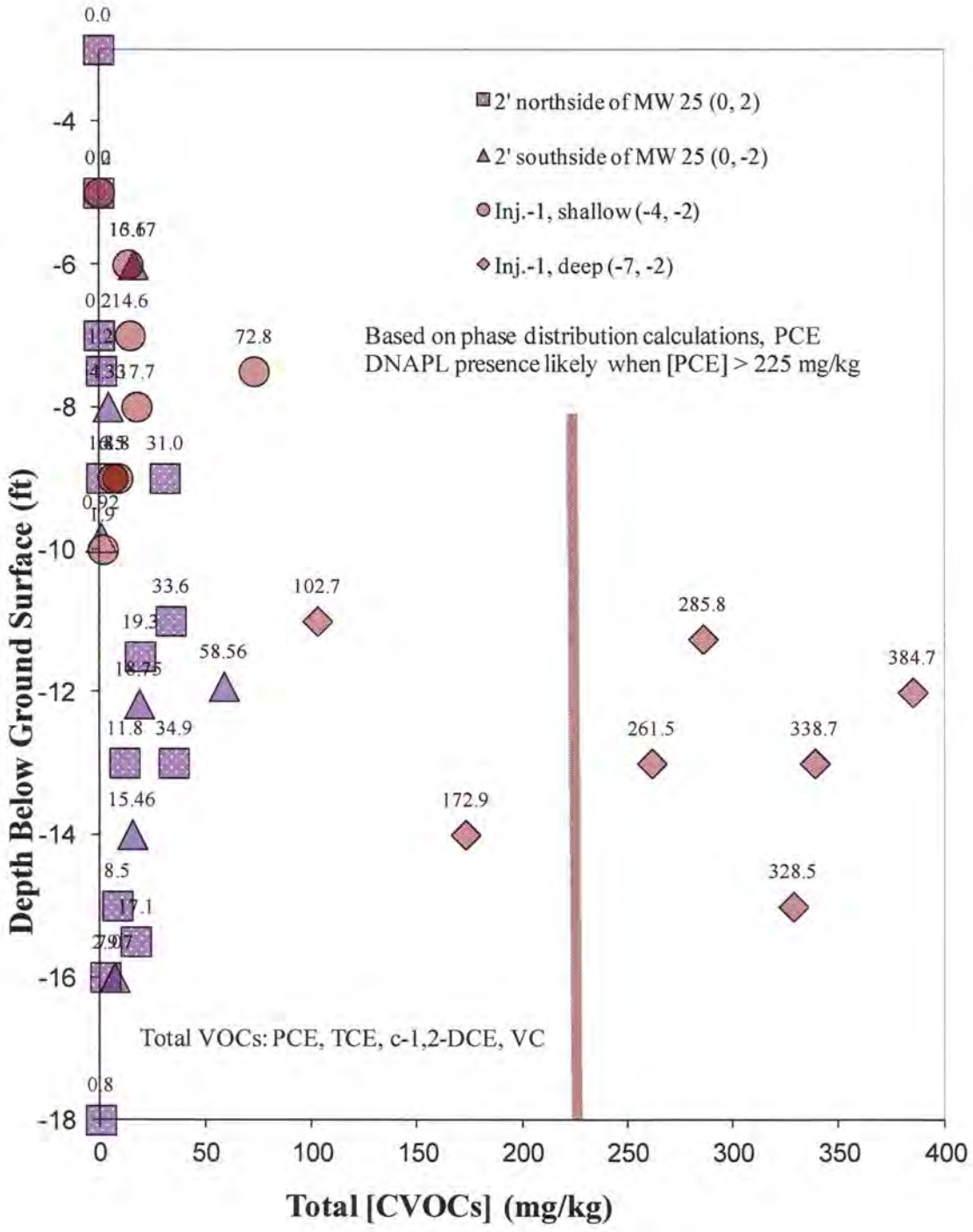

Figure D4. Vertical distribution of pre-oxidation total CVOCs in aquifer cores collected in the source area. Aquifer cores were collected adjacent to MW 25-SL and 7 ft upgradient when installing injection wells Inj.-1, Shallow and Deep (refer to Figure 4). Based on a contaminant mass distribution analysis of the total CVOCs concentration data, PCE DNAPL was likely present in the aquifer core material when PCE concentrations were greater than 225 mg/kg.

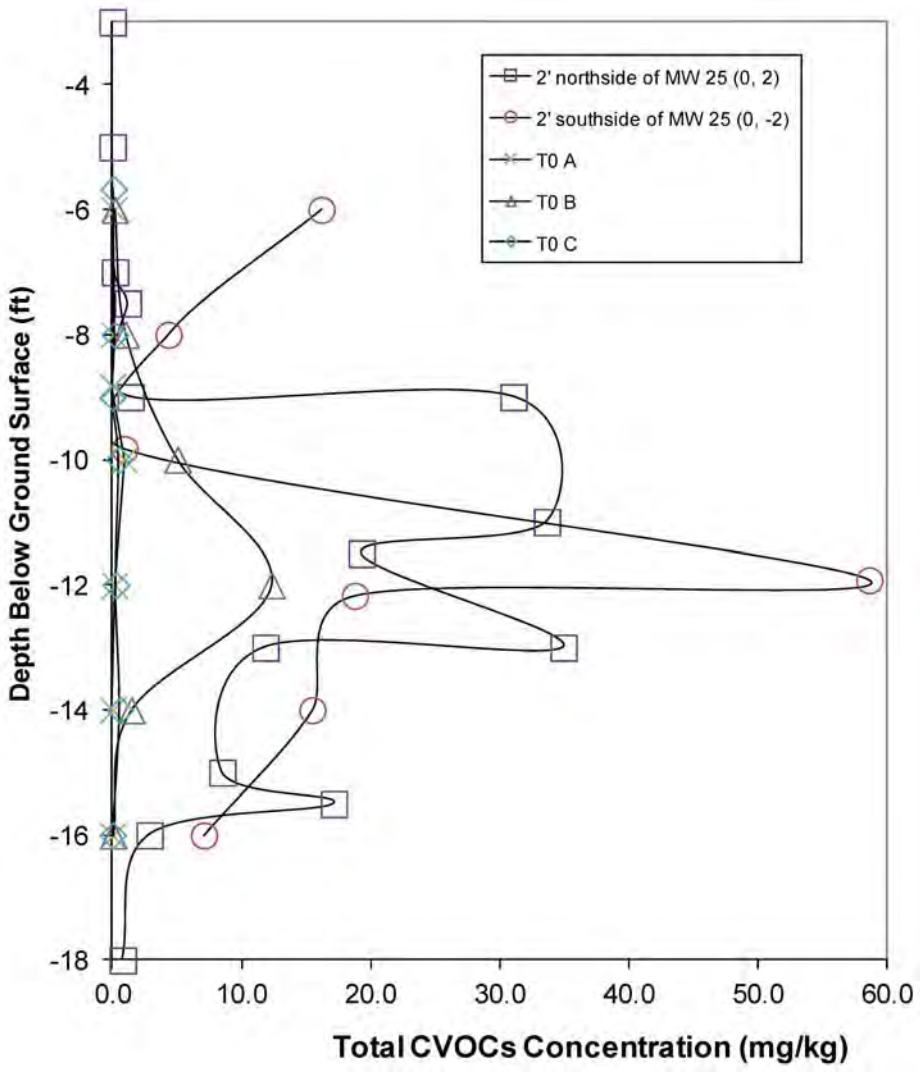

Figure D5. Vertical distribution of pre-oxidation total CVOCs at Transect T0 (refer to Figure D.1 above, and Figure 4). The T0 transect is located approximately 16.5 ft downgradient from MW 25-SL.

The contrast between pre- and post-oxidation vertical distribution of total CVOCs concentrations in soil is evident by plotting post- oxidation $[CVOCs]_{SOIL}$ with nearby aquifer locations of pre-oxidation $[CVOCs]_{SOIL}$ (Figures D6-D23). The post- oxidation $[CVOCs]_{SOIL}$ are illustrated in purple and pre-oxidation $[CVOCs]_{SOIL}$ are in red. The figures represent contrasting CVOCs profiles with increasing distance from the source zone. Sampling locations close to the ordinate at MW 25-SL and upgradient of the ordinate (0, 0) indicated a strong CVOCs source strength. The value in parentheses following the (X, Y) coordinate represents the radial distance (feet) from the post-oxidation soil sample location (as per Eqn 3, section 4.6 of the report). The bar chart inset illustrates the average pre- and post-oxidation $[CVOCs]_{SOIL}$ for each core location where the average value was based on the post-oxidation soil sample depth interval, and the post-oxidation $[CVOCs]_{SOIL}$ bar is purple.

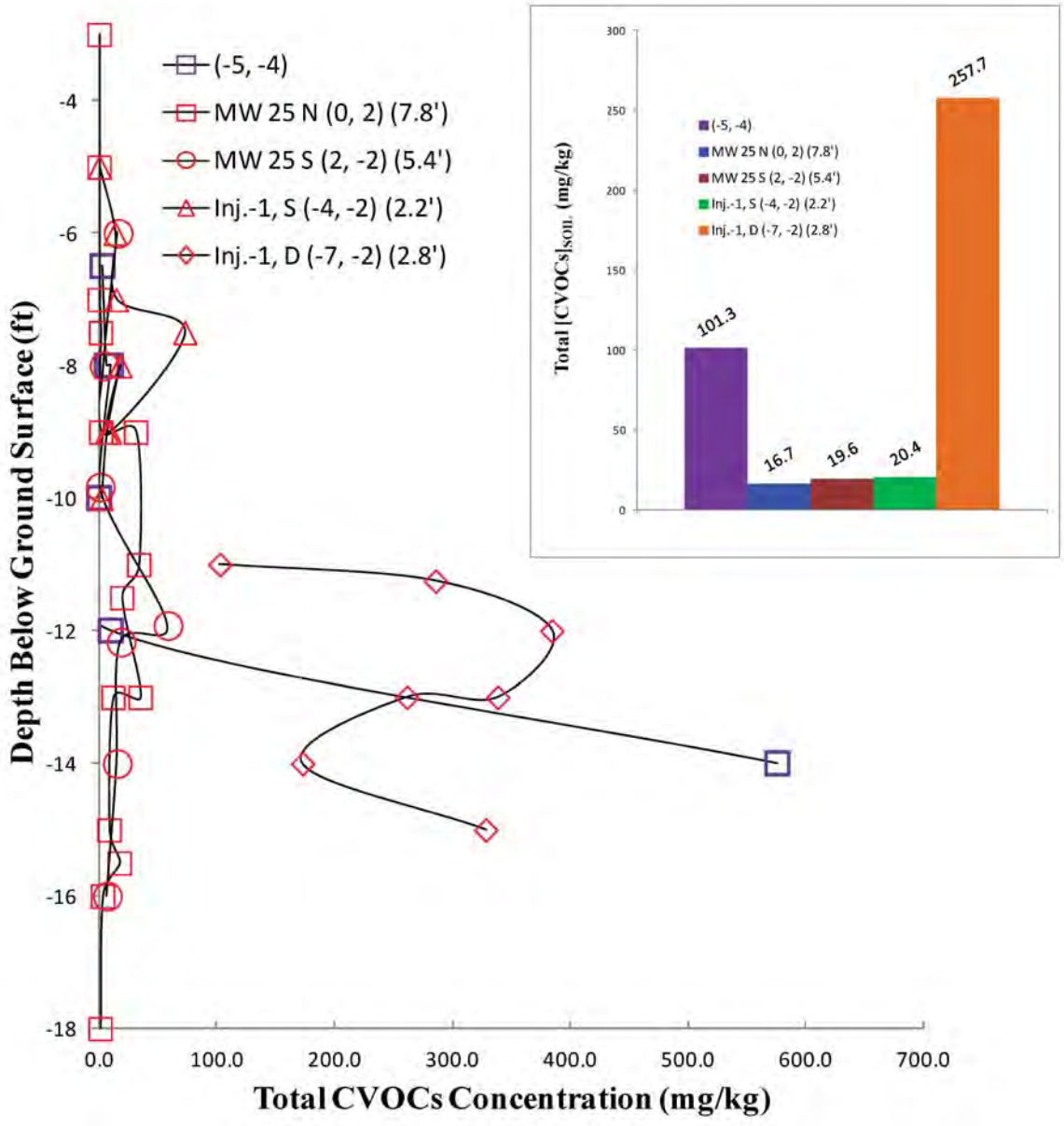

Figure D6. The depth-dependent vertical distribution of post-oxidation $[CVOCs]_{SOIL}$ (purple square symbol) at location (-5, -4) contrasted with nearby pre-oxidation $[CVOCs]_{SOIL}$ (red symbols). The (-5, -4) coordinates are based on the ordinate (*i.e.*, (0, 0) located at MW 25-SL as illustrated in Figure D1, above). The value in parentheses following the (X, Y) coordinate represents the radial distance (feet) from the post-oxidation soil sample location (as per Eqn 3, section 4.6 of the report). The bar chart inset illustrates the average pre- and post-oxidation $[CVOCs]_{SOIL}$. The average value for each core location was based on the post-oxidation soil sample depth interval.

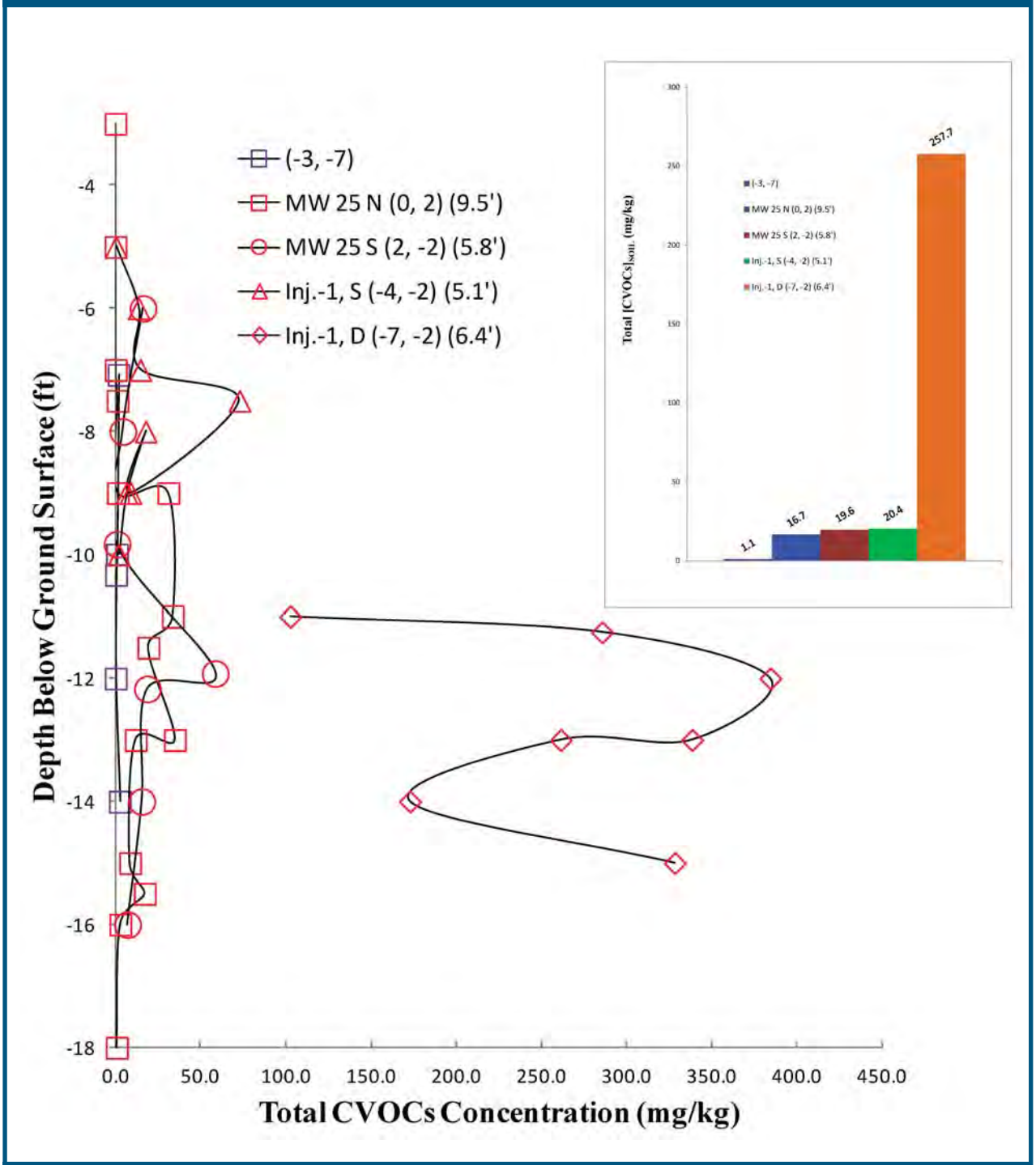

Figure D7. The depth-dependent vertical distribution of post-oxidation $[CVOCs]_{SOIL}$ (purple square symbol) at location (-3, -7) contrasted with nearby pre-oxidation $[CVOCs]_{SOIL}$ (red symbols). The (-3, -7) coordinates are based on the ordinate (*i.e.*, (0, 0) located at MW 25-SL as illustrated in Figure D1, above). The value in parentheses following the (X, Y) coordinate represents the radial distance (feet) from the post-oxidation soil sample location (as per Eqn 3, section 4.6 of the report). The bar chart inset illustrates the average pre- and post-oxidation $[CVOCs]_{SOIL}$. The average value for each core location was based on the post-oxidation soil sample depth interval.

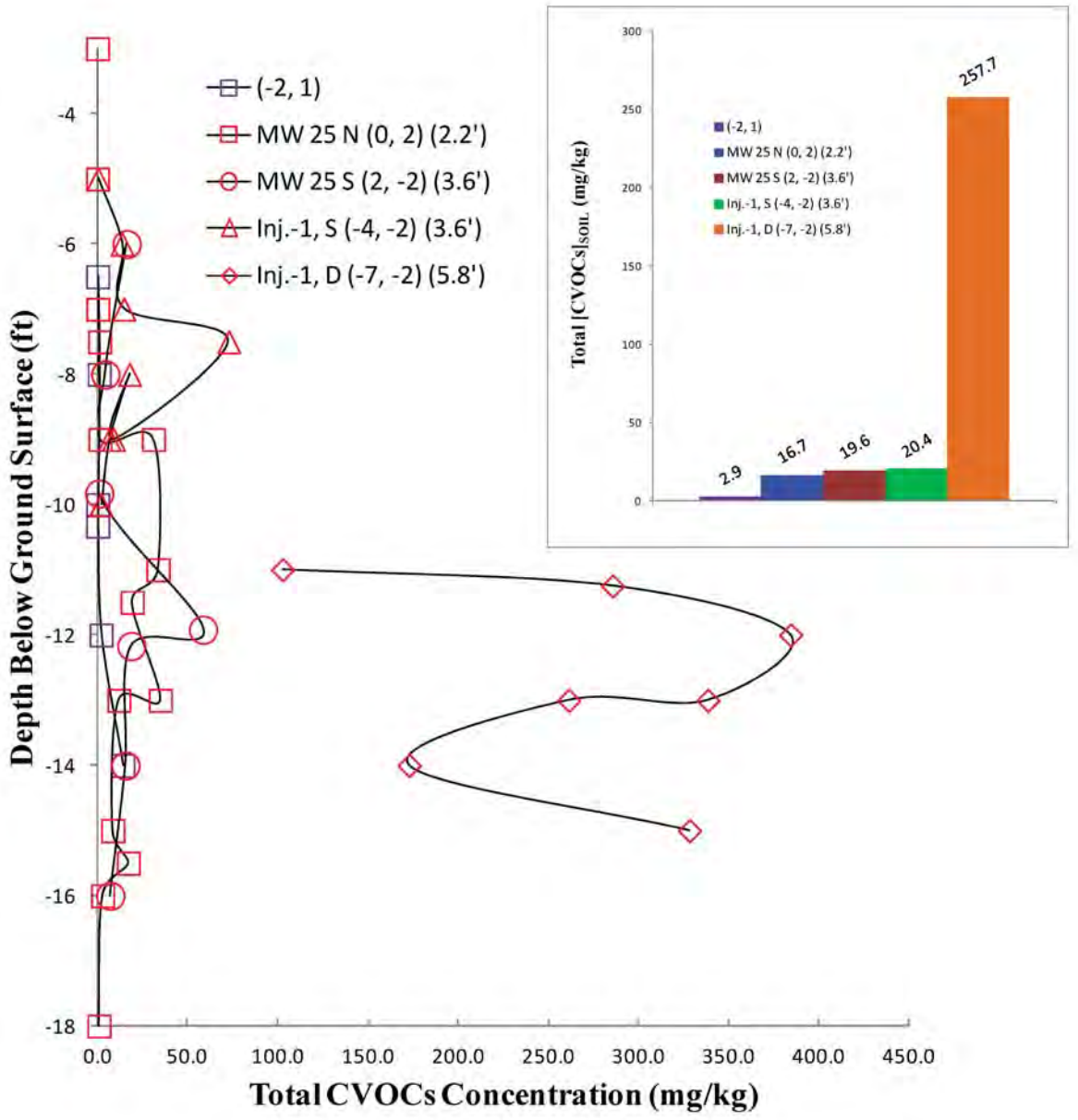

Figure D8. The depth-dependent vertical distribution of post-oxidation $[CVOCs]_{SOIL}$ (purple square symbol) at location (-2, 1) contrasted with nearby pre-oxidation $[CVOCs]_{SOIL}$ (red symbols). The (-2, -1) coordinates are based on the ordinate (*i.e.*, (0, 0) located at MW 25-SL as illustrated in Figure D1, above). The value in parentheses following the (X, Y) coordinate represents the radial distance (feet) from the post-oxidation soil sample location (as per Eqn 3, section 4.6 of the report). The bar chart inset illustrates the average pre- and post-oxidation $[CVOCs]_{SOIL}$. The average value for each core location was based on the post-oxidation soil sample depth interval.

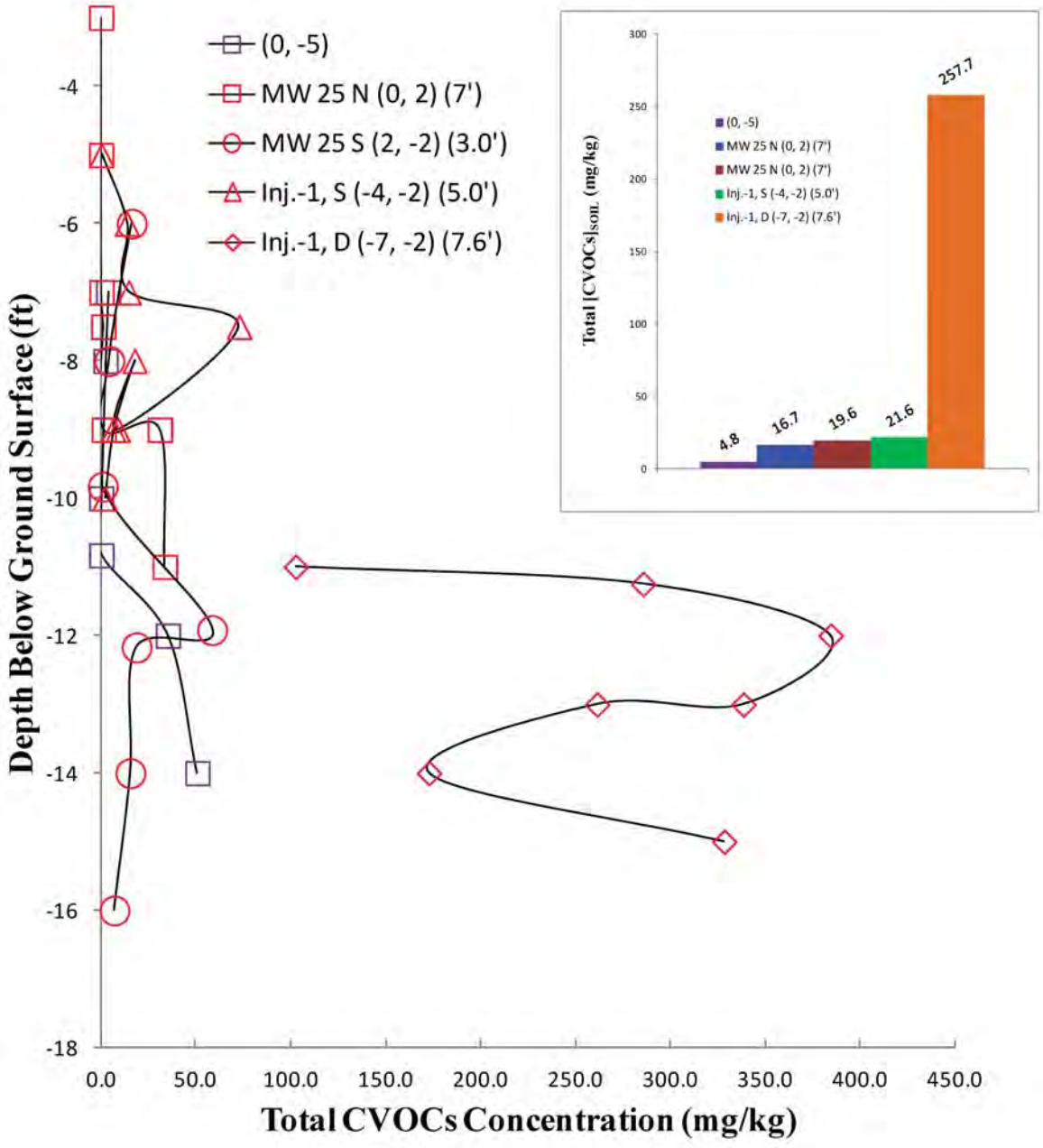

Figure D9. The depth-dependent vertical distribution of post-oxidation $[CVOCs]_{SOIL}$ (purple square symbol)) at location (0, -5) contrasted with nearby pre-oxidation $[CVOCs]_{SOIL}$ (red symbols). The (0, -5) coordinates are based on the ordinate (*i.e.*, (0, 0) located at MW 25-SL as illustrated in Figure D1, above). The value in parentheses following the (X, Y) coordinate represents the radial distance (feet) from the post-oxidation soil sample location (as per Eqn 3, section 4.6 of the report). The bar chart inset illustrates the average pre- and post-oxidation $[CVOCs]_{SOIL}$. The average value for each core location was based on the post-oxidation soil sample depth interval.

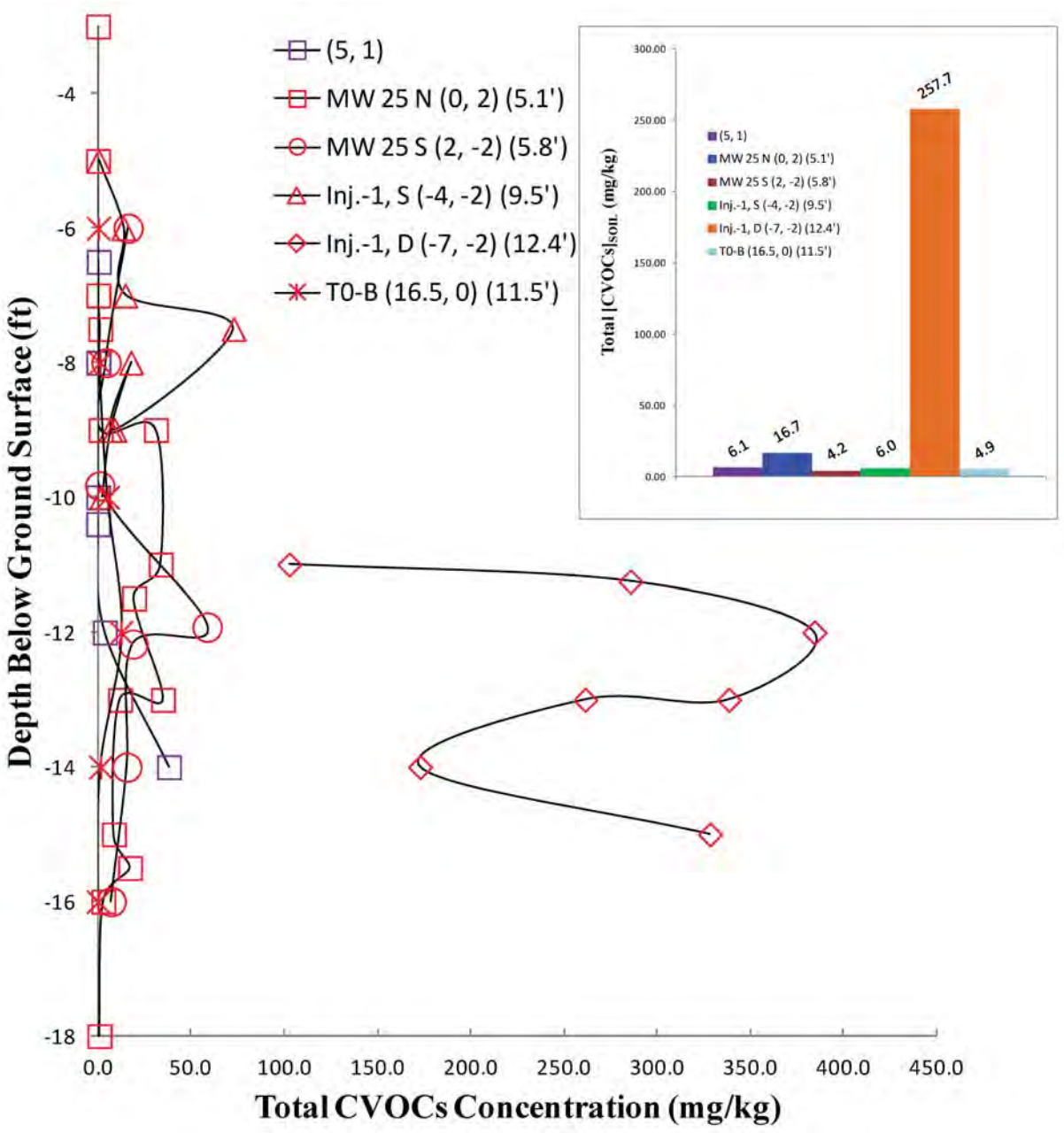

Figure D10. The depth-dependent vertical distribution of post-oxidation $[CVOCs]_{SOIL}$ (purple square symbol) at location (5, 1) contrasted with nearby pre-oxidation $[CVOCs]_{SOIL}$ (red symbols). The (5, 1) coordinates are based on the ordinate (*i.e.*, (0, 0) located at MW 25-SL as illustrated in Figure D.1, above). The value in parentheses following the (X, Y) coordinate represents the radial distance (feet) from the post-oxidation soil sample location (as per Eqn 3, section 4.6 of the report). The bar chart inset illustrates the average pre- and post-oxidation $[CVOCs]_{SOIL}$. The average value for each core location was based on the post-oxidation soil sample depth interval.

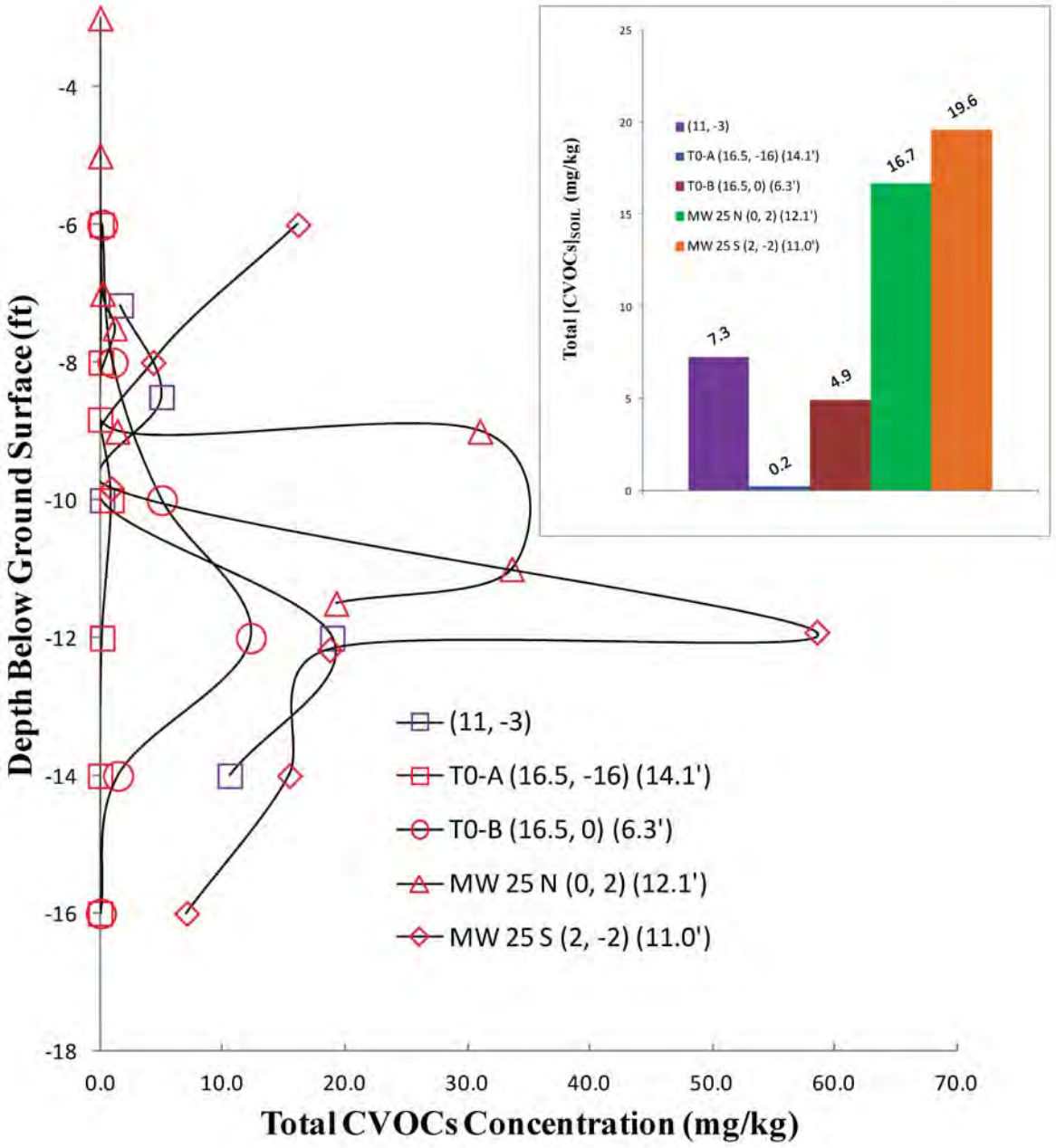

Figure D11. The depth-dependent vertical distribution of post-oxidation $[CVOCs]_{SOIL}$ (purple square symbol) at location (11, -3) contrasted with nearby pre-oxidation $[CVOCs]_{SOIL}$ (red symbols). The (11, -3) coordinates are based on the ordinate (*i.e.*, (0, 0) located at MW 25-SL as illustrated in Figure D1, above). The value in parentheses following the (X, Y) coordinate represents the radial distance (feet) from the post-oxidation soil sample location (as per Eqn 3, section 4.6 of the report). The bar chart inset illustrates the average pre- and post-oxidation $[CVOCs]_{SOIL}$. The average value for each core location was based on the post-oxidation soil sample depth interval.

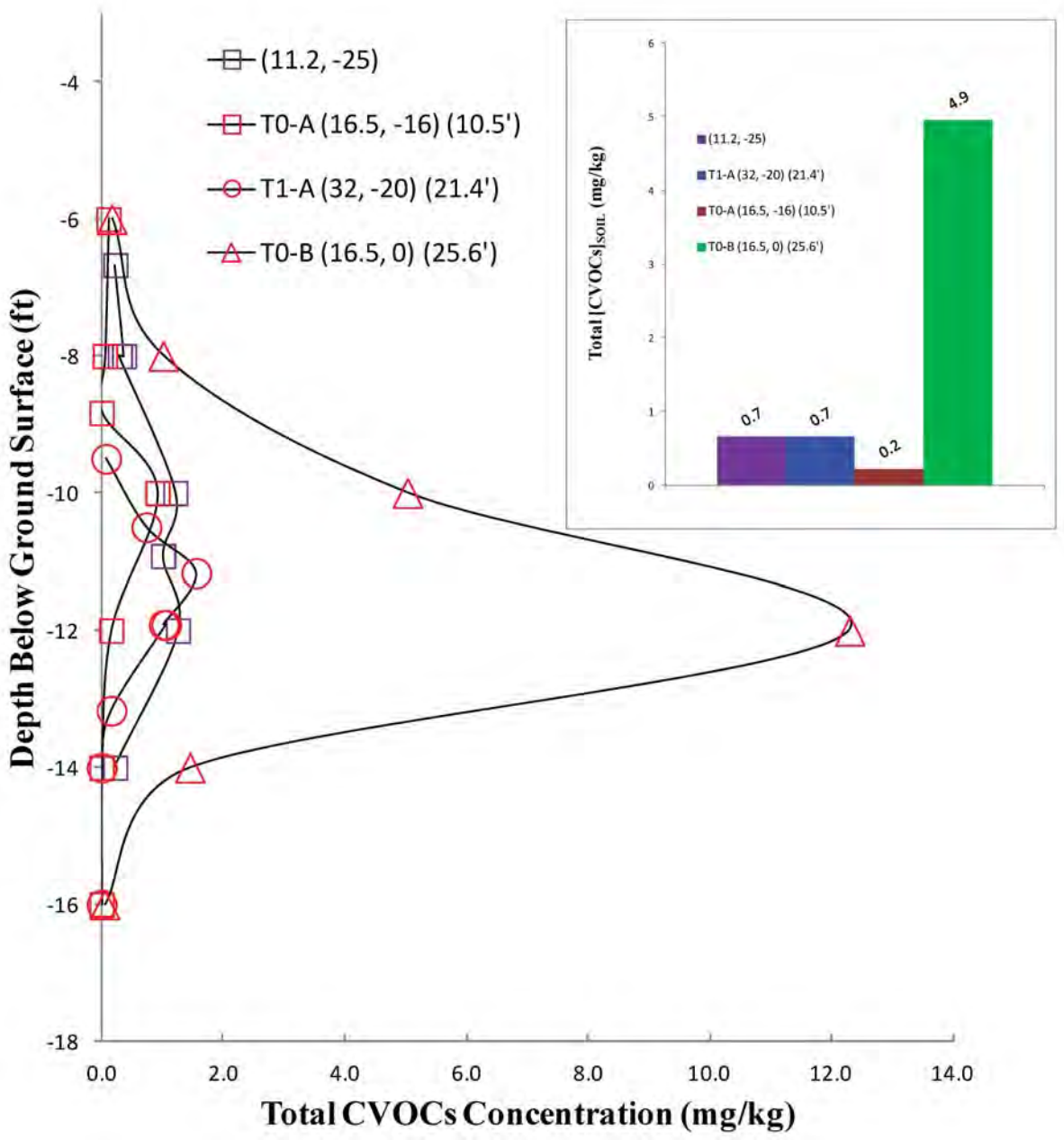

Figure D12. The depth-dependent vertical distribution of post-oxidation $[CVOCs]_{SOIL}$ (purple square symbol) at location (11.2, -25) contrasted with nearby pre-oxidation $[CVOCs]_{SOIL}$ (red symbols). The (11.2, -25) coordinates are based on the ordinate (*i.e.*, (0, 0) located at MW 25-SL as illustrated in Figure D1, above). The value in parentheses following the (X, Y) coordinate represents the radial distance (feet) from the post-oxidation soil sample location (as per Eqn 3, section 4.6 of the report). The bar chart inset illustrates the average pre- and post-oxidation $[CVOCs]_{SOIL}$. The average value for each core location was based on the post-oxidation soil sample depth interval.

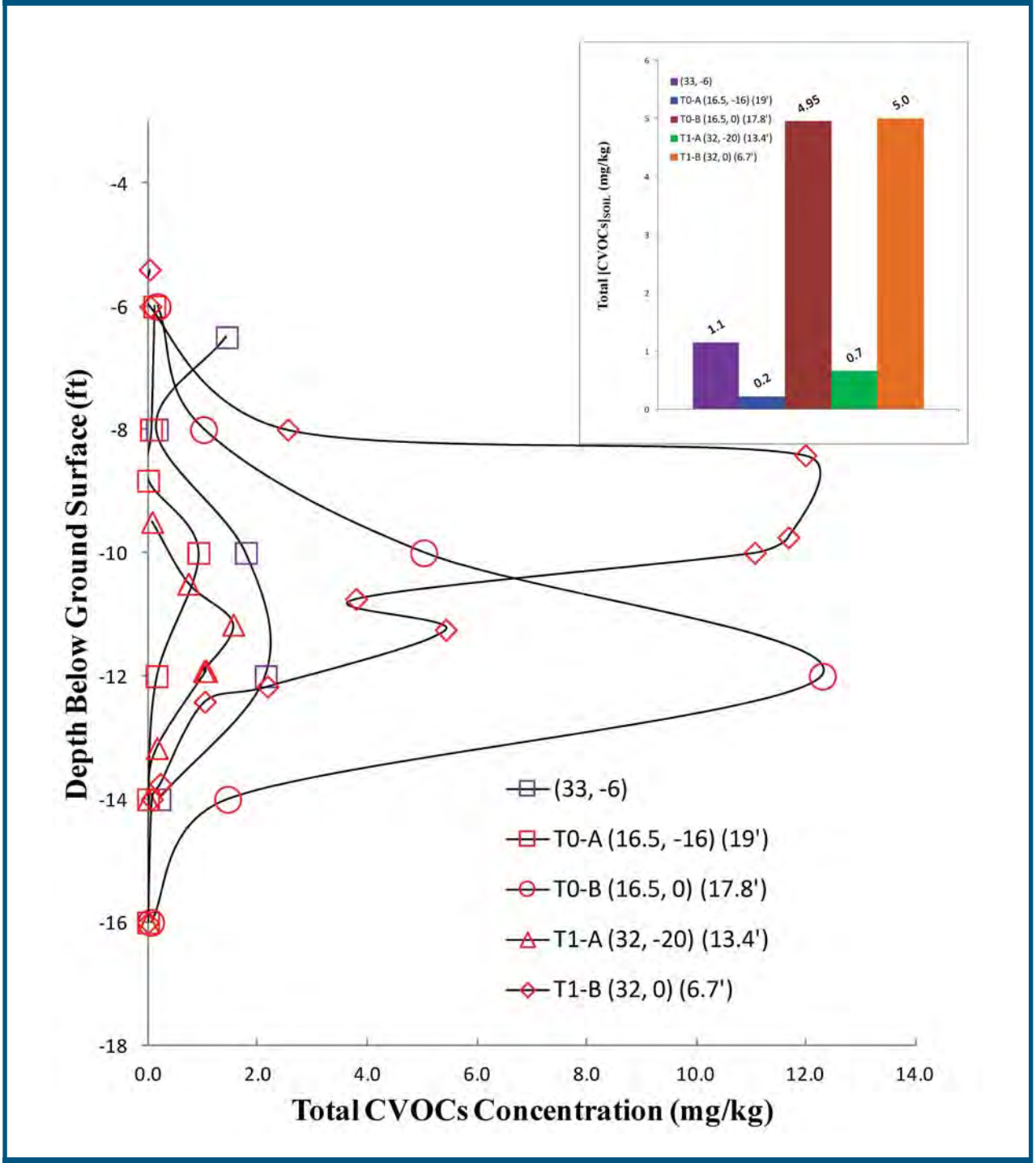

Figure D13. The depth-dependent vertical distribution of post-oxidation $[CVOCs]_{SOIL}$ (purple square symbol) at location (33, -6) contrasted with nearby pre-oxidation $[CVOCs]_{SOIL}$ (red symbols). The (33, -6) coordinates are based on the ordinate (*i.e.*, (0, 0) located at MW 25-SL as illustrated in Figure D.1, above). The value in parentheses following the (X, Y) coordinate represents the radial distance (feet) from the post-oxidation soil sample location (as per Eqn 3, section 4.6 of the report). The bar chart inset illustrates the average pre- and post-oxidation $[CVOCs]_{SOIL}$. The average value for each core location was based on the post-oxidation soil sample depth interval.

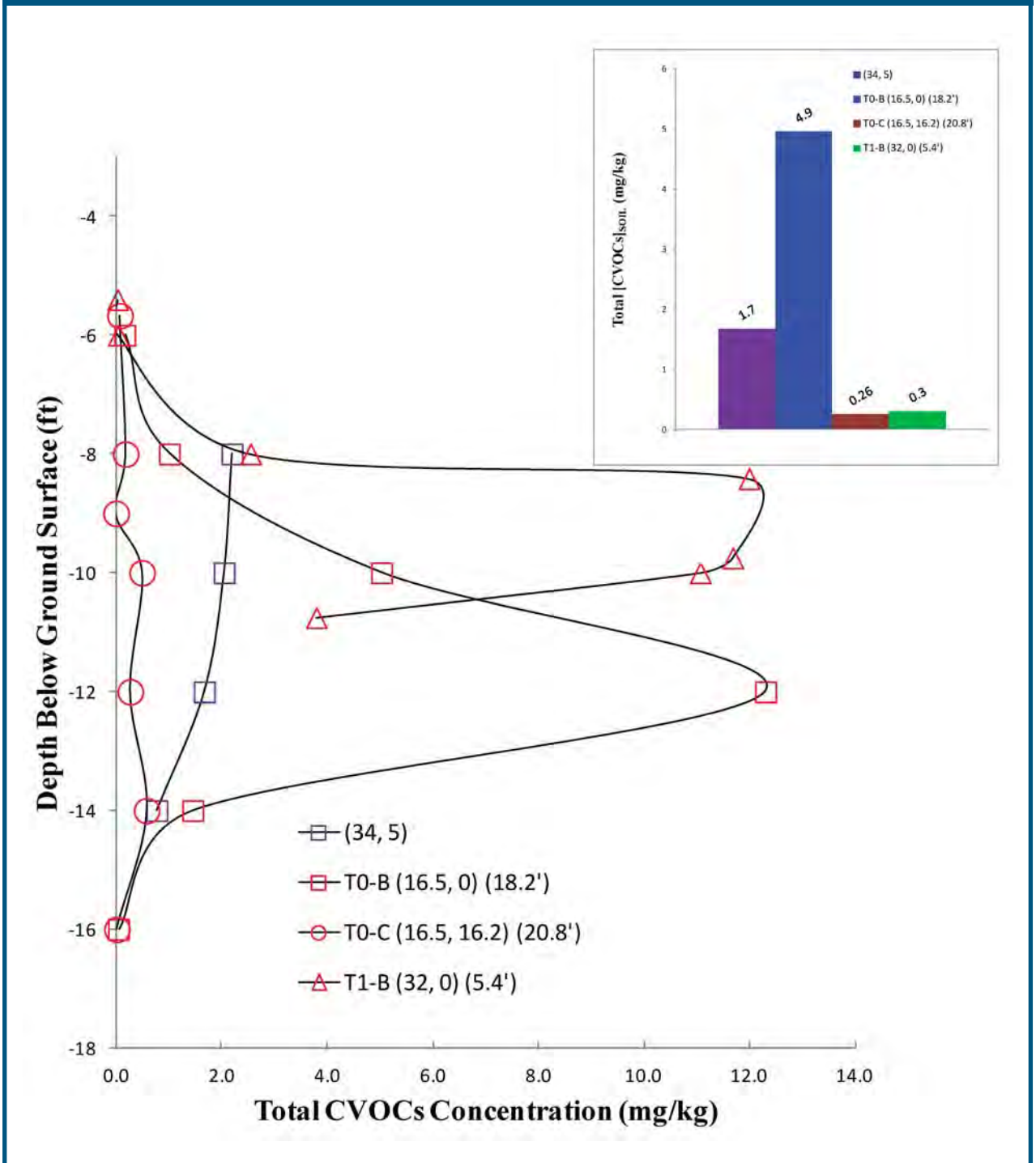

Figure D14. The depth-dependent vertical distribution of post-oxidation $[CVOCs]_{SOIL}$ (purple square symbol) at location (34, 5) contrasted with nearby pre-oxidation $[CVOCs]_{SOIL}$ (red symbols). The (34, 5) coordinates are based on the ordinate (*i.e.*, (0, 0) located at MW 25-SL as illustrated in Figure D1, above). The value in parentheses following the (X, Y) coordinate represents the radial distance (feet) from the post-oxidation soil sample location (as per Eqn 3, section 4.6 of the report). The bar chart inset illustrates the average pre- and post-oxidation $[CVOCs]_{SOIL}$. The average value for each core location was based on the post-oxidation soil sample depth interval.

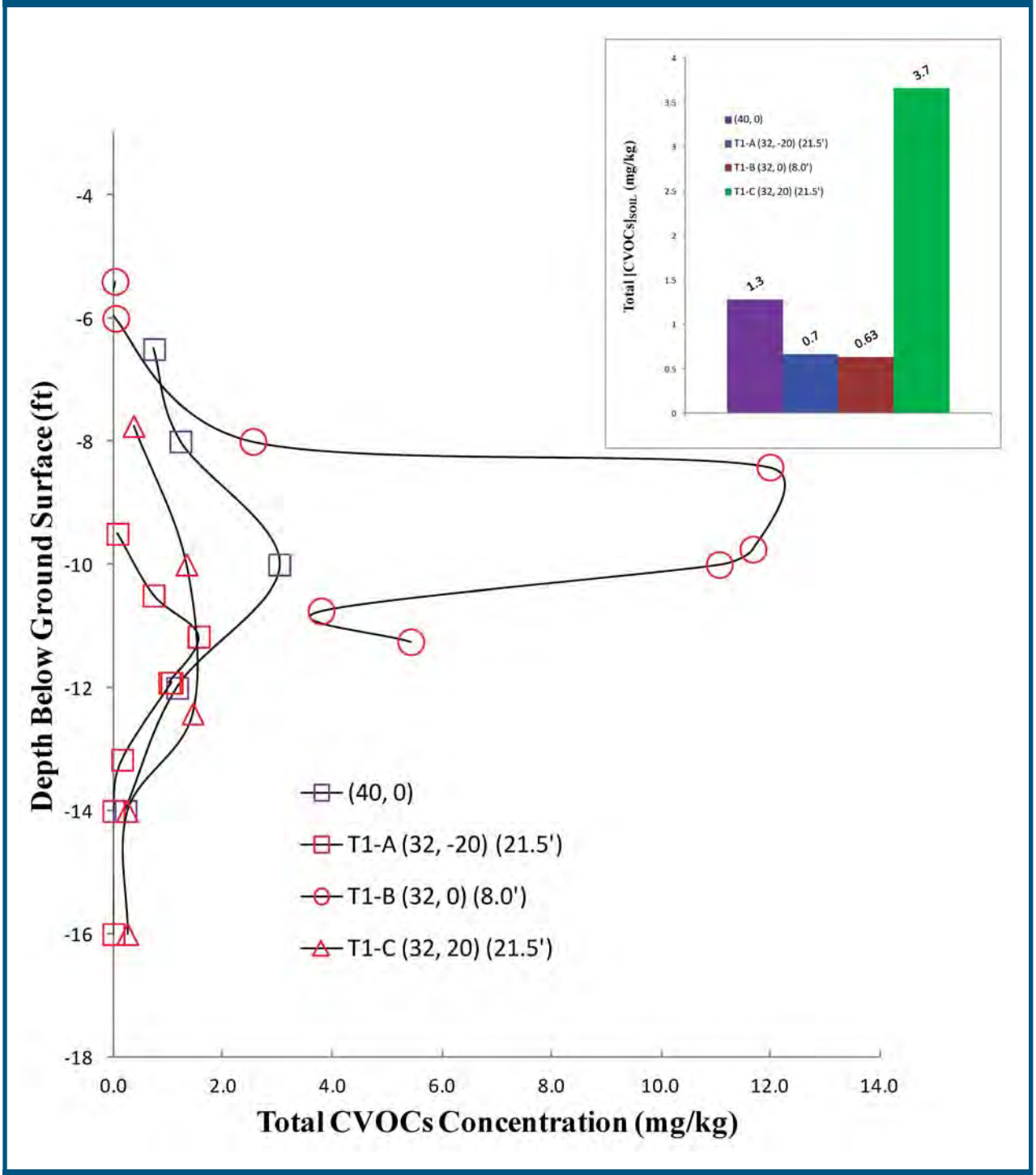

Figure D15. The depth-dependent vertical distribution of post-oxidation $[CVOCs]_{SOIL}$ (purple square symbol) at location (40, 0) contrasted with nearby pre-oxidation $[CVOCs]_{SOIL}$ (red symbols). The (40, 0) coordinates are based on the ordinate (*i.e.*, (0, 0) located at MW 25-SL as illustrated in Figure D.1, above). The value in parentheses following the (X, Y) coordinate represents the radial distance (feet) from the post-oxidation soil sample location (as per Eqn 3, section 4.6 of the report). The bar chart inset illustrates the average pre- and post-oxidation $[CVOCs]_{SOIL}$. The average value for each core location was based on the post-oxidation soil sample depth interval.

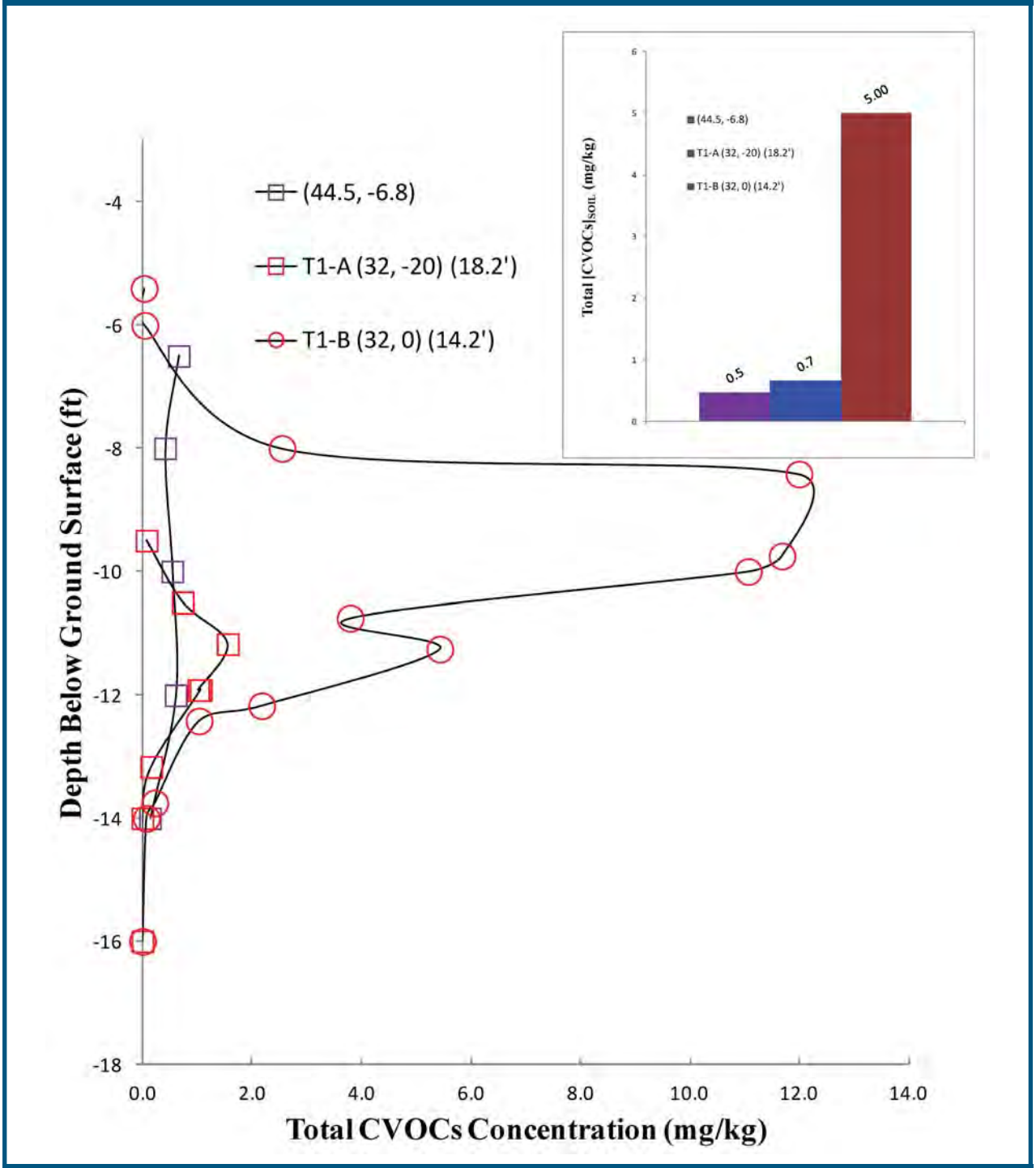

Figure D16. The depth-dependent vertical distribution of post-oxidation $[CVOCs]_{SOIL}$ (purple square symbol) at location (44.5, -6.8) contrasted with nearby pre-oxidation $[CVOCs]_{SOIL}$ (red symbols). The (44.5, -6.8) coordinates are based on the ordinate (*i.e.*, (0, 0) located at MW 25-SL as illustrated in Figure D.1, above). The value in parentheses following the (X, Y) coordinate represents the radial distance (feet) from the post-oxidation soil sample location (as per Eqn 3, section 4.6 of the report). The bar chart inset illustrates the average pre- and post-oxidation $[CVOCs]_{SOIL}$. The average value for each core location was based on the post-oxidation soil sample depth interval.

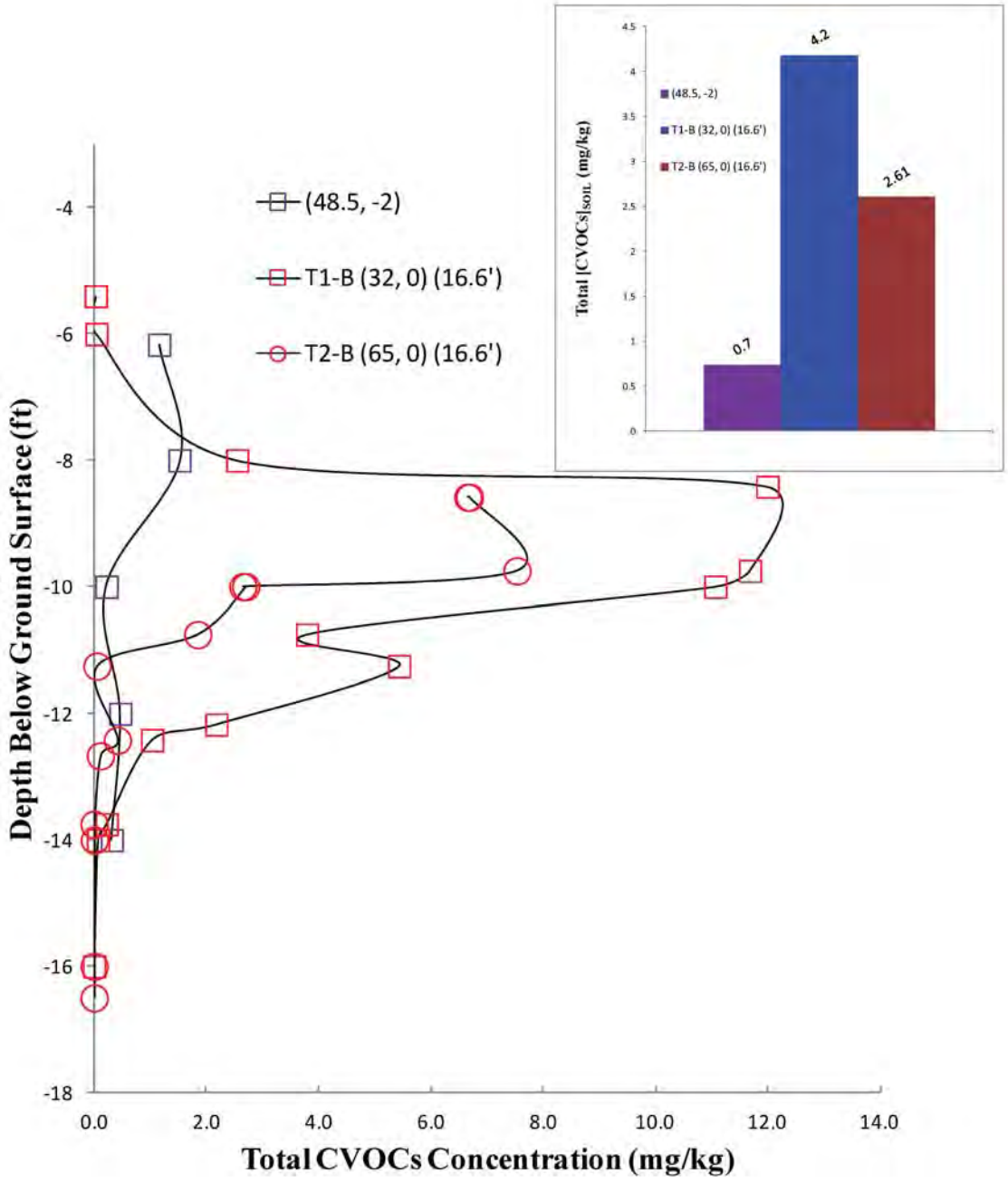

Figure D17. The depth-dependent vertical distribution of post-oxidation $[CVOCs]_{SOIL}$ (purple square symbol) at location (48.5, -2) contrasted with nearby pre-oxidation $[CVOCs]_{SOIL}$ (red symbols). The (48.5, -2) coordinates are based on the ordinate (*i.e.*, (0, 0) located at MW 25-SL as illustrated in Figure D.1, above). The value in parentheses following the (X, Y) coordinate represents the radial distance (feet) from the post-oxidation soil sample location (as per Eqn 3, section 4.6 of the report). The bar chart inset illustrates the average pre- and post-oxidation $[CVOCs]_{SOIL}$. The average value for each core location was based on the post-oxidation soil sample depth interval.

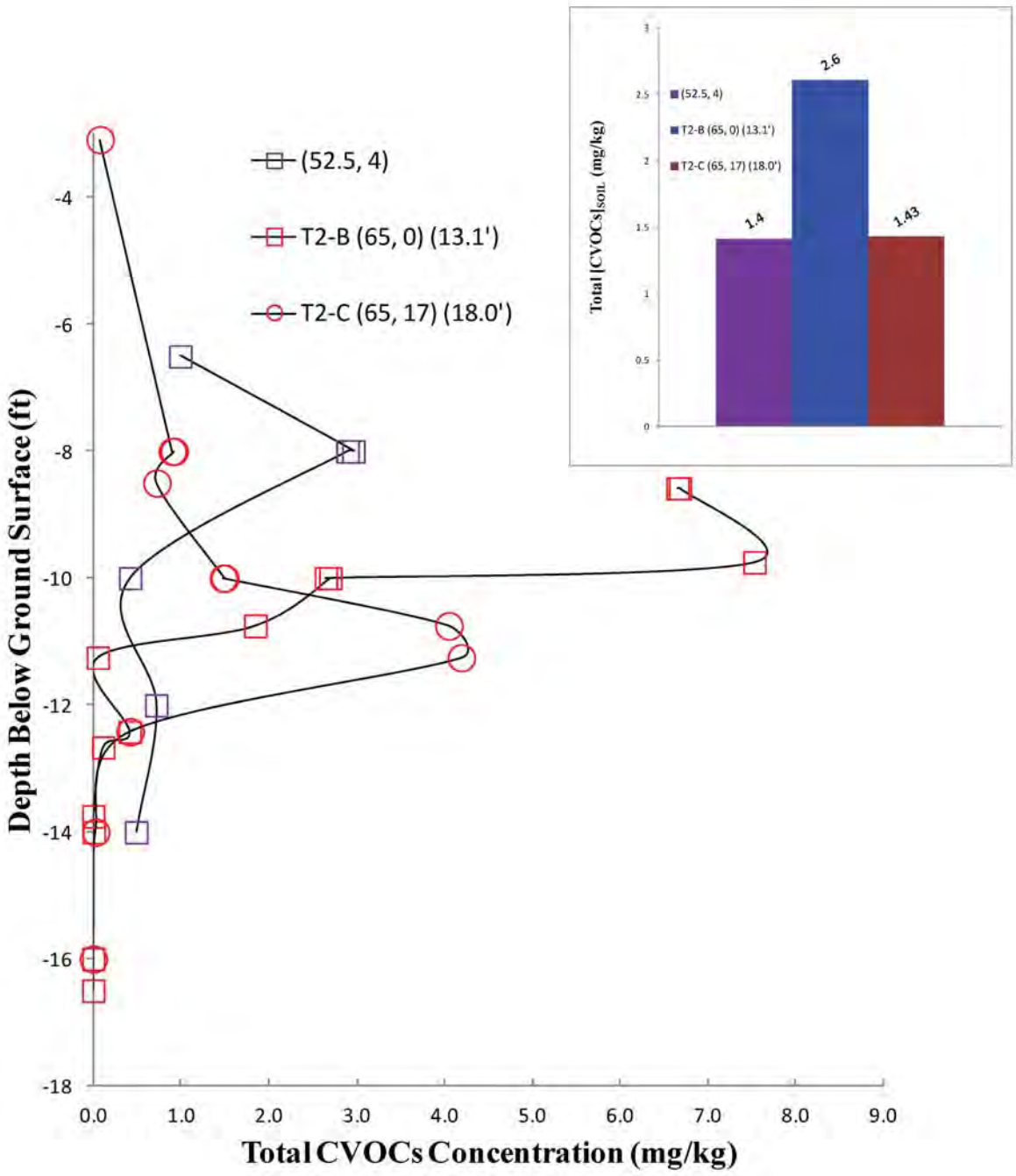

Figure D18. The depth-dependent vertical distribution of post-oxidation $[CVOCs]_{SOIL}$ (purple square symbol) at location (52.5, 4) contrasted with nearby pre-oxidation $[CVOCs]_{SOIL}$ (red symbols). The (52.5, 4) coordinates are based on the ordinate (*i.e.*, (0, 0) located at MW 25-SL as illustrated in Figure D1, above). The value in parentheses following the (X, Y) coordinate represents the radial distance (feet) from the post-oxidation soil sample location (as per Eqn 3, section 4.6 of the report). The bar chart inset illustrates the average pre- and post-oxidation $[CVOCs]_{SOIL}$. The average value for each core location was based on the post-oxidation soil sample depth interval.

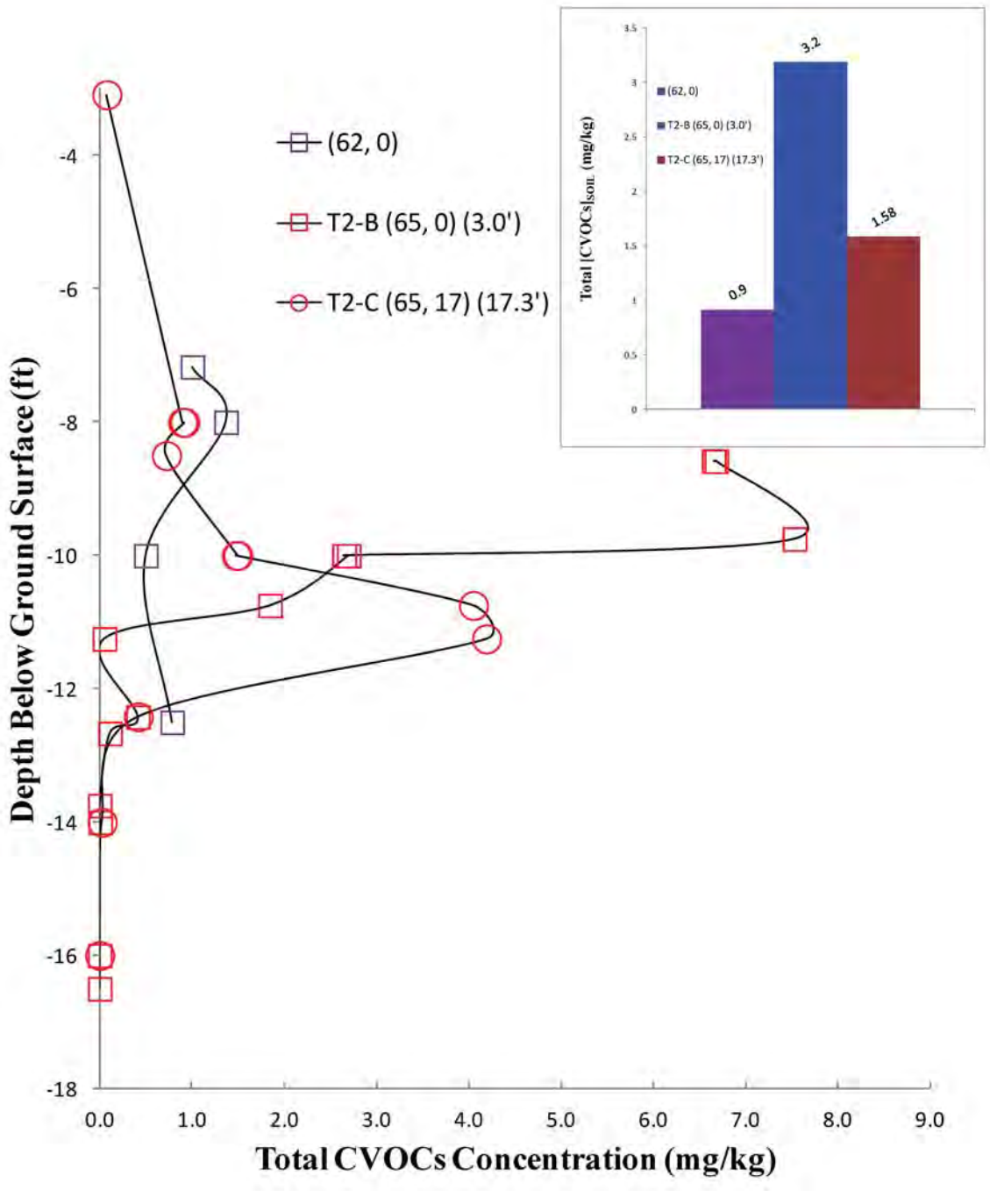

Figure D19. The depth-dependent vertical distribution of post-oxidation $[CVOCs]_{SOIL}$ (purple square symbol) at location (62, 0) contrasted with nearby pre-oxidation $[CVOCs]_{SOIL}$ (red symbols). The (62, 0) coordinates are based on the ordinate (*i.e.*, (0, 0) located at MW 25-SL as illustrated in Figure D1, above). The value in parentheses following the (X, Y) coordinate represents the radial distance (feet) from the post-oxidation soil sample location (as per Eqn 3, section 4.6 of the report). The bar chart inset illustrates the average pre- and post-oxidation $[CVOCs]_{SOIL}$. The average value for each core location was based on the post-oxidation soil sample depth interval.

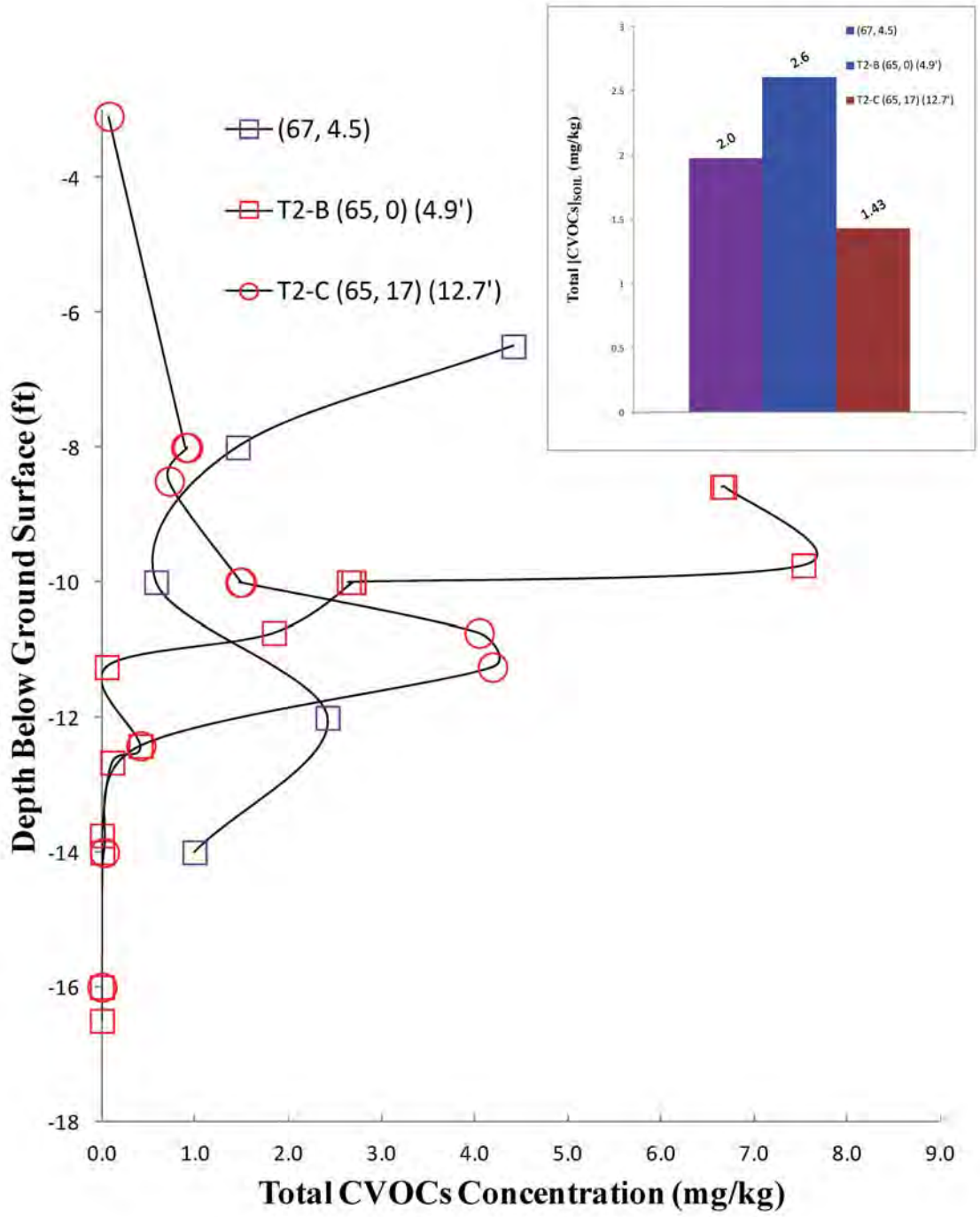

Figure D20. The depth-dependent vertical distribution of post-oxidation $[CVOCs]_{SOIL}$ (purple square symbol) at location (67, 4.5) contrasted with nearby pre-oxidation $[CVOCs]_{SOIL}$ (red symbols). The (67, 4.5) coordinates are based on the ordinate (*i.e.*, (0, 0) located at MW 25-SL as illustrated in Figure D1, above). The value in parentheses following the (X, Y) coordinate represents the radial distance (feet) from the post-oxidation soil sample location (as per Eqn 3, section 4.6 of the report). The bar chart inset illustrates the average pre- and post-oxidation $[CVOCs]_{SOIL}$. The average value for each core location was based on the post-oxidation soil sample depth interval.

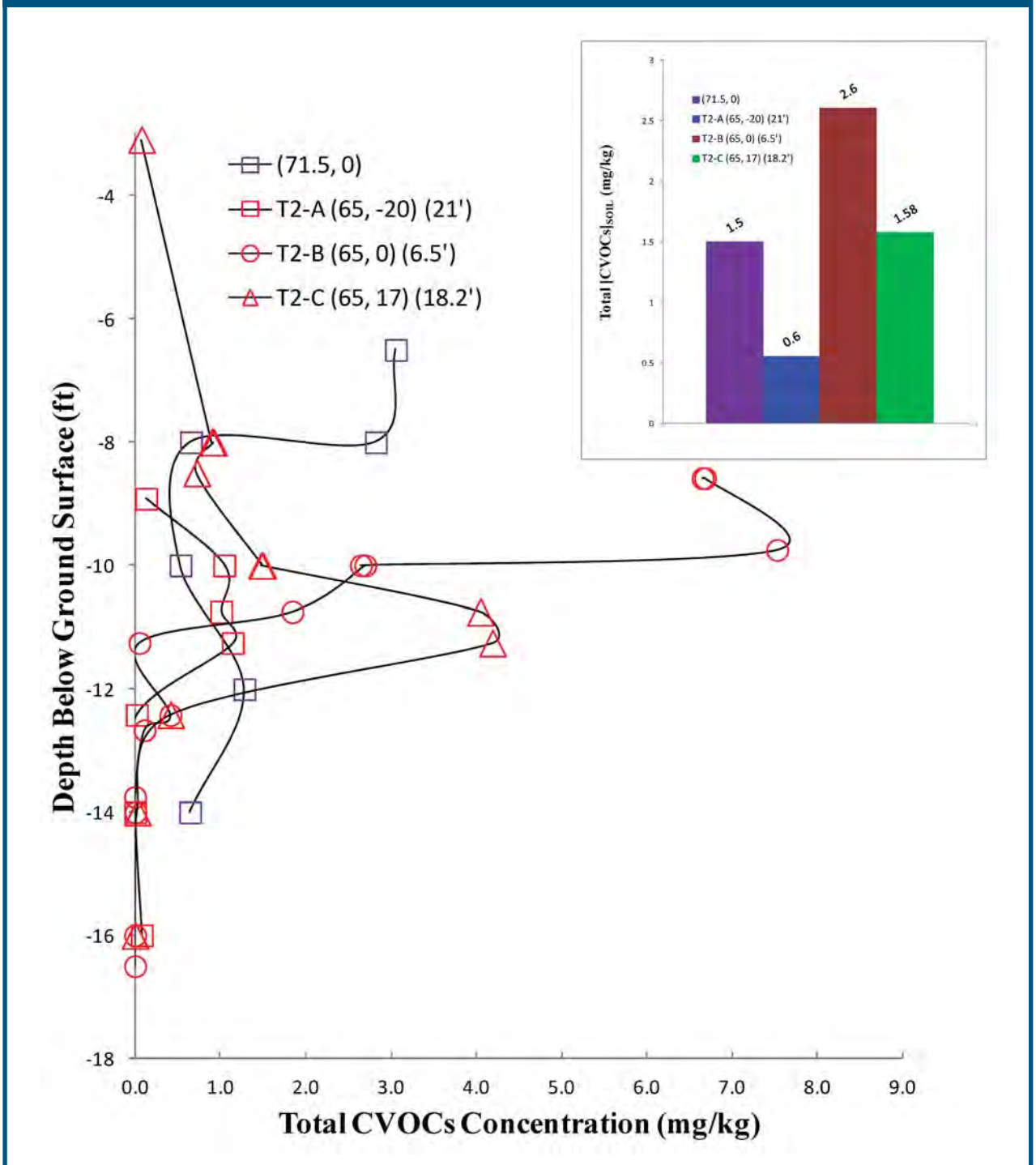

Figure D21. The depth-dependent vertical distribution of post-oxidation $[CVOCs]_{SOIL}$ (purple square symbol) at location (71.5, 0) contrasted with nearby pre-oxidation $[CVOCs]_{SOIL}$ (red symbols). The (71.5, 0) coordinates are based on the ordinate (*i.e.*, (0, 0) located at MW 25-SL as illustrated in Figure D1, above). The value in parentheses following the (X, Y) coordinate represents the radial distance (feet) from the post-oxidation soil sample location (as per Eqn 3, section 4.6 of the report). The bar chart inset illustrates the average pre- and post-oxidation $[CVOCs]_{SOIL}$. The average value for each core location was based on the post-oxidation soil sample depth interval.

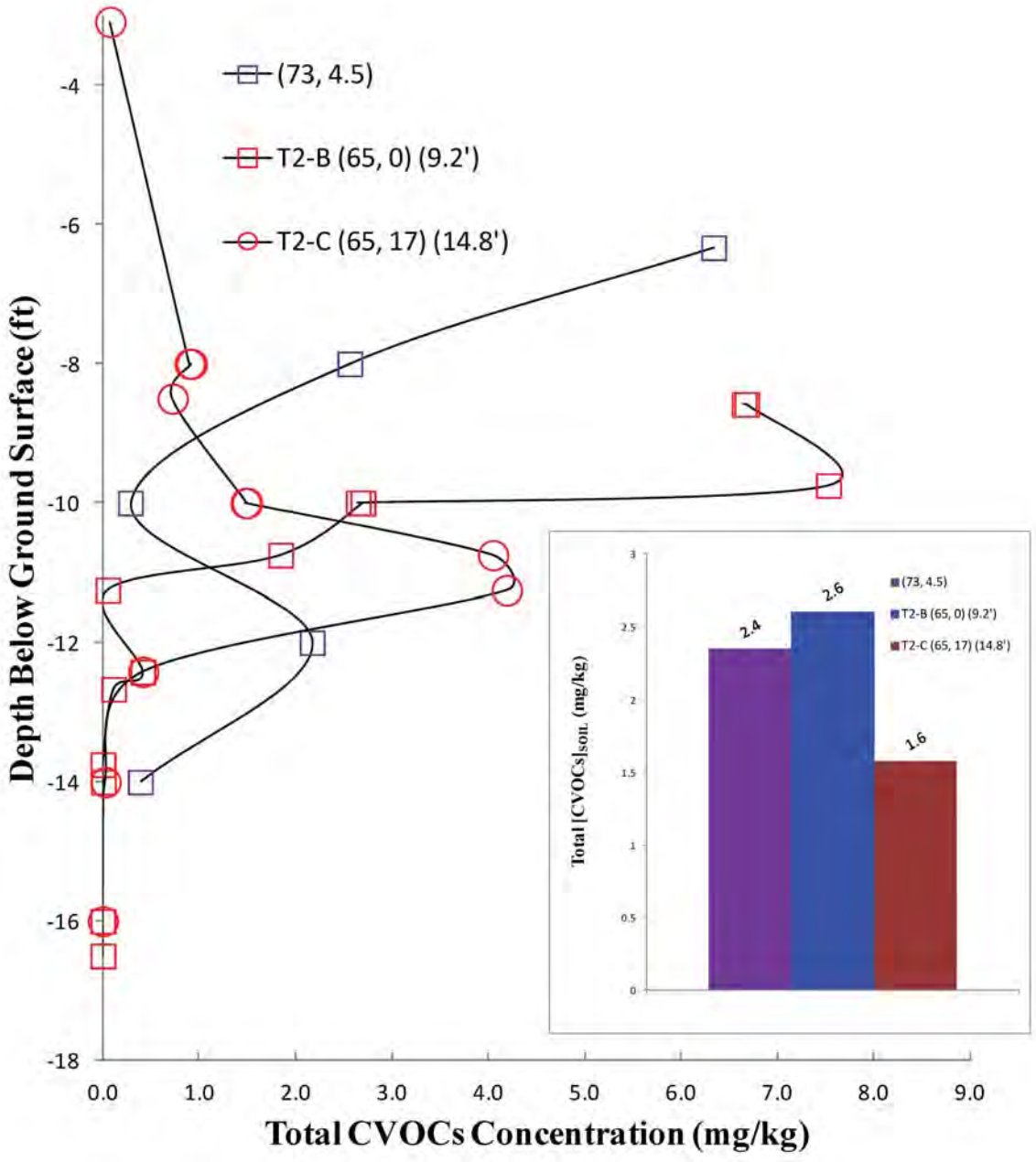

Figure D22. The depth-dependent vertical distribution of post-oxidation $[CVOCs]_{SOIL}$ (purple square symbol) at location (73, 4.5) contrasted with nearby pre-oxidation $[CVOCs]_{SOIL}$ (red symbols). The (73, 4.5) coordinates are based on the ordinate (*i.e.*, (0, 0) located at MW 25-SL as illustrated in Figure D1, above). The value in parentheses following the (X, Y) coordinate represents the radial distance (feet) from the post-oxidation soil sample location (as per Eqn 3, section 4.6 of the report). The bar chart inset illustrates the average pre- and post-oxidation $[CVOCs]_{SOIL}$. The average value for each core location was based on the post-oxidation soil sample depth interval.

Appendix E

Publication involving ISCO oxidant volume design considerations

Huling, S.G., Ross, R.R. and Meeker Prestbo, K. 2017. In situ chemical oxidation: permanganate oxidant volume design considerations. *Ground Water Monit. Remed.* (37)1, Spring.

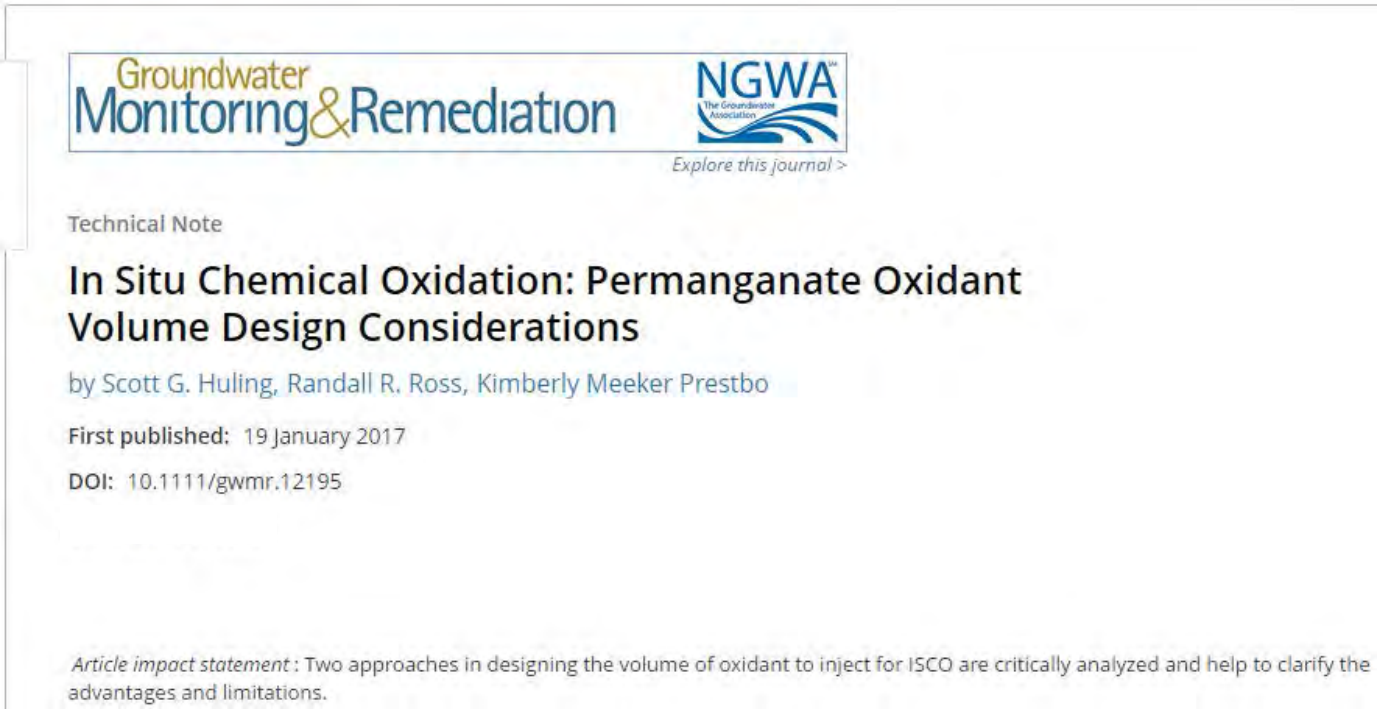

Groundwater Monitoring & Remediation

NGWA The Groundwater Association

Explore this journal >

Technical Note

In Situ Chemical Oxidation: Permanganate Oxidant Volume Design Considerations

by Scott G. Huling, Randall R. Ross, Kimberly Meeker Prestbo

First published: 19 January 2017

DOI: 10.1111/gwmr.12195

Article impact statement: Two approaches in designing the volume of oxidant to inject for ISCO are critically analyzed and help to clarify the advantages and limitations.

Groundwater Monitoring&Remediation

Technical Note

In Situ Chemical Oxidation: Permanganate Oxidant Volume Design Considerations

by Scott G. Huling, Randall R. Ross, and Kimberly Meeker Prestbo

Abstract

Contaminant rebound and low contaminant removal are reported more frequently with in situ chemical oxidation than other in situ technologies. Although there are multiple causes for these results, a critical analysis indicates that low oxidant volume delivery is a key issue. The volume of oxidant injected is critical and porosity of the aquifer matrix can be used to estimate the pore volume. The total porosity (θ_T) is the volume of voids relative to the total volume of aquifer material. The mobile porosity (θ_M) is the fraction of voids that readily contributes to fluid displacement, and is less than θ_T leading to smaller estimates of oxidant volume. Injecting low-oxidant volume may result in inadequate oxidant distribution and postinjection dispersal within the radius of influence, insufficient oxidant contact and oxidant loading, and incomplete treatment; whereas, greater oxidant volume achieves a greater oxidant footprint and may involve risk that the injected oxidant may migrate into nontarget areas and displacement of contaminated groundwater. Design guidelines and recommendations are provided that could help achieve more effective technology deployment, reduce the role of heterogeneities in the subsurface, and result in greater probability the oxidant is delivered to the targeted treatment zone.

Introduction and Background Information

The U.S. Environmental Protection Agency (US EPA) Superfund remedial program continues to select in situ chemical oxidation (ISCO) as one of the most frequently selected in situ treatment technologies (US EPA 2014). These trends in technology selection indicate the need for the continued development of ISCO, a technology that has the ability to transform contaminants in the subsurface while minimizing the use of fossil fuel energy, chemicals, and environmental impact (Siegrist et al. 2001, 2011; Huling and Pivetz 2006). A review of ISCO design and performance was performed involving 242 case studies including 83 sites where permanganate was used for the remediation of chloroethanes (Krembs et al. 2010, 2011). The median reduction in contaminant concentration in groundwater using permanganate was 51% with contaminant rebound observed at 78% of the sites. In another review of ISCO case studies, a median reduction in total chlorinated volatile organic compounds (CVOCs) concentrations of 72% was observed at 12 ISCO sites, but rebound was more prevalent relative to bioremediation, thermal, or solvent/cosolvent treatment (McGuire et al. 2006). In another remediation survey at dense nonaqueous phase liquids sites, the occurrence of rebound was reported to be more prevalent at ISCO sites compared to sites implementing other technologies (GeoSyntec Consultants 2004).

The consistency in the conclusions from these surveys regarding ISCO treatment performance possibly suggests a systematic cause and effect in technology design, deployment, and performance results. The cause of contaminant rebound and low contaminant removal reported in these cases is attributed to multiple causes and mechanisms. Here, we propose that low oxidant volume delivery is a key issue. The objectives of this manuscript are to contrast and critically analyze two methods used in estimating the volume of oxidant to inject in the targeted treatment zone (TTZ), clarify the impact of this important design parameter, and recommend injection design options that limit the role of heterogeneities and its negative impact on oxidant distribution. Several forms of oxidant can be used in ISCO but the focus of this study is potassium and sodium permanganate ($KMnO_4$ and $NaMnO_4$). A detailed description of the fundamentals of ISCO using permanganate is described elsewhere (Siegrist et al. 2001, 2011; Petri et al. 2011). ISCO is often used as a source reduction remedy in TTZs where efficient oxidation can be achieved, and is not generally applied over the entire footprint of the groundwater plume. Therefore, the TTZ defined here refers to the contaminated volume of porous media in the source area requiring oxidative treatment to achieve the treatment objective.

Article impact statement: Two approaches in designing the volume of oxidant to inject for ISCO are critically analyzed and help to clarify the advantages and limitations.

doi: 10.1111/gwmr.12195

Importance of Oxidant Volume

The delivery of a sufficient volume of oxidant is required to achieve adequate coverage of the oxidant in the TTZ. The oxidant volume must contain sufficient oxidant mass to achieve the oxidant loading and treatment objectives. The combination of both oxidant volume and oxidant concentration (i.e., oxidant loading) is required to address both oxidant distribution in the TTZ, and to target contaminant and noncontaminant oxidant losses including the natural oxidant demand (NOD) (Mumford et al. 2005; Urynowicz et al. 2008; Xu and Thomson 2009; Cha et al. 2012). The focus of this critical analysis is on the immediate contact between injected oxidant and aquifer media. The postinjection oxidant transport in the downgradient direction could result in greater contact between oxidant and aquifer solids, and is dependent on hydrogeologic conditions and oxidant loading. For example, the aquifer volume contact efficiency (E_V) is an empirical measure of the oxidant impact on aquifer solids relative to the total volume of the treatment zone (Cha and Borden 2012). In an evaluation of aquifer characteristics and ISCO injection system design, numerical simulations of oxidant injection, transport, and reaction in porous media indicate that increases in E_V are functionally dependent on oxidant loading, persistence, and advective transport. Simulation results indicated that the mass and volume of permanganate injected had the greatest impact on E_V and contaminant treatment efficiency (Cha and Borden 2012). These parameters were also identified by others as a key aspect for ISCO design (Bachiochi et al. 2014).

Estimating Pore Volume

Porosity is a design parameter used to estimate the pore volume (PV) within the radius of influence (ROI). The total porosity (θ_T) of unconsolidated porous media is the volume of voids (V_V) relative to the total volume (V_T) of aquifer material ($\theta_T = V_V/V_T$). In unconsolidated porous media, the volume of oxidant injected into the subsurface required to fill the pore spaces within the ROI can be estimated as $\theta_T \times V_{ROI}$ (i.e., PV), ideally where V_{ROI} is the total volume within the ROI and the vertical interval.

A fraction of the water in porous media is attracted to the surfaces of the solids through forces of molecular attraction and is functionally dependent on the surface area of the sediment minerals (Marsily 1986). Unconnected, poorly connected, and dead-end pores are responsible for the fraction of water in porous media that do not contribute to fluid displacement. Thus the concept of porosity is expanded to include effective porosity which is linked to the displacement of pore fluid rather than to the percentage of the volume occupied by the pore spaces. Payne et al. (2008) reported that a fraction of the total porosity that contributes to advective flow and transport of groundwater in aquifers is the mobile porosity (θ_M), and the portion of the void space that does not contribute to the advective flow of groundwater behaves as immobile or slowly moving groundwater is the immobile porosity (θ_I). The total porosity is the sum of mobile and immobile porosity ($\theta_T = \theta_M + \theta_I$). Decisions between the selection of mobile porosity and total porosity in designing the volume of oxidant to be injected into the TTZ is an important distinction and can have major implications in ISCO.

Critical Analysis of Oxidant Volume Estimation Methods

Mobile Porosity Method

Payne et al. (2008) reported that standard aquifer testing protocols obtain the average hydraulic conductivity (K) which combines the high and low K, and consequently understates the actual flow velocities. This implies that the breakthrough of a solute in groundwater, whether it is a tracer, contaminant, or oxidant will occur faster than predicted if based on the average K. The "actual groundwater velocity," determined by tracer studies and used to estimate the mobile velocity, is significantly greater than the average velocity (Payne et al. 2008). Tracer study design, implementation, and data interpretation can be complex and very few sites yield the "ideal" tracer distributions that allow easy analysis (Payne et al. 2008). Complexities include tracer selection, tracer injection rates, monitoring network, tracer detection and analysis, retardation, reactive transport, and tracer test interpretation including variability in tracer breakthrough due to localized aquifer heterogeneities, poor or skewed recovery, depth-integration, and other factors (Ptak et al. 2004; Payne et al. 2008; Suthersan et al. 2014).

A summary of tracer test results ($n = 15$) conducted in various aquifer materials yielded estimated values of mobile porosity ranging from 0.0008 to 0.18 (Table 1) (Payne et al. 2008). The mobile porosity of sand and gravel aquifers was estimated to be less than 0.1, and it was suggested that mobile porosity values ranging from 0.02 to 0.10 would be more appropriate than using the often recommended 0.20 value as the effective porosity (Payne et al. 2008). In another summary of θ_M values estimated through tracer tests in alluvial aquifers ($n = 73$), the θ_M was ≤ 0.09 at 50% of the sites, and ≤ 0.15 for about 80% of the sites (Suthersan et al. 2014). It was concluded that a small portion of the total pore space meaningfully participated in flow and advective solute transport.

Site-specific tracer tests which are used to quantify θ_M involve measuring the volume of tracer injected ($Vol._{inj50}$) to reach 50% of the maximum observed breakthrough concentration ($C_{MAX}/2$) in the dose response (i.e., monitoring) wells (Equation 1; Figure 1) (h = vertical injection interval). Ideally, the $C_{MAX}/2$ should be nearly half the injected tracer concentration (C_O); however, low tracer injection volume, long distances between injection and dose response wells, and structural failure of the aquifer matrix (Payne et al. 2008) contributes to low tracer recovery (i.e., $C_{MAX}/2 < C_O/2$) and to uncertainty in tracer transport and projections in solute transport. The inability to define tracer transport is also attributed to a poorly defined conceptual site model and insufficient monitoring well density and placement (Suthersan et al. 2014). The mobile fraction velocity (V_θ) (refer to inset in Figure 1) is greater than the average groundwater velocity (V_{AVG}) and when used in conjunction with θ_T, these parameters can be used to estimate θ_M (Equation 2; Figure 1) (Payne et al. 2008).

$$\theta_M = Vol_{inj50}/(\Pi \times ROI^2 \times h) \quad (1)$$

$$\theta_M = V_{AVG} \times \theta_T/V_\theta \quad (2)$$

In these equations, it is evident that the concept of microscale variability in mobile-immobile porosity characteristics

Table 1

Mobile Porosity Values Determined by Tracer Tests, and Total Porosity and Density of Aquifer Materials

Materials	Mobile Porosity (L^3/L^3) (θ_M)[1,2]	Location/Aquifer
Poorly sorted sand/gravel	0.085	Quebec, Canada
Poorly sorted sand/gravel	0.04 to 0.07	Central Valley, CA
Poorly sorted sand/gravel	0.09	North TX, Ogalalla
Fractured sandstone	0.001 to 0.007	NJ, Passaic formation
Alluvial formation	0.0102	Los Angeles, CA/ Gaspur
Glacial outwash	0.145	Northern NJ
Weathered mudstone regolith	0.07 to 0.10	Northern MO
Alluvial formation	0.07	Sao Paulo, Brazil
Alluvial formation	0.07	Phoenix, AZ
Silty sand	0.05	Savanah R., SC
Fractured limestone	0.0008 to 0.001	Trifels formation
Alluvium sand/ gravel	0.017	West TX
Alluvial poorly sorted sand/gravel	0.003 to 0.007	North TX/Ogalalla
Alluvial sand/ gravel	0.11–0.18	Central CO/Cherry Creek
Siltstone, sandstone, mudstone	0.01–0.05	Central CO/Denver Formation

Materials	Total Porosity (M^3/M^3) (θ_T)	Soil Density (ρ_{BULK}) (kg/m^3)
Gravel	0.24 to 0.38 [3]	2,000 to 2,350 [4]
Coarse sand	0.31 to 0.46 [3]	1,400 to 1,900 [4]
Fine sand	0.26 to 0.53 [3]	1,400 to 1,900 [3]
Silt	0.34 to 0.61 [3]	1,300 to 1,920 [4]
Clay	0.34 to 0.60 [3]	600 to 1,800 [4]
Glacial tills	0.20 [4]	1,700 to 2,300 [4]
Silts and clays (inorganic)	0.29 to 0.52 [5]	600 to 1,800 [4]
Silts and clays (organic)	0.66 to 0.75 [3]	500 to 1,500 [4]
Peat	0.60 to 0.80 [6]	100 to 300 [4]

Notes: Total porosities reflect the typical range for each material considering compaction and sorting. Soil bulk density (ρ_{BULK}) refers to the common ranges of density for unsaturated conditions and various degrees of compaction.
[1]Percentage (%) values reported by Payne et al. (2008) were changed to units of length (L^3/L^3) for contrast to total porosity values.
[2]Payne et al. (2008).
[3]Zheng and Bennet (1995).
[4]Perloff and Baron (1976).
[5]Holtz and Kovacs (1981).
[6]Bear (1988).

is intrinsically extended from one distinct layer of limited scale, across the vertical injection (i.e., screened) interval involving varying geologic and hydrogeologic characteristics exhibiting a range in permeability (Figure 1). Under this condition, it is proposed that estimates of mobile porosity correspond to cross-sections of the formation with the highest permeability and the immobile porosity with the lowest permeability. Consequently, extrapolation of mobile porosity concepts across lengthy vertical intervals introduces complexity in assessing the specific role of porosity in groundwater and solute transport as it invites the role of other parameters that impact groundwater transport, including differing depositional processes and materials.

It has been proposed that θ_M can be used to determine the injection volume to achieve adequate reagent coverage at a given radial distance from an injection well (Suthersan et al. 2014). Assuming a simplified radial flow-cylindrical porous media conceptual model, the θ_M, the vertical injection interval, and the ROI, the volume of oxidant ($V_{OXIDANT,\theta M}$) can be estimated (Equation 3) (Payne et al. 2008).

$$V_{OXIDANT,\theta M} = \Pi \, ROI^2 \, \theta_m h \quad (3)$$

Tracer Testing, Mobile Porosity, and Contaminant Distribution

The most permeable and highly conductive aquifer media characterized through tracer testing is predominantly responsible for estimates of θ_M, but may not correspond with the majority of contamination. Rigorous site characterization is needed to validate and establish a correlation between contaminated intervals in the TTZ and the intervals involved in tracer transport. Slow, steady diffusion of contaminants into low permeable materials may have occurred over decades accounting for significant contaminant storage relative to more permeable portions of the aquifer (Chapman and Parker 2005; Stroo et al. 2012) represented by mobile porosity. Specifically, "immobile pores" involving either lower permeability lenses or layers at the macro-scale, or "immobile pores" in which groundwater transport is slow or impeded at the micro-scale may not contribute to tracer transport, but may be highly contaminated.

Total Porosity Method

Total porosity measurements of aquifer media using laboratory methods (Danielson and Sutherland 1986) are relatively simple and low cost, or field geophysical methods (resistivity, neutron, and gamma-gamma radiation) can be used (Marsily 1986). Total porosity can also be calculated from site-specific measurements or estimates of the bulk density (ρ_{BULK}) and particle density (ρ_{PD}) of aquifer material (Equation 4). Values of total porosity tabulated from many measurements over a wide range of aquifer media (Table 1), and that exhibit similar compositional characteristics to the TTZ can be used for oxidant volume design. Assuming the simplified radial flow-cylindrical porous media conceptual model, total porosity, the vertical injection interval, and the ROI, the volume of oxidant ($V_{OXIDANT,\theta T}$) can be estimated (Equation 5). This method does not differentiate between mobile and immobile pores.

$$\theta_T = 1 - \rho_{BULK}/\rho_{PD} \quad (4)$$

$$V_{OXIDANT,\theta R} = \Pi \, ROI^2 \, \theta_T h \quad (5)$$

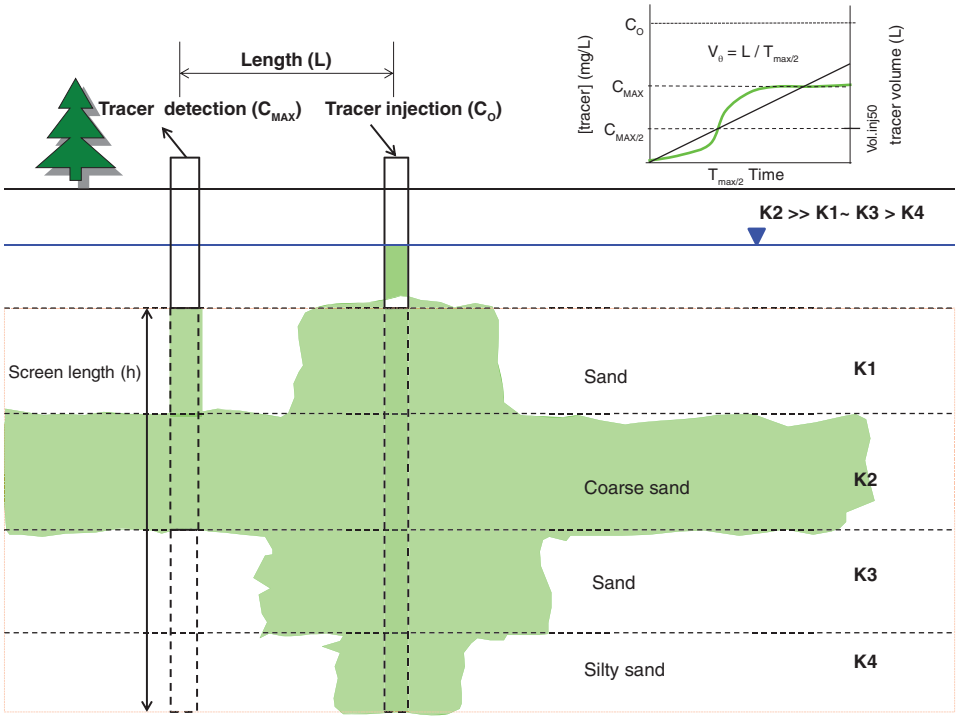

Figure 1. Schematic of tracer breakthrough in a heterogeneous porous media aquifer and mobile porosity (θ_M) calculations. The tracer volume ($Vol._{inj50}$) is measured where 50% breakthrough of the maximum tracer concentration ($C_{MAX/2}$) occurs (refer to Equations 1 and 2).

In this method, it is assumed the injected oxidant is eventually dispersed throughout the ROI PV. Consequently, long-term oxidant persistence and dispersal into the spectrum of lesser connected pores is critical. Oxidant dispersal involving the groundwater velocity continuum between mobile and immobile pores is dependent on different reactions, advection and diffusive transport mechanisms, ISCO design, and site conditions. In application of these principles to ISCO, soluble chemicals exchange between zones of mobile and immobile porosity. Preferential flow in structured media has been described using a variety of models (Simunek et al. 2003). Dual-porosity and dual-permeability models both assume that the porous medium consists of two interacting regions where solute exchange in groundwater, for example, between mobile pores and immobile pores, occurs through a rate-limiting diffusion process (Russo 2012). In some cases, oxidant persistence is insufficient, either due to reaction or transport, to effectively penetrate porous media through diffusion (Goldstein et al. 2004) suggesting that the eventual dispersal assumption may be invalid under some conditions.

Oxidant Delivery Strategies to Improve ISCO Effectiveness

Relative to long injection screened intervals, short injection screened intervals have a lower probability of being screened across lithologic layers exhibiting a wide range in hydraulic conductivity. Therefore, short injection intervals limit the risk in delivering a disproportionate volume of oxidant into higher permeability layers and greater probability of injecting the oxidant into discrete zones within the TTZ (Figure 2). Where feasible, the length of a well screen in an injection well should be no more than 10 to 15 ft (3.05 to 4.57 m), particularly in heterogeneous formations and where treating highly contaminated source zones (Simkins et al. 2011). Shorter injection well screens (<10 to 15 ft) (<3.05 to 4.57 m), and direct-push injection using short injection intervals (2 to 4 ft) (0.61 to 1.22 m) can further limit the role of preferential pathways. Overall, a combination of short-screened injection intervals, a greater number of injection locations, and smaller ROI's per injection location reduces the risk of delivering excessive oxidant volumes into preferential pathways (Figure 2) and results in greater probability that the oxidant is delivered to the TTZ. Areal coverage of the TTZ with multiple, overlapping oxidant ROIs is critical to improve contact between oxidant and contaminated media.

Oxidant breakout into higher permeability zones, mounding, surfacing, and transport beyond the TTZ in general, can result from excessive injection pressure. The rate that an aquifer can accept fluids and the lateral migration of these fluids before reaching structural failure is significantly influenced by the vertical acceptance rate. Maximum injection pressure can be estimated by the density of the dry soil and saturated soil, the thickness of the vadose zone, and the height of the saturated zone above the injection point (Los Angeles Regional Water Quality Control Board - In Situ Remediation Reagents Injection Working Group 2009). Adhering to these injection guidelines will improve oxidant delivery to the TTZ.

Assuming the contamination is mainly in the most permeable zones as defined by tracer tests, the mobile porosity oxidant volume design could be an effective approach. However, assuming contamination is present in both high and low permeability materials suggests that oxidant injection into high permeability layers limits oxidant delivery into

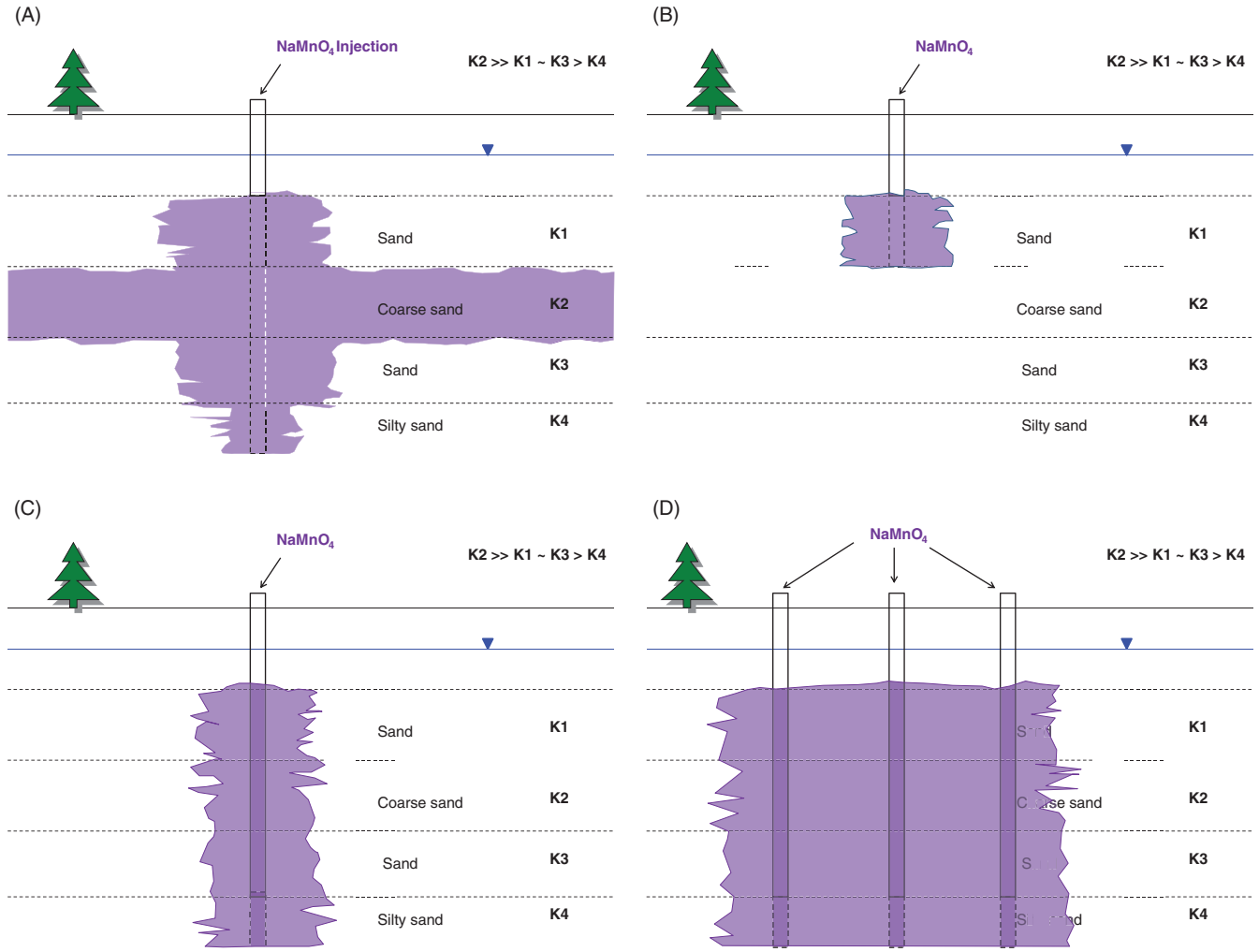

Figure 2. Schematic of idealized conceptual model illustrating the role of heterogeneities, and the impact of screen length, radius of influence, and injection spacing on the distribution of the permanganate oxidant. (A) The long well screen in heterogeneous lithology accounts for disproportionate oxidant distribution; (B to D) alternatively, advancing short, direct-push injection well screens, using small radii of influence and close injection locations, achieves more effective oxidant distribution (oxidant density effects excluded).

low permeability TTZs, and/or misses the target altogether. Chemical oxidation of contaminants in, or near, low permeability materials requires that the oxidant be delivered into or near lower permeability zones and persist for timeframes consistent with steep concentration gradients and diffusive transport (Cavanagh et al. 2014). Periodic batch delivery of oxidant could be used to address the back diffusion of contaminants. Alternatively, slow but constant oxidant delivery methods have been developed for sites with low conductivity lithology involving gravity delivery and/or constant head injection designs (Pac et al. 2014; Luhrs et al. 2015).

Critical Analysis of Mobile and Total Porosity Oxidant Injection Volume Estimation Methods

Contrasting tabulated values of θ_M and θ_T (Table 1; Equations 3 and 5) indicate that a larger volume of oxidant is estimated using total porosity vs. mobile porosity. Consider the illustrative example of an oxidant volume ISCO design where assumed values for θ_M (0.10) and θ_T (0.35) are used to estimate oxidant volume and where ROI = 10 ft (3.05 m), and h = 5 ft (1.52 m). The volume of oxidant required to achieve the ROI across the screened interval using θ_M and θ_T is 1170 gal (4428 L) and 4110 gal (15,556 L), respectively. Delivering a larger volume of oxidant associated with θ_T translates into greater oxidant handling, preparation, and labor resulting in higher remedial cost.

The potential for groundwater displacement and oxidant transport beyond the design ROI and TTZ into nontargeted zones are risks that should be evaluated. Since ISCO is usually deployed in a source area, oxidant transport beyond the ROI into lesser-contaminated aquifer conditions, and/or downgradient transport during the postinjection drift phase could also occur. In these cases, chemical oxidation of contaminants would continue to occur, potentially in nontargeted zones with less contamination. Despite the seemingly benign consequence of oxidant transport beyond the immediate ROI in this case, adjustments to the ISCO design would need to consider the loss of oxidant from the ROI. Nearby receptors beyond the TTZ and potential discharge areas (i.e., seeps, creeks, water bodies, utility corridors, etc.) should be identified to determine whether migration of oxidant beyond the contaminated TTZ could occur and what steps, if any, to implement given potential contingencies.

Contaminants are distributed between aqueous, solid, and nonaqueous phases in the subsurface and can be estimated using equilibrium partitioning calculations (Feenstra et al. 1991; Newell and Ross 1992; Cohen and Mercer 1993). Under non-aqueous phase liquid (NAPL)- or heavily contaminated source area conditions, the contaminant mass may be present in all three phases but the majority of contaminant mass is generally found in the NAPL and solid phases relative to the dissolved aqueous phase contaminant mass. Under NAPL-free conditions, based on the hydrophobicity of CVOCs and the presence of natural organic matter in aquifer material, the majority of contaminant mass is adsorbed on the solid phase material. Assuming the majority of the CVOCs mass in the ROI is immobilized either as residual NAPL or through adsorption onto aquifer solids, the displacement of the dissolved CVOC contaminant mass in the groundwater is projected to be limited relative to the total contaminant mass.

Critical Analysis of Permanganate ISCO Design Parameters

Krembs et al. (2010, 2011) compiled permanganate ISCO design parameters including the design and observed ROI (ft), oxidant dosage (g/kg), number of PVs delivered, number of delivery events, and duration of delivery events (days) (Table 2). A critical analysis of these design parameters reported is preceded by the caveat that the number of case studies for the median value of each design parameter varied, and therefore only general observations are possible.

Radius of Influence

The ROI can be estimated by measuring appreciable concentrations of the oxidant in monitoring wells located in different directions from the injection location. When the observed ROI (25 ft) ($n = 11$) (7.62 m) is considerably greater than the design ROI (14 ft) ($n = 29$) (4.27 m) (Table 2), this suggests that oxidant distribution was more extensive than designed. However, given these ROIs, the volume of oxidant required to achieve a 25-ft ROI (7.62 m), relative to a 14-ft ROI (4.27 m), would involve injecting greater than three times more oxidant volume. A firm explanation cannot be provided regarding this anomalous difference but some speculation is warranted. For example, groundwater quality parameters (i.e., ORP, DO, temperature, conductivity) are sometimes used as indirect indicators of oxidant ROI. Spikes in these parameter values can occur in groundwater after the oxidant has fully reacted, yet the effects, or the residuals of the oxidant, can still be measured yielding false-positive results for the ROI.

In some cases, the hydraulic conductivity (K) profile measured across screened intervals in groundwater wells exhibits an order of magnitude change over short vertical sections of the screened interval (Zlotnik and Zurbuchen 2003). Under this condition, a disproportionate volume of oxidant could be delivered into high K layers (Figure 1), and could also yield an ROI artifact. Injection and monitoring well screens representative of discrete vertical intervals would be useful to diagnose this condition and to obtain a more accurate assessment of oxidant transport and ROI.

Due to heterogeneities in aquifer hydraulic properties, ROIs on the order of 25 ft (7.62 m) require the injection of a large volume of oxidant which invites vulnerability to disproportionate transport of the oxidant in preferential pathways. Decreased ROIs translate into smaller injection well spacing and would include installation of additional injection wells or more direct-push injection locations. Smaller ROIs have several advantages including lower probability that preferential pathways will play a role in oxidant transport, greater potential for hydraulic control, greater accuracy in the spatial emplacement of the oxidant, and greater confidence that the oxidant can be delivered to the designed ROI.

Natural Oxidant Demand

ISCO oxidant loading, defined here as mass of oxidant per mass of soil (i.e., g oxidant/kg aquifer material) is sometimes designed based on NOD values measured in bench-scale studies. The NOD for permanganate often involves a 48-h test procedure (ASTM 2007). This batch test does not differentiate between mobile or immobile pores. Judicious interpretation of test results is warranted given that the reaction between MnO_4^- and reactants varies with time, there are multiple reactive components that exhibit varying reactivity, the NOD may increase substantially with longer testing periods, and MnO_4^- reaction is concentration dependent (Mumford et al. 2005; Hønning et al. 2007; Urynowicz 2008; Urynowicz et al. 2008; Xu and Thomson 2008, 2009; Cha et al. 2012). Most of the NOD in soil and aquifer samples is slow reacting, and 48-h NOD measurements are poor predictors of total NOD and cannot accurately estimate long-term MnO_4^- consumption (Cha et al. 2012). However, an alternative, quick and economical permanganate chemical oxidant demand test has been developed to estimate the maximum permanganate NOD for aquifer materials (Xu and Thomson 2008). Further, results from a broad range in aquifer materials indicated excellent linear relationship between the maximum NOD and the 7-day NOD test indicating that results could be used to support permanganate ISCO site screening and design (Xu and Thomson 2009). Once the fast NOD fraction is rapidly consumed, the

Table 2

A Compilation of the Median Value for ISCO Design Parameters from Field Application Case Studies (Krembs et al. 2010, 2011)

Design Parameter	Median Value Reported Krembs et al. (2010, 2011)[1]
Design ROI (ft)	14 (n = 29)
Observed ROI (ft)	25 (n = 11)
Oxidant dosage (g/kg)	0.4 (n = 24)
Number of pore volumes delivered	0.16 (n = 32)
Number of delivery events	2 (n = 65)
Duration of delivery events (days)	4 (n = 45)
Vertical injection interval (ft)	NA[2]

[1]The median design value and number of case study sites is reported.
[2]The vertical injection interval was not reported Krembs et al. (2010, 2011).

remaining MnO_4^- may persist for weeks to months, and diffuse into lower permeability zones where contaminants may reside. Samples of aquifer solids from 12 sites ($n = 50$) in the U.S. were analyzed for NOD over a long period (up to 41 days). In 80% of the samples, a broad range in NOD (0.24 to 18.8 g MnO_4^- /kg soil; median value = 3.33 g/kg) was measured and the overall range was 0.2 to 150 g/kg (Cha et al. 2012). This was similar to previously reported NOD ranges (Mumford et al. 2005; Huling and Pivetz 2006; Hønning et al. 2007; Urynowicz 2008; Xu and Thomson 2009). The median value of MnO_4^- dosage reported by Krembs et al. (2010, 2011) is low (0.4 g/kg; $n = 24$) (Table 2) relative to long-term NOD values. Assuming that long-term persistence of MnO_4^- was needed to address contaminant mass transport and mass transfer limiting processes, this low MnO_4^- dosage applied suggests that the median range value used at many ISCO sites represents an under-design either in terms of oxidant volume or concentration. Overall, this low median value of oxidant dosage would unlikely persist long enough to broadly disperse within the ROI and TTZ while satisfying both the fast- and slow-acting NOD.

Pore Volume

A PV represents the volume of voids contained within the ROI spatially defined by the ROI, vertical interval, and porosity. The median number of permanganate PVs delivered (PV = 0.16; n = 32 sites) (Table 2) (Krembs et al. 2010, 2011) is significantly less than a single PV (PV = 1.0) and suggests an under-design of oxidant volume. In this case, significant postinjection oxidant persistence and dispersal would be required to achieve both (1) coverage in the remaining 0.84 PV of the ROI where oxidant was not initially delivered and (2) to address long-term NOD requirements. Postinjection oxidant dispersal of this magnitude is unlikely.

Summary

The median values reported for oxidant dosage (0.4 g/kg) and PV delivery (PV = 0.16) (Table 2) (Krembs et al. 2010, 2011) suggests a less aggressive, low oxidant volume ISCO design which may be consistent with a mobile porosity ISCO design. This design appears likely to result in incomplete oxidant delivery, insufficient oxidant dosage within the ROI, and short duration oxidant persistence. A more aggressive ISCO design based on total porosity would involve a greater oxidant dosage ($\geq$3 g/kg) (i.e., Cha et al. 2012) and PV delivery (PV = 1) permitting greater distribution and longer duration oxidant persistence. It is noted that low oxidant concentration could have contributed to the low oxidant dosage, but oxidant concentration data were not reported by Krembs et al. (2010, 2011), and could not be evaluated.

Other Causes of Rebound and Low Contaminant Removal

Current ISCO deployment is increasingly reflective of an iterative design involving repeated oxidant injections with intermittent monitoring diagnostics used to guide subsequent oxidant injections that target persistent, high concentration source areas. Further, depletion of the "more accessible" contamination may be followed by an ISCO approach characterized by smaller oxidant batch injections, or long-term, slow oxidant delivery targeting the back diffusion of contamination (Pac et al. 2014; Luhrs et al. 2015). In the early years of ISCO design, short duration and/or single injection deployment (i.e., Table 2, number of delivery events = 2; $n = 65$) may not have fully recognized the technical challenges associated with hydrogeologic heterogeneities, oxidant distribution limitations, high contamination zones, contamination in low permeable or fractured systems, high oxidant demand zones, limited oxidant persistence, etc. Consequently, rebound and low contaminant removal through postoxidant injection groundwater monitoring would be a probable outcome. Projects involving these designs may be reflected in ISCO treatment performance conclusions in the ISCO surveys (GeoSyntec Consultants 2004; McGuire et al. 2006; Krembs et al. 2010, 2011).

Groundwater samples collected specifically to be analyzed may contain the injected oxidant and organic contaminants in a "binary mixture" (Huling et al. 2011; Johnson et al. 2012; Ko et al. 2012). Oxidative transformation of contaminants in the sample after it is collected, causes false-negative results. Upon complete reaction of the injected oxidant in the subsurface, the potential for false-negative results is eliminated and the contaminants present in groundwater samples are subsequently detected and quantified. Essentially this condition contributes to a determination of "rebound" although the contaminants may have been present all along. Given the relatively recent development in groundwater sample preservation guidelines (Ko et al. 2012), the interpretation of groundwater quality under this condition is likely reflected in the case study survey results and statistics that report rebounding contaminant concentrations at ISCO sites.

Summary

Critical reviews of in situ remediation technology treatment performance indicate that ISCO, compared to other in situ technologies, exhibits a higher degree of chemical rebound and a lower reduction in contaminant concentrations (GeoSyntec Consultants 2004; McGuire et al. 2006; Krembs et al. 2010, 2011). Although several mechanisms may provide a reasonable explanation for these observations, low oxidant volume delivery at ISCO sites is likely to be a key factor for rebound and the low reduction in contaminant concentrations.

In conjunction with porosity, a simplified radial flow, cylindrical, porous media conceptual model is often used to estimate the volume of oxidant required to achieve a ROI over a specific vertical interval. Mobile and total porosity values used in these calculations yield a wide range in estimates of oxidant volume. The mobile porosity method specifically recognizes that groundwater readily moves in "mobile pores" and can be measured using tracer tests. However, tracer tests are vulnerable to lithology-dependent variability in hydraulic conductivity where tracer transport in the most permeable sections of the media will skew estimates of

mobile porosity downward. Consequently, a smaller volume of oxidant is estimated resulting in a smaller oxidant footprint potentially leaving some TTZs oxidant-free within the ROI. Total porosity, often calculated or measured in the lab does not differentiate between mobile and immobile pores. This method involves a larger oxidant volume to inject, a larger oxidant footprint, and would likely impact ISCO field activities due to greater oxidant handling, preparation, and labor. Displacement of contaminated groundwater and oxidant migration beyond the ROI and TTZ are risks that must be evaluated. In source areas, phase distribution analysis suggests that the majority of contaminants are immobilized in soil and NAPL which limits the relative displacement of contaminants. Several oxidant injection methods and designs can be used to reduce the impact and risk of preferential pathways on oxidant delivery and provide greater probability that the oxidant is delivered to the ROI.

Acknowledgments

The authors acknowledge Dr. Kiyoung Cha (National Research Council, US EPA, Ada, Oklahoma) for technical input on this manuscript. The U.S. Environmental Protection Agency, through its Office of Research and development, funded and managed the research described here. It has not been subjected to Agency review and therefore does not necessarily reflect the views of the Agency, and no official endorsement should be inferred.

References

ASTM. 2007. *ASTM D 7262-07. Standard Test Method for Estimating the Permanganate Natural Oxidant Demand of Soil and Aquifer Solids*. West Conshohocken, Pennsylvania: ASTM International, 04.09.

Bachiochi, R., L. D'Aprile, I. Innocenti, F. Massetti, and I. Verginelli. 2014. Development of technical guidelines for the application of in-situ chemical oxidation to groundwater remediation. *Journal of Cleaner Production* 77, no. 15: 47–55.

Bear, J. 1988. *Dynamics of Fluids in Porous Media*. New York: Dover Publications.

Cavanagh, B.A., P.C. Johnson, and E.J. Daniels. 2014. Reduction of diffusive contaminant emissions from a dissolved source in a lower permeability layer by sodium persulfate treatment. *Environmental Science and Technology* 48: 14582–14589.

Cha, K.Y., M.L. Crimi, M.A. Urynowicz, and R.C. Borden. 2012. Kinetics of permanganate consumption by natural oxidant demand – Modeling approaches and statistical analysis. *Environmental Engineering Science* 29, no. 7: 646–653.

Cha, K.Y., and R.C. Borden. 2012. Impact of injection system design on ISCO performance with permanganate — mathematical modeling results. *Journal of Contaminant Hydrology* 128: 33–46.

Chapman, S.W., and B.L. Parker. 2005. Plume persistence due to aquitard back diffusion following dense nonaqueous phase liquid source removal or isolation. *Water Resources Research* 41: W12411.

Cohen, R., and J. Mercer. 1993. DNAPL site evaluation. EPA 600/R-93/022. Washington, DC: U.S. Environmental Protection Agency.

Danielson, R.E., and P.L. Sutherland. 1986. Porosity. In *Methods of Soil Analysis Part 1: Physical and Mineralogical Methods*, 2nd. Monograph 9 ed., ed. A. Klute. Madison, Wisconsin: American Society of Agronomy/Soil Science Society of America.

Feenstra, S., D.M. Mackay, and J.A. Cherry. 1991. A method for assessing residual NAPL based on organic chemical concentrations in soil samples. *Groundwater Monitoring Review* 11, no. 2: 128–136.

GeoSyntec Consultants. 2004. *Assessing the Feasibility of DNAPL Source Zone Remediation: Review of Case Studies*. Port Hueneme, California: Naval Facilities Engineering Services Center.

Goldstein, K.J., A. Vitolins, D. Navon, B.L. Parker, S. Chapman, and G.A. Anderson. 2004. Characterization and pilot-scale studies for chemical oxidation remediation of fractured shale. *Remediation Journal* 14, no. 4: 19–38.

Holtz, R.D., and W.D. Kovacs. 1981. *An Introduction to Geotechnical Engineering*. Englewood Cliffs, New Jersey: Prentice Hall.

Hønning, J., M.M. Broholm, and P.L. Bjerg. 2007. Quantification of potassium permanganate consumption and PCE oxidation in subsurface materials. *Journal of Contamination Hydrology* 90: 221.

Huling, S.G. and B. Pivetz. 2006. In-situ chemical oxidation – Engineering issue. EPA/600/R-06/072. Ada, Oklahoma: US Environmental Protection Agency, National Risk Management Research Laboratory, R.S. Kerr Environmental Research Center.

Huling, S.G., S. Ko, and B. Pivetz. 2011. Ground water sampling at ISCO sites – Binary mixtures of volatile organic compounds and persulfate. *Groundwater Monitoring and Remediation* 31, no. 2 Spring: 72–79.

Johnson, K.T., M. Wickham-St. Germain, S. Ko, and S.G. Huling. 2012. Binary mixtures of permanganate and chlorinated volatile organic compounds in groundwater samples: Sample preservation and analysis. *Groundwater Monitoring and Remediation* 32, no. 3 Summer: 84–92.

Ko, S., Huling, S.G., and Pivetz, B. 2012. Ground water sample preservation at in-situ chemical oxidation sites – Recommended guidelines, EPA Ground Water Issue Paper. EPA/600/R-12/049. Ada, OK: US Environmental Protection Agency, National Risk Management Research Laboratory, R.S. Kerr Environmental Research Center.

Krembs, F.J., R.L. Siegrist, M.L. Crimi, R.F. Furrer, and B.G. Petri. 2010. ISCO for ground water remediation: Analysis of field applications and performance. *Groundwater Monitoring and Remediation* 30, no. 4: 42–53.

Krembs, F.J., W.S. Clayton, and M.C. Marley. 2011. Chapter 8 Evaluation of ISCO field applications and performance. In *In Situ Chemical Oxidation for Remediation of Contaminated Groundwater*. SERDP/ESTCP Remediation Technology Monograph Series, C.H. Ward (Series ed), ed. R.L. Siegrist, M.L. Crimi, and T.J. Simpkin, 319–354. New York: Springer Science and Business Media, LLC.

Los Angeles Regional Water Quality Control Board - In Situ Remediation Reagents Injection Working Group. 2009. Technical report: Subsurface injection of in situ remedial reagents within the Los Angeles Regional Water Quality Control Board Jurisdiction. http://www.swrcb.ca.gov/rwqcb4/water_issues/programs/ust/guidelines/ (accessed September 16, 2009).

Luhrs, R., S. Andrews, and P.J. Dugan. 2015. Use of ISCO as a cost effective long term remedy. http://www.caruscorporation.com/page/remediation/carus-remediation-newsletters (accessed October 26, 2015).

Marsily, G. 1986. *Quantitative Hydrogeology*. San Diego, CA: Academic Press, Harcourt Brace Jovanovich.

McGuire, T.M., J.M. McDade, and C.J. Newell. 2006. Performance of DNAPL source depletion technologies at 59 chlorinated solvent-impacted sites. *Groundwater Monitoring and Remediation* 26, no. 1: 73–84.

Mumford, K.G., N.R. Thomson, and R.M. Allen-King. 2005. Bench-scale investigation of permanganate natural oxidant demand kinetics. *Environmental Science and Technology* 39: 2835.

Newell, C. and R.R. Ross. 1992. Estimating potential for occurrence of DNAPL at superfund sites, OSWER Publication 9355.4-07FS. Washington, DC.

Pac, T.J., R.W. Lewis, and E.C. Gyles. 2014. Constant head injection for enhanced in-situ chemical oxidation. *Remediation Journal* 25: 71–83.

Payne, F.C., J.A. Quinnan, and S.T. Potter. 2008. *Remediation Hydraulics*. Boca Raton, Florida: CRC Press; Taylor & Francis Group LLC, 408 p.

Perloff, W.H., and W. Baron. 1976. *Soil Mechanics: Principles and Applications*. New York: John Wiley & Sons.

Petri, B., N.R. Thomson, and M.A. Urynowisz. 2011. Chapter 3 – Fundamentals of ISCO using permanganate. In *In Situ Chemical Oxidation for Remediation of Contaminated Groundwater*. A volume in SERDP/ESTCP Remediation Technology Monograph Series, C.H. Ward (Series ed), ed. R.L. Siegrist, M.L. Crimi, and T.J. Simpkin, 89–146. New York: Springer Science and Business Media.

Ptak, T., M. Piepenbrink, and E. Martac. 2004. Tracer tests for the investigation of heterogeneous porous media and stochastic modelling of flow and transport—A review of some recent developments. *Journal of Hydrology* 294: 122–163.

Russo, D. 2012. Numerical analysis of solute transport in variably saturated bimodal heterogeneous formations with mobile–immobile-porosity. *Advances in Water Research* 47: 31–42.

Simunek, J., N.J. Jarvis, M. van Genuchten, and A. Gardenas. 2003. Review and comparison of models for describing non-equilibrium and preferential flow and transport in the vadose zone. *Journal of Hydrology* 272: 14–35.

Siegrist, R.L., M.A. Urynowicz, O.R. West, M.L. Crimi, and S.L. Lowe. 2001. *Principles and Practices of In Situ Chemical Oxidation Using Permanganate*. Columbus, Ohio: Battelle Press, 336 pp.

Siegrist, R.L., M. Crimi, and R.A. Brown. 2011. Chapter 1: In Situ Chemical Oxidation: Technology description and status. In *In Situ Chemical Oxidation for Remediation of Contaminated Groundwater*. A volume in SERDP/ESTCP Remediation Technology Monograph Series, C.H. Ward (Series ed), ed. R.L. Siegrist, M.L. Crimi, and T.J. Simpkin, 1–32. New York: Springer Science and Business Media.

Simkins, T.J., T. Palaia, B.G. Petri, and B.A. Smith. 2011. Chapter 11 Oxidant delivery approaches and contingency planning. In *Situ Chemical Oxidation for Remediation of Contaminated Groundwater*. A volume in SERDP/ESTCP Remediation Technology Monograph Series, C.H. Ward (Series ed), ed. R.L. Siegrist, M.L. Crimi, and T.J. Simpkin, 449–480. New York: Springer Science and Business Media.

Stroo, H.F., et al. 2012. Chlorinated ethene source remediation: Lessons learned. *Environmental Science and Technology* 46, no. 12: 6438–6447.

Suthersan, S., C. Divine, E. Cohen, and K. Heinze. 2014. Tracer testing: Recommended best practice for design and optimization of in situ remediation systems. *Groundwater Monitoring and Remediation* 34, no. 3: 33–40.

Urynowicz, M.A. 2008. In situ chemical oxidation with permanganate: Assessing the competitive interactions between target and nontarget compounds. *Soil and Sediment Contamination* 17: 53.

Urynowicz, M.A., B. Balu, and U. Udayasankar. 2008. Kinetics of natural oxidant demand by permanganate in aquifer solids. *Journal of Contaminant Hydrology* 96, no. 1–4: 187–194.

US EPA. 2014. Superfund Remedy Report, 14th Ed. EPA 542-R-13-016. November 2013, Washington, DC: Solid Waste and Emergency Response.

Xu, X., and N.R. Thomson. 2008. Estimation of the maximum consumption of permanganate by aquifer solids using a modified chemical oxygen demand test. *Journal of Environmental Engineering* 134, no. 5: 353–361.

Xu, X., and N.R. Thomson. 2009. A long-term bench-scale investigation of permanganate consumption by aquifer materials. *Journal of Contaminant Hydrology* 110: 73–86.

Zheng, C., and G.D. Bennet. 1995. *Applied Contaminant Transport Modeling*. New York: Van Nostrand Reinhold.

Zlotnik, V.A., and B.R. Zurbuchen. 2003. Estimation of hydraulic conductivity from borehole flowmeter tests considering head losses. *Journal of Hydrology* 281: 115–128.

Biographical Sketches

S.G. Huling, *corresponding author, is at U.S. Environmental Protection Agency, Office of Research and Development, National Risk Management Research Laboratory, Robert S. Kerr Environmental Research Center, P.O. Box 1198, Ada, OK 74820; (580) 436-8610; (580) 436-8615; huling.scott@epa.gov*

R.R. Ross *is at U.S. Environmental Protection Agency, Office of Research and Development, National Risk Management Research Laboratory, Robert S. Kerr Environmental Research Center, P.O. Box 1198, Ada, OK 74820.*

K. Meeker Prestbo *is at U.S. Environmental Protection Agency, Office of Environmental Cleanup, Region 10, 1200 Sixth Avenue, Suite 900, Seattle, WA 98101.*

Appendix F

Recommended Ground Water Sampling Plan for PI MCRD Site 45

Background

It is recommended to perform post-oxidation ground water sampling and analysis to continue the assessment of treatment performance of ISCO at site 45. Recommended guidelines are provided that are consistent with methods used in previous ground water monitoring events.

Ground Water Sampling

Post-oxidation ground water samples would include 39 wells and micro-wells (Table F1; Figure F1). It is recommended that ground water samples be analyzed for CVOCs, metals and $NaMnO_4$ (*i.e.*, MnO_4^-), and other optional ground water parameters listed below (*i.e.*, dissolved methane gas, ferrous and total iron, chloride, sulfate). Prior to ground water sample collection, a YSI multi-parameter probe with a flow through cell should be used to collect field parameters, including pH, dissolved oxygen, oxidation reduction potential, temperature, specific conductivity, and turbidity. Ground water samples could then be collected when field parameters stabilize. Previously, a peristaltic pump (MasterFlex Easy Load II, L/S, model 77200-62; MasterFlex PharMed-24 tubing; MasterFlex speed Controller) was used and connected to the micro-well and pumped at 100-300 mL/minute. Similar methods to retrieve a sample from the micro-wells is recommended. A ground water purge log is included below, and could be used to keep track of readings until the parameters stabilize. The purge log includes a record of time, temperature (°C), specific conductivity (mS/cm), DO (mg/L), pH, ORP (mV), and field comments.

Parameters	Method
CVOCs (PCE, TCE, cis-1,2-DCE, trans-1,2-DCE, 1,1-DCE, VC)	EPA Method 8260B GC/MS
Metals	EPA Method 6010C (ICP-AES)
Dissolved Methane Gas	RSKSOP-194/175, Rev. 5
Ferrous and total iron	EPA Method 3500-Fe D
Chloride and sulfate	[(1)]EPA Method 6500 (refer to RSKSOP-276, Rev. 4 below).

EPA Method 8260B - Volatile organic compounds by purge and trap GC/MS.

EPA Method 6010C (EPA SW-846) - Inductively coupled argon plasma with atomic emission Spectrometry.

RSKSOP-194, Rev. 4 - Gas Analysis by Micro Gas Chromatograph (see Table 3).

RSKSOP-175, Rev. 5 - Sample Preparation and Calculations for Dissolved Gas Analysis in Water Samples Using a GC Headspace Equilibration Technique (see Table 3).

EPA Method 3500-Fe D - Phenanthroline method.

RSKSOP-276, Rev. 4 - Determination of Major Anions in Aqueous Samples Using Capillary Ion Electrophoresis with Indirect UV Detection and Empower 2 Software.

[(1)]There is no existing EPA method for dissolved methane gas. Refer to Kampbell and Vandegrift, 1998.

Table F-1. Micro-well and 2" monitoring wells to be sampled during the post-oxidation 3 sampling event (total wells = 39).

Micro-well Monitoring Transect	Micro-well Number				
M1	M1-SB-S M1-SB-D	M1-SA S M1-SA D	M1-Mid-S M1-Mid-D	M1-NA-S M1-NA-D	M1-NB-S M1-NB-D
M2	M2-S-S M2-S-D		M2-Mid-S M2-Mid-D		M2-N-S M2-N-D
M3	M3-S-S M3-S-D		M3-Mid-S M3-Mid-D		M3-N-S M3-N-D
M4	M4-S-S M4-S-D		M4-Mid-S M4-Mid-D		M4-N-S M4-N-D
T1		T1-S-S T1-S-D		T1-N-S T1-N-D	
T2		T2-S-S T2-S-D		T2-N-S T2-N-D	
2 inch wells		MW-25, Inj.-1, Deep, MW-31 SL			

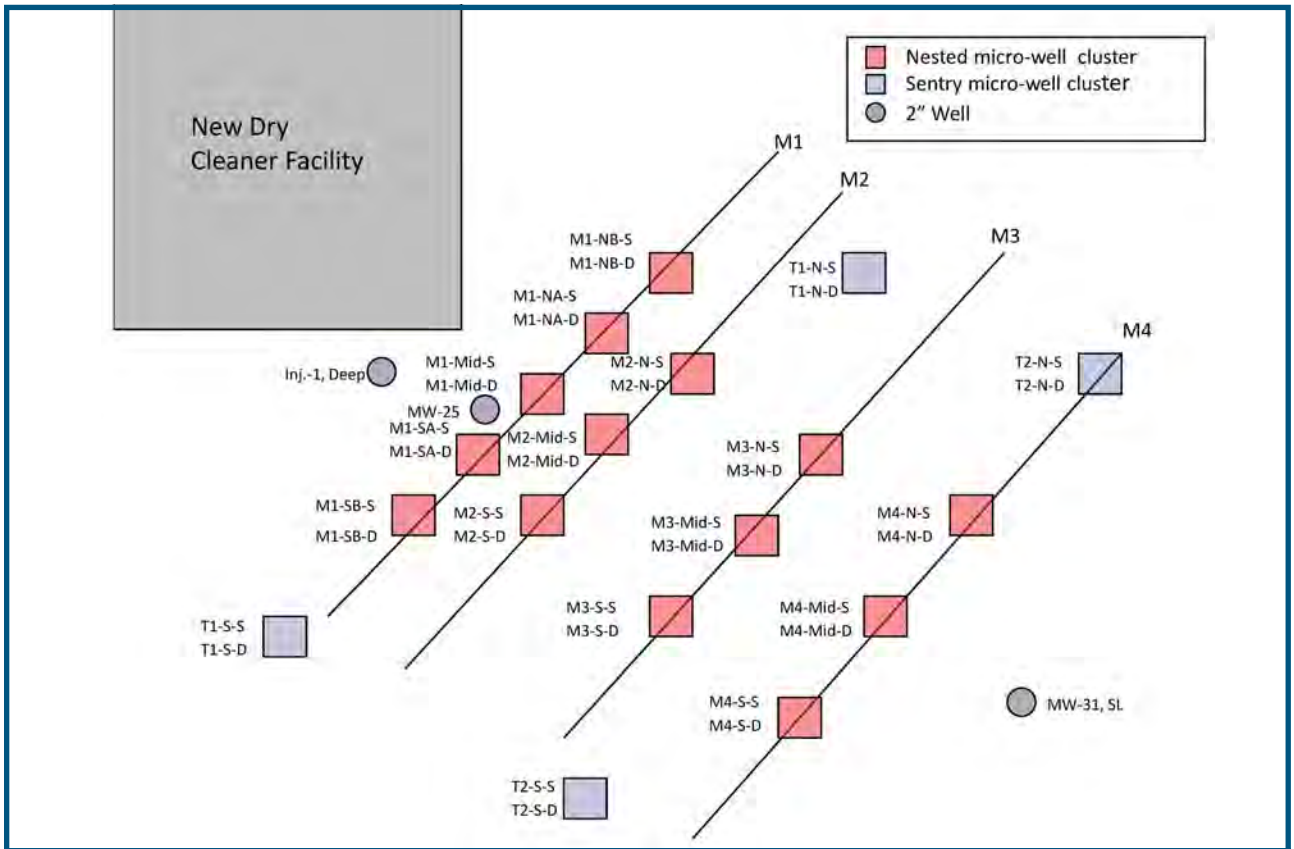

Figure F1. Conceptual layout of 2 inch wells and micro-wells at the U.S. MCRD Parris Island, SC Site 45.

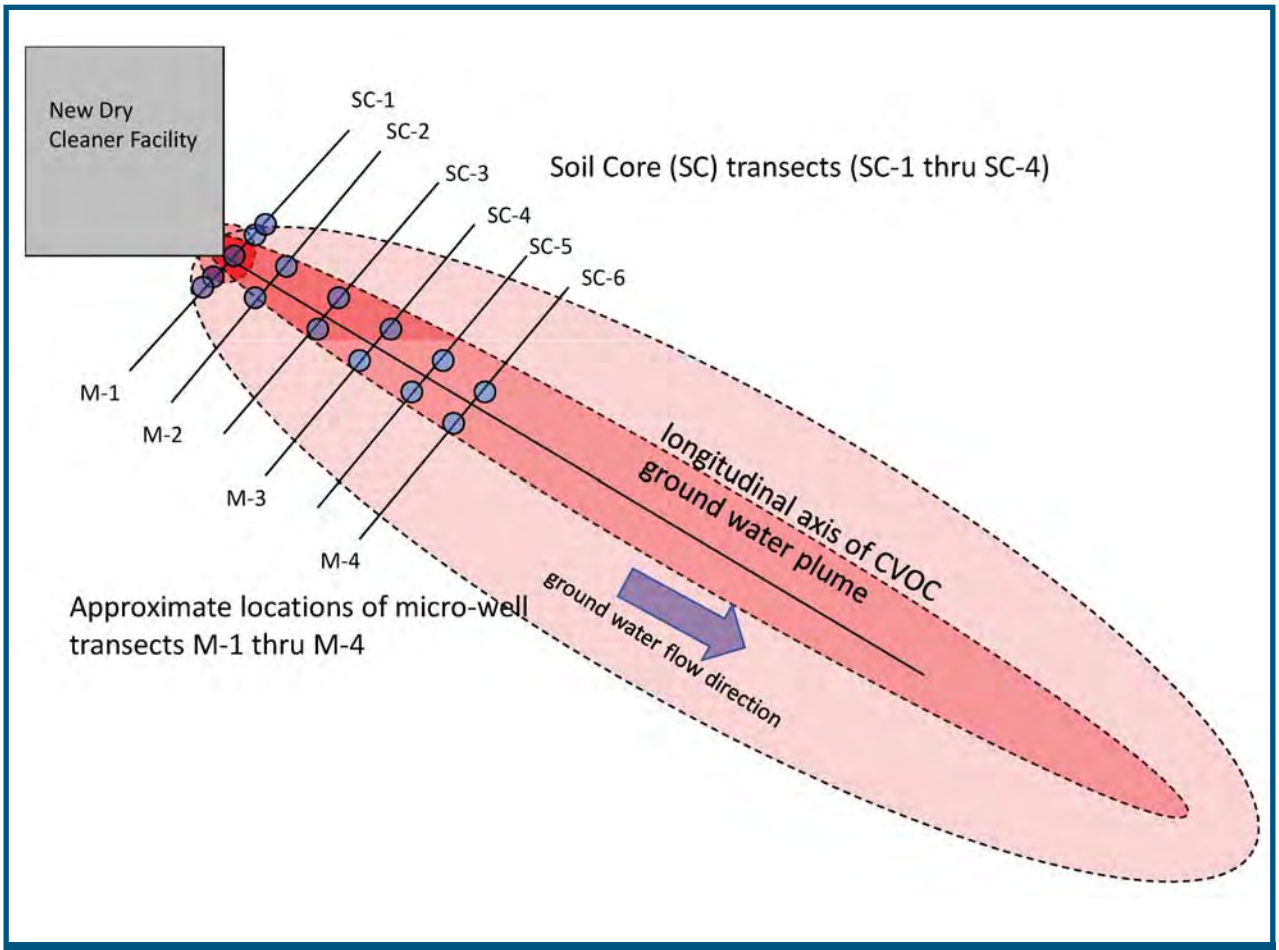

Figure F2. Conceptual model of approximate locations of soil core and micro-well transects used in soil core sample collection.

Sample Handling, Labeling, Packaging and Shipping, and QA/QC

Ground water samples. Ground water samples should be collected in pre-labeled 40 mL vials, preserved with HCl for CVOCs and HNO_3 for metals, and stored in ice chests with blue ice. Upon completion, samples will be transported/shipped overnight to the analytical laboratory (*i.e.*, Shealy Environmental Services, Columbia, SC), using the appropriate chain of custody forms.

The presence of $NaMnO_4$ in a ground water sample can be visually determined as either a pink or purple color (Johnson *et al.*, 2012). Assuming the presence of MnO_4^- is ascertained in the ground water sample, it is recommended to (1) note the presence and the nature of the color in the ground water purge log notes, (2) collect a sample to measure the $NaMnO_4$ concentration via spectrophotometer analysis (*i.e.*, wavelength = 525 nm), and (3) neutralize the sample with ascorbic acid, as described in Johnson *et al.* (2012) or Ko *et al.* (2012).

Johnson, K.T., Wickham-St. Germain, M., Ko, S. and Huling, S.G. 2012. "Binary Mixtures of Permanganate and Chlorinated Volatile Organic Compounds in Groundwater Samples: Sample Preservation and Analysis." *Ground Water Monit. Remed.* 32(3), Summer 84–92.

Ko, S., Huling, S.G., and Pivetz, B. 2012. Ground Water Sample Preservation at In-Situ Chemical Oxidation Sites – Recommended Guidelines, EPA Ground Water Issue Paper. US Environmental Protection Agency, National Risk Management Research Laboratory, R.S. Kerr Environmental Research Center, Ada, OK. EPA/600/R-12/049.

QA/QC. Laboratory, field, equipment, and trip blanks, will be used for aqueous samples analyzed for CVOCs, metals, Cl^-, SO_4^{2-}, Fe^{+2}, and Fe_T; it is recommended that 10-15% duplicates for aqueous samples should be collected and analyzed. Method blanks, practical quantitation limits, method detection limits, matrix spikes, and percent recoveries are to be used and reported by the analytical contractor. The analytical contractor will issue a case narrative and discuss whether samples adhered to the quality assurance management plan and SOPs.

Investigation-Derived Waste

Less than 1 drum of contaminated ground water will likely be produced as investigation derived waste (IDW). The contaminated ground water is produced as a result of the micro-well and 2 in well purging prior to sample collection. The production, handling, and storage of IDW should be communicated and coordinated with the Installation Restoration Program Manager, Lisa Donohoe at (843) 228-2779.

Description of Operating Procedures for the YSI MPS 5600

The ground water flow will be diverted through a flow cell equipped with a YSI 5600 multi-parameter probe. The rate of pumping will be approximately 100-300 mL/minute. The YSI probe is used to track the stabilization of pH, oxidation-reduction potential (ORP), specific conductance (SC), dissolved oxygen (DO), and temperature. In general, the following criteria are used to determine when parameters have stabilized: a pH change of less than or equal to 0.02 units per minute, an oxidation-reduction potential change of less than or equal to 0.002 V per minute, and a specific conductance change of less than or equal to 1% per minute. These criteria are initial guidelines; professional judgment in the field is used to determine on a well-by-well basis when stabilization has occurred. The time-dependent changes in geochemical parameters recorded by the YSI probe are logged by the handheld instrument and recorded for each well on the ground water purge log sheet (see below). Once stabilization occurs, the final values for pH, ORP, specific conductance, dissolved oxygen, and temperature are recorded. After the values for pH, ORP, SC, DO, and temperature have been recorded, the flow cell is disconnected. For background information, the EPA NRMRL SOP for field analytical QA/QC (NRMRL-GWERD-23-0) is available.

Parris Island, SC MCRD Site 45 – ISCO Project: Ground Water Purge Log

Well ID:_____ Date:_____

Start Purge Time:_____ Initial Purge End Time:_____

Purge Rate:_____

End of Sampling Time:_____

Weather Conditions:_____

Time	Temp (ºC)	Specific Cond. (mS/cm)	TDS (g/L)	DO (mg/L)	pH	ORP (mV)	Comments

United States
Environmental Protection
Agency

Office of Research and Development (8101R)
Washington, DC 20460